MAY 18 1960

OAK RIDGE NATIONAL LABORATORY

operated by

UNION CARBIDE CORPORATION

for the

U.S. ATOMIC ENERGY COMMISSION

ORNL-TM-201

247

MASTER

CONCEPTUAL DESIGN OF THE PEBBLE BED REACTOR EXPERIMENT

NOTICE

This document contains information of a preliminary nature and was prepared primarily for internal use at the Oak Ridge National Laboratory. It is subject to revision or correction and therefore does not represent a final report. The information is not to be abstracted, reprinted or otherwise given public dissemination without the approval of the ORNL patent branch, Legal and Information Control Department.

DISCLAIMER

This report was prepared as an account of work sponsored by an agency of the United States Government. Neither the United States Government nor any agency Thereof, nor any of their employees, makes any warranty, express or implied, or assumes any legal liability or responsibility for the accuracy, completeness, or usefulness of any information, apparatus, product, or process disclosed, or represents that its use would not infringe privately owned rights. Reference herein to any specific commercial product, process, or service by trade name, trademark, manufacturer, or otherwise does not necessarily constitute or imply its endorsement, recommendation, or favoring by the United States Government or any agency thereof. The views and opinions of authors expressed herein do not necessarily state or reflect those of the United States Government or any agency thereof.

DISCLAIMER

Portions of this document may be illegible in electronic image products. Images are produced from the best available original document.

ORNL-TM-201

Contract No. W-7405-eng-26

CONCEPTUAL DESIGN OF THE PEBBLE BED REACTOR EXPERIMENT

Staff
Oak Ridge National Laboratory

DATE ISSUED

MAY 17 1962

OAK RIDGE NATIONAL LABORATORY
Oak Ridge, Tennessee
operated by
UNION CARBIDE CORPORATION
for the
U. S. ATOMIC ENERGY COMMISSION

CONTENTS

		Page
1.	SUMMARY	1
2.	INTRODUCTION	3
	Features of the Pebble-Bed Reactor	4
	Objectives of the Reactor Experiment	5
	Flexibility Provided by Replaceable Core Design	7
	Applications of High-Temperature Energy	7
3.	REACTOR DESIGN	10
	System Design	10
	General Arrangement	10
	Selection of Design Conditions	17
	Reactor Core and Graphite Structure	18
	Control Rods and Control Rod Drives	19
	Primary Coolant System	22
	Pressure Vessel and Support	24
	Main Coolant Blower	27
	Steam Generator and Steam System	30
	System Shielding and Maintenance	37
	Fuel-Handling System	37
	Helium Storage, Transfer, and Purification System	40
	Pressure-Relief System	43
	Leaktightness Requirements	44
	Secondary Containment System	46
	Ventilation System	47
	Offgas System	50
	Decontamination Facility	52
	Reactor Building Layout	52
	Layout No. 1	52
	Layout No. 2	58

Plant Layout 60
Site 60
Facilities 60
4. CORE SELECTION AND THERMAL ANALYSIS 63
Core Design 63
Pressure Drop and Levitation Limit 63
Thermal Stress in Fuel Sphere 64
Fuel Temperature 68
Selection of Core and Fuel Sphere Dimensions 73
Shutdown Cooling by Natural Circulation 74
System Pressure Drop 77
Pressure Vessel Temperature 79
5. FUEL-HANDLING SYSTEM 82
Fuel-Element-Addition System 84
Fuel-Discharge Mechanism 87
Fuel Inspection and Storage Area 90
Fuel Element Movement Through the Core 91
6. REACTOR PHYSICS 98
Fuel Composition 98
Temperature Coefficient 103
Reactor Control 104
Power and Flux Distribution 107
Fast Flux Distribution 110
Reflector and Shield 110
Economic Basis for Reference Design 118
7. COOLANT SYSTEM ACTIVITIES AND IMPURITIES 131
Purification System 131
Gaseous Fission-Product Activity 132
Deposited Fission-Product Activity 134
Oxidizing Impurities 137
Coated Fuel 137
Uncoated Fuel Spheres 138
Nonoxidizing Impurities 140
Coolant Purity Requirements 141

Impurity Sources 142
Main Stream Filtration 143
System Analysis 143
8. REACTOR CONTROL AND SAFETY SYSTEMS 145
Reactor Control System 145
System Control Characteristics 149
Reactor Safety System 150
Primary Coolant System Instrumentation 153
9. STRUCTURAL ANALYSIS OF SYSTEM 155
Pressure Vessel 157
Heads and Cylindrical Portion of Vessel 158
Nozzle Attachment Regions 160
Liner 168
Core Support Plate 169
Pressure Vessel Support System 170
Design and Stress Analysis for Normal Operating Conditions 171
Effects of Seismic Loads 172
Steam Generator Support System 175
Graphite Reflector Structure 179
10. FUEL ELEMENTS AND GRAPHITE COMPONENTS 185
Fuel Elements 185
Requirements and Operating Conditions 185
Fission-Product Retention 186
Mechanical Effects 188
Thermochemical Effects 190
Irradiation Effects 191
The Reference Fuel Element 192
Status of Coated Particle Fuel Element Development 192
Pyrolytic-Carbon-Coated Uranium Carbide Particles 193
Pyrolytic-Carbon-Coated Uranium-Thorium Carbide Particles 196
Pyrolytic-Carbon-Coated Uranium Dioxide Particles 196
Al_2O_3-Coated Uranium Dioxide Particles 197
BeO-Coated Uranium Dioxide Particles 198

Sphere Surface Coatings and Low-Permeability Graphite 198
Sphere Surface Coatings 198
Low-Permeability Graphite 199
Graphite Components 199
Reflector Graphite 200
Boronated Graphite for Thermal-Neutron Shield 205
11. MAINTENANCE OF CONTAMINATED SYSTEMS AND COMPONENTS 207
Main Circulating Blower 210
Heat Exchanger 211
Core Servicing 212
Control-Rod and Fuel-Discharge-Machine Drives 214
Control Rods 214
Fuel-Discharge Machine 214
Auxiliary Equipment 215
Decontamination Procedures 215
12. HAZARDS 217
Integrity of the Containment Shell 217
Fission-Product Leakage from Containment Shell 224
Direct Radiation Dose Rate 229
Shield Ventilation System 231
Emergency Cooling 232
Release of Fission Products from Fuel 235
Results of Analyses 239
13. HIGH-TEMPERATURE OPERATION 241
Alterations Required for High-Temperature Operation 241
Fuel Problems of High-Temperature Operation 245
Reactor Physics and Control 246
Hazards Considerations 246
Additional Costs of High-Temperature Operation 247
Conclusions 247
14. SITE SELECTION 249
Introduction and Conclusions 249
Hazards Considerations 251
Utilization of the Facility 253

Sites at ORNL 254
Site 1, at HRE-2 Facility 254
Site 2, East of the HRE-2 Facility 255
Sites at NRTS 255
Site 1, Between SPERT and GCRE Areas 255
Site 2, at ANP Area 255
Site Cost Comparison 257
15. CONSTRUCTION COST ESTIMATE 259
16. RESEARCH AND DEVELOPMENT 263
Fuel Element Development 264
Mechanical and Physical Properties 265
Nondestructive Inspection of Fuel Elements 265
Fabrication Studies 266
Chemical Stability 266
Fission-Product Behavior 267
Effects of Irradiation 267
Chemical Processing 268
Graphite Components 268
Physical and Mechanical Property Tests 269
Irradiation Tests 269
Boronated Graphite Studies 270
Coolant Purification 270
Gas Evolution from Reflector and Fuel Graphite 270
Graphite Oxidation and Mass Transfer 271
Purification System and Components 272
Purification System Mockup 273
Fission-Product Transport and Deposition 274
Chemical Studies 275
Activation Studies 275
In-Pile Experiments 276
Core Cooling Problems 276
Mean Bed Void Fraction 277
Flow Distribution and Pressure Drop 277
Additional Flow Problems 278

Full-Scale Flow Model 279
Thermal Studies 280
Fuel Handling 280
Movement of Spheres in the Core 280
Component Development 281
PBRE Instrumentation and Contrcl 281
Analog Analysis 282
Reactor Control and Safety System 282
Nonnuclear Instruments and Equipment for Reactor Safety and Control 282
Containment System Equipment 283
Fuel-Handling System 283
Development of Thermocouples for Measurements in the Range 2000 to 2500°F 283
Component Development 284
Control Rods and Drives 285
Blowers 285
Joints and Closures 287
Slip Joints 288
Valves 289
Steam Generator Development 289
Experimental Stress Analyses 290
Materials Problems 290
Compatibility of Coolant and Decontamination Reagents with Metals 290
Compatibility of Graphite and Metal 291
Welds of Upper Shroud, Concentric Tubing, etc. 291
Special Compatibility Problems in High-Temperature Operation 292
Control Rods 292
Maintenance Problems 293
Maintenance in the PBRE Cells 294
Decontamination Studies 294
Physics 295

Hazards Studies 296
Over-All Research and Development Program 299
17. SCHEDULE FOR DESIGN AND CONSTRUCTION 303

1. SUMMARY

Pebble-bed reactors have advantages associated with the simplicity of the fuel element, ease of fuel handling, suitability for high-temperature operation, and good neutron economy. In common with other all-ceramic reactors not having purged fuel elements, they suffer the disadvantage that some fission-product activity will enter the coolant system. The Pebble-Bed Reactor Experiment (PBRE) will advance the pebble-bed concept by providing a test of these features and will make important contributions to the general development of all-ceramic gas-cooled reactors as well. To this end the following objectives were established for the reactor experiment: (1) to investigate key features of the pebble-bed concept, including on-stream fuel handling, movement of fuel through bed, and performance of core; (2) to obtain operation and maintenance experience with a system contaminated with fission-product activity; and (3) to investigate the behavior of graphite fuel elements. A fourth objective, study of the behavior of core materials at conditions occurring with exit gas temperatures in the range 2000 to 2500°F, was tentatively included.

The preliminary design of a 5-Mw (thermal) reactor for achieving these objectives has been prepared. The core of the PBRE is a 2 1/2-ft-diam, 4-ft-tall cylinder containing approximately 12 000 spherical graphite fuel elements 1 1/2 in. in diameter. Fuel spheres are added to and removed from the core by gravity flow, and these operations are performed while the reactor is at power by using pairs of valves for passage of elements into and out of the high-pressure system. Exposed fuel can be recycled to the top of the core.

Helium coolant at 500 psia enters the bottom of the core at 550°F and emerges from the top at 1250°F. Concentric ducting connects the reactor to a single heat exchanger, which is located sufficiently high above the core that natural circulation will suffice to remove afterheat in the event the blower ceases to function. The coolant flow path is such that the entire pressure envelope is swept with helium at the temperature at which it emerges from the heat exchanger.

Provision for semiremote maintenance of contaminated components is emphasized in the layout, and most of the equipment in the primary and auxiliary systems is accessible from above by the removal of modular shielding units. The design permits replacement of the entire core graphite structure. The reactor can be adapted for testing core materials at high temperature by attemperation of the hot helium emerging from the core with cool gas in a plenum in the upper graphite structure.

Location of the PBRE at the site of the HRE-2 facility is proposed to take advantage of available buildings and services, but the reactor and auxiliary equipment will be contained in a completely new vessel located adjacent to the existing building. The design and direct construction cost of the reactor plant is estimated to be $7,958,000; allowance for contingencies, overhead, and escalation brings the total to $12,260,000. High-temperature operation can be achieved when desired for an additional expenditure of less than $500,000.

2. INTRODUCTION

The pebble-bed reactor concept is an old one, having been among the proposals considered for the Daniels Pile in 1945.[1] Little attention was devoted to it, however, until five years ago when the Sanderson & Porter Company, with AEC support, began to investigate the design and development of pebble-bed reactors. Most of their effort was devoted to the study of fuel-handling problems and to development of a fuel for the reactor, with, in particular, the aid of the Battelle Memorial Institute.

In Germany, a combine of the Brown-Boveri Company and Krupp began actively in 1956 to develop a pebble-bed reactor and to plan for its construction.[2] A 15-Mw (electrical) reactor has been designed, and its construction in Germany began recently. The BBC-Krupp reactor will undoubtedly make major contributions to the development of the pebble-bed concept.

The Oak Ridge National Laboratory was requested by the Atomic Energy Commission in the fall of 1960 to perform design studies of both an experimental reactor and a large power reactor based on the pebble-bed concept. Results of these studies are presented in refs. 3 and 4. Further studies of a pebble-bed reactor experiment were initiated at ORNL in July 1961, and this report contains a preliminary description of the design which has emerged. It also presents an estimate of the construction cost of such a reactor, a proposed schedule for design and construction, and a discussion of the research and development effort which it is believed should accompany the design program.

---

[1]F. Daniels, High Temperature Pebble Pile (Minutes of lecture on April 14, 1945), CF-2860(5), May 31, 1945.

[2]F. Schulten, The Development of High Temperature Reactors, pp. 109–26, Franklin Institute Monograph No. 7, May 1960.

[3]A. P. Fraas et al., Preliminary Design of a 10-Mw(t) Pebble-Bed Reactor Experiment, CF 60-10-63 rev. (May 8, 1961).

[4]A. P. Fraas et al., Design Study of a Pebble-Bed Reactor Power Plant, CF 60-12-5 rev. (May 11, 1961).

Features of the Pebble-Bed Reactor

The unique feature of the pebble-bed reactor concept is the formation of the core from a bed of randomly packed spherical fuel elements. Graphite is used as the primary sphere material; the fissile and fertile material are refractory compounds of low cross-section elements, and helium is the coolant. As presently conceived, a pebble-bed reactor has the following features:

1. A simple fuel element. There is hope that the simple geometry of the fuel without close tolerances will result in relatively low fabrication costs.

2. Ease of fuel handling. Fuel spheres are added at the top of the core and discharged at the bottom by gravity flow. These operations are performed while the reactor is at power by utilizing a series of valves for passage of elements into and out of the high-pressure system. This simple at-power refueling concept makes an equilibrium fuel cycle quite practical. In addition, provision of multiple fuel removal and addition points in a large reactor would make it possible to shift fuel radially, as well as transfer it from the bottom to the top of the core. The simplicity of the fuel-handling system suggests that a relatively small capital investment in equipment will be required to provide for on-stream refueling.

3. High-temperature operation. Fuel elements of refractory materials permit operation at high temperatures. This basic advantage of refractory materials is not compromised by requirements of structural properties or close tolerances; for example, a bed of spheres which is not restrained at the top expands upward to accommodate thermal volume increases, the load on individual spheres from the weight of the bed is small, and exact fuel element dimensions are not necessary.

4. Good neutron economy. The absence of metal cladding and structural materials in the core reduces the loss of neutrons by parasitic absorptions and thus permits operation with good neutron economy.

5. Activity in coolant. There has been no demonstration to date of an all-ceramic fuel element that completely retains fission products

when operated at the temperatures and burnups of interest for power reactors. Although this does not imply that a high degree of fission-product retention will not be achieved, the assumption must be made that a small but significant amount of activity will enter the coolant and deposit on surfaces in the reactor system. Hence the pebble-bed reactor, in common with other ceramic-core reactors which provide no purge for the fuel elements, must be considered a contaminated system. The activity level, while far below that of a fluid fuel reactor, may be enough higher than that of gas-cooled reactors with metal-clad fuel elements to dictate different requirements for leaktightness and to necessitate special provisions for decontamination and maintenance.

6. Randomness of coolant flow and temperature distribution. The random variation in void fraction associated with an unordered sphere arrangement results in local variations in coolant velocity. As a consequence, temperature distribution in the core is somewhat statistical in nature, although the extremes of temperature are limited.

Objectives of the Reactor Experiment

The construction and operation of a reactor experiment will advance the pebble-bed concept by providing an integrated test of its key features. Important contributions to the general development of high-temperature all-ceramic systems will be made as well. To these ends the following objectives were established as a basis for the PBRE design:

1. to investigate in an operating reactor the key technical features of the concept, such as the performance of a nuclearly heated ball bed, operation of an on-stream fuel-handling system, and movement of fuel through the bed;
2. to gain experience in the operation and maintenance of reactors in which a small but significant fraction of the fission products escapes from the fuel and passes into the coolant system; and
3. to obtain information at power reactor conditions on the behavior of graphite fuel elements, with particular emphasis on the characteristics of dispersion elements containing coated fuel particles.

The first objective encompasses those factors which are unique to the pebble-bed concept. Although valuable information can be obtained from out-of-pile and in-pile experiments, many aspects of these features can only be investigated by actual operation of a reactor.

The second objective is intended to answer questions of interest to all gas-cooled reactor concepts in which activity is expected to enter the coolant system. Prismatic fuel elements, such as those for Dragon and HTGR, can be purged to keep the level of activity in the coolant circuit low. This is achieved in present designs, however, at the expense of constructing a more expensive fuel element and providing an elaborate fission-product cleanup system for the purge stream, and at the penalty of increased thermal resistance between fuel and coolant, resulting in higher fuel temperatures. These disadvantages could be avoided with prismatic as well as spherical fuel elements by using a fuel that retains most of the fission products and permitting the activity which does escape to enter the coolant. A coolant purification system would still be provided to reduce the activity level, but acceptance of the presence of some activity greatly reduces the demands on the cleanup system and results in an appreciable simplification. The question of how much penalty will be paid in operating and maintaining a contaminated system will only be answered by operation of a reactor. Since it seems unlikely that a full-scale power plant will be built or an existing reactor deliberately operated as a test of a contaminated system, a major function is to be served by an experimental reactor that will provide this information.

The third objective, of course, relates most directly to pebble-bed reactor fuel elements. Statistically significant data on the behavior of coated particles or other means for retaining fission products will, however, be of value to reactors with different fuel geometries.

It is to be noted that the objectives of the Pebble-Bed Reactor Experiment do not include its being designed as a prototype of a large power reactor, other than with regard to the features mentioned above. This omission is deliberate, since the factors included are considered to represent sufficient motives for the experiment, and attempting to

serve too many purposes with one reactor would increase the difficulty and the cost of achieving the primary objectives.

Flexibility Provided By Replaceable Core Design

As discussed later in detail, the possibility of damage to the graphite reflector by radiation shrinkage or oxidation is of sufficient concern that provision has been made in the design for removal and replacement of the entire graphite structure. If the graphite structure is replaceable, it should be possible to substitute a core with a geometry appropriate for testing fuel elements of a different type. It may be of interest in particular to test prismatic graphite fuel elements, and provision for such a test seems quite feasible. Insertion of a BeO core in place of one of graphite may also be possible.

Applications of High-Temperature Energy

The possible applications of high-temperature energy are of sufficient interest that a tentative fourth objective for the PBRE appears, that is, the generation of helium temperatures in the range 2000°F and above. The temperature levels of gas-cooled reactors have been increasing rapidly in recent years, and the Dragon and HTGR will have outlet gas temperatures in the 1350 to 1400°F range. The goal of producing steam conditions comparable to the most modern of conventional power plants will thus soon be achieved.

There is interest in still higher temperature levels, however, for direct-cycle gas turbines and for process heat; in fact, the motivation for much of the early interest was the potential use of pebble-bed reactors as energy sources for direct-cycle gas turbines. Development of the metallurgy of refractory metals, notably molybdenum, which offer promise of machines that will operate at temperatures well beyond present levels has renewed interest in gas turbines coupled to reactors for central station use. One possible arrangement is the use of a high-temperature gas turbine in a topping cycle preceding a heat exchanger in which steam at conventional conditions would be produced; with this scheme high efficiencies

could be achieved with only conventional materials required beyond the gas turbine. The feasibility of maintaining a turbine which has been exposed to fission-product-laden gas, of course, is a major question.

Use of nuclear energy in the synthesis of gas from coal[5] appeared sufficiently promising in 1955 that a joint AEC-Department of Interior project was established at the Morgantown Research Center of the Bureau of Mines to investigate the problems and to test and develop components for a coal-gasification system heated by a nuclear reactor. The Morgantown program includes operation of a loop in which an induction-heated bed of graphite spheres is used to simulate a reactor; uninterrupted operation of this loop with an outlet gas temperature of 2500°F has been sustained in a run of over 1000 hr.[6] A gasifier in which a steam-coal mixture will be heated with hot helium is presently being constructed for installation in the loop.

An application that may be economically more attractive than coal gasification, at least in the near future, is the production of hydrogen by the reforming of methane, other hydrocarbons, or coal. It has been stated[7] that nuclear energy for this process could cost over $1 per million Btu's and still be competitive with conventional processes for the production of hydrogen.

Nuclear reactors are said[5] to have two advantages for these applications: (1) there are no stack losses and (2) reactor pressures are comparable to those at which the products of coal gasification or hydrogen production systems are used and at which conditions for their production are favorable. The latter feature permits balancing of pressures across a high-temperature heat exchanger (to reduce stresses) without additional pumping costs. In both of the applications mentioned the gas temperatures

---

[5]R. Carson Dalzell and J. P. McGee, Indirect Cycle Nuclear Reactor System to Furnish Process Heat, pp. 111–18 in Chemical Engineering Progress Symposium Series, Vol. 55, No. 22, 1959.

[6]N. H. Coates, J. P. McGee, and G. E. Fasching, Simulated Nuclear Reactor System for High-Temperature Process Heat: 1000-Hour Demonstration Run at 2500°F, RI-5886, 1961.

[7]J. P. McGee, High-Temperature Systems for Nuclear Process Heat, IC 7954, 1960.

of interest are in the 2000 to 2500°F range. As with a gas turbine, the most favorable economics might result from following the process heat reactor with a heat exchanger in which steam for a conventional power cycle is generated.

With the reactor described in this report it would be considered sufficient to produce high-temperature gas as a test of core materials. This objective would be accomplished even if the hot gas were attemperated with cold gas at the core exit without being conducted elsewhere.

3. REACTOR DESIGN

System Design

The PBRE plant design is governed by the basic requirement that it provide a system for studying (1) the behavior of pebble-bed fuel elements, (2) the performance of the fuel-handling system, and (3) the problems associated with the operation and maintenance of a system contaminated with fission products. The design conditions for the system selected to satisfy these objectives are given in Table 3.1 and the over-all arrangement is illustrated in Figs. 3.1 and 3.2.

General Arrangement

Initial decisions that flow of coolant through the core would be upward and that the upper surface of the ball bed would not be mechanically restrained strongly influenced the design of the reactor. Upward flow of coolant avoids problems associated with having high-temperature gas pass through the core structural support system. In addition, less over-all height is required to provide for natural-circulation cooling of an upflow core; natural-circulation (by thermal convection) is desirable for removal of core afterheat in case of a primary loop blower failure.

Lack of a hold-down device at the top of the core creates restrictions on the core design because of the possibility of levitation of the fuel spheres. A restraining structure would, however, complicate the addition of fuel and, further, would require special provisions to allow for expansion of the ball bed. These problems were avoided by leaving the core unrestrained.

As may be seen in Fig. 3.3, helium emerging from the top of the core passes through the center of concentric ducts to a steam generator located in a separate shielded compartment. After being cooled, the helium is conducted to a single, separately mounted blower from which it returns through the steam generator and through the outer of the concentric ducts to the reactor vessel.

Fuel is charged at the top of the vessel and is discharged at the bottom to a separate inert-gas-filled compartment designed for the required

Table 3.1. Principal Performance and Dimensional Data for the PBRE Design

Power generation	
Design thermal output, Mw	5
Levitation-limited thermal output,[a] Mw	6.2
Design power density of bed, w/cm^3	9
Core dimensions and characteristics	
Diameter, ft	2.5
Height, ft	4
Inlet face area, ft^2	4.9
Volume, ft^3	19.6
Average void fraction	0.39
Number of fuel spheres	11 700
Total weight of fuel spheres, lb	1 300
Total heat transfer area, ft^2	574
Diameter of core plus reflector, ft	8.5
Height of core plus reflector, ft	10.0
Initial fissionable inventory, kg of U^{235}	17.2
Rate of bed temperature rise at 5 Mw (no coolant flow), °F/min	565
Weight of graphite, lb	57 000
Number of control rods	4
Fuel element characteristics	
Sphere outside diameter, in.	1.5
Sphere surface-to-volume ratio, ft^2/ft^3	48
Sphere composition, wt %	
U^{235}	2.91
U^{238}	0.21
Thorium	1.88
Carbon	95.00

[a]Based on a coolant inlet temperature of 550°F and outlet temperature of 1250°F.

Table 3.1. (Continued)

Initial specific power in core, kw/kg of U^{235}	3 000
Average fuel element burnup, Mwd/ton (U + Th)	130 000
Fissions per initial U + Th, at. %	13.9
Average heat flux, Btu/hr·ft^2	29 700
Volumetric average fuel temperature, °F	1 090
Maximum sphere surface temperature, °F	<1 900
Average internal temperature drop (uniformly fueled sphere), °F	120
Stress-limited power density,[b] w/cm^3 of bed	45
Coolant characteristics	
Gas	Helium
Pressure, psia	500
Inlet temperature, °F	550
Outlet temperature (mean), °F	1 250
Flow rate through bed, lb/hr	19 500
Superficial mass velocity, lb/ft^2·hr	3 970
Circuit pressure drop, psia	2.7
Core pressure drop, psia	0.83
Recirculation time, sec	14.5
Average core heat transfer coefficient, Btu/hr·ft^2·°F	200
Coolant blower (one)	
Type	One stage, centrifugal, gas bearing
Drive	Variable-speed electric motor
Motor drive power, hp	100

[b]For uniformly fueled sphere and 1500-psi stress, k = 8 Btu/hr·°F·ft, and the void fraction is 0.39.

Table 3.1. (Continued)

Pressure vessel	
Shape	Cylinder with torispherical heads
Outside diameter, ft	9.5
Height, ft	20
Thickness, in.	2.5
Material	A 212, grade B, steel
Design pressure, psig	625
Design membrane stress, psi	17 500
Maximum design temperature, °F	650
Total weight, including contents, lb	145 000
Steam generator (one) and emergency cooler	
Type	Saturated steam, natural recirculation
Capacity	
Steam generator, Mw	6.2
Emergency cooler, Mw	0.2
Heat transfer area	
Steam generator, ft^2	620
Emergency cooler, ft^2	85
Gas pressure drop (max), psi	1
Gas-side film coefficient, $Btu/hr \cdot ft^2 \cdot °F$	160
Over-all heat transfer coefficient, $Btu/hr \cdot ft^2 \cdot °F$	130
Tube (steam) side conditions	
Operating pressure, psia	600
Design pressure, psig	750
Operating temperature, °F	486
Design temperature, °F	600
Shell (gas) side conditions	
Operating pressure, psia	500
Design pressure, psig	625
Operating temperature, °F	550
Design temperature, °F	650

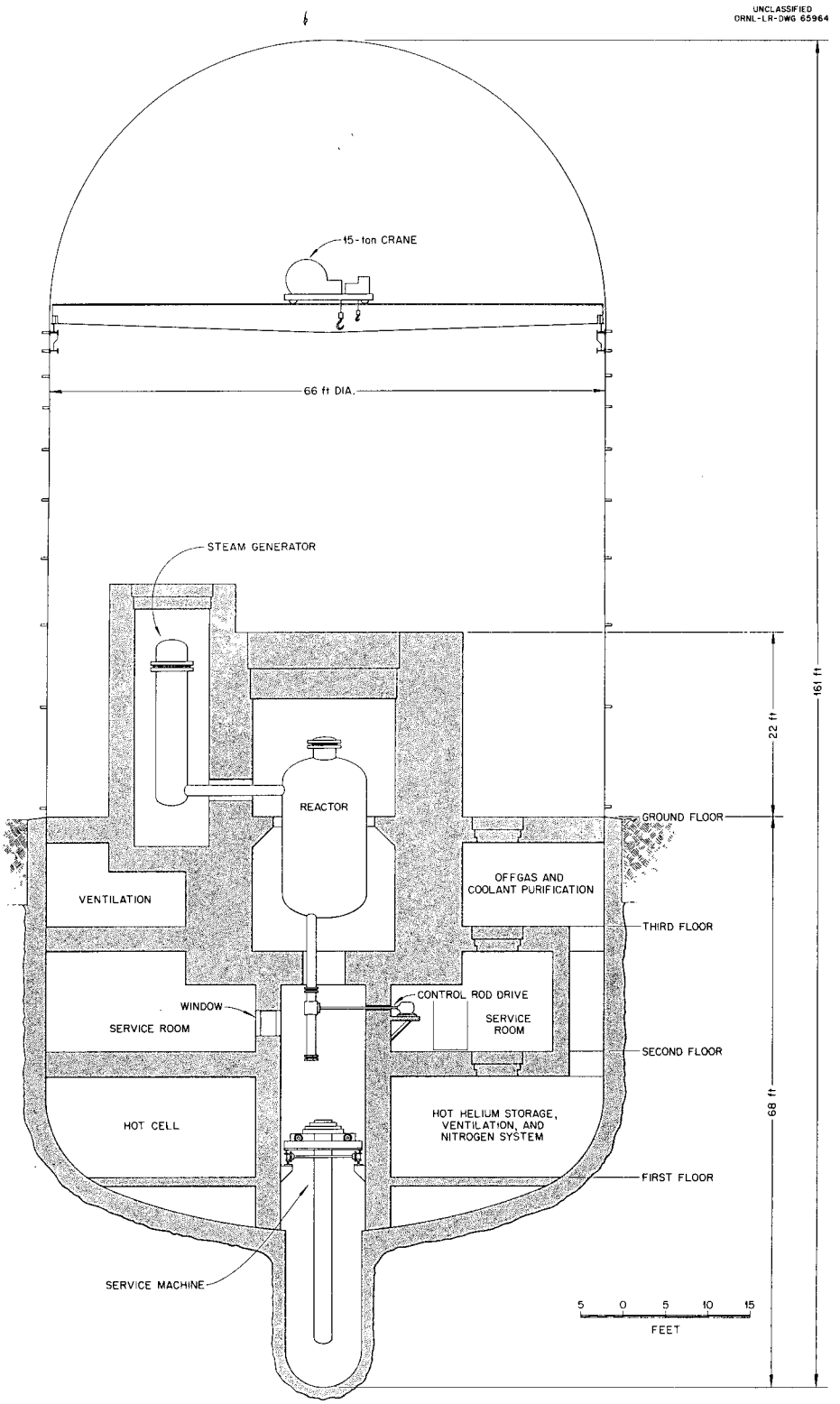

Fig. 3.1. Vertical Section Through Reactor Building Showing Relative Positions of Reactor and Steam Generator.

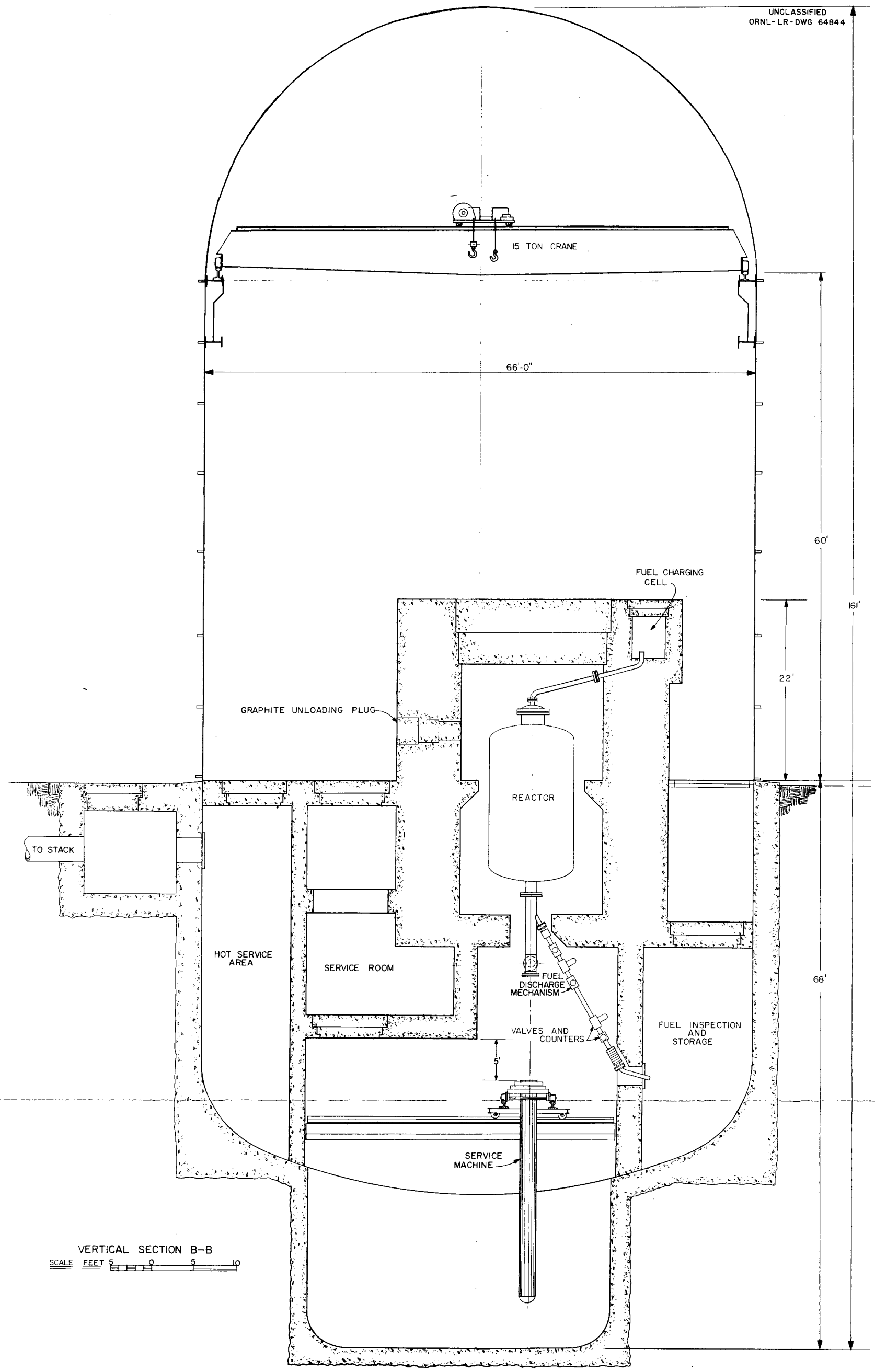

Fig. 3.2. Vertical Section of Reactor Building Showing Fuel-Handling System.

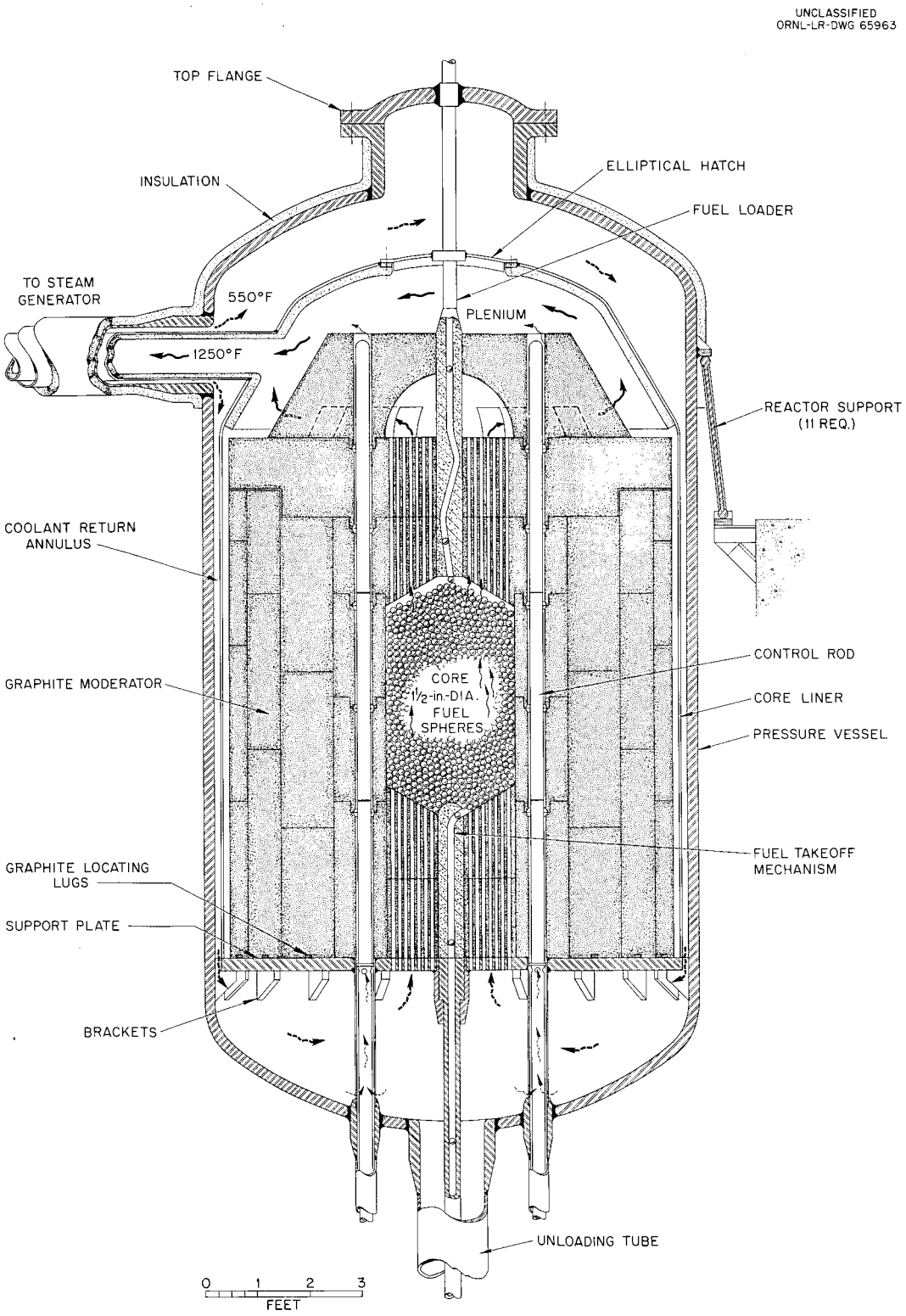

Fig. 3.3. Sectional View of PBRE Assembly.

fuel-handling, classification, and storage operations. Fuel elements can be added and removed while the reactor is at power, and normal fuel-handling operations can be performed from outside the containment vessel.

The experimental nature of the reactor dictates that certain components be accessible for periodic maintenance and replacement operations. Accordingly, the design provides for (1) maintenance and replacement of the blower, steam generator, and fuel-handling system, as well as all of the auxiliary system components, (2) replacement of the reactor graphite, and (3) maintenance and replacement of control rods and drives. The service machine located below the reactor is utilized for replacement of control-rod-drive subassemblies and the fuel-discharge and inspection assembly. Most other maintenance operations can be performed using semi-remote techniques.

Selection of Design Conditions

A thermal power of 5 Mw was selected as adequate to meet the objectives of the experiment while minimizing the capital investment. Core dimensions appropriate for this power represent sufficient multiples of the fuel diameter to allow adequate reproduction of the ball-bed behavior in a power reactor.

Reactor inlet and outlet temperatures were established as 550 and 1250°F, respectively, primarily from materials and steam-cycle considerations. Outlet gas temperatures of 1250 to 1400°F, although sufficiently high for cycle efficiencies comparable with those of advanced conventional power plants, do not introduce new materials problems. The lower end of this range was selected for the design point because, with an unrestrained up-flow core, the levitation restriction is more severe with a smaller temperature rise across the core; the reactor can, however, be operated with outlet gas temperatures up to about 1400°F. An inlet gas temperature of 550°F results in favorable power plant efficiency but is low enough to permit use of mild steel as the pressure envelope material.

High pressures (with high gas densities) are desirable for pebble-bed reactors, since they permit greater power densities within the levitation limit; an operating pressure of 500 psia was therefore chosen for

the PBRE. The pressure selected represents an extension from the levels of the present generation of gas-cooled reactors, but is not so high that it will present unusual design problems or add excessively to the construction cost.

Reactor Core and Graphite Structure

The core contains 11 700 spherical fuel elements 1 1/2 in. in diameter in a 2.5-ft-diam 4.0-ft-high volume surrounded by a graphite reflector. Selection of the core dimensions and fuel element size is discussed in Section 4, and the design data are summarized in Table 3.1.

The minimum reflector thickness has been made 3.0 ft to protect the pressure vessel from radiation damage by fast neutrons. This results in a cylindrical graphite structure with an outside diameter of 8.5 ft and a height of 10 ft (see Fig. 3.3). Borated graphite is used for the outer 4 in. of the cylinder to reduce the current of thermal neutrons into the pressure vessel; the factors which make this desirable are discussed in Section 6 and the properties of borated graphite are reviewed in Section 10. Four 4-in.-diam control-rod channels having centers on a 40-in. circle penetrate the reflector parallel to the core axis.

The graphite regions immediately above and below the fuel cavity are designed with passages for coolant flow through the bed. Openings for the fuel addition and removal equipment are also provided in these regions, and the lower surface of the bed is shaped to ensure free flow of balls into the fuel-discharge device.

An additional graphite bridge structure is mounted on top the reflector. This structure forms a cavity for collecting the hot gas from the core, and provides cooling channels for control rods projecting into the upper plenum. Core exit gas flows from the cavity into the plenum by way of four passages through the graphite. Provision is made for use of the cavity as an attemperation chamber during special experiments with the exit gas from the core above the design temperature; cold helium (550°F) from the space between the pressure vessel and liner dilutes the hot gas so that the temperature of the gas emerging from the graphite structure does not exceed 1250°F. This is discussed further in Section 13.

Shrinkage of graphite from fast-neutron irradiation is anticipated at the temperatures in the PBRE. Uneven shrinkage from flux gradients could result in severe stresses in the region immediately surrounding the fuel cavity. The graphite in this region must, therefore, be designed to minimize these stresses in order to achieve adequate life (see Sections 9 and 16).

Since damage from oxidation, as well as from irradiation, is possible, provision is made for replacement of the graphite structure by working through the closure at the top of the vessel. The reflector will therefore need to be made up of sections that can pass through the openings in the liner and vessel. If the upper closure is only 27 in. in diameter, the segments will have to be keyed together, as in Fig. 3.4, to form the surface of the ball bed. However, if the closure is increased in diameter to 4 ft, as discussed later, graphite cylinders could be used to contain the bed. The details in Figs 3.3 and 3.4 are intended to show the type of structure which might be used and do not depict a specific design. Techniques that can be used in replacement of the core structure are described in Section 11.

Provision will be made in the design of the core for the exposure and removal of surveillance specimens of steel and graphite. Steel specimens made from pressure vessel material will be located in positions at which they will be subjected to environmental and flux conditions representative of those that are most severe for the reactor vessel. Graphite specimens made of reflector material will be at positions in which the temperature and flux are similar to those in the regions in which appreciable radiation damage to the reflector is expected.

Control Rods and Control Rod Drives

The reactor is controlled by four absorber rods located in the reflector graphite adjacent to the core. Each rod provides regulating, shim, and safety functions. The control-rod and drive arrangement are shown in Fig. 3.5. Each rod has three tubular sections with outside diameters of 3 in. The absorber section, which is top-most, is 4 ft long and consists of B_4C bushings contained between concentric metal tubes. A 5-ft-long

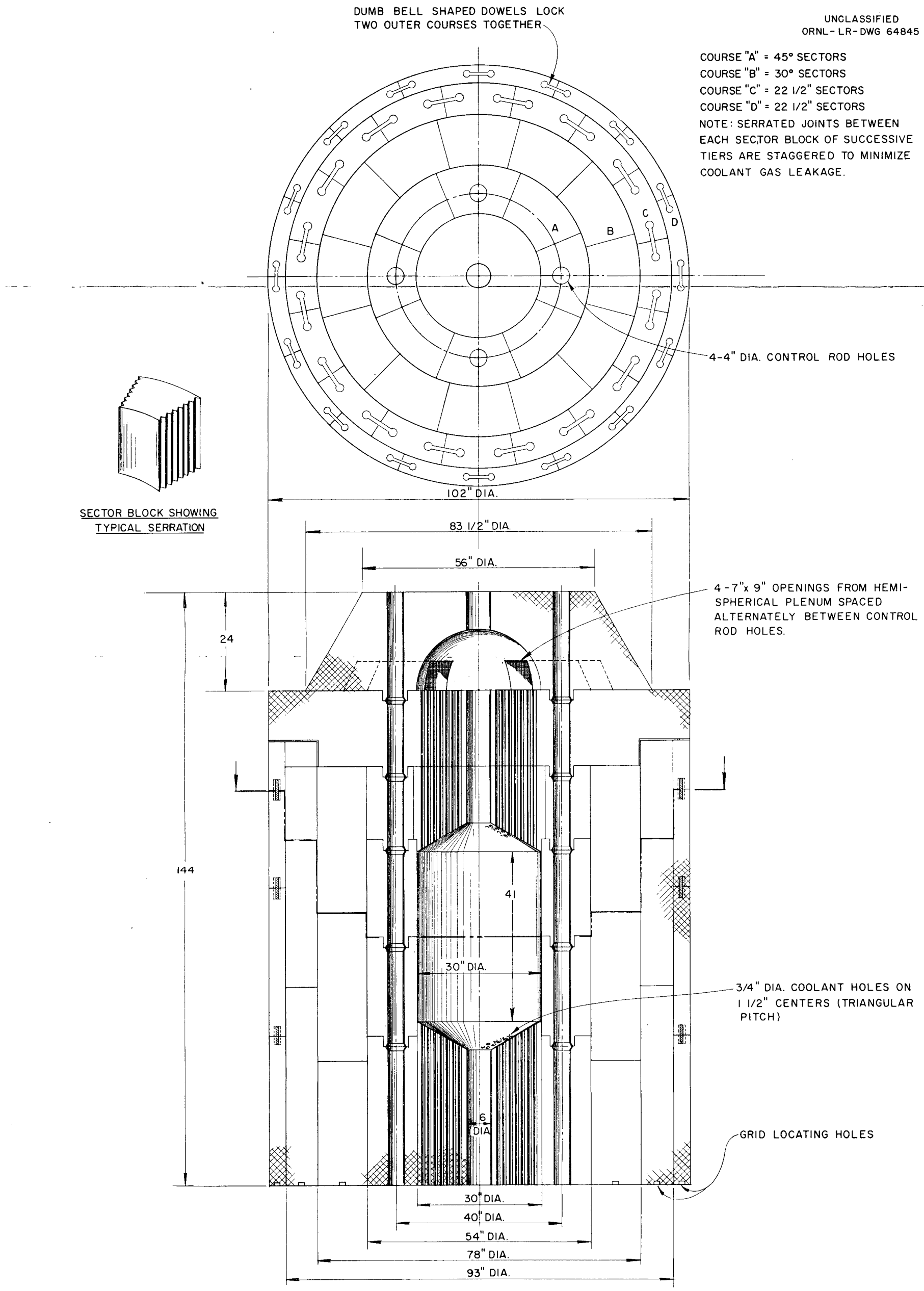

Fig. 3.4. PBRE Core Graphite Arrangement.

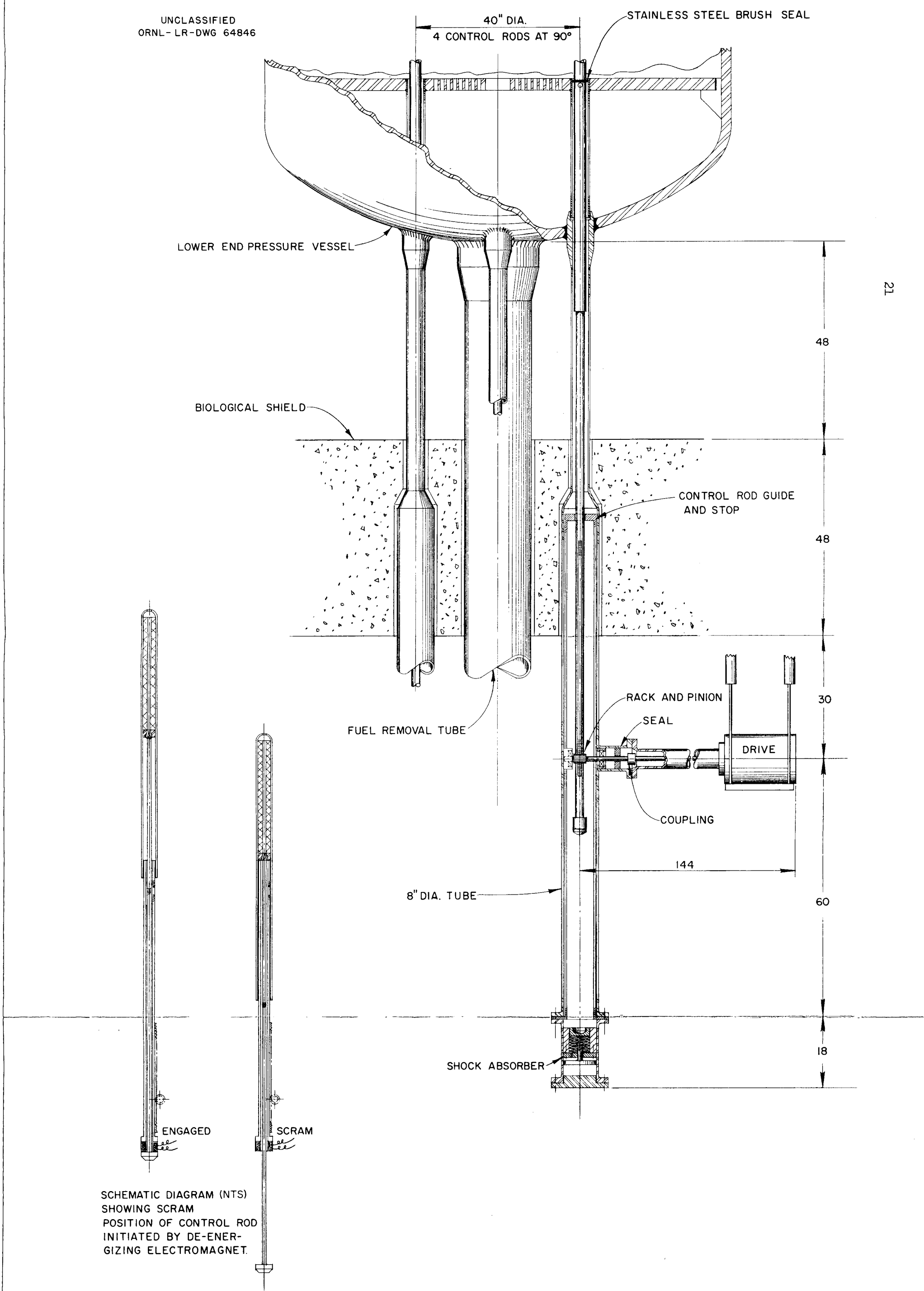

Fig. 3.5. Control Rod and Drive Arrangement.

central section is made from a heavy-walled graphite tube, and the lower section is a metal tube. A metal rod or cable passing up the center of the graphite tube connects the lower-metal tube to the absorber section. When the reactor is critical, the absorber section is in the upper part of the reflector and the graphite section is opposite the core. Shutdown is achieved by dropping the rod to bring the absorber alongside the core.

Cooling is accomplished during normal operation by helium passing upward through the rod sections and emerging at the top. Passage of gas up the annulus between the rod and the rod channel is restricted by a brush-type seal on the outside of the drive tube. On rod insertion, however, movement of the brush to a position below the point of entry of gas into the rod channel allows flow through the annulus. This feature automatically provides adequate cooling of the control rods when coolant circulation is provided only by natural convection.

Rod drive thimbles are located at the bottom of the pressure vessel. The control rods are coupled to the drive mechanism through magnets which are de-energized to scram the reactor. Provision is made for pulling the absorber section into the core region if for any reason it does not drop by gravity. The arrangement shown in Fig. 3.5 requires that removal and replacement of control rods be through the bottom of the thimbles. An alternate design, which has a larger access nozzle at the top of the reactor vessel permits replacement of rods from the top, even though they are driven from below the reactor.

Primary Coolant System

The primary system flowsheet is shown in Fig. 3.6. Helium emerging from the core flows through the center of concentric ducts to the heat exchanger, passes upward through the center of the heat exchanger, and then downward in an annular region next to the wall to the blower. From the blower it passes back through the heat exchanger and through the annular region of the concentric ducts to the reactor. Inside the reactor vessel the helium passes downward between a shroud and the vessel wall to again enter the core at the bottom. The heat exchanger is located above the level of the reactor vessel to provide natural-convection cooling in the event of a coolant blower failure.

UNCLASSIFIED
ORNL-LR-DWG 64847

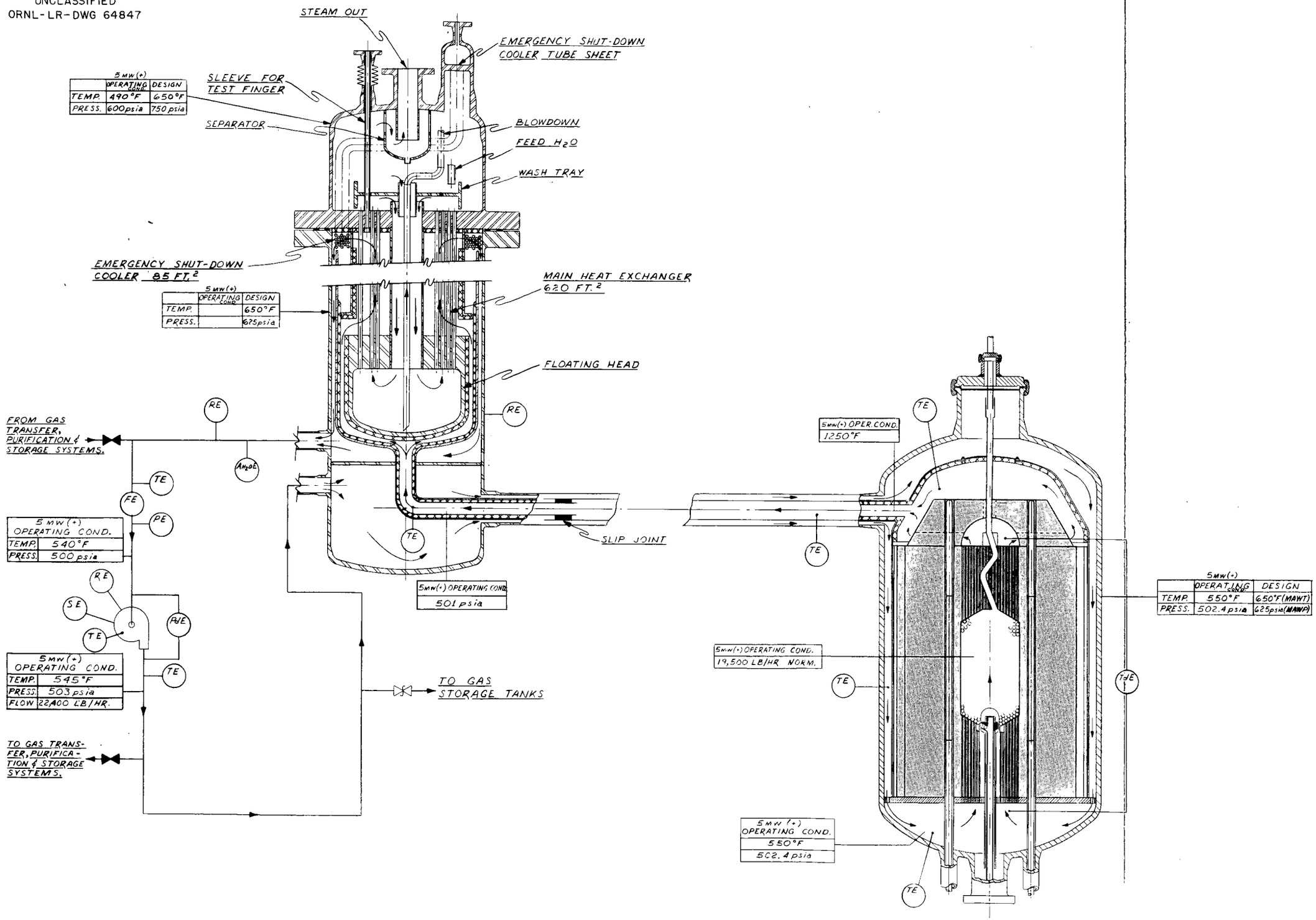

Fig. 3.6. Schematic Flow Diagram of Primary Coolant System.

A stainless steel shell (or liner) is used inside the pressure vessel to separate the cool return gas from the hot gas leaving the reactor core (Fig. 3.3); the liner surfaces that would contact hot gas are covered with reflective insulation. The flow distribution obtained by returning the cool gas into the plenum between the pressure vessel and the liner dome should provide uniform cooling for the support region and cylindrical sides of the vessel.

The outer member of the concentric ducts is a carbon steel pipe and the central member is a stainless steel pipe with 1 in. of reflective insulation on its inner surface. A slip joint accommodates the difference in axial thermal expansion between the carbon and stainless steel pipes. Flexible runs of carbon steel piping connect the heat exchanger to the blower. The use of a full-flow particulate filter for the primary coolant stream is under consideration. If a filter is used, it can be mounted in the horizontal run of piping to the suction side of the blower.

Sweeping the entire pressure envelope with helium returning from the heat exchanger permits the use of carbon steel for the pressure vessel and piping; that this is achieved at forced or natural circulation conditions without auxiliary circuits enhances the simplicity and reliability of the sytem. As discussed in Section 13, an additional benefit is gained from the design because attemperation of the gas leaving the core may be achieved without employing another circuit.

Pressure Vessel and Support

The reactor pressure vessel is cylindrical with torispherical heads, as illustrated in Figs. 3.7 and 3.8. The concentric piping for primary coolant gas ties into the cylindrical portion of the vessel. One fuel-removal and four control-rod-drive nozzles are located in the bottom head. Locating the control-rod-drive nozzles at the bottom avoids penetrating the vessel liner and leaves the entire upper region unobstructed for installation of fuel loading equipment and for core servicing operations (including control rod replacement if, as discussed later, a larger access nozzle is provided). The top head of the vessel has a single large nozzle, and below it is a bolted opening in the metal liner; removal of

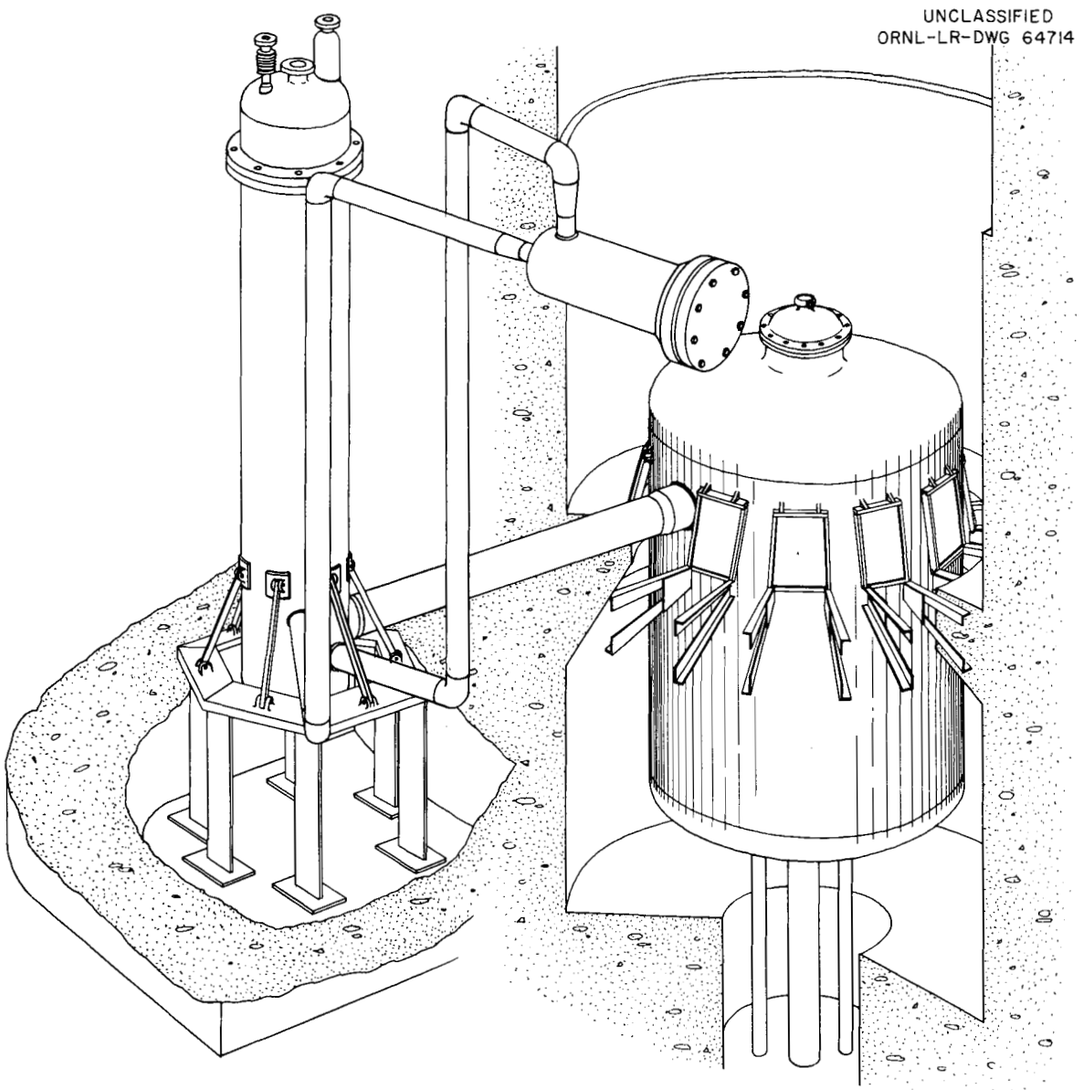

Fig. 3.7. PBRE Primary System Vessels and Support Arrangements.

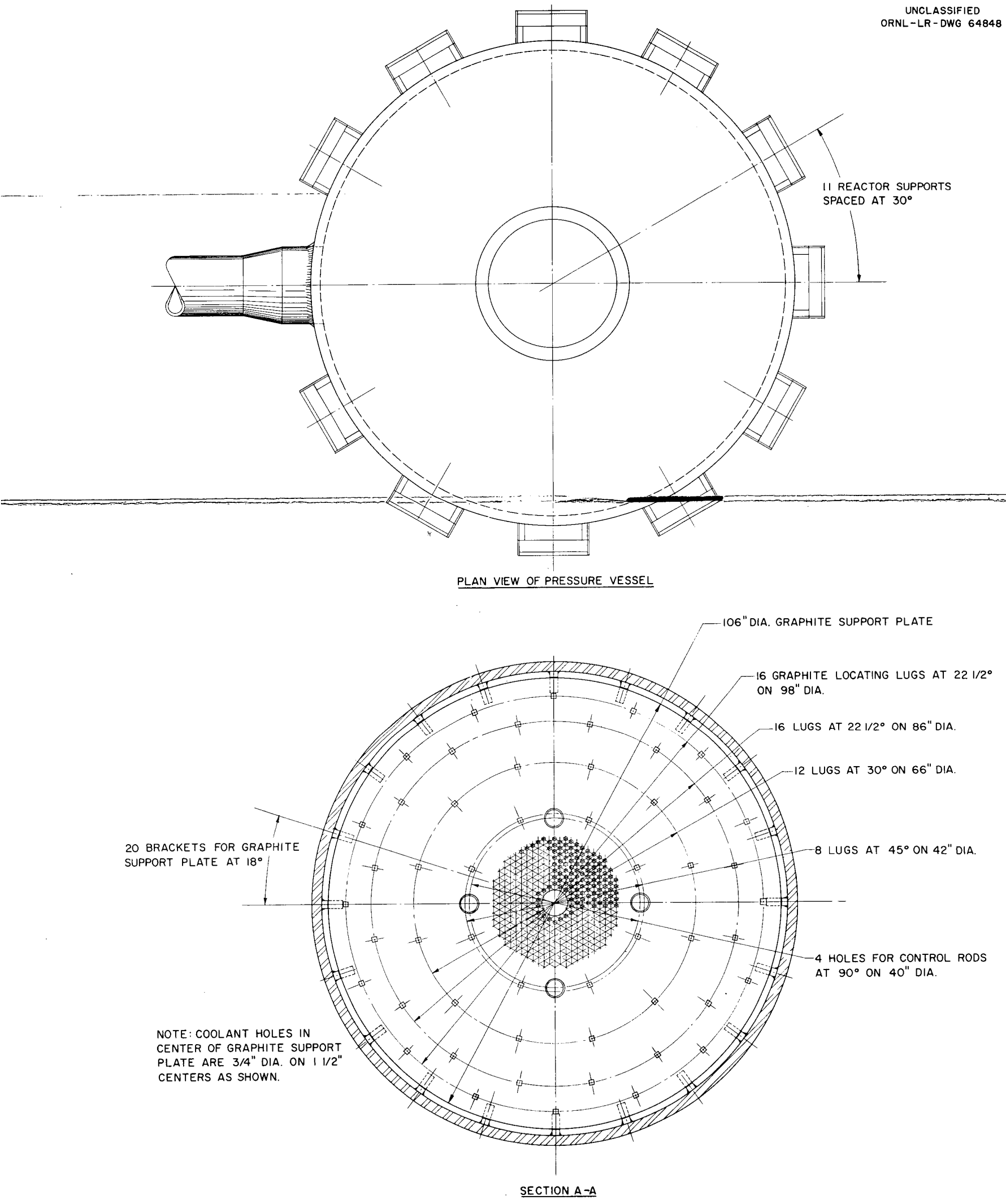

Fig. 3.8. Plan and Section View of PBRE Pressure Vessel.

both closures provides access to the core. Nozzles for insertion of replaceable thermocouples are also provided. Pressure vessel design information is summarized in Table 3.1 and the structural analysis of the vessel is discussed in Section 9.

The pressure vessel is supported in a horizontal plane through the gas inlet nozzle by a structure similar to that used on the British AGR. Lugs on the vessel rest on flat-plate columns with cylindrical ends which, in turn, bear on structural members attached to the adjacent biological shielding (Figs. 3.7 and 3.9). These columns can rotate to accommodate the radial expansion of the vessel. Lateral translation is prevented by side plates that restrain the cylindrical ends, and slippage on the bearing surfaces is prevented by a gear-tooth arrangement. Column length is chosen so that vertical movement of the primary coolant inlet line is small when the vessel is heated from room temperature to operating temperature.

A steel plate with perforations sized and spaced to satisfy the primary coolant flow requirements supports the graphite structure in the core and the steel vessel liner (Fig. 3.10). A 2-in. layer of stainless steel reflective insulation covers the inner surface of the liner dome. The outer surface of the pressure vessel is insulated down to 1 ft below the support plane to help maintain uniform temperatures in the support region. There is no insulation on the lower portion of the vessel.

Main Coolant Blower

A single main coolant blower is used, based on studies which indicate that the reactor core can be adequately cooled by thermal convection in the event of blower failure. Blower design conditions are as follows:

Helium flow rate, lb/hr	
Maximum	28 500
Minimum	4 500
Normal inlet pressure, psia	500
Normal inlet temperature, °F	550
Required pressure rise at maximum flow rate, psi	4.5

UNCLASSIFIED
ORNL-LR-DWG 65966

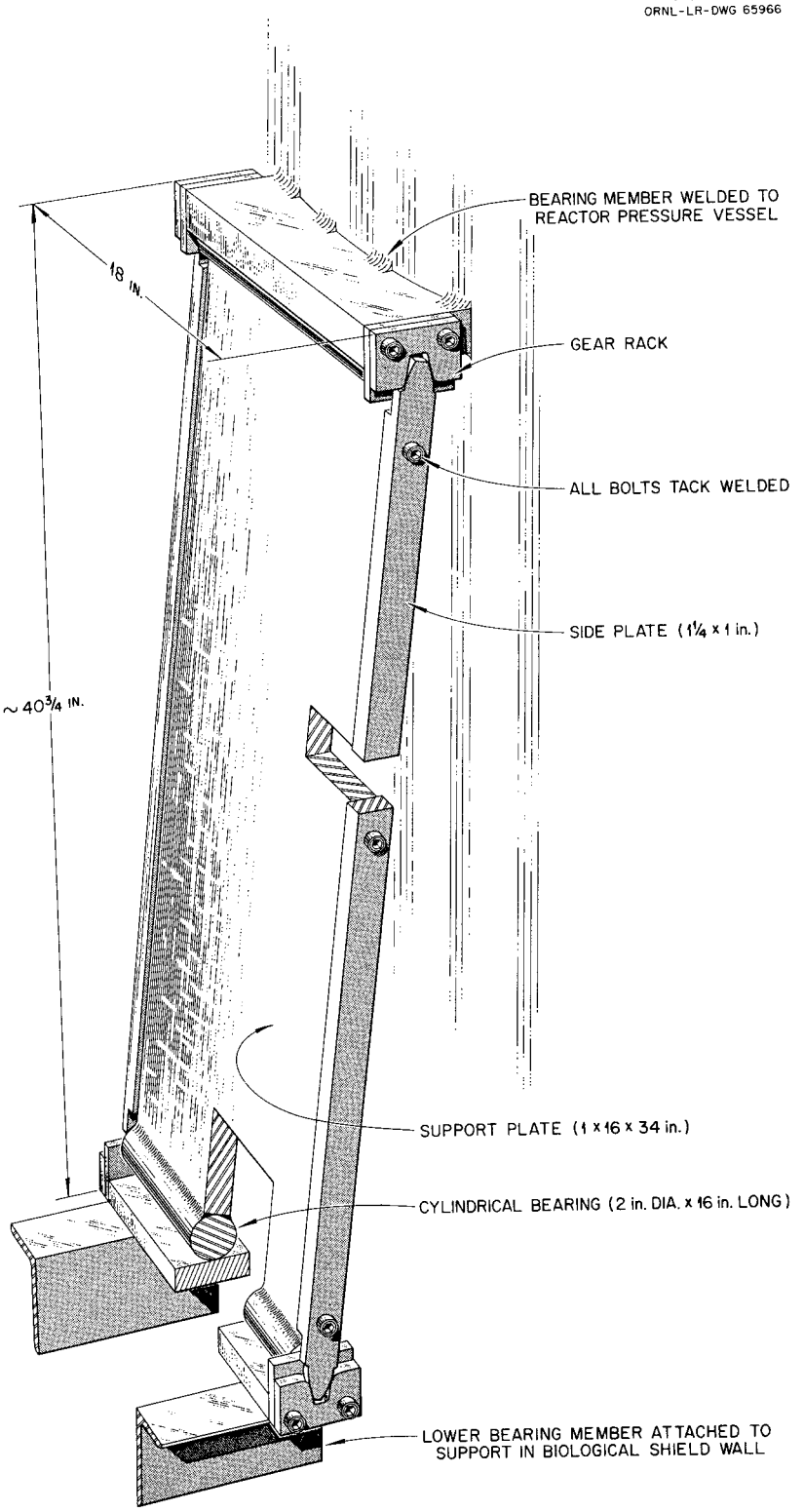

Fig. 3.9. Reactor Vessel Support.

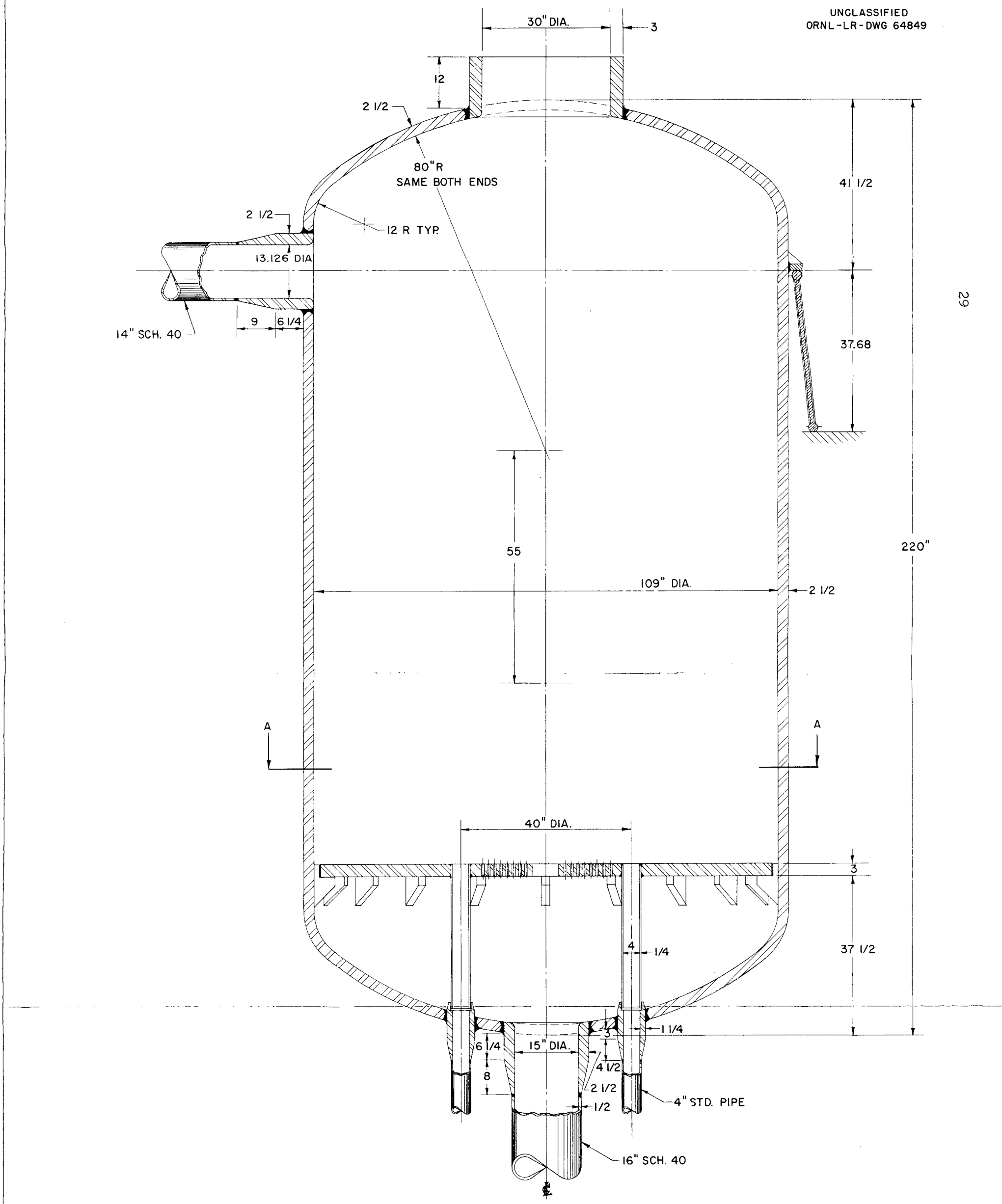

Fig. 3.10. PBRE Pressure Vessel Layout.

Flow rate is varied by changes in blower motor speed through use of a variable-frequency motor-generator set.

As illustrated in Fig. 3.11, the blower is of the hermetically sealed type, with impeller, bearings, and motor enclosed in a common pressure vessel. The blower shaft is approximately horizontal. A flange at the cool end of the 18-in.-o.d. casing permits removal of the entire internal assembly as a unit, including impeller, motor, bearings, and internal cooling system, without disturbing the main coolant piping.

Gas-lubricated bearings of the self-acting (hydrodynamic) type are used. This construction eliminates shaft seals and their auxiliary equipment, and also avoids complexities associated with high-pressure oil-lubricated bearings. In addition, a gas-bearing compressor, being capable of higher speed operation, is smaller in physical size than an oil-lubricated unit of the same capacity. The blower motor is rated at 100 hp at the maximum operating speed of 12 000 rpm.

The present state of development of gas-bearing compressors and the successful production of several such units in the capacity range of interest lends confidence to this choice of blower. If, however, developments in the near future do not continue to support this degree of confidence, the alternative will be to resort to an oil-lubricated blower.

Steam Generator and Steam System

The PBRE heat-removal system has a capacity of 6.2 Mw with helium entering and leaving the reactor at temperatures of 550 and 1250°F. The gas stream is cooled by generating steam in a heat exchanger and condensing the steam in an air-cooled condenser.

Steam Generator Design. The steam generator design is based on the following criteria:

1. Reliability — The probability of steam leakage into the helium system must be minimized.

2. Natural Circulation — The unit is to be installed in an elevated position with respect to the reactor to promote natural circulation of helium for afterheat removal in the event of blower failure.

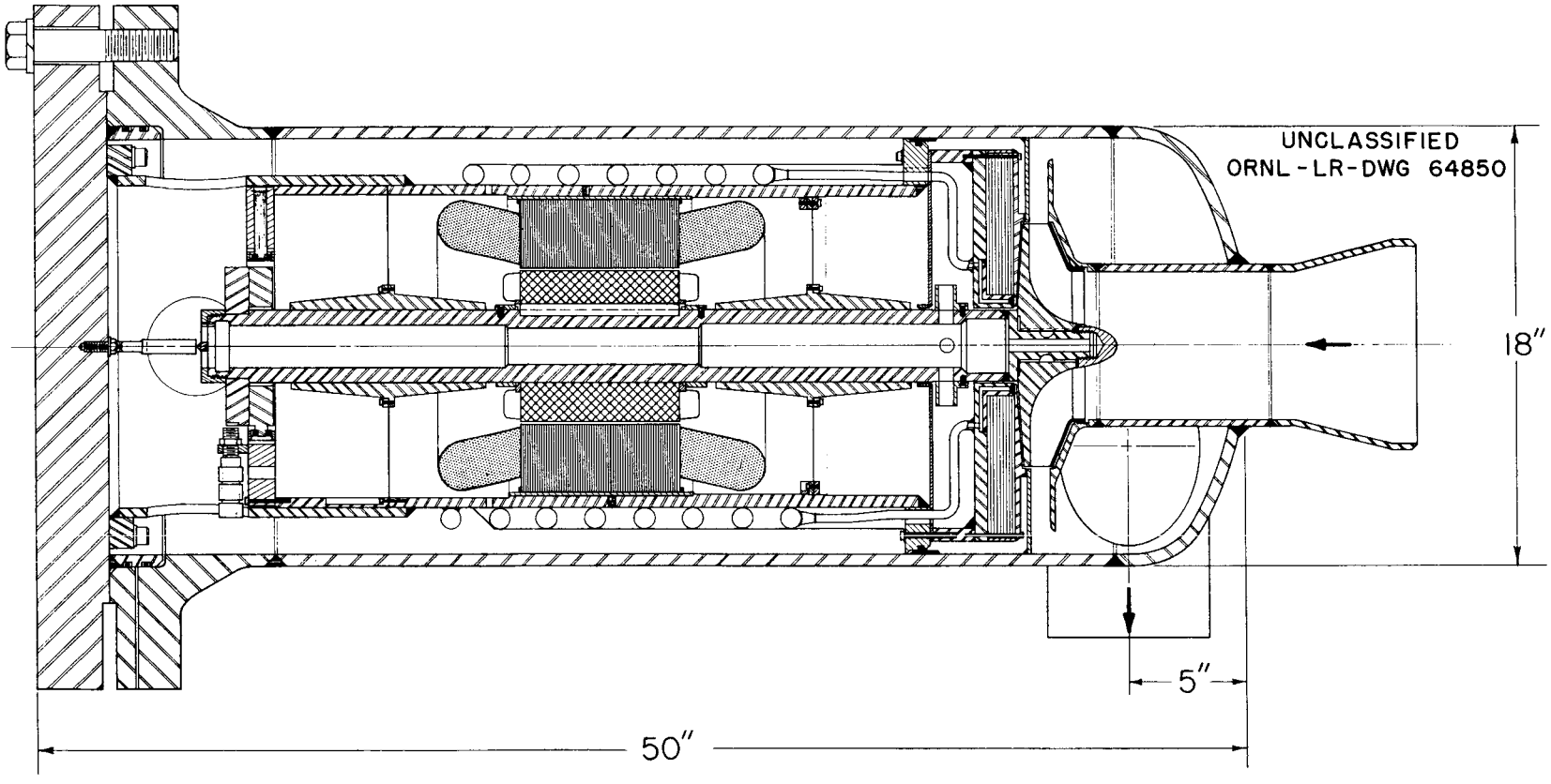

Fig. 3.11. PBRE Main Coolant Blower.

3. Emergency Cooling — An independent emergency shutdown cooler will be incorporated in the steam generator.

4. Maintenance — Tube leaks must be repairable, but not necessarily by in-place (remote) plugging of tubes.

The absence of electrical-generating facilities largely removes the incentive for generating high-temperature, high-pressure steam. However, consideration was given to the effect on steam plant control of having superheated steam vs saturated steam in the system and to the effect of a superheater section in the steam generator on fission-product deposition. It is felt that the control characteristics of a 5-Mw reactor are not sufficiently applicable to a full-scale plant to justify selection of steam conditions of interest for power generation. The effect that the higher surface temperature in a superheater has on fission-product deposition, however, relates to an important objective of the experiment. Because of the difficulty of obtaining reliable quantitative information on deposition without internal access to the steam generator, this effect will be studied by providing surfaces which can be withdrawn for examination. Removable deposition fingers will be installed within the tube matrix of the steam generator, with means provided for varying and monitoring the surface temperatures of the fingers. The decision was therefore made that production of superheated steam was not a requirement of the experiment (but a provision is made in the design for a Phase-2 heat exchanger with superheat).

The steam pressure was selected as 600 psia to ensure that steam would enter the helium system rather than activity enter the steam system if a leak occurred. Contamination of the steam system would thus be avoided.

A conceptual drawing of a type of heat exchanger which would be appropriate for the PBRE is presented in Fig. 3.12. The heat exchanger is a natural-circulation system with an integral steam drum and floating mud drum contained within the pressure shell. Feedwater added through a wash tray mixes with the saturated recirculating liquid in the top drum, flows down the central downcomer to the floating drum, and returns up through the tubes. Gas from an internally insulated central duct moves axially

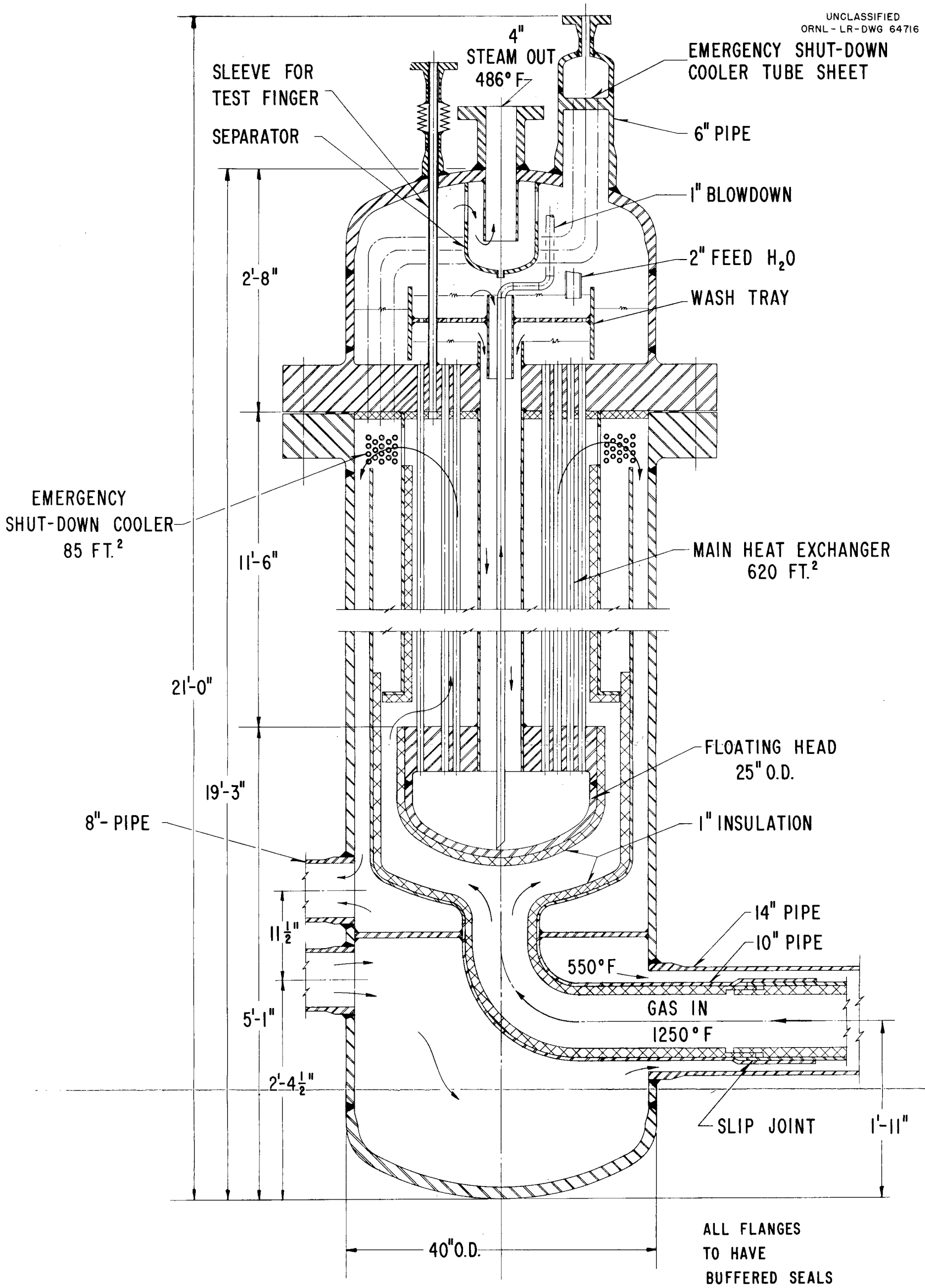

Fig. 3.12. Steam Generator.

through the tube bundle and passes down the outer annulus to a duct which leads to the blower. The return gas from the blower passes through the lower chamber of the pressure shell and out the concentric-pipe annulus. With this design, the entire pressure shell is swept only by the cool gas. Additional details of the steam generator are given in Table 3.1.

In the event of a tube leak, the steam drum and tube bundle would be removed as a unit and replaced, using the procedures described in Section 11. The damaged bundle would then be decontaminated and repaired. The removable tube bundle concept obviates the development and construction of specialized remote equipment for in situ tube plugging. In addition, the unit illustrated is conventional in design and fabrication.

Support System. A flexible support system for the steam generator is provided to accommodate the lateral movements required for thermal expansion of piping between the steam generator and the reactor vessel, the radial expansion of the pressure vessel, and the radial expansion of the steam generator. The support system, shown in Figs. 3.7 and 9.2 (see Sec. 9), consists of six beam columns sized so that only a small force is required for the necessary displacement; the design of the beam columns is discussed in detail in Section 9. This support system has an advantage over more conventional systems in that no maintenance is required. All attachments to the steam generator, including water and steam lines, will be designed so as not to impede significantly the free lateral movement of the steam generator. The support system will also permit any lateral movement required to connect or disconnect the steam generator to the primary coolant, steam, and water piping during steam generator replacement operations.

Phase-2 Steam Generator. Provisions are made with respect to space and shielding requirements for complete replacement of the initial steam generator with a unit of more advanced design capable of producing superheated steam and amenable to in-place plugging of the tubes. Substitution of a new unit would be made when the progress of experiments with the reactor indicated its desirability. Removable plugs are placed in the shielding where the helium piping connects to the steam generator to facilitate this alteration. The technique which would be used for replacement of the heat exchanger is described in Section 11.

Steam System. The steam system, illustrated in Fig. 3.13, uses many components available from the HRE-2 system. Saturated steam at 600 psia flows from the steam generator to a pressure-reducing station where it is throttled down to 40 psia before entering an air-cooled condenser. The condensate flows to a combined deaerator and surge tank, which is maintained at a pressure of 2 to 6 psig. Feedwater is supplied from the surge tank through a feedwater heater where its temperature is increased to 400°F. Two feed pumps are provided, one being a spare.

During startup the deaerator is heated using building steam. Later, steam is bled from the high-pressure portion of the system to heat the deaerator. Condensate from the building steam system is used for makeup water, and a feed station is provided for introducing treatment chemicals into the system.

Alternate Steam System. An alternate steam system is being considered wherein an intermediate heat exchanger is provided between the primary steam system and a low-pressure secondary steam loop connected to an air-cooled condenser. In such a system the primary steam loop would be located entirely within the containment shell to obtain an additional measure of protection against escape of fission products to the outer atmosphere. The existence of this intermediate system would permit operation with a steam pressure less than that of the primary helium, if that were desired. In addition, it would eliminate the need for a feedwater heater and high-pressure feed pumps. The advantages, disadvantages, and relative costs of the two steam systems will be studied in greater detail before a decision is reached as to which will be used.

Emergency Shutdown Cooling System. Removal of afterheat from the reactor in the event of a steam generator failure or failure of a vital component in the heat-removal system must be ensured. This requirement often is satisfied by duplicating vital components, such as the steam generator, pumps, and auxiliary equipment. In the present design there was a strong incentive to avoid two separate steam generators with the additional piping, shielding, and containment space which would be required. An emergency shutdown cooler, shown in Fig. 3.12, was therefore incorporated within the main steam generator shell.

UNCLASSIFIED
ORNL-LR-DWG 64866

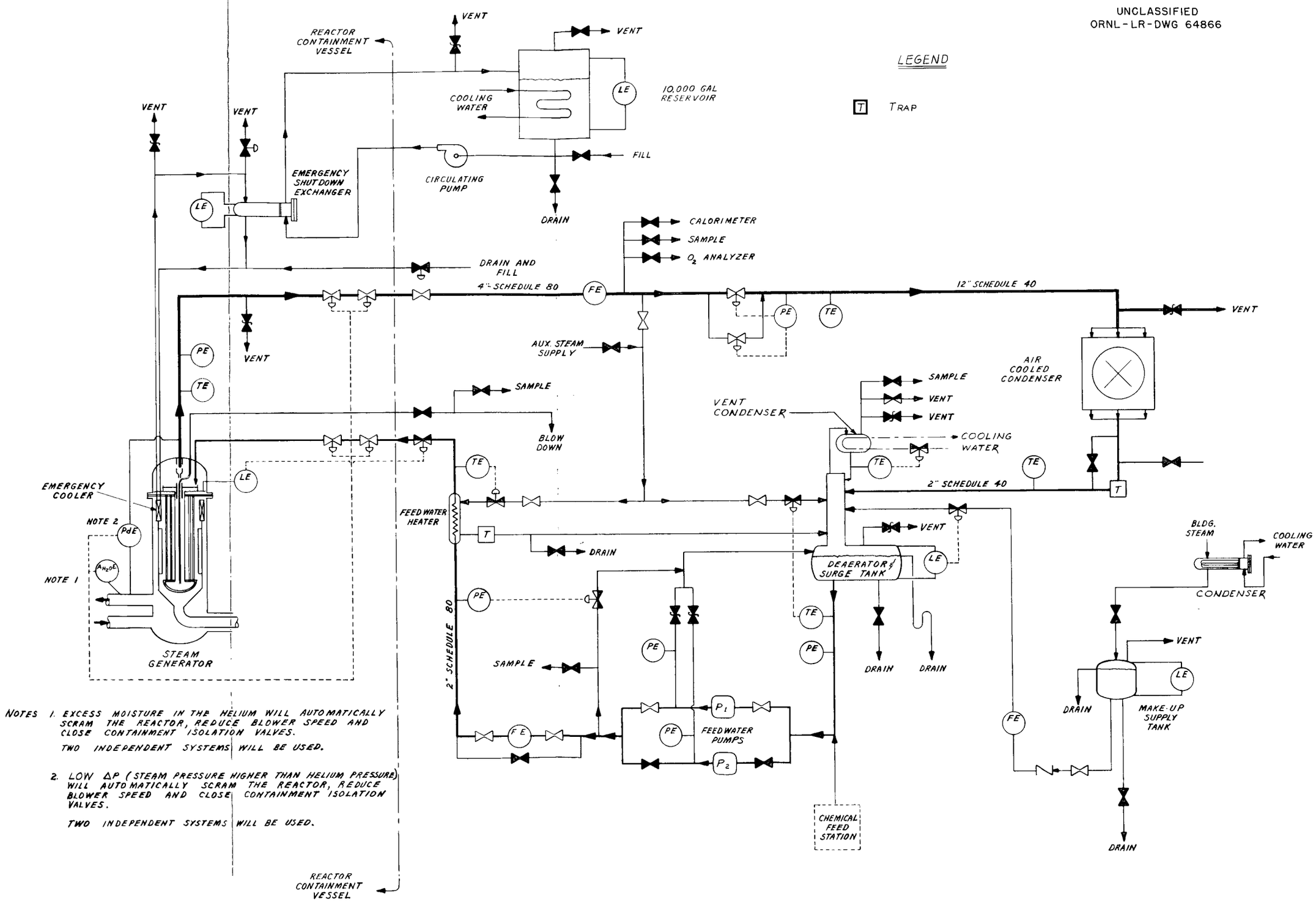

NOTES 1. EXCESS MOISTURE IN THE HELIUM WILL AUTOMATICALLY SCRAM THE REACTOR, REDUCE BLOWER SPEED AND CLOSE CONTAINMENT ISOLATION VALVES.
TWO INDEPENDENT SYSTEMS WILL BE USED.

2. LOW ΔP (STEAM PRESSURE HIGHER THAN HELIUM PRESSURE) WILL AUTOMATICALLY SCRAM THE REACTOR, REDUCE BLOWER SPEED AND CLOSE CONTAINMENT ISOLATION VALVES.
TWO INDEPENDENT SYSTEMS WILL BE USED.

Fig. 3.13. Schematic Flow Diagram of Steam System.

Steam generated in the emergency cooler is condensed in an intermediate heat exchanger located within the containment vessel. A water system containing a 10 000-gal tank cools the intermediate exchanger. During normal reactor operation and during emergencies not involving the steam system, heat is removed from the helium principally by the main heat exchanger, and little energy is transferred to the emergency cooler. When the main steam system is not operating, however, higher temperature helium reaches the emergency cooler; the cooler is then capable of removing 200 kw from the helium stream. The intermediate heat exchanger will be supplied automatically by gravity feed from the storage tank which, with vaporization and venting of fluid, has sufficient capacity to remove afterheat for several months.

A leak in the heat exchanger requires the closure of isolation valves in the steam lines. To permit identification of the section which is faulty, the emergency system will be operated at 400 psia. Hence, detection of moisture in the helium will indicate a leak in the primary heat exchanger, whereas activity in the emergency cooler system will indicate a leak in that unit.

System Shielding and Maintenance

The reactor vessel, heat exchanger, and main coolant blower have been placed in separately shielded compartments, as illustrated in Fig. 3.14, to reduce the radiation encountered during maintenance. Each shielded compartment is provided with shield plugs or modular shielding units that can be removed to provide access for the indirect maintenance procedures described in Section 11. Provision that the ventilation system draw air into a contaminated compartment during maintenance will protect personnel from particulate contamination. Use of separate compartments may make possible direct access to a compartment for installation of a replacement unit after removal of the original contaminated component.

Fuel-Handling System

The fuel-handling system is shown schematically in Fig. 3.15 and is described in detail in Section 5. The equipment layout uses gravity flow

UNCLASSIFIED
ORNL-LR-DWG 65230

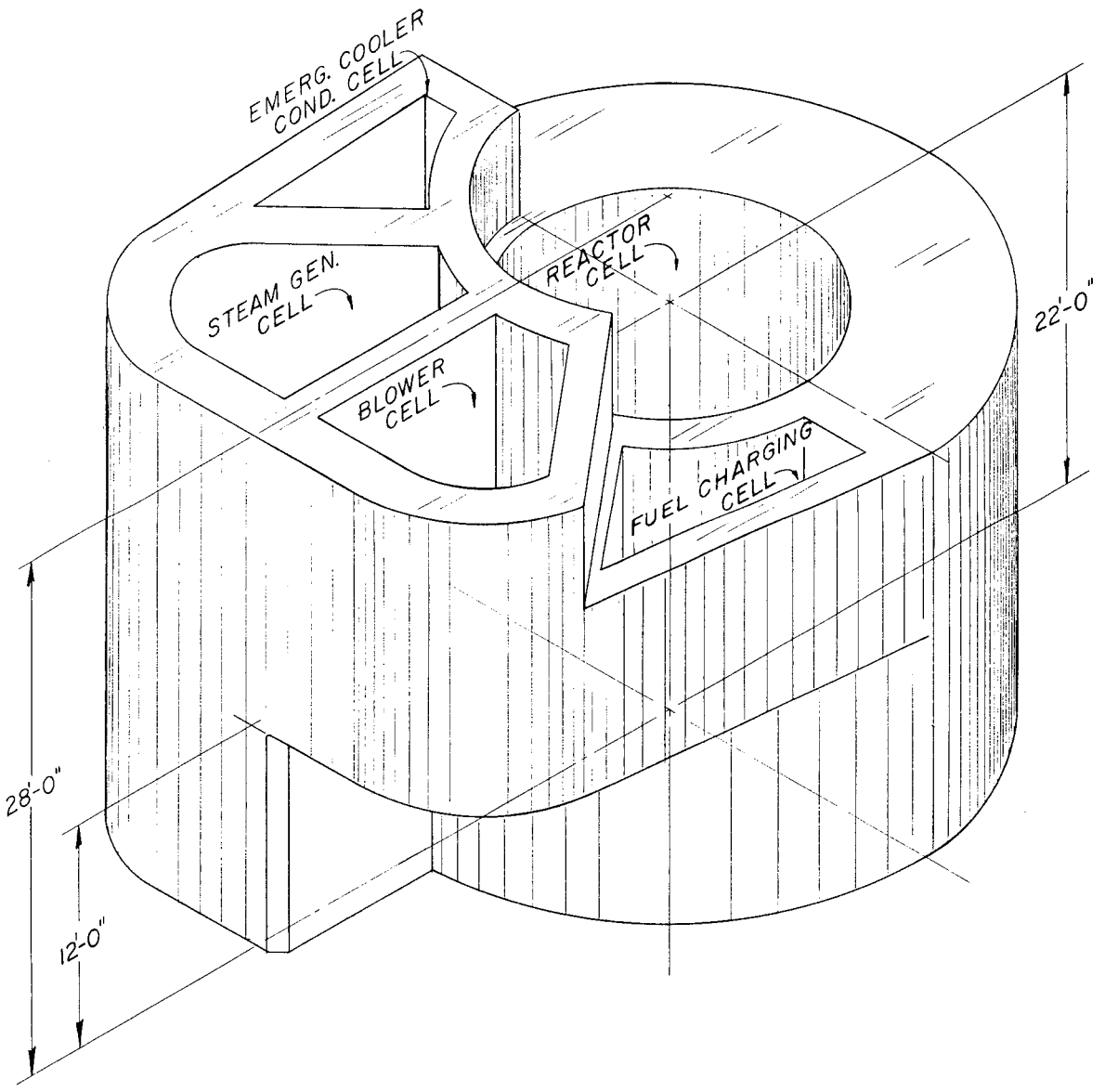

Fig. 3.14. Primary Reactor Shielding Cells.

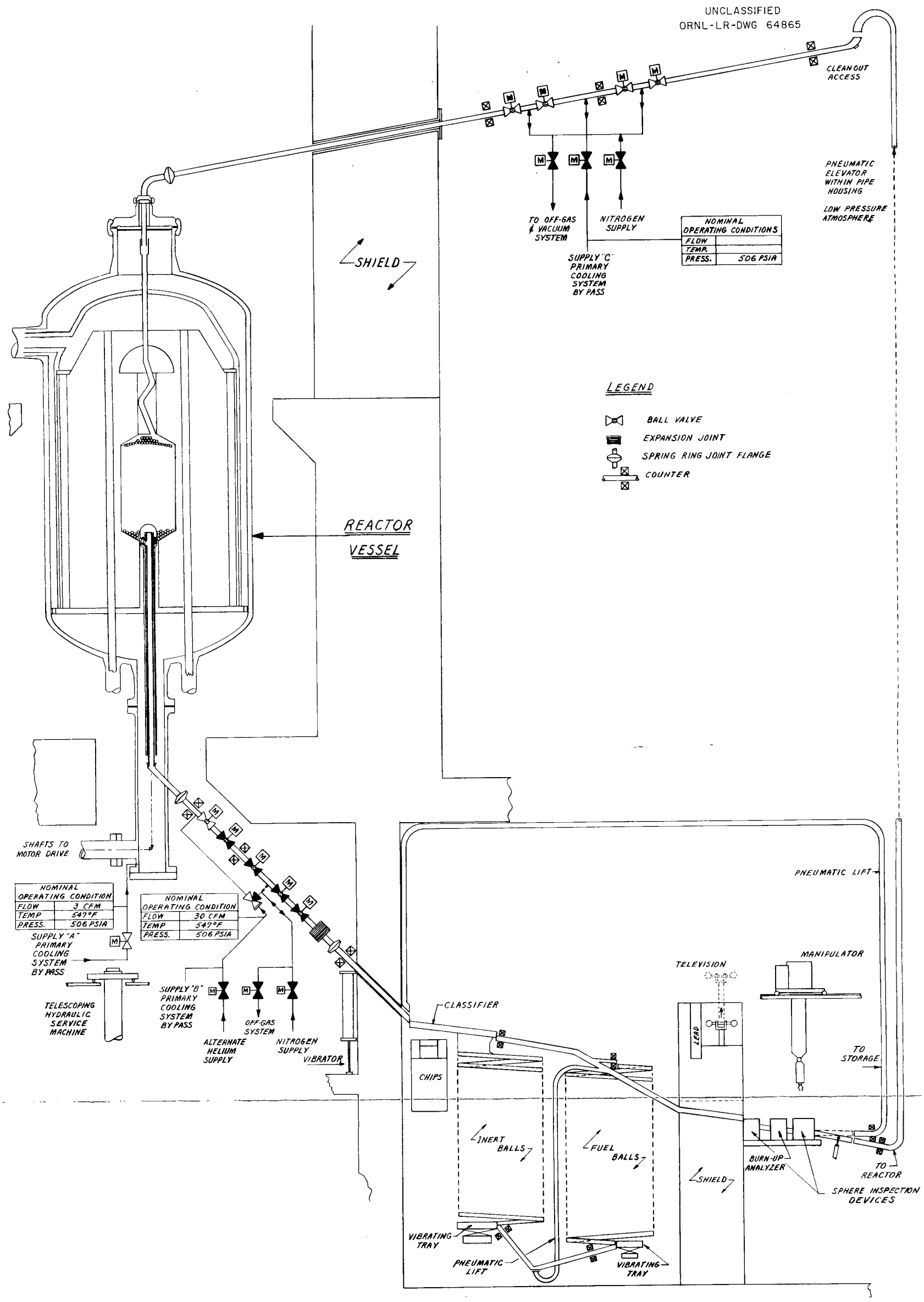

Fig. 3.15. Schematic Flow Diagram of Fuel-Handling System.

to feed fuel into the core and to discharge fuel from the core to the fuel-inspection area. The fuel-discharge port is in a rotating dome at the bottom of the core. A pneumatic elevator lifts fresh or recycle fuel to the top of the reactor. Fuel can be added and removed when the reactor is at power; valves are arranged to form gas locks for passage of fuel into and out of the primary system. All normal fuel-handling operations can be controlled from outside the containment vessel.

The fuel-addition gas lock is located in the biological shielding at the top of the reactor and can be replaced from above using the techniques discussed in Section 11. The unloading system is in a shielded compartment beneath the reactor pressure vessel. For maintenance, the fuel-discharge assembly will be uncoupled from the reactor by the service machine and removed as a unit.

Unloaded fuel is transferred to the fuel-inspection room where, after determination of its burnup and integrity, it is either stored, returned to the core, or put in a shielded cask for removal. Since the fuel will probably contain uranium and thorium carbides, which are reactive with oxygen and moisture, and since the protective coatings on the fuel may be defective after irradiation, an inert atmosphere of nitrogen is specified in the fuel-handling areas. The nitrogen system is designed to cool irradiated fuel and to remove fission products which are evolved by drawing nitrogen downward through the fuel containers. The withdrawn gas passes through cleanup equipment to remove particulate contamination and offgases and, possibly, chemical contaminants, and then passes through a cooler and a blower before being returned to the compartment. This arrangement restricts contamination of the fuel-handling areas. A negative pressure is maintained in the room so that leakage will be inward.

Helium Storage, Transfer, and Purification System

The helium storage, transfer, and purification system is provided to serve the following purposes:

1. evacuate the reactor coolant system,
2. provide initial charge for pressurizing the reactor coolant system,
3. provide makeup gas for the primary coolant system during operation,

4. circulate ~2% of the maximum coolant system flow through the purification system when the reactor is operating and circulate gas from the contaminated helium storage tanks through the purification system when the reactor is shut down,
5. provide for discharging gas from the primary cooling system, either directly to the storage tanks or via the gas-purification system,
6. store the reactor coolant for future use,
7. receive and store any gas discharged from the primary loop pressure-relief valves.

Clean Helium Supply System. Clean helium for both the initial charge and makeup is supplied to the reactor coolant system from a standard helium supply trailer. Silica-gel dryers and a filter are provided to reduce the moisture content and clean the helium before it is fed into the coolant system. Instrumentation is provided for monitoring the oxygen content.

Helium Purification. The purification system, shown in Fig. 3.16, is subdivided into two parallel systems, one for the removal of fission products and the other for the removal of chemical contaminants. The fission-product removal system consists of a helium cooler and charcoal delay traps through which 1% of the total purification system flow is diverted; the charcoal beds have no special provisions for cooling and therefore operate at ambient temperature. The chemical-contaminant-removal system consists of a gas heater, a copper oxide oxidizer, a gas cooler, and a molecular-sieve adsorber bed. On leaving the adsorber bed, the helium stream recombines with the effluent from the fission-product-removal system, passes through an absolute filter, and is then pumped back into the main coolant circuit by the gas-purification-system blower. Provisions are made for supplying heated air to the oxidizer and adsorber for regeneration purposes. The performance of the purification system is discussed in Section 11.

Purification System Compressor. A single auxiliary compressor will be used to return the helium effluent from the cleanup system to the reactor system. This compressor will be of the regenerative type (also called "drag" or "peripheral"), and the impeller and motor will be mounted on a common horizontal shaft supported by gas-lubricated bearings.

UNCLASSIFIED
ORNL-LR-DWG 68055

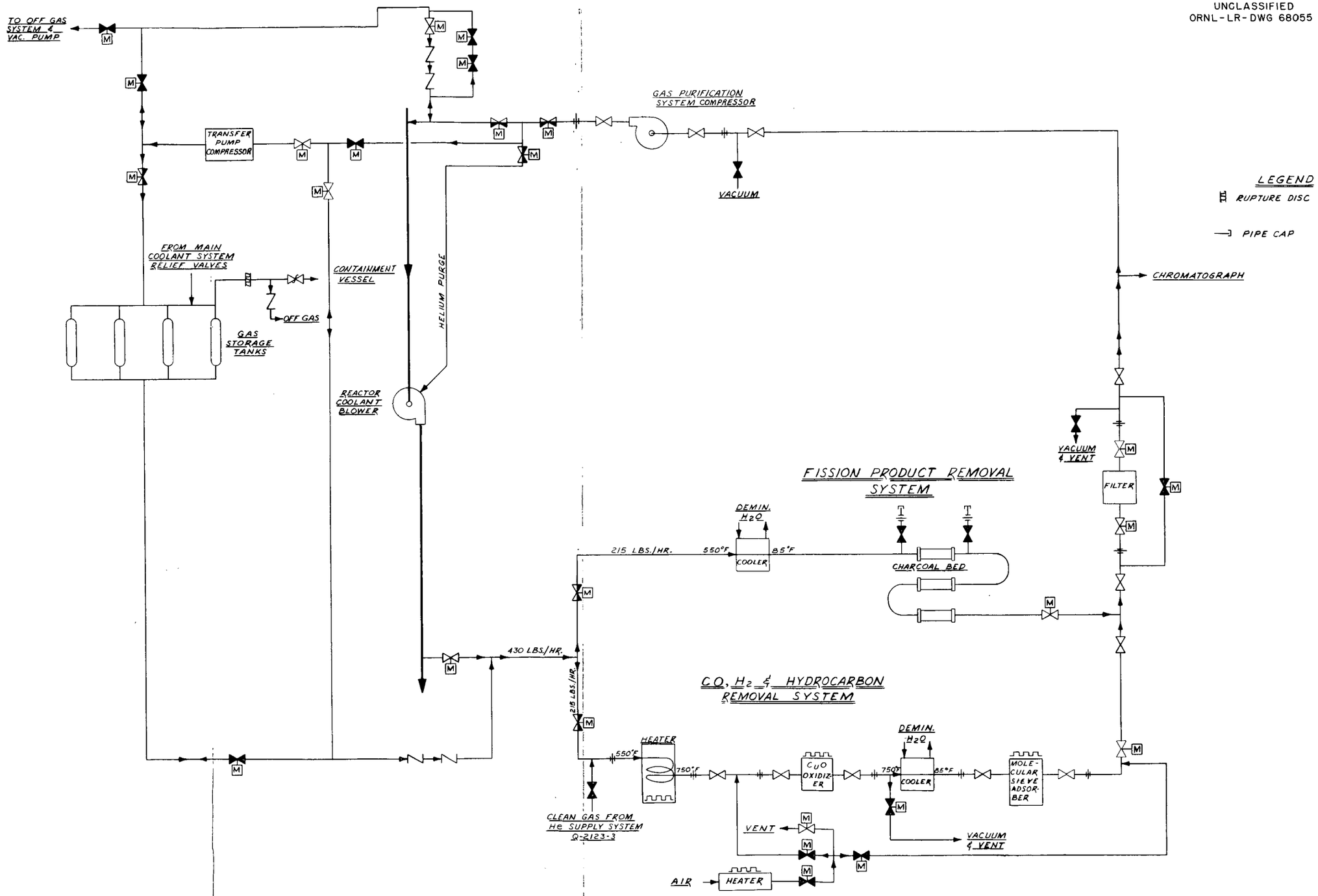

Fig. 3.16. Schematic Flow Diagram of Gas Transfer, Purification, and Storage Systems.

The operating conditions for the auxiliary compressor are:

Helium flow rate, lb/hr	
Maximum	600
Minimum	100
Normal inlet pressure, psia	500
Normal inlet temperature, °F	70

The motor rating will be about 20 hp at 12 000 rpm, and power will be furnished by a 40-kva motor-generator set at 400 cps. The use of a single auxiliary compressor for the purification system is permissible, since its failure will not endanger the safety of the reactor.

Contaminated Helium Storage. Contaminated-gas storage tanks are located in the lower level of the containment vessel. Provision is made for gaseous discharge from the fuel-handling system, helium purification system, and other auxiliary systems to enter either the storage tanks or pass through filters to the stack.

Transfer Compressor. A helium transfer compressor is provided to charge the primary system with gas from the contaminated helium storage tanks and to transfer helium to the storage tanks from the reactor when the pressure in the tanks is higher than in the primary system. This compressor, as shown in Fig. 3.16, can also be used to circulate gas from the storage tanks through the helium purification system for cleanup.

The transfer compressor is to be of the metallic diaphragm, positive-displacement type. For additional reliability, a standby unit can be installed in parallel. Since the compressor must be capable of compressing helium from the storage pressure to 500 psia, a two-stage machine may be required.

Pressure-Relief System

Pressure-relief devices are installed in the helium coolant system to provide overpressure protection. Relief valves are located in all sections of the reactor system that are capable of generating a pressure when isolated from the remainder of the system. All pressure-relief devices discharge to the contaminated gas storage tanks, as indicated in Fig. 3.16; this system avoids the escape of gases that discharge or leak

across the valve seats. The gas storage tanks themselves are pressure relieved to the containment vessel.

Leaktightness Requirements

The maximum allowable leakage of contaminated helium from the reactor has been arbitrarily set at 0.1% per day of the system inventory, since this rate appears to be attainable and creates no operating problems or unacceptable hazards. Helium can only escape to shielded spaces which are normally inaccessible to personnel. The ventilation system, described later, is arranged to prevent the passage of activity from those spaces to accessible areas.

Gases discharged from the containment vessel pass through filters and absorbers before release from the stack. Even without purification, however, release to the atmosphere of 0.1% per day of the activity circulating in the reactor is shown in Section 12 to be acceptable.

Closure Flanges. Wherever possible, welded joints are used in the reactor to reduce leakage potential. Many types of mechanical joints, however, appear to satisfy leakage specifications and are used where provision for maintenance is required. A leakage rate of less than 0.1% per day should be readily achievable with mechanical joints, even if there are as many as 1000 of them.

Connection of components in the various reactor systems requires the use of many flanged joints or closures in pipe sizes ranging from a fraction of an inch up to several feet in diameter. For each application more than one type of flanged joint can be considered, and provisions for seal welding can be incorporated, if required; seal welding is minimized, however, to reduce remote maintenance operations, downtime, and related expense. Five types of double-gasketed joints are shown in Fig. 3.17. Preferable design choices, subject to change as influenced by the results of future developmental work, appear to be:

1. single-gasketed joints with a minimum of leak-detection equipment for joints of less than 1 in.,
2. Marmon "Conoseal"-type double-gaskets, or oval-ring gaskets for joints in the range of 1 in. IPS to 12 in. IPS,

UNCLASSIFIED
ORNL-LR-DWG 68056

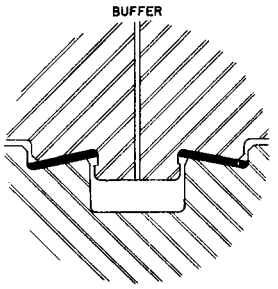

1. MARMAN "CONOSEAL"

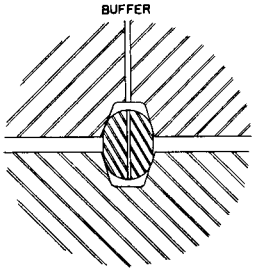

2. OVAL RING GASKET

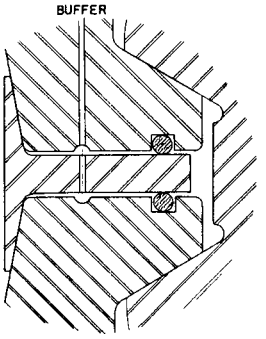

3. "GRAYLOC" AND ELASTOMER

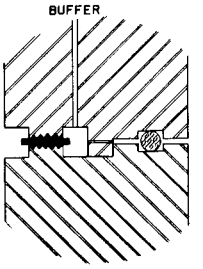

4. SOFT METAL AND ELASTOMER

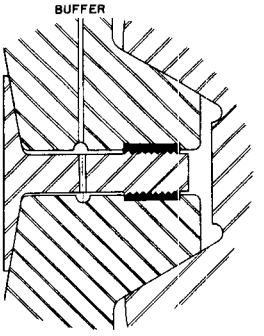

5. "GRAYLOC" AND SOFT METAL

Fig. 3.17. Types of Mechanical Closures.

3. soft-metal plus elastomer gaskets for joints larger than 12 in. and possibly larger than 6 in. at temperatures less than 400°F,
4. Grayloc plus soft-metal gaskets for joints greater than 12 in. and possibly for joints greater than 6 in. at temperatures greater than 400°F.

Buffering of intergasket regions by pressurization appears to be preferable to purging by evacuation, since the need for shielding, remote operation, and indirect maintenance of the pressurization lines and equipment should be less than would be required if activity were expected to enter the system.

Secondary Containment System

The entire reactor area is enclosed in a containment vessel, as shown in Fig. 3.1. The vessel is designed to withstand pressures and temperatures which would result from the maximum credible accident. Permissible leakage from the vessel is tentatively specified as 0.4% per day of the contents of the vessel with the ventilation valves closed and a pressure equivalent to the maximum which could exist in the containment vessel during emergency conditions. The entire system within the containment vessel will be examined for the possible generation of missiles, and potential missiles will be shielded to protect the containment shell. Hazards problems involving the containment system are discussed in detail in Section 12.

An equipment air lock is provided for transferring equipment between the containment vessel and service area, and a smaller air lock is provided for personnel access to the containment vessel. Should an accident block the personnel air lock, the equipment air lock could be used as an emergency exit. The integrity of the containment envelope is protected by providing that both doors on one access lock cannot be open at the same time, and the entire lock system is capable of meeting leakage and pressure requirements.

To ensure that no process line which penetrates the containment vessel is capable of violating its integrity, each line satisfies at least one of the following conditions: (1) the line has valves that are normally

closed; (2) the line has valves that will automatically close in the event of an accident; (3) the line has check valves that are directed so that no flow can proceed out of the containment shell; and (4) if the line cannot be isolated by any of the above three means, it is considered as an extension of the containment envelope, and it and all the equipment to which it is connected meet containment requirements. Valves and control systems involved in isolation of the containment vessel are duplicated when required.

Consideration will be given to providing an additional containment barrier by making the shield volume a pressure-tight enclosure. This would not only retain fission products but, as discussed in Section 12, could also be used to limit the access of oxygen to the core in the event of a primary system rupture. The advantages of this feature will be evaluated and compared with the cost and difficulty of making the structure capable of withstanding a pressure rise and having pressure-tight seals on all penetrations into the enclosure.

Ventilation System

The ventilation system is designed to restrict the spread of fission-product activity within the containment building and to limit the release of activity to the atmosphere. The first objective is achieved by recirculation of air through absorbers and filters and by control of air movement between compartments; the second objective is achieved by use of filters and adsorbers to remove activity (other than noble gases) from air which is discharged from the stack. An additional function served by the ventilation system is the control of temperatures within the various compartments of the system.

The reactor building is divided into two major ventilation zones: a "clean" zone (I), which includes areas such as the ground floor, stair well, and service room to which access is required for normal operation and maintenance of the reactor, and a "hot" zone (II), which includes the cells containing contaminated helium equipment, the sub-pile room, the hot cell, and other compartments from which personnel are normally excluded. Figure 3.18 shows the ventilation system schematically. The

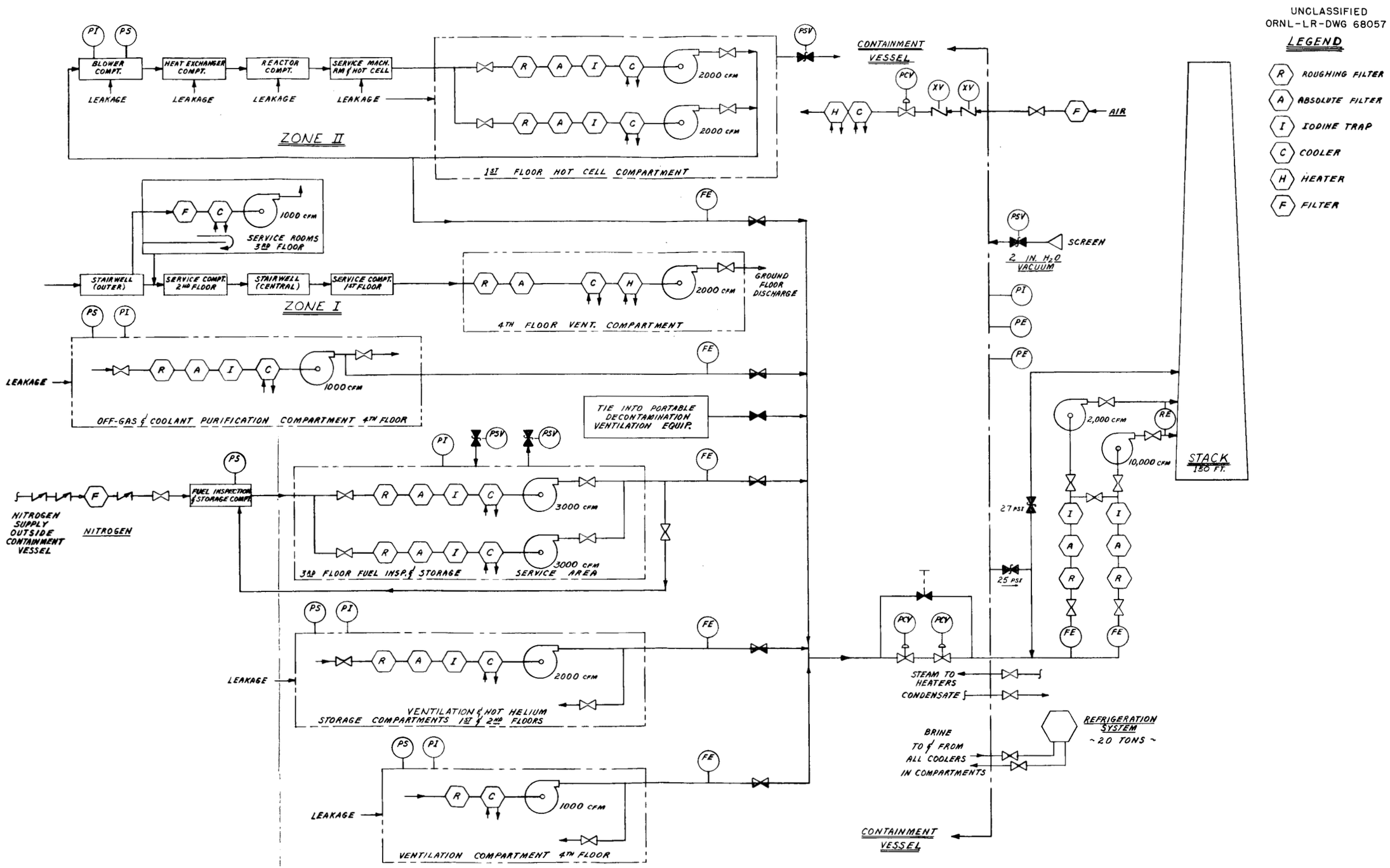

Fig. 3.18. Schematic Flow Diagram of Containment Vessel Ventilation System.

nitrogen-filled fuel-inspection and storage cell has an independent ventilation system that is discussed separately with regard to fuel handling (see Sec. 5).

Zones I and II of the ventilation system are isolated from each other. Air is recirculated separately within the two zones to maintain acceptable environmental conditions (Zone I) and to control radioactivity which may escape from the contaminated helium system (Zone II). Connected in series within some ventilation systems are a roughing filter, an absolute filter, a room-temperature iodine trap, an air-to-water cooler, and an air-circulating blower. Duplicate equipment is used for the reactor and fuel-inspection compartments because of the necessity of ensuring continued operation during maintenance.

Heat generated in the shield plus that lost from the reactor, blower, and heat exchanger is removed by a cooler lining the wall of the reactor compartment. Much of the heat transferred from the reactor vessel is radiated directly to the cooler, whereas energy from the other compartments is transferred to the cooler by circulating air. If an accident renders all other heat removal systems ineffective, afterheat will be radiated to this cooler from the reactor vessel (see Sections 4 and 12); a water system similar to that described for the emergency cooler in the primary steam generator (Fig. 3.13) will be capable of removing afterheat for several months.

Zones I and II are not positively sealed from each other, but possible leakage paths from one to the other (by way of hatch covers, etc.) are sealed as well as practicable. Leakage of the contaminated gas from the hot to the clean areas is minimized by maintaining a pressure differential between them so that gas flow is always into the hot zone. This is accomplished by establishing a small flow rate from the external atmosphere into the containment vessel (Zone I), through the imperfect seals into Zone II, and then from Zone II to the stack via an external filter and blower system; a portion of the circulating air from each ventilation system (except Zone I) is continuously bled off and discharged to the stack through a final cleanup system having components similar to those in the individual ventilation systems. Filtered makeup air is admitted

to the containment vessel through tandem check valves and shutoff valves that are closed in the event of activity release within the containment vessel. In addition to the low-flow bleed system, a higher capacity discharge system is provided for establishing a large air flow into a contaminated area during maintenance operations.

Should an excessive pressure develop within the containment vessel, it would be relieved by venting gas to the stack through the cleanup system. A pressure-relief valve would vent the containment vessel directly to the stack, however, if the cleanup system plugged and impeded relief of the pressure excess.

Offgas System

The offgas system is designed to handle gas from both high-pressure and low-pressure sources; high-pressure sources include the primary coolant system, buffer gas from the seals of mechanical joints, and gas which is discharged from the fuel-handling system when the gas locks are operated; low-pressure sources are the contaminated helium storage tanks, excess flow through valves in the pressure-relief system, the bypass flow from the gas-sampling system, and the gas from the decontamination system (which will contain condensible vapors and entrained liquid from the decontamination solutions). The offgas system is shown in Fig. 3.19.

Flow from the high-pressure offgas sources passes through a pressure-reducing station and is combined with the low-pressure offgas. A liquid trap installed in the low-pressure inlet portion of the system removes the liquids and dumps them to the intermediate-level waste system. The gas than passes through a roughing filter, an absolute filter, and an iodine trap, after which it is vented to the stack.

A vacuum pump is used to evacuate the gas systems before charging, to evacuate isolated gas system components before removal from the system, to purge the gas locks in the fuel-handling system, and to remove gas and vapor from the decontamination system. The vacuum pump has an oil trap and oil separator to ensure that none of the pump oil enters the system. A flow of air from the containment vessel is provided to purge the low-pressure inlet piping of any condensate where there is no appreciable flow from any of the low-pressure sources.

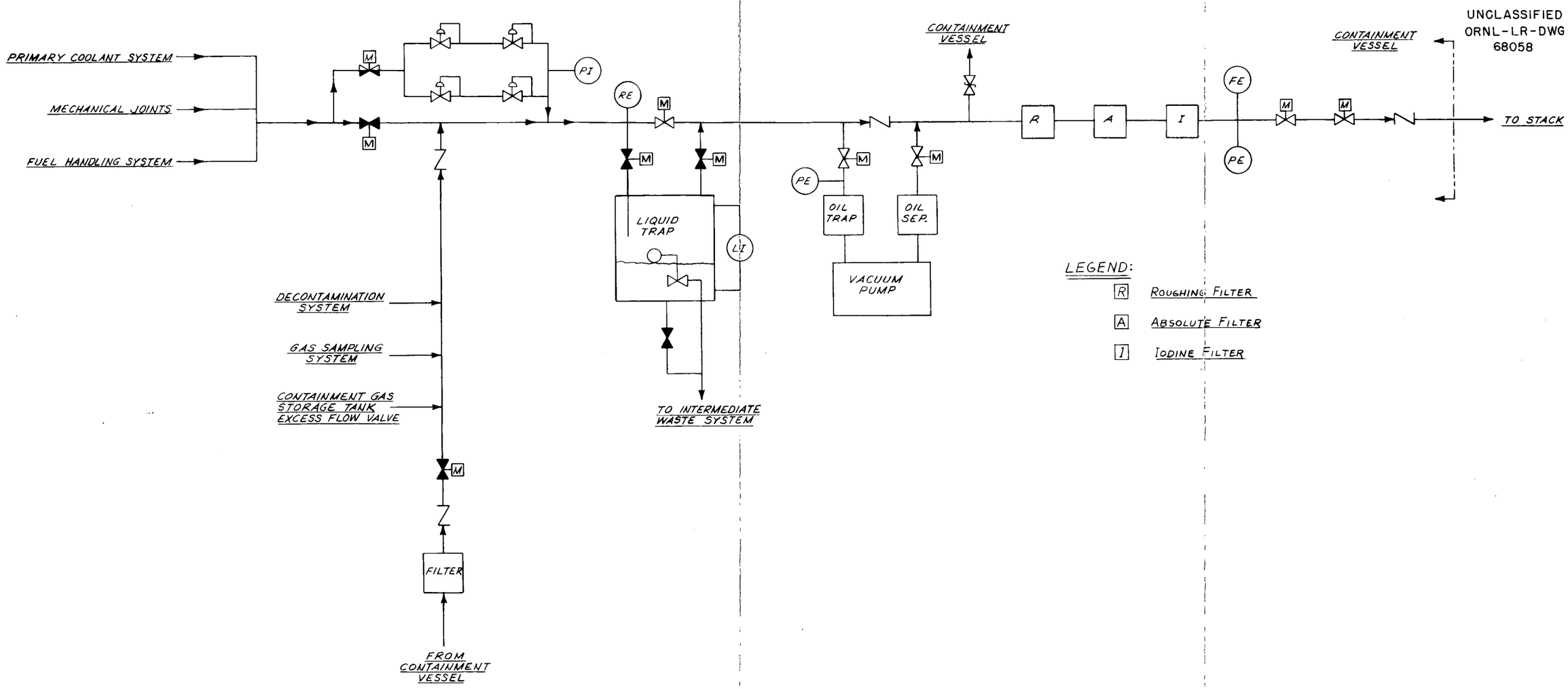

Fig. 3.19. Schematic Flow Diagram of Offgas System.

Decontamination Facility

A facility is provided in the containment vessel for the decontamination of equipment removed from the reactor. Principle items in the facility include shielded decontamination tanks, a transfer pump, contaminated solution storage tanks, and piping and valves for transferring the solutions. A scintillation gamma spectrometer, used also for other purposes, will be available for scanning equipment, and a gross gamma monitor will be installed on the solution drain line. Contaminated solution storage tanks are shielded by burying them in the earth outside the containment vessel.

Procedures to be followed in use of the facility are outlined in Section 11.

Reactor Building Layout

Two possible arrangements of the reactor building have been considered. The first, which is based on removal of control rods from below the core, provides a canyon for the long service machine which performs this operation. In the second layout, removal of rods is from above and the need for the canyon is avoided. Layout No. 2 has other features which may prove attractive in either basic arrangement. Selection of a layout will be made after the design of the reactor system is developed in greater detail.

Layout No. 1

As shown in Figs. 3.1 and 3.2, the reactor system is enclosed in a sealed metal containment vessel that is 66 ft in diameter and 144 ft high. Access to the building is provided by two air locks located at ground level. A 15-ton bridge crane runs on a circular track in the upper part of the structure.

The building, illustrated in Figs. 3.20 through 3.24, contains three floors below ground level. The first floor (lowest level) provides space for contaminated helium storage, ventilation equipment, the nitrogen system, a hot cell, and a lower service room. The second floor is largely a service area; the fuel discharge and control-rod-drive motors are located

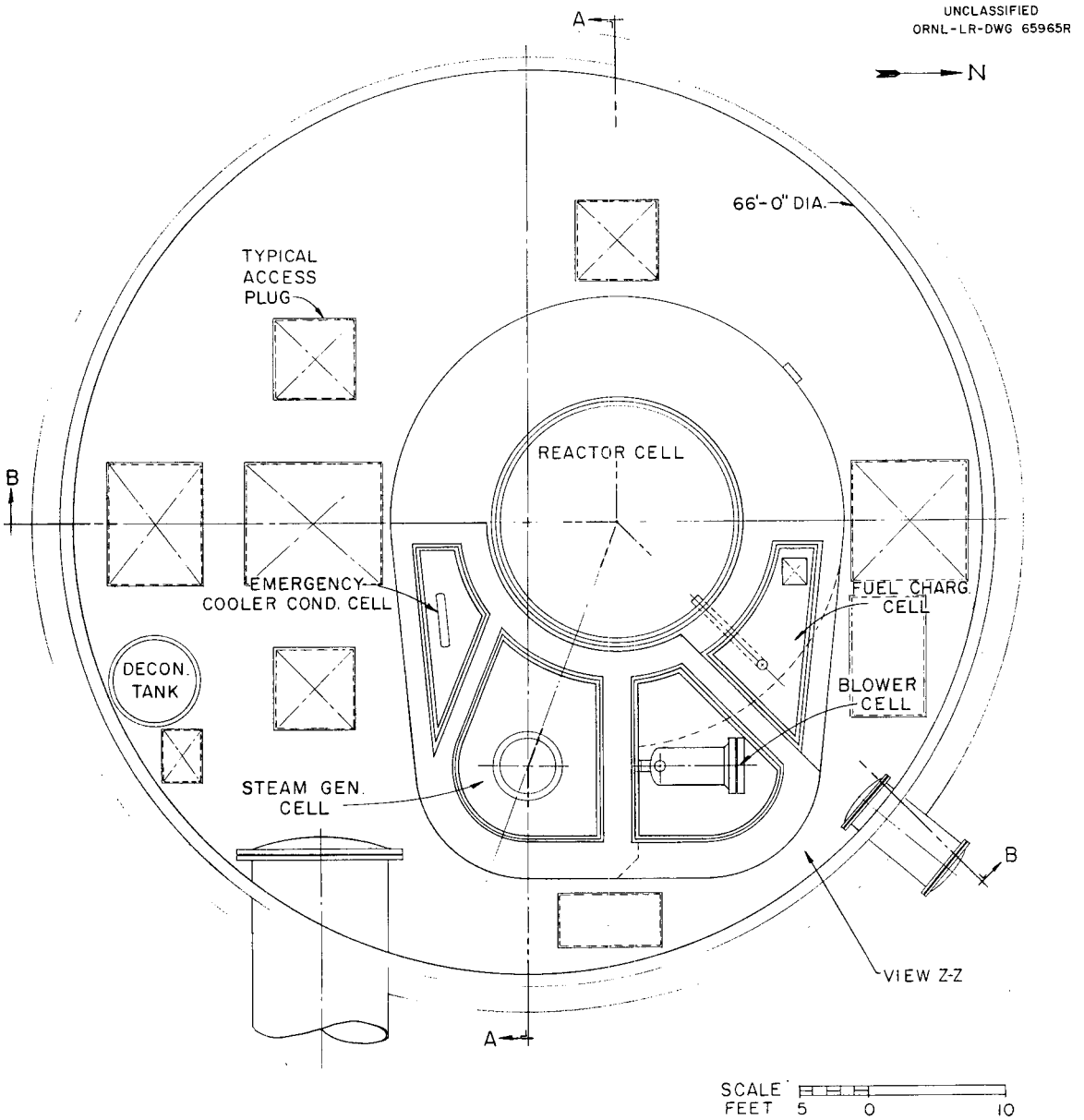

Fig. 3.20. Plan Section of Reactor Building.

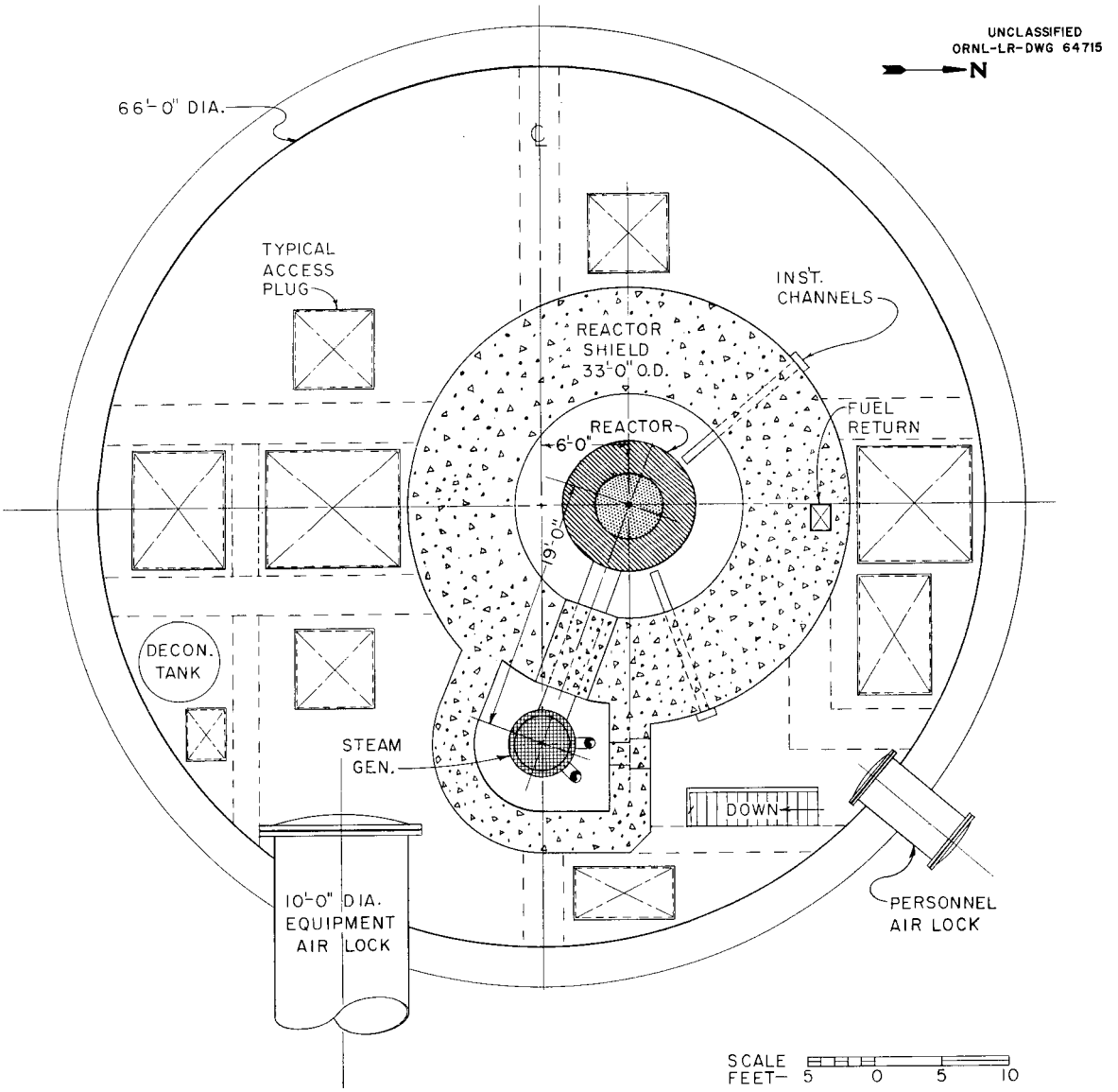

Fig. 3.21. Ground Floor Plan of Reactor Building.

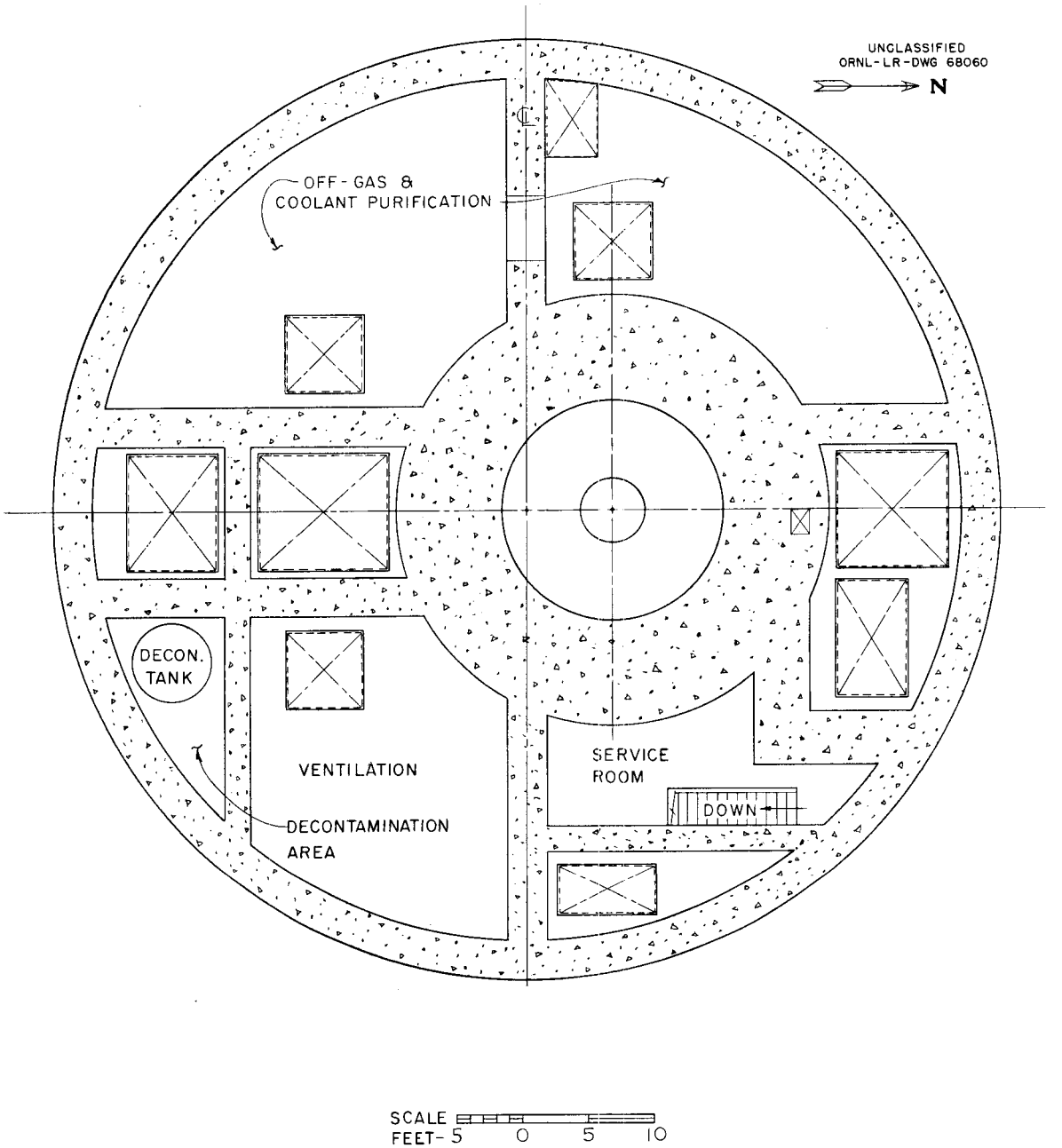

Fig. 3.22. Third Floor Plan of Reactor Building.

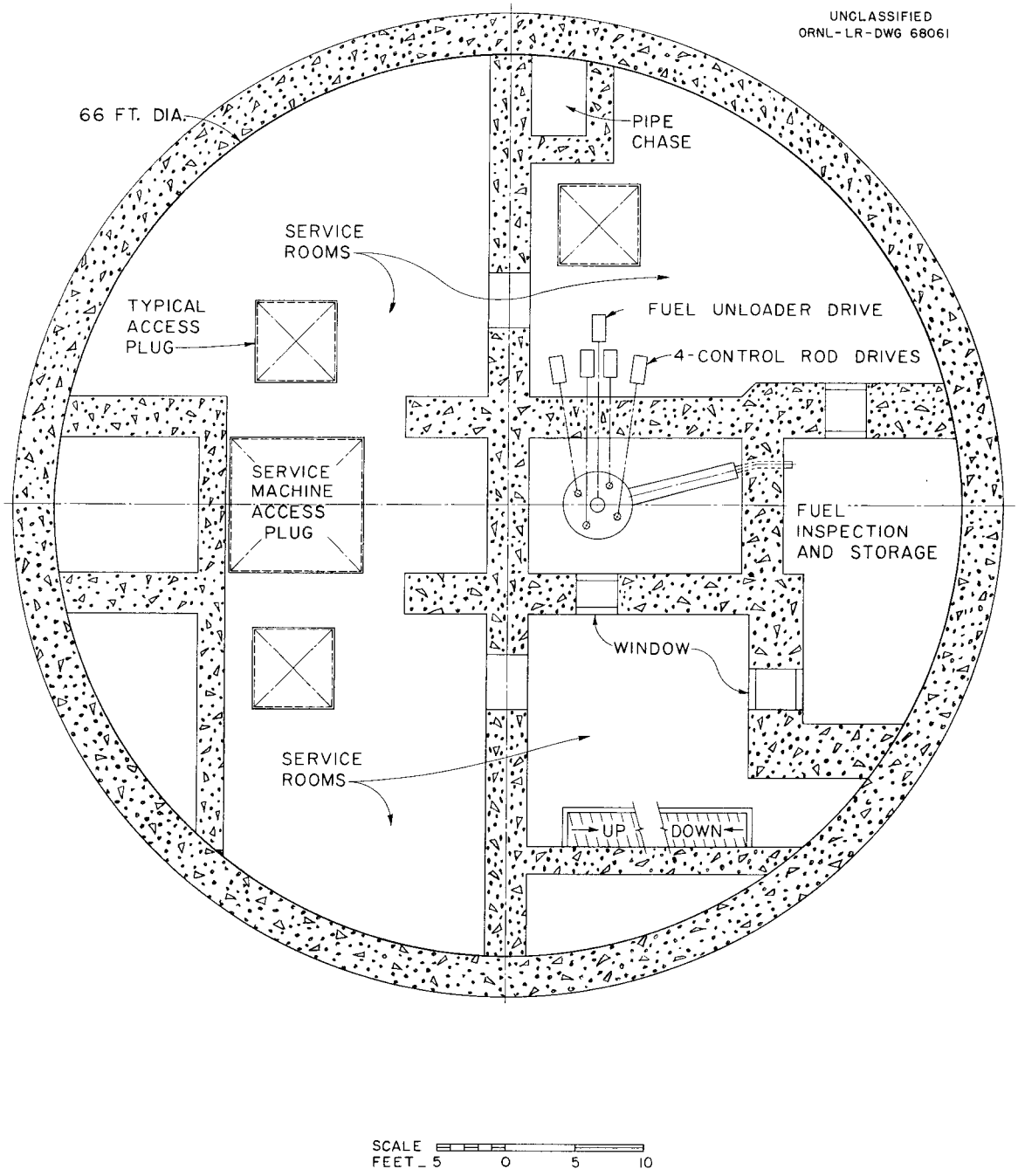

Fig. 3.23. Second Floor Plan of Reactor Building.

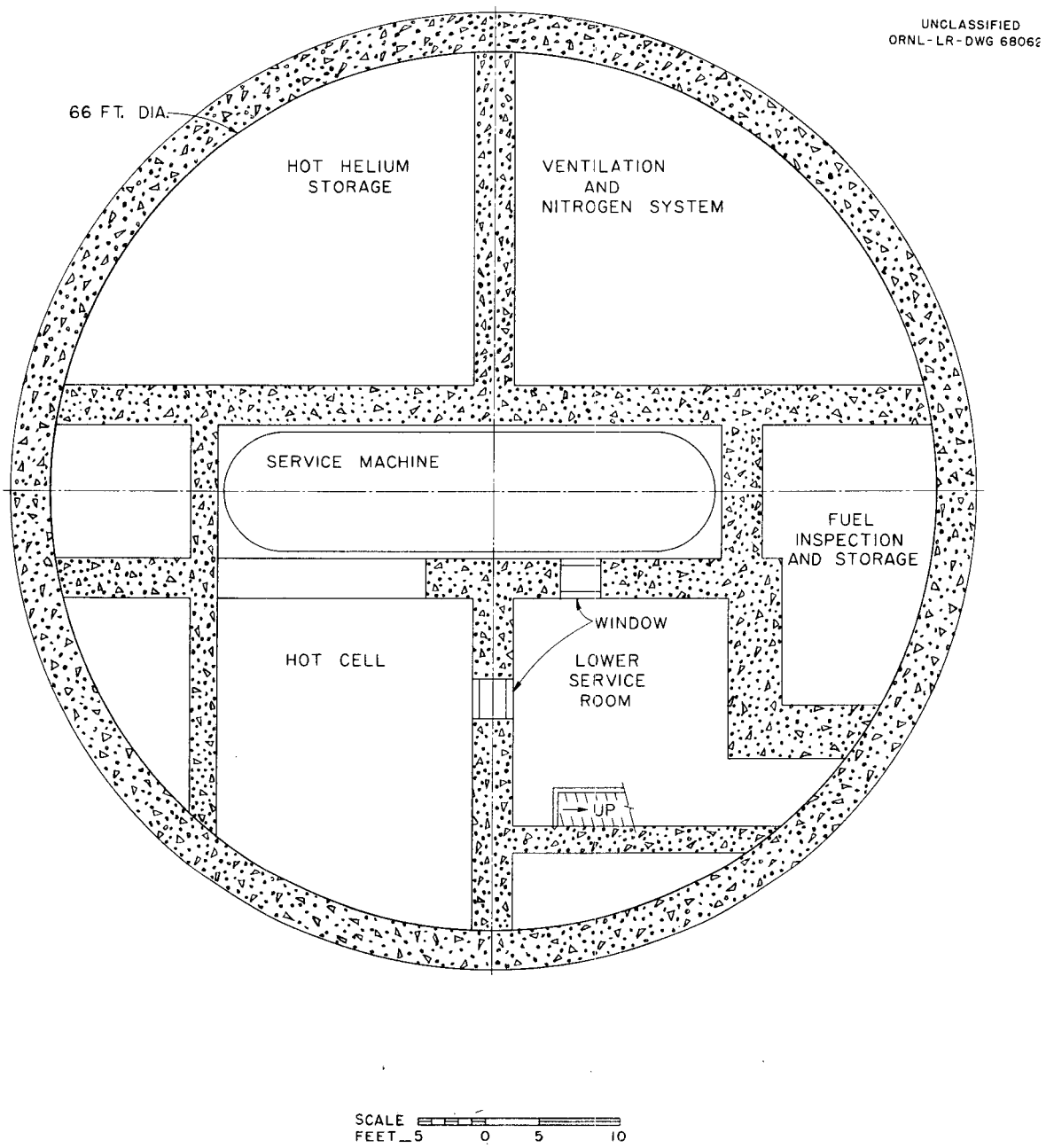

Fig. 3.24. First Floor Plan of Reactor Building.

on this level. Offgas, coolant purification, and additional ventilation equipment is located on the third floor. The reactor primary system extends through several levels, as does the fuel-inspection and storage space and the decontamination equipment.

A major consideration in the building arrangement was the provision of access from above, wherever possible, to components subject to contamination. This feature has generally been achieved, with the major exception of the subpile area. The ground and second floors are largely reserved as service areas; maintenance operations, using the techniques discussed in Section 11, can be performed on equipment located on the first and third floors by working downward through openings in the shield. Removable access plugs are located over most areas in which indirect maintenance will be required. Windows are provided on the first and second floor for viewing operations performed remotely in the subpile, fuel-handling, and hot-cell areas. No operating personnel are stationed in the containment vessel during reactor operation; however, access for minor maintenance is permitted.

Layout No. 2

The layout illustrated in Fig. 3.25 mainly differs from the one described above in the following features:

1. An enlarged reactor vessel top closure is used to permit removal and insertion of control rods from above.

2. The reactor vessel is positioned below ground level, and both vessel and steam generator are located adjacent to the containment vessel wall, thereby utilizing earth shielding on one side to reduce concrete shield requirements.

3. Portable concrete shield blocks are utilized in the annuli between the permanent shield and the reactor and steam generator vessels; the blocks are put in place after installation of equipment.

Placing shielding more closely about the primary system components and reducing the height requirements below the reactor permits the containment vessel dimensions to be reduced to 64 and 125 ft. There is,

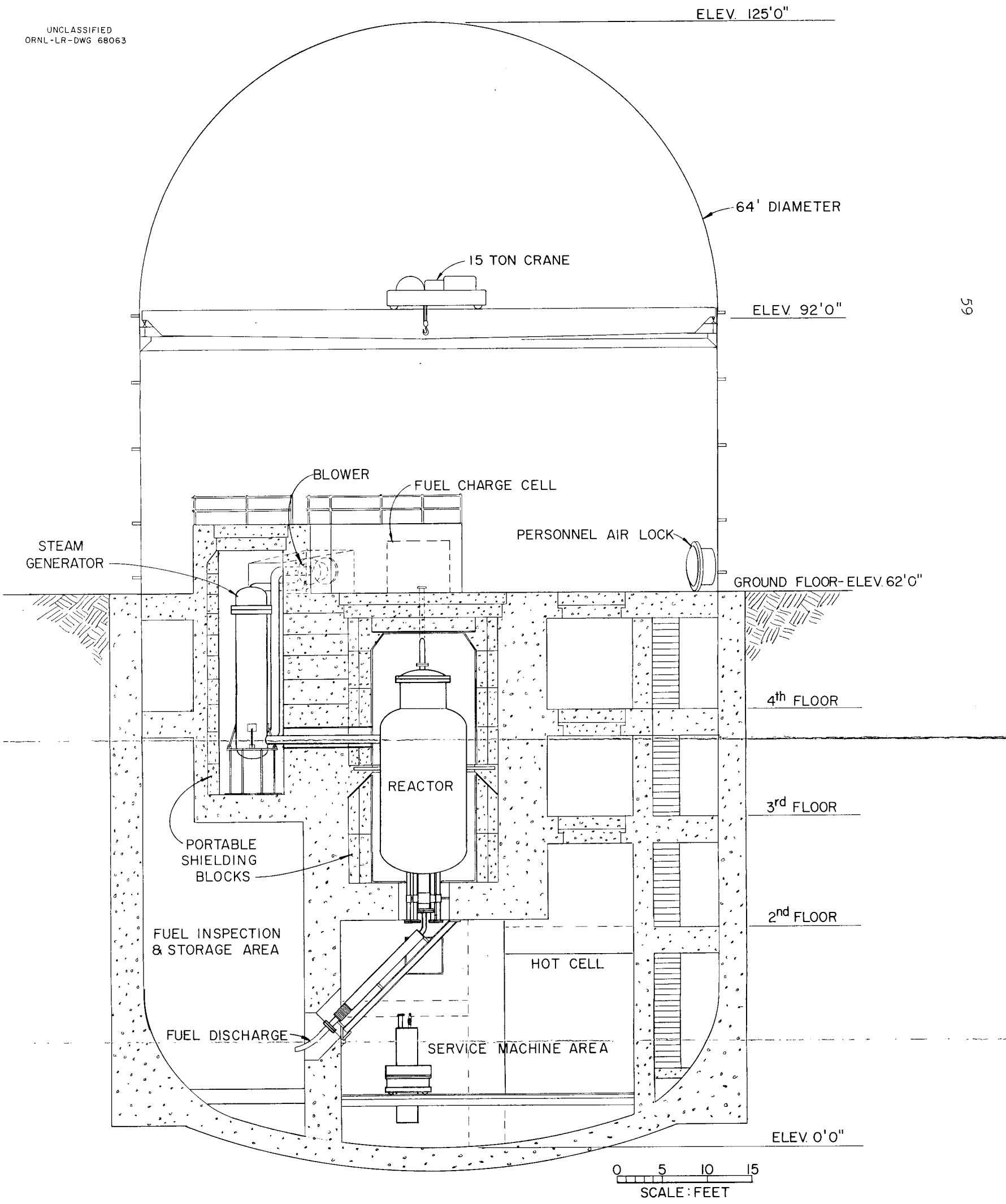

Fig. 3.25. PBRE Reactor Layout No. 2.

however, a gain in space available for auxiliary equipment, since the shield volume is decreased and an additional floor is provided.

Plant Layout

Site

The design of the reactor and the associated plant is based on use of the HRE-2 site and existing facilities at the Oak Ridge National Laboratory. Selection of the site is discussed in Section 14. The plant layout using the HRE-2 site is shown in Fig. 3.26.

Facilities

The HRE-2 building has the advantage that it was designed for a reactor similar in size to the PBRE and most utilities such as water, electricity, waste disposal, steam, plant air, instrument air, and a heat dump system can be utilized as they exist or with minor modifications.

Dismantling and Service Area. The dismantling and service area is located in the high bay of the existing HRE-2 building. A 7 1/2-ton crane and adequate space are available in this area for extensive maintenance work. The high-bay enclosure and crane rails are extended to meet the containment vessel and to enclose the equipment air lock. A smaller space equipped with a 5-ton crane provides an additional work area and truck access.

Equipment requiring major repair or replacement is removed when the reactor is shut down, cleaned in the decontamination facility, and transferred to the maintenance and service area.

Control Room. The existing control room in the HRE-2 building is enlarged by eliminating the hallway and offices in the northwest corner of the building. The PBRE control room contains the reactor control panel and is the monitoring and control center for the entire plant.

Office Area. Office space is available in the existing office building east of the HRE-2 building.

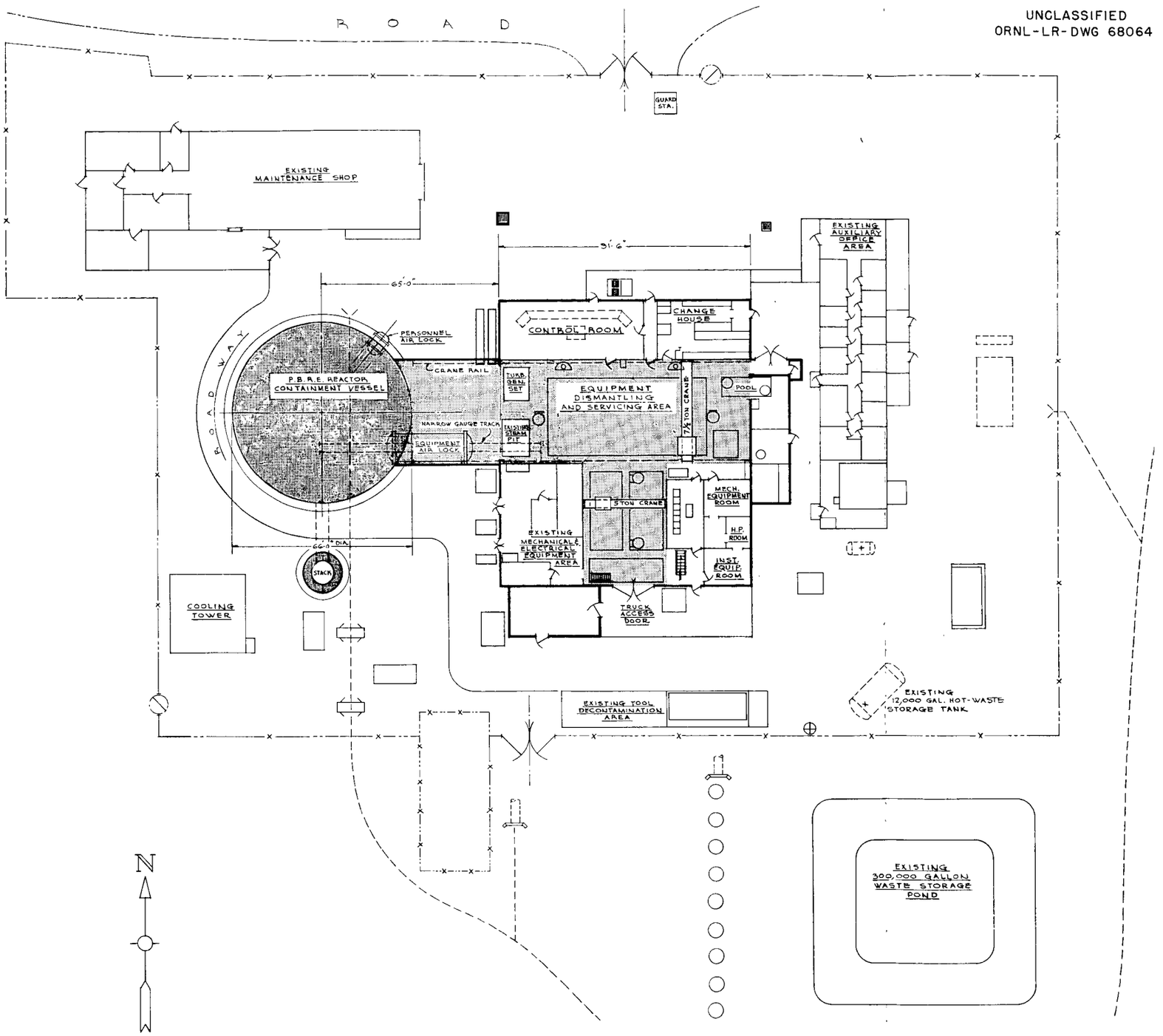

Fig. 3.26. PBRE Plot Plan — 7500 Area.

Maintenance Shop. A maintenance shop available in the existing building northwest of the HRE-2 building is equipped with machine tools to handle on-site repairs and modifications to reactor components. Storage space is available in this building for spare parts.

Change Facilities. Existing change facilities in the HRE-2 building are adequate for operation and maintenance personnel.

Waste-Disposal Facilities. An existing waste storage pond can be used for low-level waste storage; however, addition of a pumping station for transferring liquid to the existing ORNL low-level waste line will be required. Intermediate-level waste can be stored in an existing 12 000-gal waste tank, but a pumping station must also be added for transfer of liquids to a planned intermediate-level waste line.

Stack. A new 150-ft-high stack is located south of the containment vessel.

4. CORE SELECTION AND THERMAL ANALYSIS

The decision to employ an unrestrained core with upflow of coolant imposes on the design the fundamental restriction that the gas flow rate not be high enough to cause levitation of the fuel spheres. Other restrictions on the core design relate to limiting fuel temperatures and avoiding excessive thermal stresses in the fuel. These limitations conflict with the desirability of having a high power density to yield information rapidly on fuel performance. Reconciliation of these features in the selection of the core parameters is discussed in this section. Analyses of natural-circulation-cooling conditions, pressure drops in the coolant circulating system, and temperatures in and about the core are also presented. In the performance of these analyses, considerable use was made of the work done in previous studies.[1-3] The basic equations used and their sources are discussed in ref. 2.

Core Design

Although no precise method is available for optimizing the core and ball size in an experimental reactor of this type, the restrictions mentioned above place rather narrow limits on these variables. Evaluation of these limits and application of the results in the selection of the PBRE design are described in the following paragraphs.

Pressure Drop and Levitation Limit

The pressure drop through a bed of spheres may be expressed as

$$\Delta p = \frac{15(1-\epsilon)^{1.27}\, G^{1.73}\, \mu^{0.27} L}{g_c \epsilon^3 \rho D_s^{1.27}} , \qquad (1)$$

---

[1] Sanderson & Porter, Design and Feasibility of a Pebble Bed Reactor-Steam Plant, NYO-8753 (May 1, 1958).

[2] A. P. Fraas et al., Preliminary Design of a 10-Mw(t) Pebble Bed Reactor Experiment, ORNL CF 60-10-63 Rev. (May 8, 1961).

[3] A. P. Fraas et al., Design Study of a Pebble Bed Reactor Power Plant ORNL CF 60-12-5 Rev. (May 11, 1961).

where

Δp = pressure drop,

ϵ = mean void fraction,

G = superficial mass velocity,

μ = dynamic viscosity of gas,

L = bed length,

g_c = conversion constant, 32.2 $lb_m \cdot ft/lb_f \cdot sec^2$,

ρ = gas density,

D_s = sphere diameter.

Experiments[4] with gas flowing upward through beds of spheres have indicated that when the pressure gradient equals 80% of the bulk bed density, spinning of the balls in the upper layer begins; at still higher flow rates, actual levitation of the bed will occur. This limits the pressure gradient in a randomly packed bed of graphite spheres to 56 lb/ft^3 (based on an average bed bulk density of 70 lb/ft^3) if ball movement is to be avoided. In applying this restriction, the gas properties used in Eq. (1) are those corresponding to the exit temperature from the core.

With the helium pressure and temperature specified, the limiting superficial gas velocity through the core and, consequently, the power which can be removed per unit of bed cross section, are functions only of sphere size. The effect of this limitation on the power level of the reactor is shown in Fig. 4.1, in which the maximum power is plotted as a function of core diameter.

Division of the levitation-limited power per unit bed cross-section by the core height gives the maximum power density that can be achieved in the core. This limit is plotted in Fig. 4.2 for various core heights as a function of sphere size (the other curves in Fig. 4.2 are discussed later in this section).

Thermal Stress in Fuel Sphere

The maximum thermal stress in an elastic sphere with uniform internal generation of heat and uniform surface temperature can be computed from

[4]D. E. Randall and S. S. Millwright, Experimental Determination of the Pressure Drop Through A Pebble Bed, SC-4354(TR), Sept. 1959.

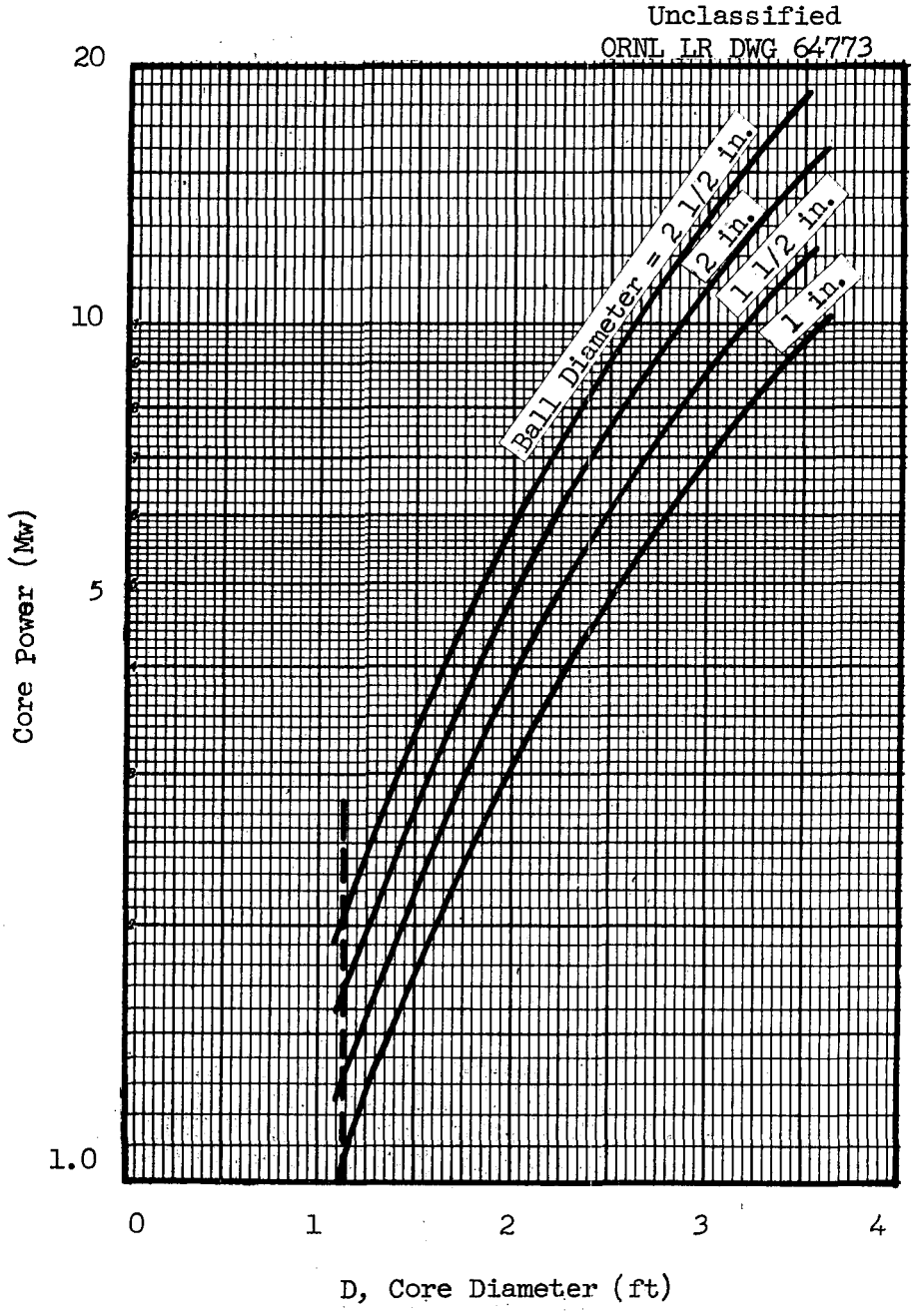

Fig. 4.1. Power Level Versus Core Diameter for Several Ball Diameters with Pressure Gradient Equal to the Levitation Limit for Inlet and Outlet Temperatures of 550 and 1250°F and a Pressure Level of 500 psia. The dashed vertical line represents a cross-sectional area of 1.0 ft^2.

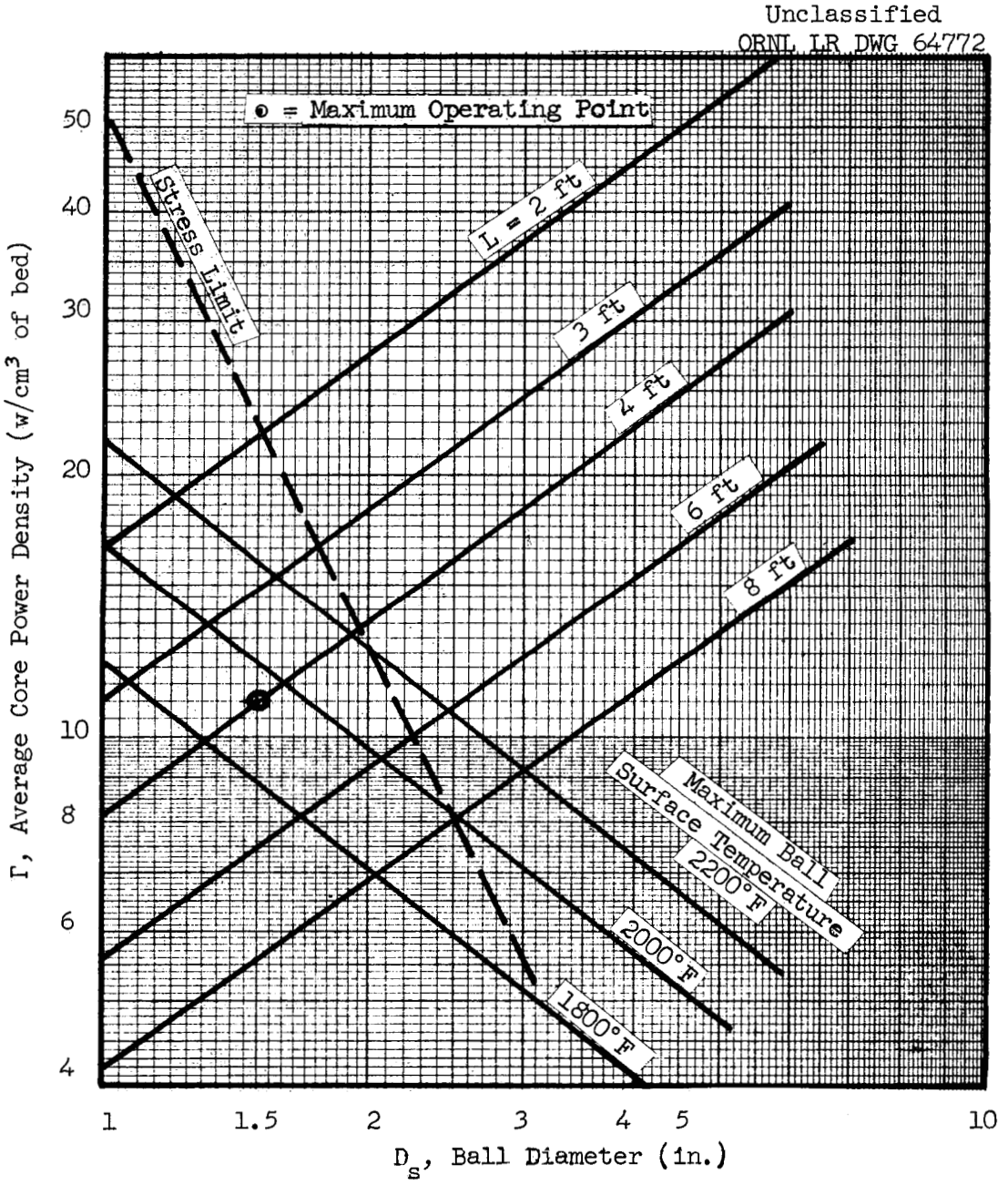

Fig. 4.2. Power Density Versus Ball Diameter for Helium Inlet and Outlet Temperatures of 550 and 1250°F and a Pressure Level of 500 psia. Curves for various lengths indicate power density for gas flow rate corresponding to the levitation limit. Curves with temperature parameter indicate maximum power density that can be achieved at the levitation limit without exceeding specified surface temperature. Stress limit curve has allowance for peak-to-mean power density ratio of 2.0.

$$\sigma_{max} = \frac{\alpha E D_s^2 \gamma}{60k(1 - \nu)} , \qquad (2)$$

where

σ_{max} = maximum stress in sphere,
α = coefficient of linear thermal expansion, $3 \times 10^{-6}/°F$,
E = modulus of elasticity, 1.5×10^6 psi,
D_s = sphere diameter,
γ = power density in sphere,
k = thermal conductivity, 8 Btu/hr·ft.°F,
ν = Poisson's ratio, 0.3.

The physical property values used in the design analysis are those listed above. Although the actual values are uncertain, those selected are believed to be conservative.

The limit that thermal stress places on the mean power density in the ball bed is obtained from Eq. (2) by inclusion of the terms $(1 - \epsilon)$ and $\gamma_{max}/\overline{\gamma}$ and the substitution of σ_{ult} for σ_{max}:

$$\overline{\Gamma}_{\sigma\text{-lim}} = \frac{60(1 - \nu)\, k\sigma_{ult}(1 - \epsilon)}{\alpha E D_s^2 (\gamma_{max}/\overline{\gamma})} , \qquad (3)$$

where

$\overline{\Gamma}_{\sigma\text{-lim}}$ = maximum allowable mean power density in bed as determined by stress limit,
σ_{ult} = ultimate tensile strength of fuel ball (design value, 1500 psi),
$\gamma_{max}/\overline{\gamma}$ = ratio of maximum power density in a fuel sphere to the mean for all spheres in the core.

The peak-to-mean power density ratio in Eq. (3) must allow for differences in the amount of fissile material remaining in the fuel spheres, as well as for flux peaking. (In the PBRE, the ratio of fissile material in a fresh fuel ball to that remaining in an average ball at equilibrium is about 1.2.) The stress-limited mean power density computed from Eq. (3) is plotted in Fig. 4.2 for a peak-to-mean power density ratio of 2.0.

The maximum stress in a fuel element may differ from that computed using Eq. (2) if the fuel is not distributed uniformly throughout the sphere, the neutron flux is not uniform, the heat removal is not uniform around the sphere surface, or the physical properties of the sphere are not uniform. The increase in stress from nonuniform heat removal is analyzed in ref. 3, and the effects of flux depression and the presence of an unfueled shell on the fuel elements are discussed in ref. 5. As shown in Fig. 4.2 and discussed later, the design power density selected for the PBRE is less than one-half the limit imposed by Eq. (3). Making liberal allowances for nonuniformities, based on the results in ref. 3 and 5, would not lower the stress limit curve enough to make thermal stress a factor in the core design.

Fuel Temperature

The mean heat transfer coefficient for a bed of spheres is given by

$$h = \frac{0.5(1 - \epsilon)^{0.3} G c_p}{Pr^{0.66} Re^{0.3}} , \tag{4}$$

where

h = mean heat transfer coefficient,

c_p = specific heat of coolant, 1.25 Btu/lb·°F,

Pr = Prandtl number, 0.703,

Re = Reynold's number, $D_s G/\mu$.

The heat transfer coefficient for helium as a function of ball diameter and mass velocity is given in Fig. 4.3.

The mean gas-film temperature difference may be expressed in terms of the bed parameters as

$$\Delta T_{f,m} = \frac{\bar{\Gamma} D_s}{6(1 - \epsilon)h} , \tag{5}$$

[5]Sanderson & Porter Co., Fuel Element Development Program for the Pebble Bed Reactor, May 1, 1959 to October 31, 1959, NYO-2706, Section 3.0.

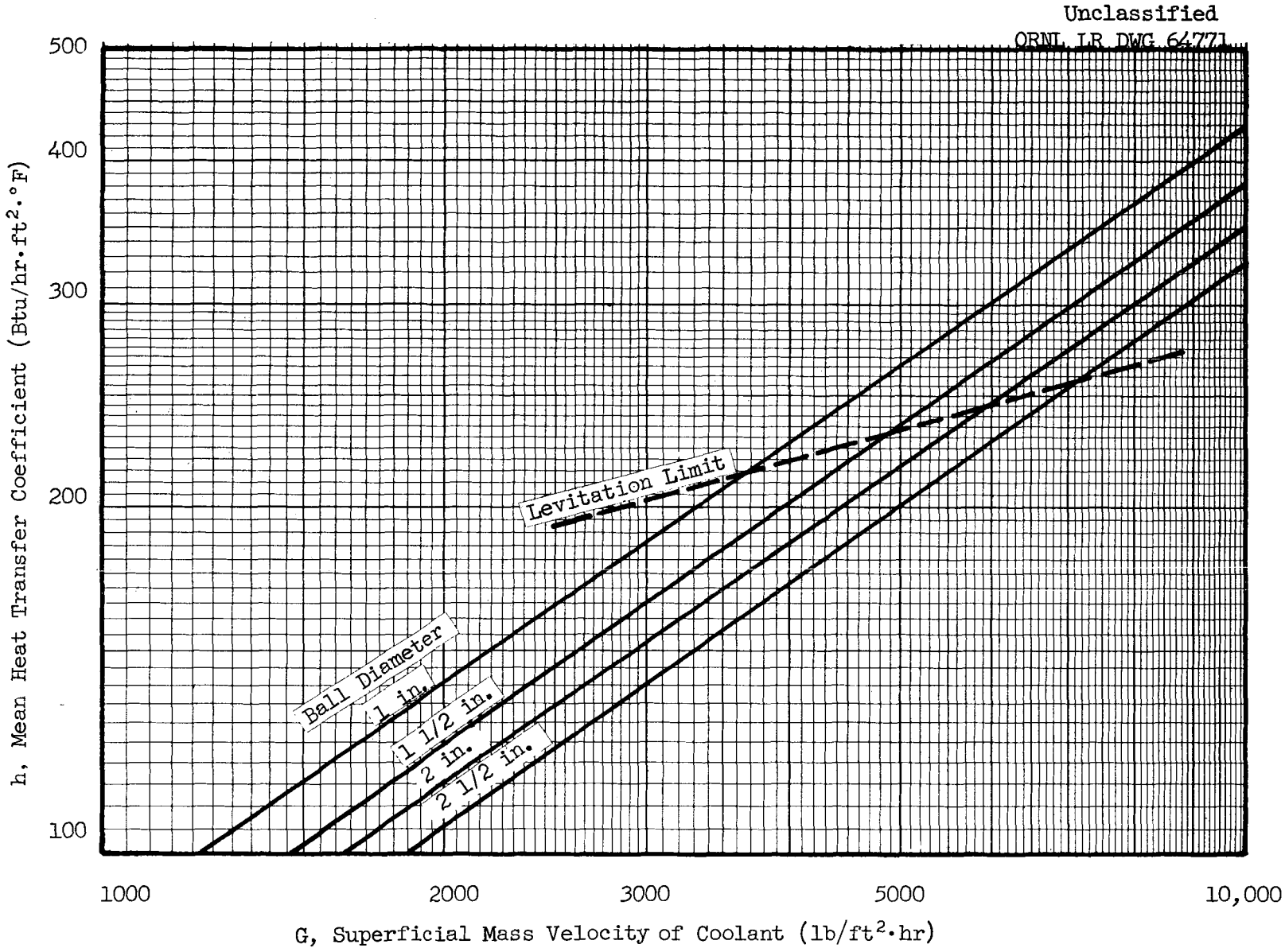

Fig. 4.3. Heat Transfer Characteristics of PBRE Core with a Helium Pressure of 500 psia, an Average Gas Temperature of 900°F, and a Bed Void Fraction of 0.39.

where

$\bar{\Gamma}$ = mean power density in the bed.

The central temperature in a fuel element, of course, exceeds the surface temperature by the internal temperature drop. This difference is given by the following equation for the case of uniform power density throughout the sphere, uniform heat removal at the surface, and uniform thermal conductivity:

$$\Delta T_i = \frac{\gamma D_s^2}{24k} , \tag{6}$$

where ΔT_i is difference between central and surface temperatures of sphere. An unfueled shell increases the internal temperature drop if the power generation per ball is the same. For example, a shell whose thickness is one-sixth of the ball radius would increase the difference between the central and surface temperatures by 60% over that for the same diameter sphere with uniform fuel distribution; a shell one-third of the radius in thickness would increase the temperature drop by 150%.

Variation of the heat transfer coefficient around the sphere surface makes the center-to-surface temperature difference somewhat higher than that for uniform cooling; the effect in practical cases, however, is shown in ref. 3 to be insignificant. Only a small additional increase in temperature occurs within a coated particle. In the peak flux region of the PBRE, the temperature difference between the surface of the coating and the center of the particle is less than 10°F.

The maximum fuel-surface temperature in a pebble-bed reactor core, may be significantly higher than that obtained using Eqs. (4) and (5). The hot-spot problem rises mainly from the variations in heat transfer coefficient about the surface of a sphere, variations in packing density of elements in the bed, and variations in power density throughout the bed. Variations in packing density in a randomly packed bed are of two types: (1) a predictable alteration in void fraction starting at 1.0 at a flat wall, falling to about 0.23 one-half ball diameter away, rising and falling several times again, and leveling off about 4 to 5 diameters

from the wall, to give an average void fraction in the bed of 0.39 for a bed diameter-to-ball diameter ratio of 20; and (2) a statistical variation in sphere arrangement resulting in local void fractions ranging from the minimum possible (0.26) to above 0.47. These nonuniformities in void fraction result in there being random local deviations in velocity and heat transfer coefficient superimposed on the alteration that is a function of radial position.

A primary concern associated with local differences in bed density is that coolant may bypass a closely packed region and thus starve the area of the bed downstream. If this downstream area has a normal or low packing density, the velocity and heat transfer coefficient will be reduced, making the gas and fuel temperatures higher than average.

Various aspects of the hot-spot problem are considered in references 2 and 3. Based on the reasoning and values reported in ref. 2 and an overall peak-to-average power density of 2, the following equation was derived to estimate the maximum fuel-element surface temperature for an outlet gas temperature of 1250°F:

$$T_{s,max} = 1300 + 4\Delta T_{f,m} \quad , \tag{7}$$

where

$T_{s,max}$ = maximum fuel-element surface temperature, °F,
$\Delta T_{f,m}$ = mean gas film temperature drop computed from Eqs. (4) and (5), °F.

Equation (7) has been used with the equations which precede it to estimate hot-spot temperatures for various PBRE core designs. The maximum power densities that can be achieved without exceeding surface temperatures of 1800, 2000, and 2200°F are shown in Fig. 4.2 for flow rates corresponding to the levitation limit.

The analysis on which Eq. (7) is based is conservative in that it assumes an unfavorable conjunction of power density, sphere arrangement, and gas temperature. Actually, the radial peak in the neutron flux occurs near the core wall where the gas flow rate is highest. Further,

with control rods located in the top of the reactor, the axial flux peak occurs at the bottom of the core where the gas temperature is lowest.

Another factor affecting the hot-spot analysis is the height of packed bed required to achieve equilibrium flow conditions, since the maximum fuel temperature is postulated to occur in a loosely packed section preceded by a closely packed cluster. An estimate of this mixing length has been computed for the isothermal case, as follows:

1. The reactor core was divided into nine axial sections and four radial sections. The void fraction of the radial sections varied with radial position, the minimum value of 38% occurring in the central section.

2. Flow rates based on pressure drop and velocity head considerations were estimated for each radial section, with allowance for material balance requirements at each axial position.

3. It was assumed that there was no resistance to cross flow in the bed.

4. Mass velocity at the inlet and static pressure at all levels were assumed to be uniform across the bed.

Results of this analysis indicated that the flow would shift from the low-void central section to the higher void outer section and that equilibrium flow conditions would be very closely approached within about three ball diameters; 60% of equilibrium was found to be achieved within a height equivalent to one ball diameter.

This relatively rapid flow shifting should reduce the effect of closely packed clusters on the fuel temperature. In addition, the ratio of gas flow rate calculated for the outside section to that for the central section is reasonably close to the ratio of the fluxes for these sections, indicating a balance between heat generation and heat removal. (The equilibrium velocity profile obtained in the analysis compared favorably with experimental data[6,7] in terms of the ratio of the maximum to the minimum

---

[6]C. E. Schwartz and J. M. Smith, Flow Distribution in Packed Beds, Industrial Engineering Chem., 45: 1209 (1953).

[7]V. P. Dorweiler and R. W. Tahier, Mass Transfer at Low Flow Rates in a Packed Column, American Journal of Chemical Engineering, 5: 139 (1959).

velocity.) Conduction and radiation will also have the effect of reducing temperature gradients in the bed. Consideration of these factors indicates that the hot-spot analysis used in ref. 2 and adopted in obtaining Eq. (7) and Fig. 4.2 is quite conservative. However, a detailed analysis of existing information and data from the proposed research and development programs will be required to determine the temperature of the hot spots more exactly.

Selection of Core and Fuel Sphere Dimensions

The criteria used in selecting the core and fuel dimensions were: (1) to obtain a high power density so that fuel burnup can be obtained in a reasonably short period; (2) to have the ratios of core dimensions to ball diameter high enough to reproduce the ball behavior in a large reactor and to reduce wall effects on the gas flow; and (3) to stay within the limits imposed by core levitation, thermal stress, and hot-spot considerations. In addition, the fuel requirements and other physics characteristics of the core must be acceptable.

The hot-spot restriction was applied by limiting the fuel surface temperature to 2000°F to prevent damage to the siliconized silicon-carbide sphere coating, if such is used. There are no limits on internal fuel temperatures that would be exceeded if the surface were at 2000°F, although problems of uranium migration and fission-product escape become more severe at higher temperatures.

From the above criteria and Fig. 4.2, the fuel sphere size was chosen as 1 1/2 in. and the core length as 4 ft. The core diameter selected was 2 1/2 ft, which at design conditions gives a maximum pressure gradient equal to 70% of the levitation value; as seen in Fig. 4.1, the power capability of this size core is 6.2 Mw at the levitation limit.

At the design power of 5 Mw, the average power density in the 2 1/2-ft-diam, 4-ft-high core is 9 w/cm^3 of bed, and the estimated maximum surface temperature is about 1900°F. The internal temperature drop at the mean power density is 120°F for a uniformly fueled sphere having a thermal conductivity of 8 Btu/hr·ft.°F; this value would be 240°F for a sphere with power density equal to twice the average. The maximum value would

be increased to 380°F if a 1/8-in.-thick unfueled shell were provided and would be increased to 600°F if the shell were 1/4 in. thick. The volumetric average fuel temperature without an unfueled shell is only 1090°F for an exit gas temperature of 1250°F. These and other design parameters are given in Table 4.1.

After allowance for a peak-to-mean power density ratio of 2.0, the thermal stress in a sphere with uniform power generation throughout its volume is only 40% of the stress limit; an unfueled shell would, therefore, still not make the stress excessive.

The core diameter is equal to 20 sphere diameters, and the height equal to 32 sphere diameters, which are quite reasonable for simulation of ball behavior in a large reactor. Also, as shown in Section 6, the core geometry and dimensions are satisfactory with regard to reactor physics requirements, and the rate of fuel burnup is acceptable.

To provide flexibility, the PBRE blower is sized to give sufficient head and flow for operation at the levitation-limited condition. In addition, the piping system is capable of operating at higher exit gas temperatures than the design point of 1250°F, and the exit coolant can be attemperated with cool helium if desired. Thus, the reactor can be operated at a higher power density if the fuel development program shows that the Si-SiC coating is not necessary, of if further analysis indicates that the hot-spot allowance has been overly conservative.

Shutdown Cooling by Natural Circulation

The reactor system is designed so that in the event of a blower failure, afterheat may be removed by natural circulation of the coolant without any appreciable increase in the core exit temperature. This is accomplished by locating the heat sink high enough above the reactor for the buoyancy driving force to overcome the flow resistance of the system components, including a "seized" blower. Further, a separate small cooler section is provided within the heat exchanger shell, so that this cooling is achieved, even if the main heat exchanger becomes inoperative.

Figure 4.4 serves as a basis for determining the required height of the heat exchanger above the reactor core. This figure was obtained from

Table 4.1. Data for PBRE Preliminary Core Design

Power Level	
Design thermal power level, Mw	5
Power density, w/cm^3 of bed	9
Core Dimensions and Characteristics	
Diameter of bed, ft	2.5
Height of bed, ft	4.0
Bed void fraction	0.39
Bed face area, ft^2	4.91
Bed volume, ft^3	19.6
Number of fuel spheres	11 700
Total heat transfer area, ft^2	574
Bed pressure drop, psi	0.82
Rate of temperature rise (no coolant flow), °F/min	565
Fuel Element[a]	
Sphere outside diameter, in.	1.5
Average heat flux, $Btu/hr \cdot ft^2$	29 700
Stress-limited power density (for 1500-psi stress and k = 8 Btu/hr·°F·ft, ϵ = 0.39), w/cm^3 of bed	45
Mean fuel temperature, °F	1090
Estimated maximum sphere surface temperature, °F	<1900
Maximum thermal stress (peak-to-mean power density of 2.0), psi	600
Mean surface-to-gas temperature drop, °F	150
Mean internal temperature drop, °F	120
Maximum internal temperature drop (peak-to-mean power density of 2.0), °F	240
Coolant Characteristics	
Gas	Helium
Pressure level, psia	500
Inlet temperature, °F	550
Mean outlet temperature, °F	1250
Flow rate through core, lb/hr	19 500
Superficial mass velocity, $lb/ft^2 \cdot hr$	3970
Flow rate as percentage of levitation value,[b] %	80
Average heat transfer coefficient, $Btu/hr \cdot ft^2 \cdot °F$	200
Reactor Parameters When Operated at Levitation Limit[b]	
Power level, Mw	6.2
Power density, w/cm^3	11.0
Flow rate through core, lb/hr	24 000
Superficial mass velocity, $lb/ft^2 \cdot hr$	4890
Bed pressure drop, psi	1.20
Average heat flux, $Btu/hr \cdot ft^2$	38 000
Average heat transfer coefficient, $Btu/hr \cdot ft^2 \cdot °F$	233

[a]Temperatures and stresses estimated for a uniformly fueled sphere.

[b]With gas in at 550°F and out at 1250°F; based on pressure gradient equal to 87% of bed density using fuel density of 1.7 g/cm^3.

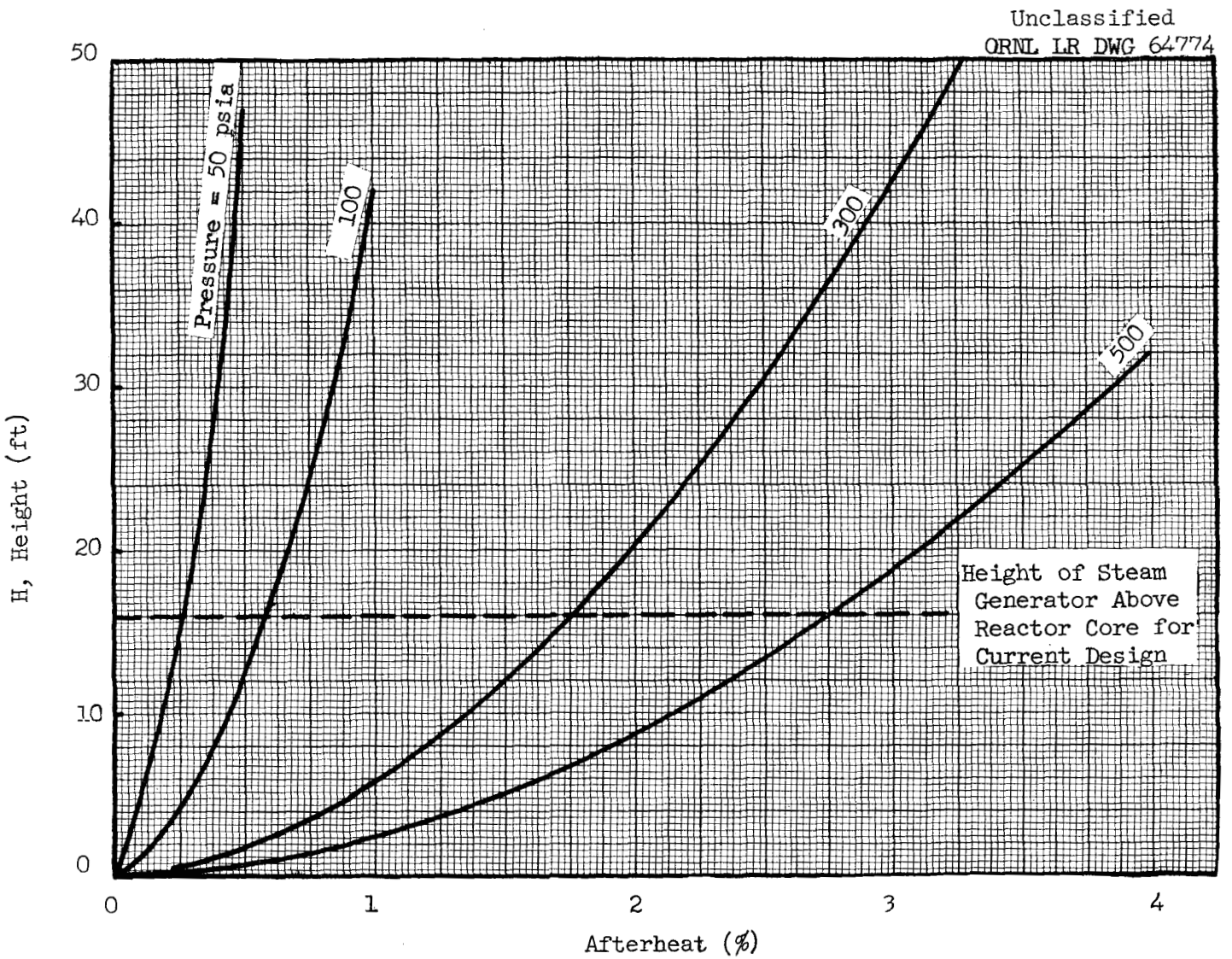

Fig. 4.4. Natural-Convection Cooling of PBRE. Plot of height (centerline to centerline) from steam generator to core versus afterheat removable for several system pressure levels and a reactor power level before shutdown of 6.2 Mw.

calculations based on the following assumptions:

1. gas temperatures remain at 550°F into and 1250°F out of the core,
2. prior to shutdown, the reactor has been operating at 6.2 Mw,
3. the pressure drop through the steam generator is scaled down from 1.0 psi at full flow (6.2 Mw) according to the ratio of the square of the flow rates,
4. the resistance of a seized blower is half of the design head multiplied by the ratio of the square of the flow rates.

A height of 16 ft was chosen as sufficient to remove most of the afterheat and yet not require an excessively high containment structure. As may be seen from Fig. 4.4, natural circulation will remove 2.7% of 6.2 Mw with the inlet and exit gas temperatures at 550 and 1250°F. Although this is not adequate to remove all the afterheat during the first 3 to 4 min. after shutdown, storage of all energy above 2.7% in the fuel elements would raise their average temperature only about 10°F.

Figure 4.5 was prepared to illustrate the effect of pressure level and the replacement of helium by nitrogen on afterheat removal by natural circulation. This figure shows the slight superiority of nitrogen at pressures below 140 psia; for example, at one day after shutdown, a system pressure of 70 psia is required to remove the afterheat with helium, while a pressure of only 56 psia is required if nitrogen is used.

System Pressure Drop

The helium coolant circuit pressure drop was computed to provide the required blower design information. The calculated pressure drop through the system may be summarized for the case of 6.2-Mw operation at a pressure of 500 psia with a 550°F inlet gas temperature and a 1250°F outlet gas temperature, as follows:

	Pressure Drop (psi)
Core	1.28
Steam generator (estimated)	1.00
Blower loop piping	0.97
Concentric piping, etc.	0.81
Core inlet and outlet	0.16
Total	4.32

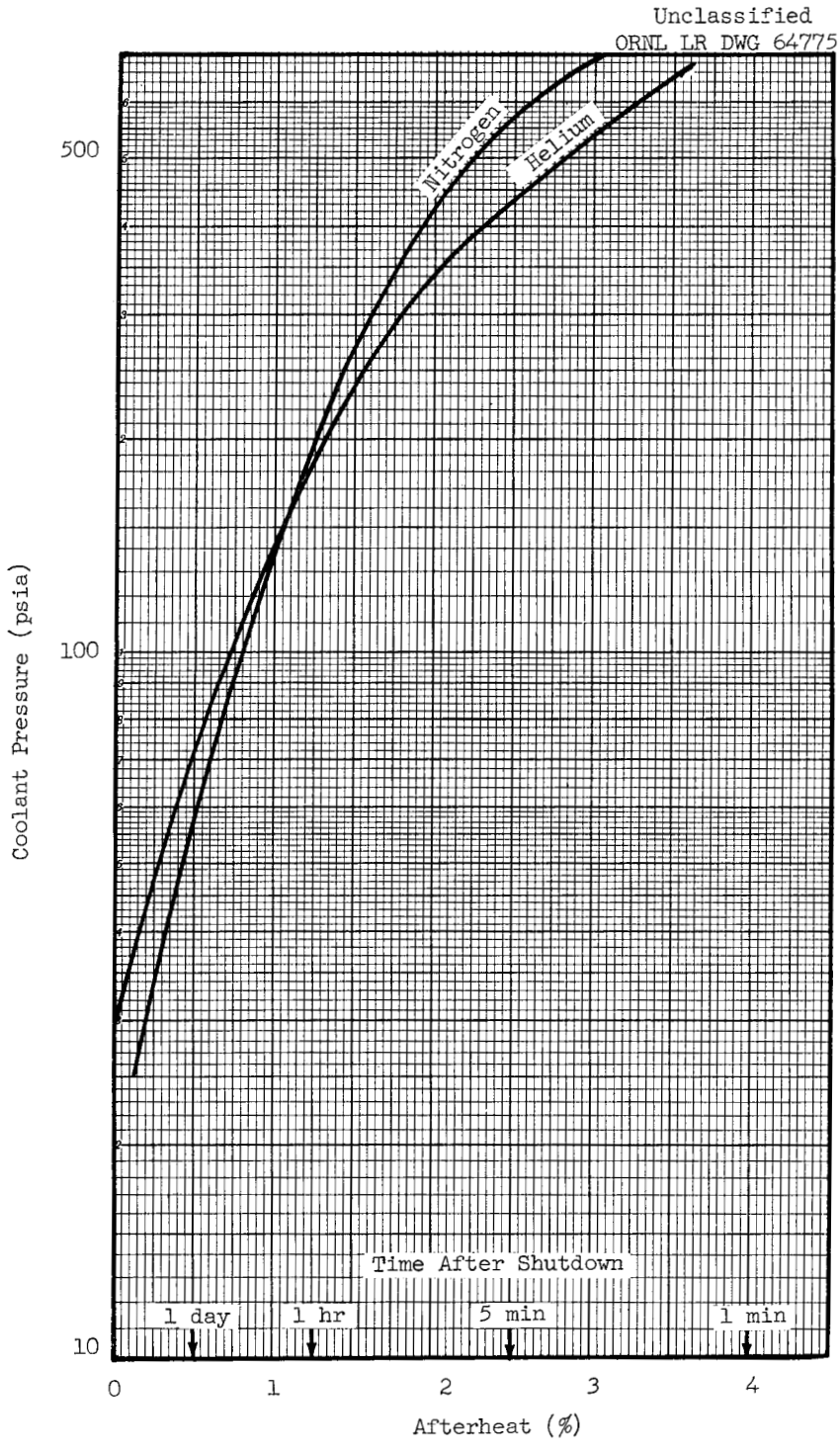

Fig. 4.5. Natural-Convection Cooling. Plot of coolant pressure vs afterheat removal capability for helium and for nitrogen for a height of 16 ft between core centerline and steam generator centerline. Reactor power before shutdown of 6.2 Mw.

These pressure drops were computed for a flow of 24 700 lb/hr of helium through the core and 29 600 lb/hr through the piping, to allow for control rod and reflector cooling and for additional leakage through the reflector. The relationship used in computing the core pressure drop was based on Eq. (1), assuming the bed void fraction to be 0.39. The highest gas velocity attained in the system, 210 ft/sec, occurs in the inside pipe leading from the pressure vessel to the steam generator.

Pressure Vessel Temperature

The temperature of the pressure vessel was estimated for several conditions to aid in determining the desirability of using internal (reflective) or external pressure vessel insulation. Insulation between the graphite and the pressure vessel might seem beneficial, since the use of type A212, grade B, steel requires that the pressure vessel temperature at 500 psia not be greater than 650°F. In a loss-of-pressure and -power accident, however, it is desirable to minimize the heat flow resistance in order to discharge afterheat from the surface of the reactor vessel without overheating the core.

Figure 4.6 shows the temperature of the pressure vessel with external insulation as a function of gas flow rate through the cooling annulus for two reflector temperatures. In the calculations required for this figure, allowance was made for energy transferred to the pressure vessel from the graphite reflector, as well as for that generated in the vessel. Heat was assumed to pass from the reflector to the flow liner by radiation and conduction, from the liner to the pressure vessel by radiation, and from the liner and pressure vessel to the helium coolant by convection. The results indicate that the pressure vessel temperature is relatively insensitive to the reflector temperature and that it is controlled by the gas flow rate. The rate of heat transfer from the graphite increases, however, by 57% for a reflector temperature increase from 1050 to 1250°F.

The effects of using boronated graphite in the outer edge of the reflector are shown in the lowest curve of Fig. 4.6. This curve was obtained by assuming that the heat generation rate in the pressure vessel wall was

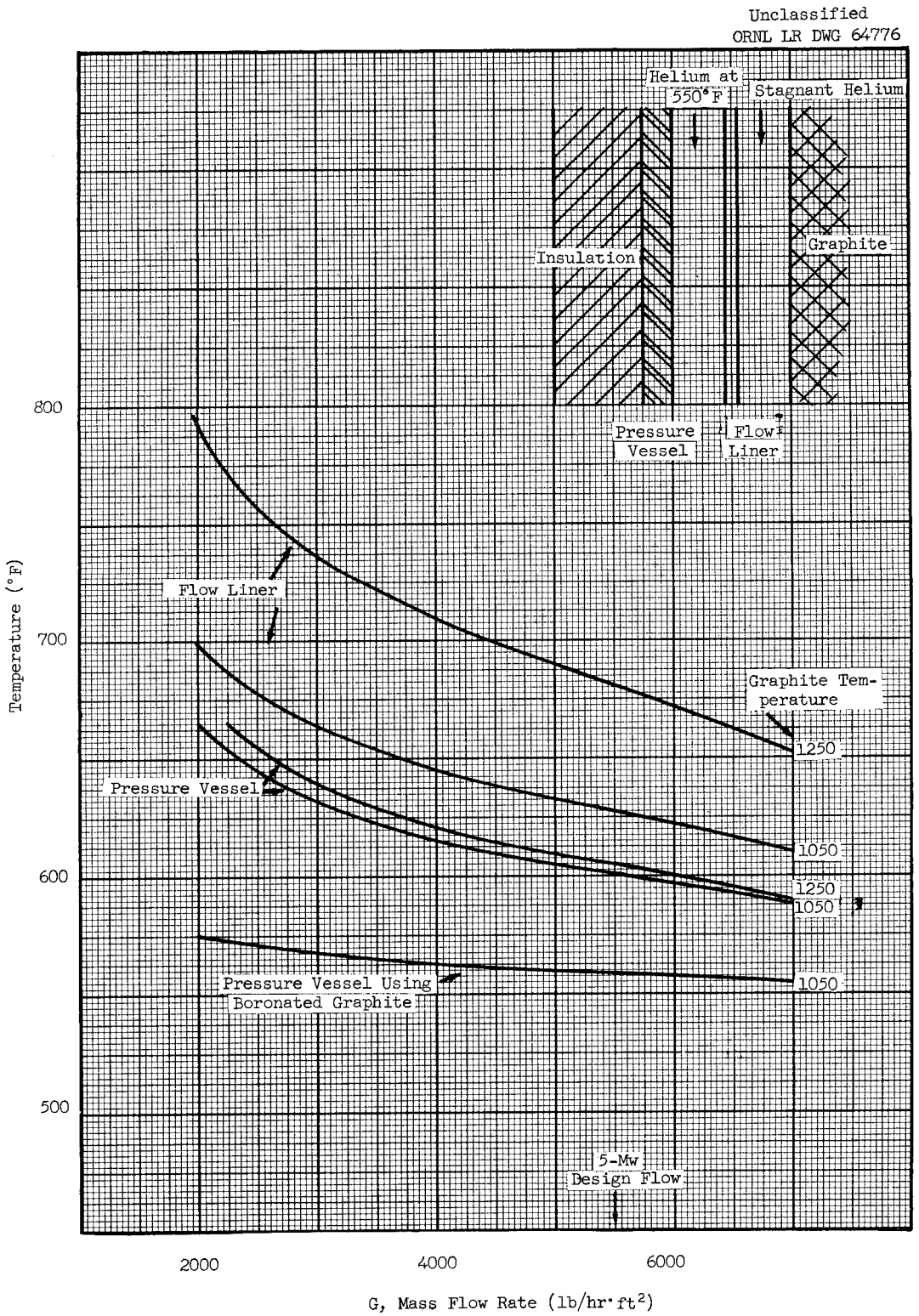

Fig. 4.6. Temperature of Pressure Vessel with Insulation. Plot of temperature of shield and pressure vessel versus flow rate inside pressure vessel for two graphite temperatures.

reduced by a factor of 10 from that used for the case with no boron. In addition to reducing the pressure vessel temperature by about 40°F, the sensitivity to the gas flow rate is also reduced, indicating that temperature nonuniformities may not be a significant problem with this arrangement.

The temperature of the insulated pressure vessel was also estimated for the case of natural circulation at a 500-psia system pressure after reactor shutdown. Assuming that no heat is generated in the pressure vessel and, using 1050°F for the outside graphite temperature, the vessel temperature was computed to be 700°F, which is above the design value. Removing the insulation allows heat to be radiated to the surroundings and thus decreases the pressure-vessel temperature. Radiation from the uninsulated pressure vessel would keep its temperature below 710°F with no helium circulation, and, with natural convection cooling by helium at 500 psia, the vessel temperature would remain below 650°F. These conditions appear to be satisfactory, since zero helium circulation would correspond, essentially, to a depressurized situation in which the pressure vessel is unstressed. More refined calculations, including, for example, consideration of external (air) thermal-convective cooling, are required to firmly establish these temperatures.

With no pressure vessel external insulation, the heat loss would only amount to about 1 1/2% of the reactor heat generated at 5 Mw. Thus insulation is not required to reduce the heat loss, and, in fact, is actually undesirable from the hazards analysis standpoint.

5. FUEL-HANDLING SYSTEM

A major attraction of the pebble-bed reactor is the possible ease of fuel addition and removal when the reactor is at power. A fuel-handling system that makes optimum use of this feature must be simple and reliable, and, of course, investigation of fuel-handling problems is a principle objective of the PBRE. Since the fuel-handling system must be capable of operation and maintenance even though highly contaminated with fission-product activity and it must provide for the sampling and examination of exposed fuel elements, other basic features of the experiment are involved in the design. The design conditions listed below were established for the system.

1. The fuel-handling system must be capable of operating at all reactor conditions, that is, conditions ranging from shutdown and depressurization to full nuclear power. It must be capable of routinely discharging and replacing a small number of balls, and, in addition, must provide for fairly rapid removal of all fuel elements from the core and for their storage. Provision must be made for the addition of fresh fuel and for the recycle of exposed fuel, both at the rate of a small number per day or fairly rapidly, in the event an entire core has been discharged. The fuel-handling system must also provide storage and transfer facilities for a complete nonnuclear fuel charge to permit reactor startup and shakedown studies.

2. In order to determine which fuel spheres should be recycled, means must be provided for examination of exposed fuel to determine its physical integrity and either the uranium burnup which has occurred or the amount of fissile material remaining.

3. It must be possible to operate the fuel-handling system from outside the reactor containment vessel in order to avoid the presence of personnel in the vessel when the reactor is at power.

4. Provision must be made for the routine transfer of small numbers of fuel spheres from the reactor system for hot cell examination elsewhere and for the occasional transfer of large quantities of spheres for reprocessing or disposal.

5. Since the fuel elements will contain uranium and thorium carbides, all spaces through which they will pass after exposure to the reactor environment must contain an inert atmosphere.

6. Full advantage must be taken of movement of balls under gravity in their passage through the core and their handling and transfer in the external system.

7. A close correspondence between radial variations in neutron flux and fuel residence time in the core is desirable in order to produce approximately the same burnup in all spheres. Achieving a favorable ball-movement pattern in the core must therefore be an objective in the design of the fuel-discharge device.

8. The experimental nature of the PBRE makes desirable the ability to test fuel elements of various mechanical strengths. Hence, an attempt should be made to limit the free fall in the reactor. (Irradiated fuel discharged from the PBRE can be tested in hot cells in statistically significant quantities to determine crushing strength and permissible impact loading.)

9. Reliable counters must be located at points in the fuel-handling system to provide knowledge at all times of the movement and location of fuel elements.

10. The entire system must be capable of being maintained and the design must be such as to make maintenance as simple and straightforward as possible.

11. Alternate means must be provided for removal of fuel from the core in the event gross malfunction of the fuel-handling system or damage to the ball bed makes the normal fuel-discharge system ineffective.

12. In recognition that the PBRE is primarily an experimental facility, consideration must be given in the design to the possibility of changes in operating conditions and future alteration of the system.

The fuel-handling system for the PBRE is illustrated schematically in Fig. 3.15. Fuel is inserted into a sloping tube at the top of the reactor and flows by gravity through a gas lock into the core. Fuel entering this upper tube can be either fresh fuel, recycled fuel, or dummy elements transferred from the fuel-handling room below the reactor.

Fuel is discharged from the core through an opening in a rotating removal port at the bottom. It then passes downward through a gas lock into a nitrogen-filled, shielded room that is maintained at near atmospheric pressure. In the fuel-handling room, spheres move by gravity either directly to subcritical storage containers or pass through inspection devices under the control of the operator. New fuel, recycled fuel, or dummy spheres can be released from storage containers into a pneumatic lift for transfer to the inspection area, to the top of the reactor, or to shielded casks for removal from the reactor. These operations can be controlled completely from a position external to the reactor containment vessel.

Two methods of operation are possible. Under normal circumstances the reactor will be at pressure and power and a small number of spheres will be removed and replaced in the core each day. (At equilibrium conditions under full-power operation, about 15 spheres per day will be replaced to maintain criticality.) It is possible, however, to remove fuel rapidly when the reactor is shut down by replacing the helium with nitrogen at atmospheric pressure. The valves in the gas-lock system can then be left open and the fuel discharged from the core in a continuous stream. Return of fuel to the core is relatively rapid also, if the upper gas lock is left open. All routine fuel-handling operations can be controlled by personnel outside the containment vessel.

Fuel-Element-Addition System

The arrangement of the fuel-addition system for the PBRE is shown in Fig. 3.15. New or exposed fuel will be transferred from the fuel-handling room to the fuel-addition system by a pneumatic tube. The spheres will pass from the nitrogen system into the primary helium system through a gas lock.

In preparation for introducing fuel, the space between the valves will be evacuated to remove any gaseous fission-product activity and then permitted to fill with nitrogen. The outer valve will then be opened and the fuel added; the ball counter will indicate the passage of each

sphere. When the proper number of balls has been added, the outer valve will be closed, the nitrogen evacuated from the lock, and helium readmitted. Opening of the lower valve will then permit the spheres to enter the reactor. All fuel-handling lines are slightly sloped, probably 10 to 15 deg, in order to keep the ball velocity low; at these angles the spheres will roll at about 7 ft/sec.

The system of valves, assembled as a unit between mechanical joints, is located in the upper shielding, as shown in Fig. 3.15. Flexible snakes can be used to ram out jammed balls if this becomes necessary. Two spare valves are provided for use in case the others malfunction, and the entire system can be removed and replaced using the semiremote techniques described in Section 11.

After passing through the pressure lock, the fuel elements will roll down to the reactor core. Within the pressure vessel, they will be decelerated to limit the velocity with which they fall on the top of the ball bed. To do this, two schemes are being considered. The first method lets the balls roll down an inclined pipe which takes the shape of a spiral within the core pressure vessel. This system has two major disadvantages. First, if a broken ball should jam in the spiral, it would be difficult to get a flexible rod down to ram it out. Second, there is apparently no good way to assure the operator that a ball has actually left the spiral and entered the core.

In order to eliminate these disadvantages, the alternate system illustrated in Fig. 5.1 is proposed. In this method, the fuel elements are dropped vertically through a counter-current flow of helium that cushions the fall. The presence of a fuel element in the line will be indicated by the pressure difference between the core and the helium withdrawal point. The disadvantages of this system are that precise control of the helium flow may be necessary and that an auxiliary system may be required to provide gas flow when the reactor is not at pressure. Further investigation will be required to determine the practicality of this scheme.

Lines that the fuel balls roll through should be sized so that the inside diameter is 20 to 30% greater than the ball outside diameter. For

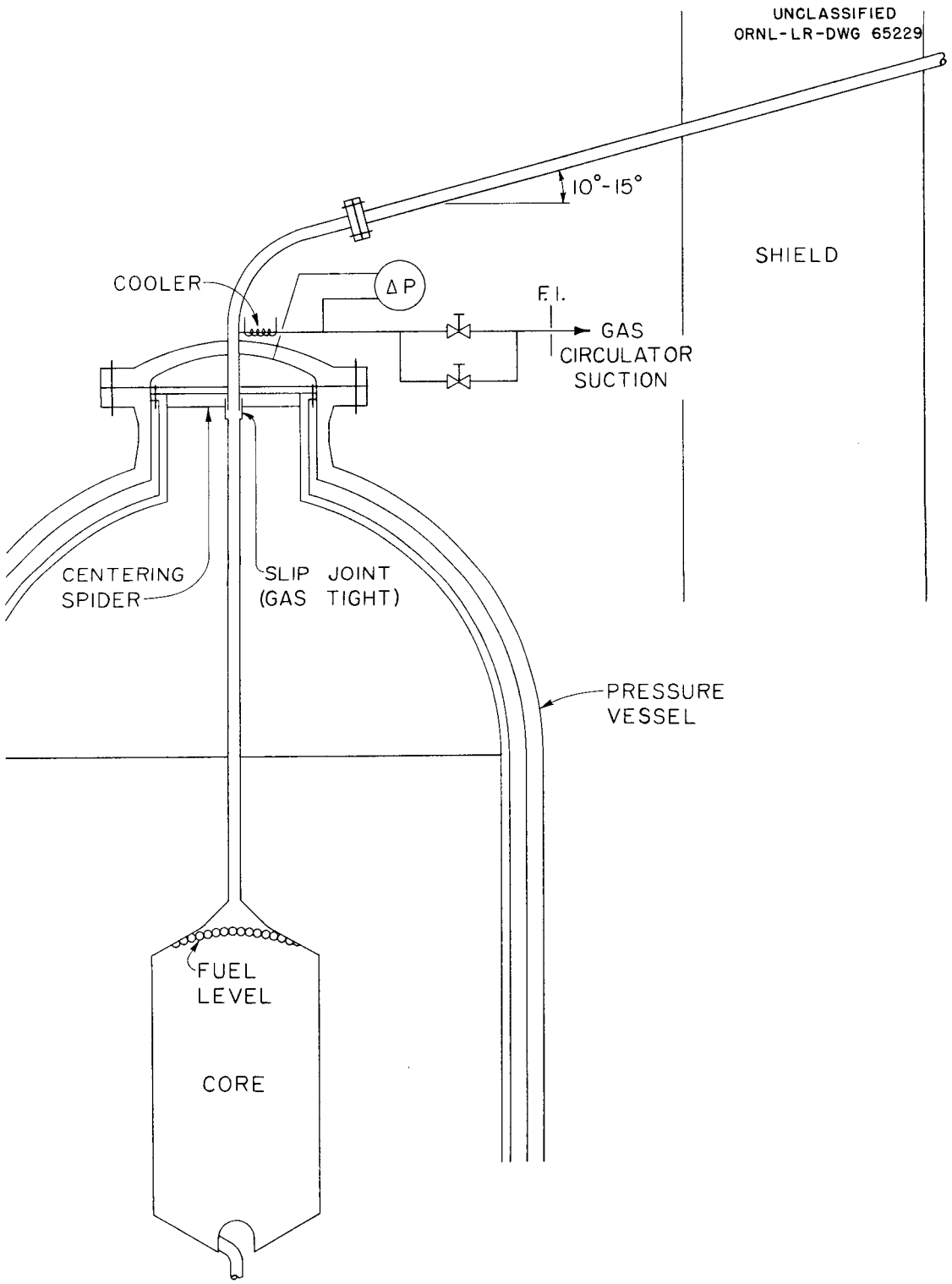

Fig. 5.1. Fuel Ball Inlet Device with Pneumatic Feed.

the countercurrent helium-cushion concept, the closer the pipe inside diameter is to the ball outside diameter, the less gas flow is required to suspend the ball. A very rough estimate indicates that at reactor operating conditions, about 7-cfm of helium flow would be required to suspend a single graphite fuel ball in 1 1/2-in. sched.-40 pipe and about 30-cmf in 2-in. sched.-80 pipe. These values would have to be determined more precisely by experiment.

The initial loading technique would be the same for both fuel-element feeding schemes. First, the core would be filled with inert graphite balls that could tolerate the drop into the core cavity. When the ball level approached the top, the operator would start adding fuel elements while simultaneously withdrawing inert balls from the bottom. Since the fuel elements would not be forced into the core, it would be necessary to maintain a gas phase above the ball level to assure that all balls fell out of the inlet line.

Fuel-Discharge Mechanism

Various techniques that might be used for discharging fuel from a pebble-bed reactor were discussed and evaluated in a previous ORNL study.[1] Among these, it appears that a rotating-dome discharge mechanism of the type shown at the left in Fig. 5.2 will best meet the objectives of the PBRE. The rotating dome serves to collimate the fuel elements at the point of exit from the core and thus allows the entire fuel discharge system to have a size slightly greater than the diameter of a fuel element; studies have shown[1] that unbroken spheres will not jam in a tube that has an inside diameter of 1.1 to 1.7 ball diameters. A rotating mechanism also has the advantage of removing spheres symmetrically about the axis of the bed.

A right-angle drive will be used to rotate the discharge device. This will conserve vertical distance and, in addition, allow placement of the drive motor beyond a shield wall in an area accessible for direct

[1]A. P. Fraas et al., Preliminary Design of a 10-Mw(t) Pebble-Bed Reactor Experiment, CF 60-10-63 rev. (May 8, 1961).

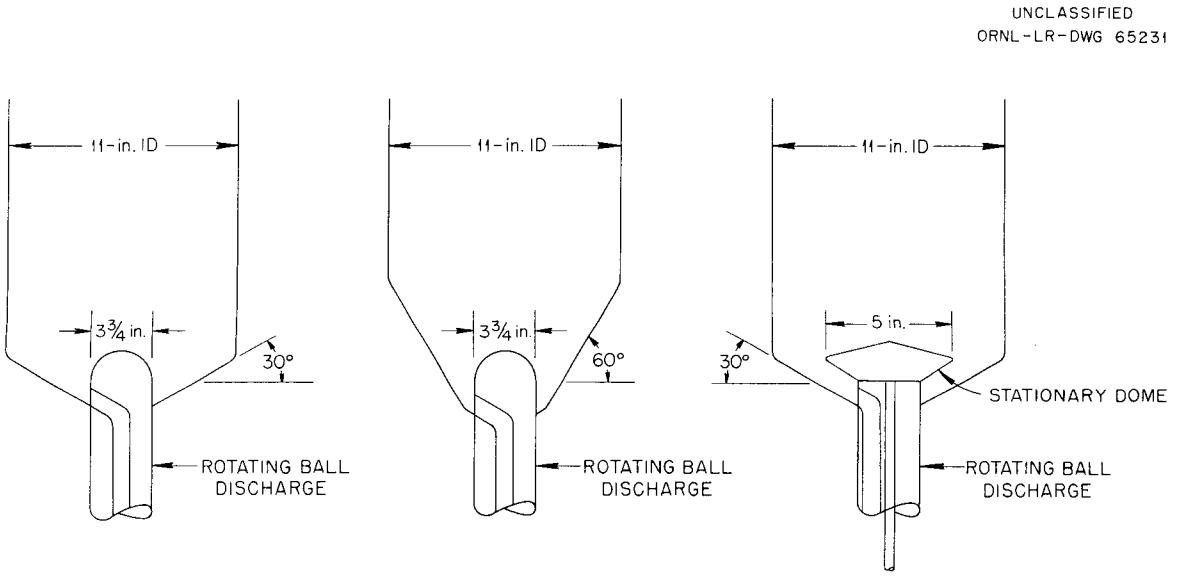

Fig. 5.2. Fuel-Element Discharge Devices.

maintenance. A small amount of clean helium will normally flow through the drive mechanism for cooling and to keep out particulate matter.

The question as to how much fuel, if any, will be allowed to reside continuously in the discharge line is as yet unresolved. One possibility is to have a mechanism for stopping the flow of spheres into the discharge head and thus keep the line free of fuel except during unloading operations. Mechanical shutters or detents might be used or, possibly, gas could be passed up through the discharge line at a rate sufficient to prevent the entry of fuel; at a reduced flow rate the gas would serve to cushion falling spheres. An alternative is to allow the discharge line to remain full of spheres down to some level below the reactor. A mechanical device at this point would control admission of spheres to the lower gas lock.

Replacement or repair of any of the components in the discharge dome drive-shaft housing would be accomplished by withdrawing the drive motor and horizontal drive shaft and removing the lower blind flange. The lower sections of the discharge assembly could then be withdrawn. On lowering the discharge tube, the dome would drop enough to block the discharge port before coming to rest on a support in the lower plenum. Thus it might be possible to replace inoperative components below the rotating dome without unloading the core. To replace the dome, it would probably be necessary to remove the fuel by some alternate technique, such as vacumming the spheres through the top of the reactor vessel.

Five valves in series are shown in Fig. 3.15 as comprising the lower gas lock, whereas actually only two are required for normal operation; the extra three valves are spares. Whether all these spares are necessary will be shown by the valve development and testing program outlined in Section 16. It may be desirable for the valves to have a finger-like extension built into them, or possibly a separate finger ahead of the seat, to prevent hot fuel elements from coming in contact with the valve trim. A vibrator attached near the lock exit may be utilized to clear the transfer line and lock piping should fuel fragments block the passage. A flexible plumbers type of snake may also be introduced via a cleanout connection. An expansion joint precedes the low-pressure flanged

connection to assure placement alignment and to compensate for operational line shifts.

Tentative provisions for disconnection and replacement of the gas-lock assembly include remotely operable mechanical joints above and below the station. A sloped-track system might be employed in conjunction with the lower reactor service machine to transfer a defective unit to an adjacent hot-cell facility for repairs.

Fuel Inspection and Storage Area

After the fuel passes through the pressure lock and through a short section of pipe, it enters a shielded compartment designated as the fuel-element inspection and storage cell (see Fig. 3.2). The passage of fuel through this cell is somewhat complex, and it is desired to use gravity flow as much as possible. At first the fuel passes a classifying device which will reject chips to a storage drum, and, next, the inert spheres, made slightly undersized for easy identification, will fall out onto a spiral storage tray. The fuel elements will roll off the end of the classifier in single file onto an inclined chute.

If a large number of balls is being discharged, the first deflector gate will divert them into the fuel storage tray. This tray, which can hold a complete reactor loading, is a 16-turn spiral containing a single layer of balls. It does not appear to present a criticality problem, although a complete analysis will be made to assure this. A vibrating feeder is used to discharge balls from the spiral storage trays into a pneumatic tube which lifts them back to the ramp leading into the inspection area.

In normal daily operations (10 to 50 balls), the first deflector gate is positioned to allow the balls to continue down a chute to a second gate. Here they are held up for cooling and fed one-at-a-time through a shielding wall into the inspection area.

The inspection area is equipped with devices for detecting cracked or chipped balls and with an analyzer for determining the burnup experienced by an element or the amount of uranium remaining. This area, as well

as the rest of the cell, can be viewed with a television camera. A one-arm manipulator is available for use in both areas. After passing inspection the balls are lifted by pneumatic tube to the fuel-addition lock at the top of the reactor or returned through another tube to the storage area of the cell. Means will be provided to divert used fuel into drums for long-term storage.

Nitrogen is withdrawn from the cell through the fuel storage trays and drums and passes through a filter, cooler, and absorber before being returned to the cell by a blower. This serves to cool the fuel and to restrict the dispersal of activity in the cell. Each nitrogen line is equipped with an orifice having a pressure drop that is high compared with the pressure drop through the drum or tray; the coolant flow rate is therefore independent of whether the unit is full of fuel, and valves are not needed to control the flow.

Counters located in the cell allow the movement of balls to be monitored and a continuous record of ball location to be kept. The counter being developed consists of a differential transformer around the pipe, an oscillator-amplifier, and an electronic counter. For ease of maintenance, all equipment in the cell is visible and accessible from overhead. Removal of shielding blocks, as discussed in Section 11, will permit equipment in the room to be repaired or replaced.

Sampling, introduction of fresh fuel, or removal of spent fuel will be accomplished through air locks separating the cell from the adjacent service room. The cell will normally contain a supply of fresh fuel that is adequate for the scheduled period of operation.

Fuel Element Movement Through the Core

The power density at the edge of the PBRE core is higher than at the center line, and fuel elements near the wall may undergo a higher burnup there than at the center. Ultimately, it would be desirable to be able to match the fuel velocity distribution to the core power distribution and attain uniform fuel burnup. For this reason, flow studies have been undertaken to determine the velocity distribution of the fuel as it travels through the core and the variable that affect this distribution.

A small plastic model, approximately in scale to the PBRE core, was built to operate with ordinary 5/8-in. glass marbles and was tested with the outlet configurations illustrated in Fig. 5.2. For the tests of each core configuration, the model was filled with enough marbles to cover the conical bottom discharge device to a depth of two or three layers to get out of the region of influence of the core bottom. A lower layer of numbered control marbles, as indicated in Fig. 5.3, was placed in the model by hand. The model was then filled to a point near the top, and another layer of numbered control marbles was added directly above the identically numbered marbles of the lower layer. The ball-discharge device was then turned on and each time a control marble came out of the model the total number of marbles removed up to that time was recorded. Marbles discharged from the model were added back to the top to maintain a constant level.

Of the several configurations tested, only the results for the model shown at the left of Fig. 5.2 will be presented here. In this particular configuration, the conical bottom makes an angle of 30 deg with the horizontal, and the entire discharge-dome rotates. The lower plot of Fig. 5.4 shows the average residence time, in terms of numbers of marbles removed, of each circular ring of control marbles in each layer plotted against the dimensionless radius. The upper plot of Fig. 5.4 gives the results of subtracting the "lower layer" curve from the "upper layer" curve and shows that the flow of marbles in the cylindrical part of the vessel is piston-like. The flow of marbles in the cylindrical parts of the vessels described in the center and right-hand arrangements of Fig. 5.2 was also piston-like, with one slight exception. In the case of the discharge device illustrated at the right, the dome is stationary and does not rotate; apparently the dome was not perfectly centered in the model and the velocity distribution, while piston-like, was skewed to one side. This demonstrates the advisability of having a rotating dome.

The piston-like flow of marbles found in the cylindrical part of the core did not agree with data obtained by the Sanderson & Porter Company; their results showed a velocity profile somewhat analogous to

UNCLASSIFIED
ORNL-LR-DWG 65232

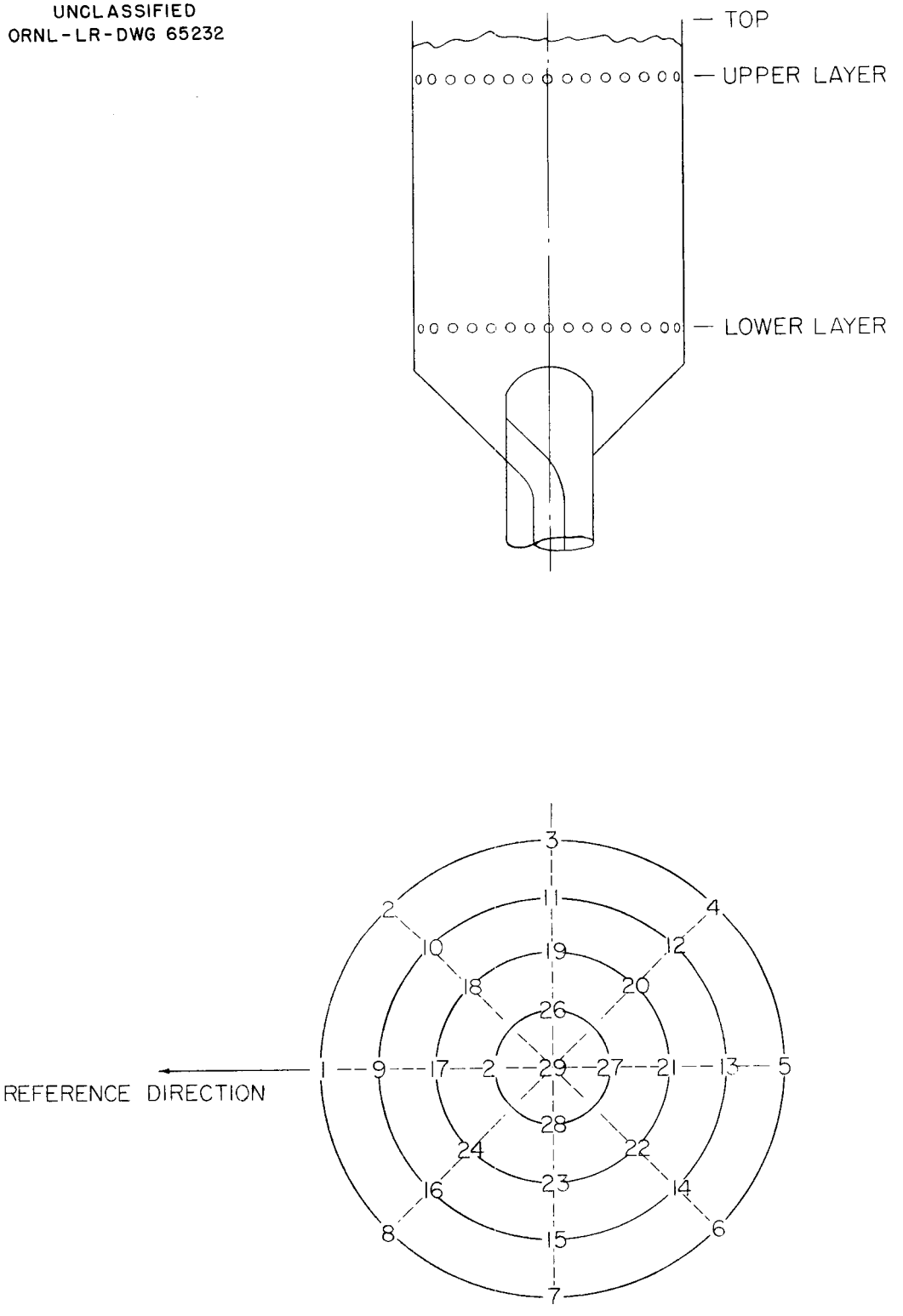

Fig. 5.3. Experimental Model for Testing Discharge Device.

UNCLASSIFIED
ORNL-LR-DWG 65233

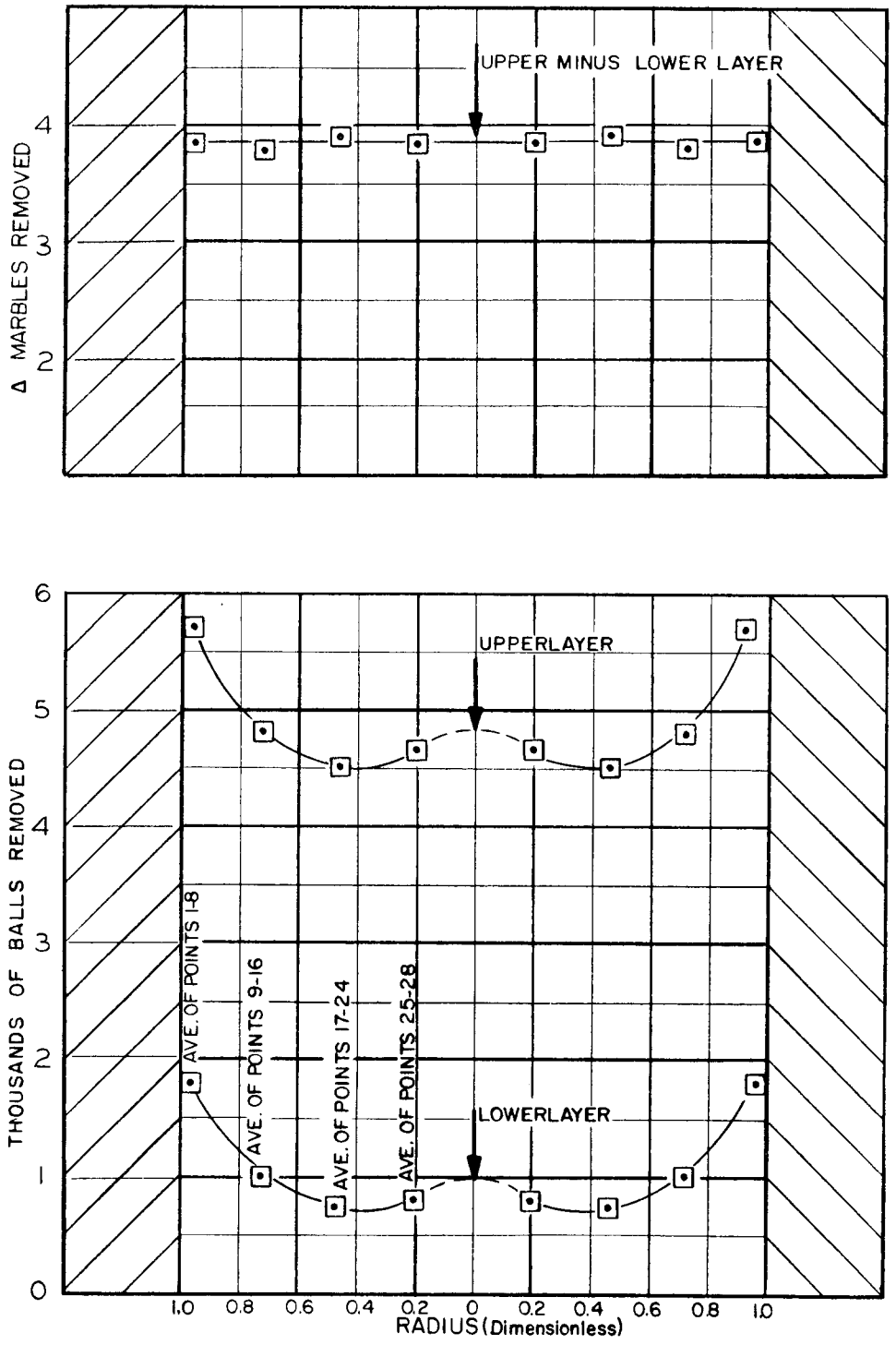

Fig. 5.4. Plots Showing Flow of Balls in Cylindrical Part of Vessel.

water flow in a pipe, that is, high at the center and lower (but not zero) at the walls. The model and plastic balls used by Sanderson & Porter are now at ORNL, and the Sanderson & Porter results have been confirmed using the technique described above. The Sanderson & Porter model, which is smaller than the models illustrated in Fig. 5.2, was used with plastic spheres rather than glass marbles, but the discharge device,[2] although different from those illustrated in Fig. 5.2, was expected to behave similarly.

The differences in the velocity distributions were found to be due, in part, to differences in model configuration, but, in particular, to differences in the coefficients of friction of the materials used. The static coefficient of friction between spheres and a wall was determined from the force required to start pulling a plate vertically out of a bed of spheres, and the coefficient of friction between randomly packed spheres and a flat array of spheres was determined similarly by pulling a tray vertically out of the bed. The tray had sides 3/4 of a sphere diameter high and therefore carried a layer of spheres with it. The coefficients of friction were measured with the plate and tray immersed 10 sphere diameters into the bed. The data obtained are given in Table 5.1.

[2]Pebble Bed Reactor Program Progress Report, Period of June 1, 1959, NYO-9071 (October 31, 1960).

Table 5.1. Static Coefficients of Friction Measured with Plastic Spheres, Glass Marbles, and Graphite Spheres

Material	Specific Gravity	Static Coefficient of Friction (psi)	
		Spheres vs Flat Plate	Spheres vs Spheres
3/8-in. plastic spheres with plastic plate or tray	1.19	0.013	0.027
5/8-in. glass marbles with plastic plate or tray	2.58	0.048	0.119
1 1/2-in. graphite spheres with graphite plate or tray	1.71	0.021	0.068

The absolute difference between the sphere-to-sphere and plate-to-sphere coefficient in Table 5.1 is about 5 times as great for the marbles as it is for the plastic spheres. The ratio of coefficients is also greater for the marbles, being 2.5 versus 2.1 for the plastic spheres. It is not known whether the parameter that determines the ball flow pattern is the ratio of coefficients, difference between coefficients, or some more complicated relation involving such things as solid density, sphere diameter, or other properties. Both the ratios and differences are consistent, however, in indicating that it is the comparative sphere-to-sphere and sphere-to-wall forces that determine whether the flow is piston-like.

The importance of drag forces on the pattern of ball movement was indicated further by tests in which sandpaper was used to increase the drag of the wall on glass marbles. Ball movement studies with marbles in a sandpaper-lined model showed velocity profiles similar to those with plastic spheres in a plastic vessel, rather than the flat profiles obtained before with marbles. The coefficient of friction between a sandpaper-covered plate and marbles was found to be 0.070, which gave a sphere-to-sphere vs plate-to-sphere ratio of 1.7 and reduced the difference between the two coefficients to 69% of what it was without sandpaper.

Coefficients of friction values obtained with 1 1/2-in. uncoated graphite spheres and a graphite plate are given in Table 5.1. The ratio of coefficients is 3.2, and the difference in coefficients is 3.4 times that of the 3/8-in. plastic spheres. From this it can be tentatively concluded that the flow of fuel elements in the cylindrical part of the PBRE core will be nearly piston-like. This conclusion, however, involves the uncertain assumptions that the friction coefficients of the actual fuel elements will be similar in dry helium at reactor conditions to those measured with graphite spheres in air at room temperature, and that the lifting force of upward flowing gas will not change the ball flow pattern. It should also be recognized that the addition of ceramic sphere coatings or the slitting of the core wall (as suggested to reduce stresses from radiation shrinkage) could change the coefficient of friction enough to significantly alter the flow pattern. A full-scale model of the PBRE core

is currently being built to operate with upward flow of air through a bed of 1 1/2-in. graphite spheres. Studies using this model will resolve several of the unknown factors in ball-velocity distribution.

Although the preceding discussion has concerned only the pattern of ball movement through the cylindrical portion of the core, the converging section at the bottom is of equal importance and requires study. Clearly the discharge device and the core bottom must be shaped so that no long-hold-up zones exist in the lower part of the core. This is particularly important in the PBRE because of the flux peaking which occurs in that region.

One example of the influence of the discharge region on the total residence time in the core can be seen in the curve for the upper layer of balls in Fig. 5.4. The spheres originating near the wall were in the core 27% longer than those which passed through the most rapidly, even though their velocities were the same in the cylindrical portion. This difference, however, is only 12% for spheres starting at the top of the core, rather than half way up as in the experiment. Thus, relatively uniform residence times can be expected if care is taken in the specific design of the lower core region.

6. REACTOR PHYSICS

Fuel Composition

There are two quantities to be fixed in regard to fuel composition, since both the U^{235} and the thorium content of the fuel can be varied. The criteria which have been used are, first, that the total weight percentage of uranium plus thorium in a fuel ball should be the same as would be anticipated in a full-scale power reactor, and, second, that there should be sufficient reactivity to give the same burnup density (fissions per cubic centimeter) as would be anticipated in a full-scale reactor. The first criterion gives a fuel ball matrix which has the desired mechanical and physical properties, while the second criterion provides a meaningful test of the radiation stability and fission-product retention characteristics. The ratio of thorium to uranium in the fuel for the experimental reactor will, of course, be much lower than in the full-scale reactor because of the much higher neutron leakage from the smaller core.

The economic analysis that was used to establish a reference design for a full-scale power reactor of the pebble-bed type is described later in this section. On the basis of this analysis it was concluded that a reasonable fuel composition for the PBRE would be 5 wt % uranium plus thorium and that this fuel would have sufficient reactivity to give a burnup density of 3.1×10^{19} fissions/cm^3 of fuel sphere. To obtain this burnup density in the PBRE at an average power density of 14.8 w/cm^3 of fuel sphere requires a fuel lifetime of 2.1 years.

The initial enrichment for the PBRE fuel was computed by calculating the k_{eff} for equilibrium mixtures of nuclides where the final burnup was 3.1×10^{19} fissions/cm^3 of fuel, the initial uranium plus thorium content of the fuel was 5 wt %, and the initial enrichment of the fuel was allowed to vary. The equilibrium conditions were defined as those of graded exposure, in which the fuel is well mixed within the core so that composition is not a function of position. The equilibrium reactivity corresponding to various initial fuel enrichment is shown in Fig. 16.1. An enrichment of 58% was chosen. The associated k_{eff} of 1.03 allows 0.01 k for shim control and 0.02 k for minimum control rod poisoning.

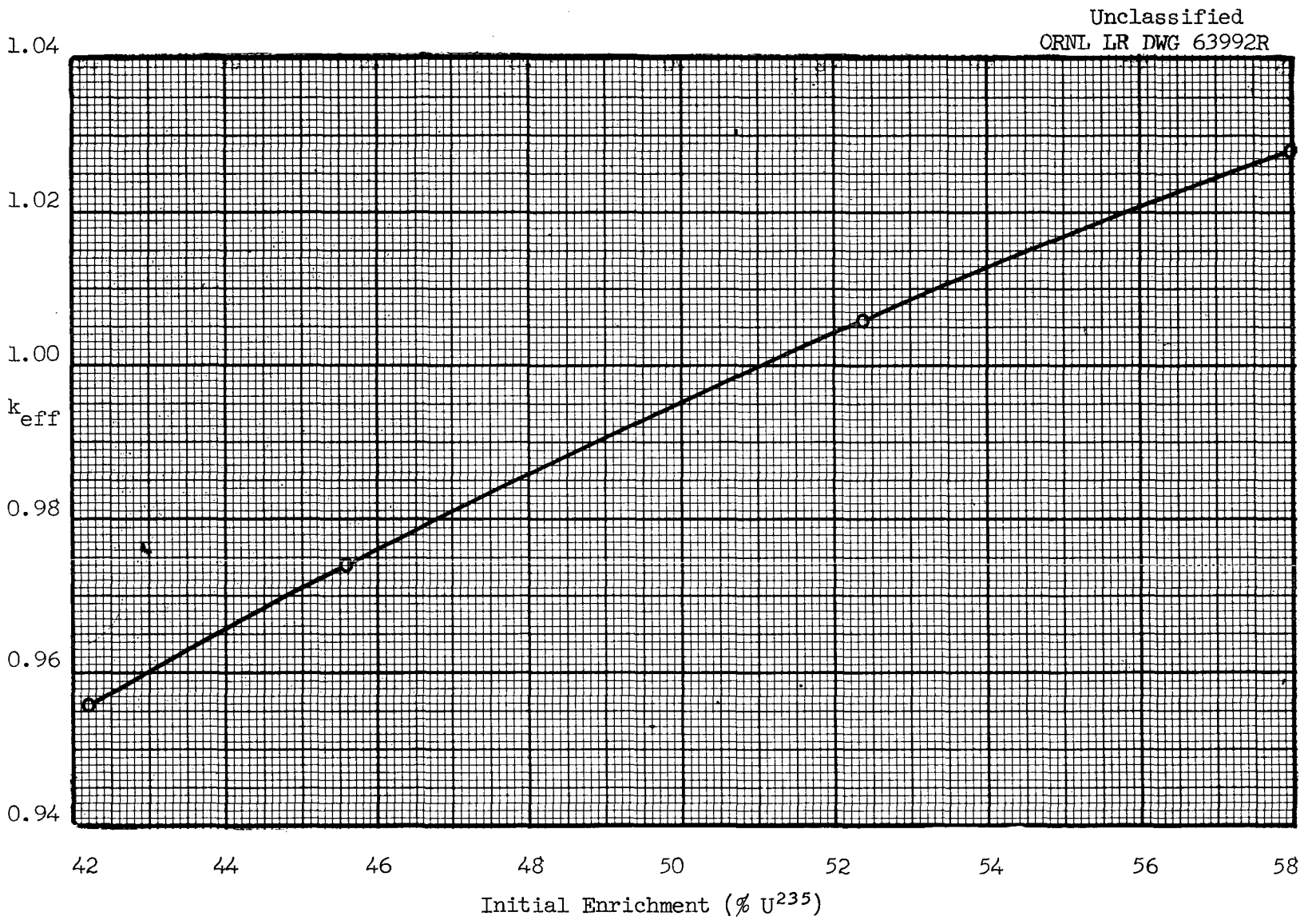

Fig. 6.1. Equilibrium k_{eff} for PBRE with 5 wt % Thorium plus Uranium in Fresh Fuel, 3.1×10^{19} Fissions per cm^3 of Fuel in Spent Fuel, and Graded Exposure.

In calculating the reactivity of fuel on an equilibrium cycle it is not intended to imply that the PBRE will ever actually reach such conditions. In an experimental reactor, with a principal aim of providing a test of fuel materials, it would be expected that various types and compositions of fuel spheres would be inserted from time to time and that fuel would be withdrawn for analytical purposes, as well as when dictated by core reactivity. The equilibrium reactivity does, however, provide a useful yardstick by which to measure fuel-lifetime capability. If the PBRE is operated for the first part of its lifetime with no withdrawal or change in position of the fuel, then substantial refueling will have to occur when the average fuel exposure is a little less than one-half the target value and the maximum exposure (the outer fuel layer at the bottom) is at approximately the target value. If some fuel removal and reinsertion occurs during burnup of the first core loading, then substantial refueling will be necessary when all the fuel approaches one-half its target burnup.

The criticality calculations were performed with the one-dimensional multigroup GNU code. The burnup calculations were done by analytical solution of the nuclide-concentration equations, using the effective cross sections from the GNU calculations. Xenon and samarium concentrations were computed explicitly, while the poisoning from the remainder of the fission products was allowed for by the eight pseudo-elements taken from Nephew's study.[1] An iteration between the two types of calculations was done for each enrichment to assure that the effective cross sections corresponded to the nuclide-concentrations being used. The results of these calculations are given in Tables 6.1 and 6.2 for 58% enrichment of the fuel.

The burnup in the PBRE would be 0.24 fissions per initial fissile atom or 1.3×10^5 Mwd/T of uranium plus thorium. The equilibrium conversion ratio would be 0.080. The initial core loading would be 17.2 kg of U^{235}. The initial specific power would be 0.3 Mw/kg. The macroscopic fission cross section of fresh fuel would be 1.2 times the average value in the core at equilibrium.

---

[1]E. A. Nephew, Thermal and Resonance Absorption Cross Sections of the U^{233}, U^{235}, and Pu^{239} Fission Products, ORNL-2869 (Jan. 18, 1960).

Table 6.1. Nuclide Concentrations of 58%-Enriched Fuel

Nuclide	Nuclide Concentrations (atoms per barn-cm of core volume)		
	Fresh Fuel	Equilibrium	Spent Fuel
Th^{232}	5.18×10^{-5}	5.10×10^{-5}	5.02×10^{-5}
Pa^{233}		7.47×10^{-8}	7.75×10^{-8}
U^{233}		6.23×10^{-7}	1.22×10^{-6}
U^{234}		1.88×10^{-8}	4.72×10^{-8}
U^{235}	7.91×10^{-5}	6.66×10^{-5}	5.55×10^{-5}
U^{236}		2.63×10^{-6}	4.93×10^{-6}
U^{238}	5.50×10^{-6}	5.32×10^{-6}	5.14×10^{-6}
Pu^{239}		1.33×10^{-7}	2.26×10^{-7}
Xe^{135}		4.78×10^{-10}	
Sm^{149}		4.48×10^{-9}	4.48×10^{-9}

Specified Conditions

1. Fresh fuel has $\dfrac{N^{25}}{N^{25} + N^{28} + N^{02}} = 0.58$

2. Fresh fuel has $\dfrac{(235)N^{25} + (238)N^{28} + (232)N^{02}}{(235)N^{25} + (238)N^{28} + (232)N^{02} + 12N^{C}} = 0.05$

3. For all nuclides the equilibrium concentration is

$$N_j^{equil.} = \frac{1}{t} \int_0^t N(t)\, dt$$

4. $t = 6.76 \times 10^7$ sec

5. $\sum_j \int_0^t \sigma_j^f N_j(t)\, \phi\, dt = 3.1 \times 10^{19}$ fissions/cm^3 of fuel

Table 6.2. Neutron Balances for 58%-Enriched Fuel

	Neutron Balances[a] (neutrons per source neutron)					
	Hot Clean Core		Fresh Fuel with Xe and Sm		Equilibrium	
	Absorptions	Productions	Absorptions	Productions	Absorptions	Productions
Th^{232}	0.0358		0.0357		0.0363	
Pa^{233}					0.0005	
U^{233}					0.0059	0.0130
U^{234}					0.0001	
U^{235}	0.5793	1.1022	0.5641	1.0718	0.5293	1.0098
U^{236}					0.0028	
U^{238}	0.0082		0.0081		0.0082	
Pu^{239}					0.0029	0.0056
Xe^{135}			0.0100		0.0110	
Sm^{149}			0.0068		0.0068	
Other fission products					0.0137	
Core graphite	0.0023		0.0023		0.0026	
Core escapes	0.3744		0.3730		0.3799	
Total	1.0000	1.1022	1.0000	1.0718	1.0000	1.0284

[a]These neutron balances were computed with zero control rod poisoning in all cases; since there is actually a 0.02 δk poisoning from the control rods in their most retracted position, the excess reactivities are 0.02 lower than indicated.

Temperature Coefficient

A preliminary estimate of the magnitudes of the thermal-neutron-spectrum temperature coefficient of reactivity was made by means of one-dimensional multigroup calculations (GNU code). The calculations were done for the clean core, that is, for fuel with no burnup or fission products. In each case the calculations were for isothermal conditions across the core and reflector. The calculation gave a temperature coefficient from the thermal-neutron spectrum of $-1.2 \times 10^{-5}/°F$.

The temperature coefficient from Doppler broadening of the thorium resonance integral was calculated in two steps. First the change in k resulting from a change in thorium resonance integral, I, was computed with the GNU code to be

$$\frac{\delta k}{k} \Big/ \frac{\delta I}{I} = -0.071 \quad .$$

Then the change in resonance integral for a given change in temperature, T, was computed from the resonance parameters at a fuel temperature of 1080°F. The result was

$$\frac{1}{I}\frac{\delta I}{\delta T} = 5.6 \times 10^{-5}/°F \quad .$$

Multiplication of these two quantities gives the fuel temperature coefficient

$$\frac{1}{k}\frac{\delta k}{\delta T} = -0.4 \times 10^{-5}/°F \quad .$$

The combined temperature coefficient is thus $-1.6 \times 10^{-5}/°F$, or $-2.9 \times 10^{-5}/°C$. It is believed that the reflector makes a positive contribution to this coefficient, so the core coefficient alone should be more negative than the above value. Considerable improvement in the calculations will be necessary, however, before much reliance can be placed in the results. In particular, the effects of changes in neutron spectrum as a result of neutron diffusion from reflector to core must be explored by more elaborate calculations than those used so far in this study. As a result of this uncertainty in temperature coefficient, the preliminary analog computer studies of reactor transients have been carried out with the temperature coefficient as a parameter.

Reactor Control

The required amount of reactivity control is given below:

	δk
Temperature defect	0.016
Equilibrium xenon poisoning	0.018
Equilibrium samarium poisoning	0.012
Other fission products and burnup	0.044
Shim control	0.010
Total	0.100

The control rods are located in the reflector where there is no interference with ball flow or coolant flow from internal boundaries. Since the reactor is largely reflector moderated, it is possible to obtain sufficient reactivity control with absorber rods outside the core.

Calculations on the effectiveness of control rods were made for several combinations of rod diameter and number of rods. The calculations were two-dimensional and four-group in (x,y) geometry with the circular control rods approximated by squares. With B_4C rods it was assumed that an approximate result could be obtained with a calculational model in which the rods were black to neutrons of each energy group. Since the high-energy group accounted for only 13% of the control rod absorptions, the overestimate of control rod effectiveness should not be large. The rods were located with centers on a 40-in.-diam circle (5 in. outside the core boundary). The reflector thermal flux peak reached a maximum at about 8 in. outside the core, indicating that the rods will be in a region of high thermal flux.

The change in reactivity, δk, that will be obtained by complete insertion of the rods is indicated in Fig. 6.2. The design which was chosen has 4 rods, each 3 in. in diameter. The B_4C control rods are to be supported from below by a graphite rod with a steel core. Hence the reactivity effect of the steel core must be subtracted from the calculated control rod effectiveness. This effect is shown in Fig. 6.3 as a function of the diameter of the steel core. It was concluded that 0.01 δk would be an

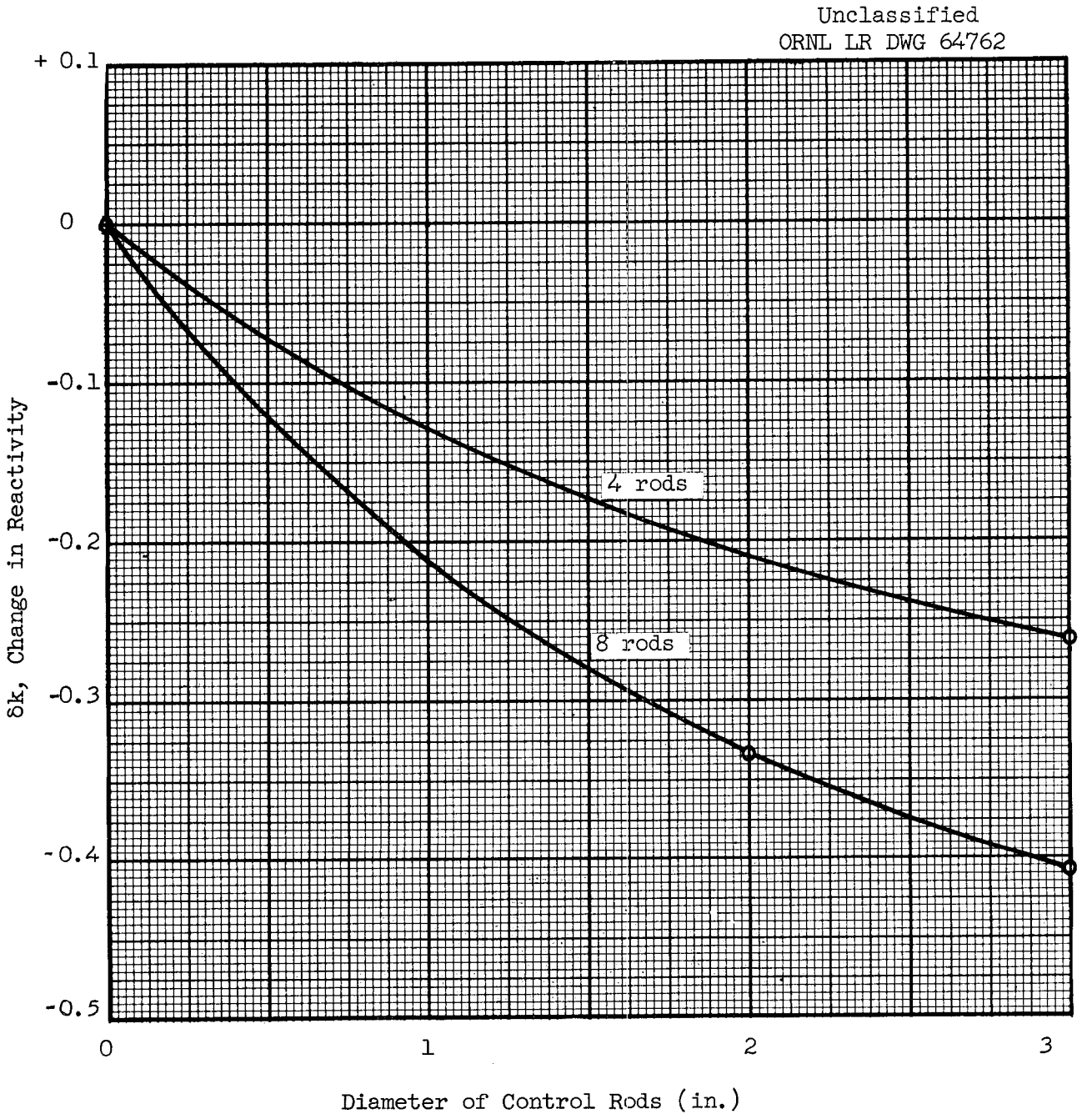

Fig. 6.2. Effectiveness of Black Control Rods on a 40-in.-diam Circle.

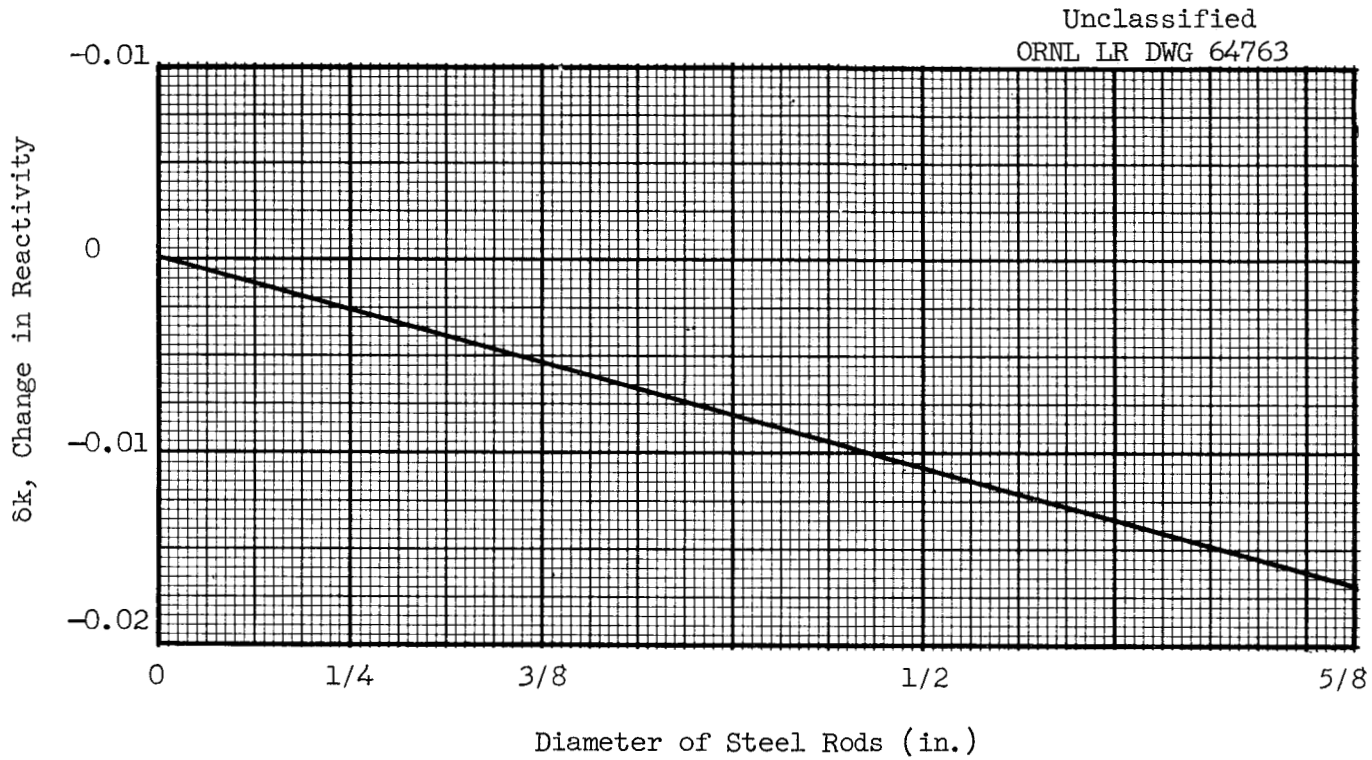

Fig. 6.3. Reactivity Effect of Four Steel Rods on a 40-in.-diam Circle.

adequate allowance for the effect of the steel core. An additional 0.03 δk must be subtracted since the rods are only 4 ft long and do not blanket the entire core and reflector when inserted. A 0.01 δk must be subtracted for residual poisoning after the rods have been withdrawn to the maximum design point, with the bottom of the active section 1 ft above the core. The total control rod worth is then 0.21 δk, leaving a shutdown margin in the order of 0.11 δk. Further calculations will be required, however, with more exact mathematical models of the control rods and surrounding regions, in order to establish a precise value for the shutdown margin.

Power and Flux Distribution

It is characteristic of a small pebble-bed reactor that the thermal flux shows very high peaking in the reflector, and thus the power density tends to be at a maximum at the outer walls and ends of the core. A typical power distribution is shown in the curves of Fig. 6.4. These curves were computed for the hot, clean core and uniform axial and radial reflectors with void fractions of 0.20 and 0.10, respectively. The control rods were assumed to be fully withdrawn, so the axial power distribution is symmetrical about the midplane of the core.

It is noteworthy that the highest radial power occurs near the core walls where the gas flow is highest because of the greater void fraction. With the control rods partially inserted, the power would be depressed in the upper part of the core, and the axial distributions would be at a maximum at the bottom where the gas temperatures would be lowest. Both these factors are favorable in limiting the maximum fuel temperature.

The "scalloping" of the circumferential power distribution that is caused by the presence of control rods is indicated in Fig. 6.5. It does not appear to be serious, and, in any case, would be in a region of low power density and would affect only a small portion of the core.

Axial power distributions for the core with partially inserted control rods (inserted as a bank) were obtained by doing two-dimensional calculations in (r,z) geometry with the control rods represented by a homogeneous annulus. The group cross sections for the control annulus were obtained by

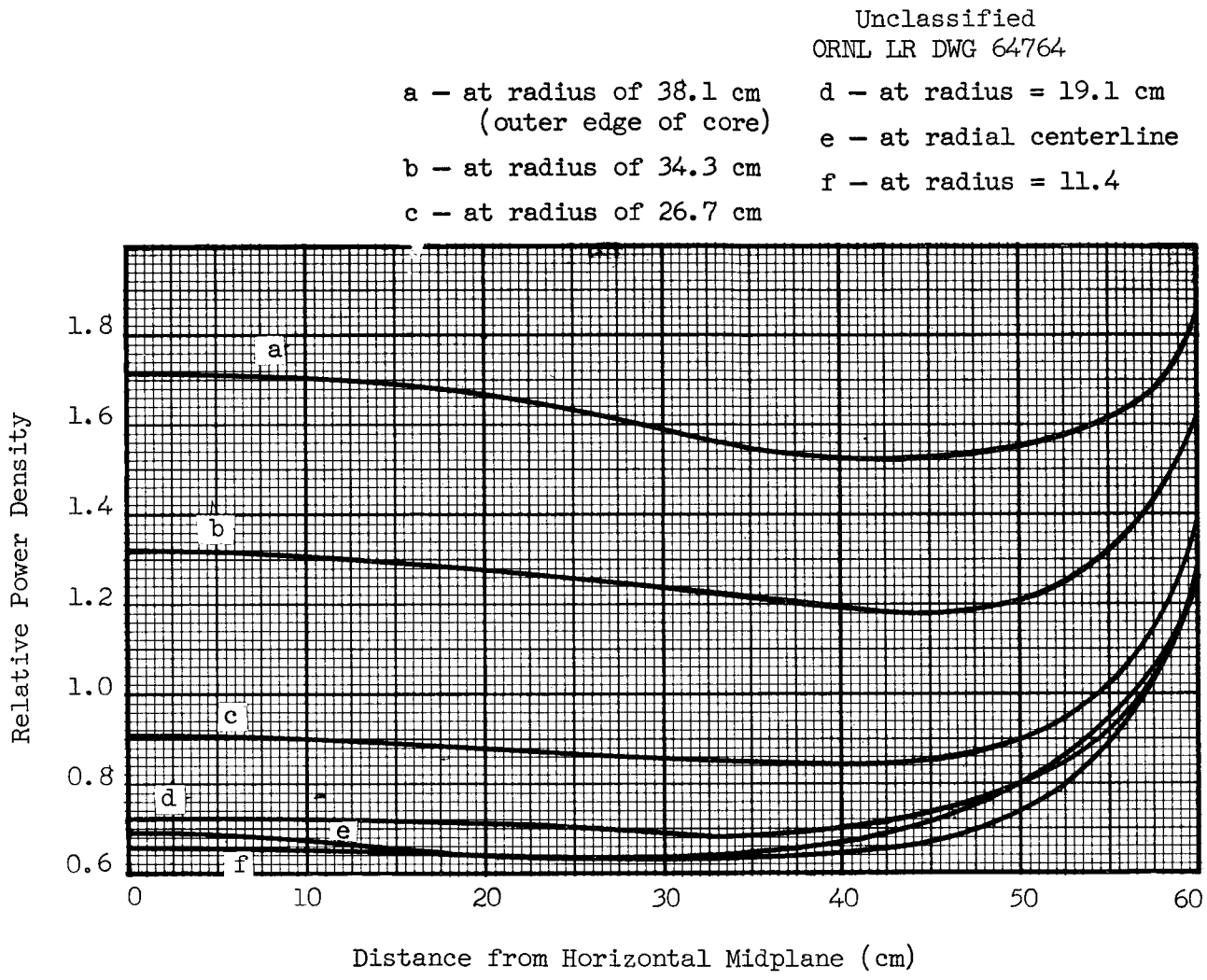

Fig. 6.4. Axial Power Distribution with Control Rods Withdrawn (Relative to 1.0 for the Entire Core).

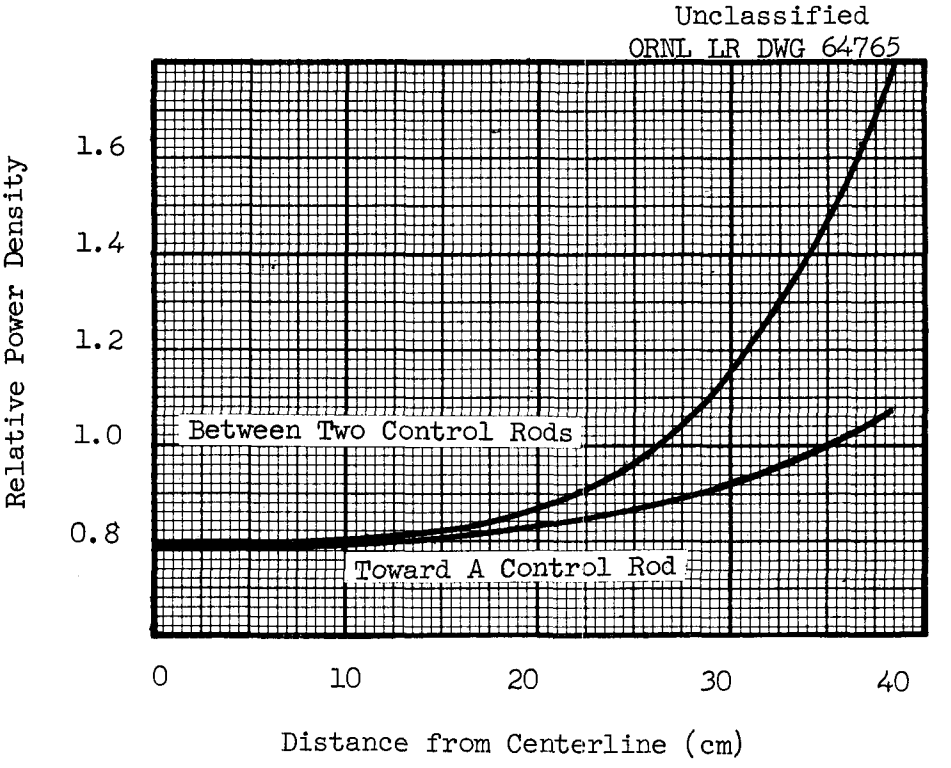

Fig. 6.5. Radial Power Distributions with Control Rods Inserted (Relative to 1.0 for the Entire Core).

specifying that they should give the same absorptions in each energy group as was obtained in the calculation in which the four rods were represented explicitly. Typical power distributions are given in Fig. 6.6. The effects of partial control rod insertion on k and on the ratio of peak-to-average power are shown in Figs. 6.7 and 6.8.

Fast Flux Distribution

The fast flux distribution in the core and inner portions of the reflector is given in Fig. 6.9. The fast flux at the inner surface of the pressure vessel is of particular interest because this quantity is controlling in determining the reflector thickness. In this case the flux of neutrons with energy greater than 0.10 Mev is calculated to be 6×10^9 neutrons/cm^2·sec at the inner surface of the pressure vessel at the reactor midplane. Using as a design criterion that the pressure vessel radiation exposure must not exceed 4×10^{18} neutrons/cm^2, a lifetime of 21 years of full-power (5-Mw) operation is obtained.

Reflector and Shield

The addition of a small amount of boron in the outer few inches of the reflector may have a number of desirable effects, although perhaps introducing some materials development problems. A tentative conclusion has been reached that the outer 4 in. of the reflector should include 0.5 wt % boron. The advantages are (1) reduction, by a large factor, of the gamma-ray heating in the pressure vessel, (2) reduction of biological shield thickness by as much as 2 ft because of a decrease in pressure vessel capture gamma rays, (3) reduction of shield heat load, and (4) reduction, by a large factor, of the pressure vessel activation, which gives a possible advantage in performing major maintenance. Possible disadvantages are (1) the risk of contaminating the core with boron and (2) the reduction of the neutron flux at the location of reactor control and safety instruments outside the pressure vessel. Most of these points are discussed briefly in the following paragraphs.

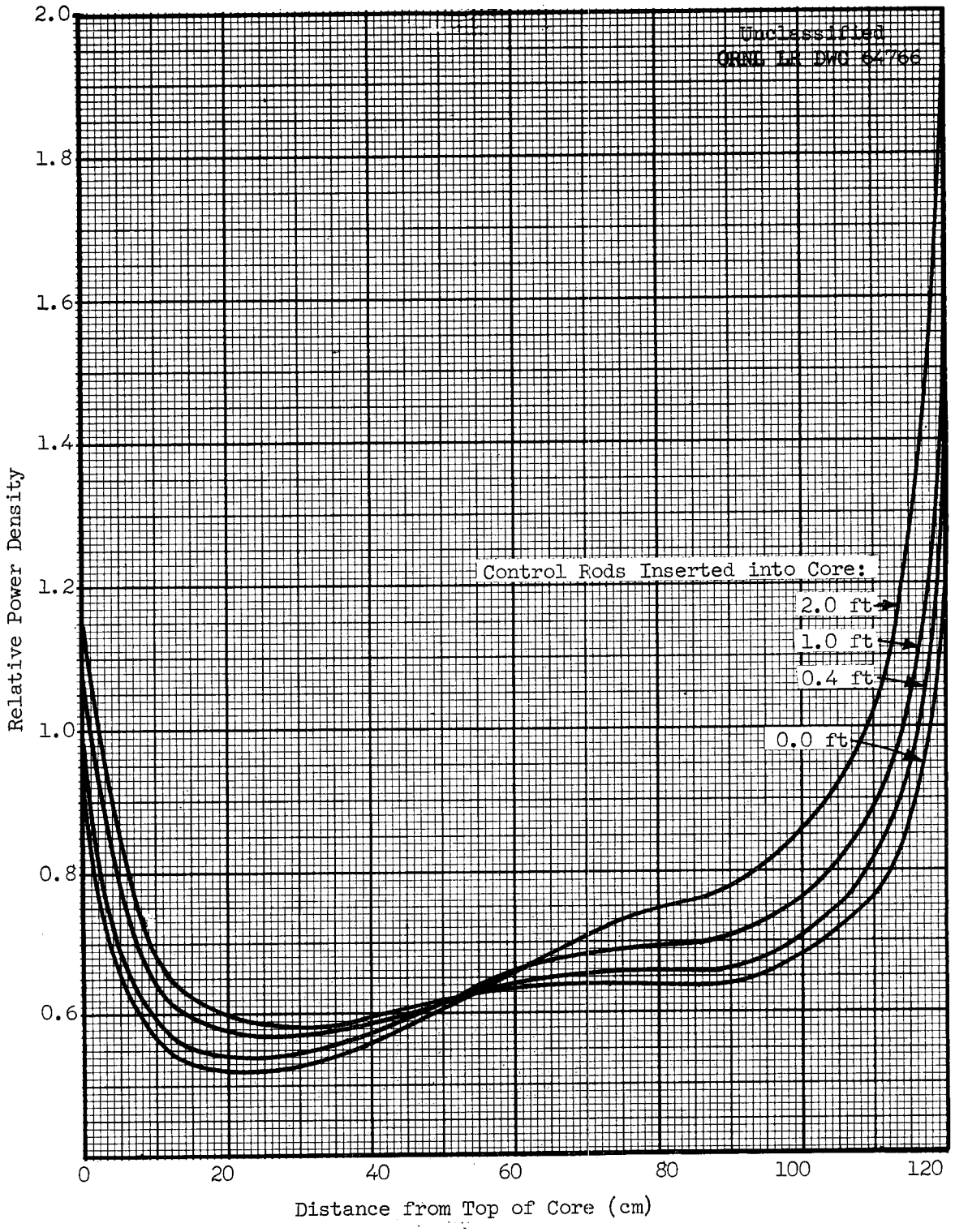

Fig. 6.6. Axial Traverses of Relative Power Density at Centerline as a Function of Control Rod Bank Insertion (Power Densities Normalized to an Average of 1.0 for Entire Core).

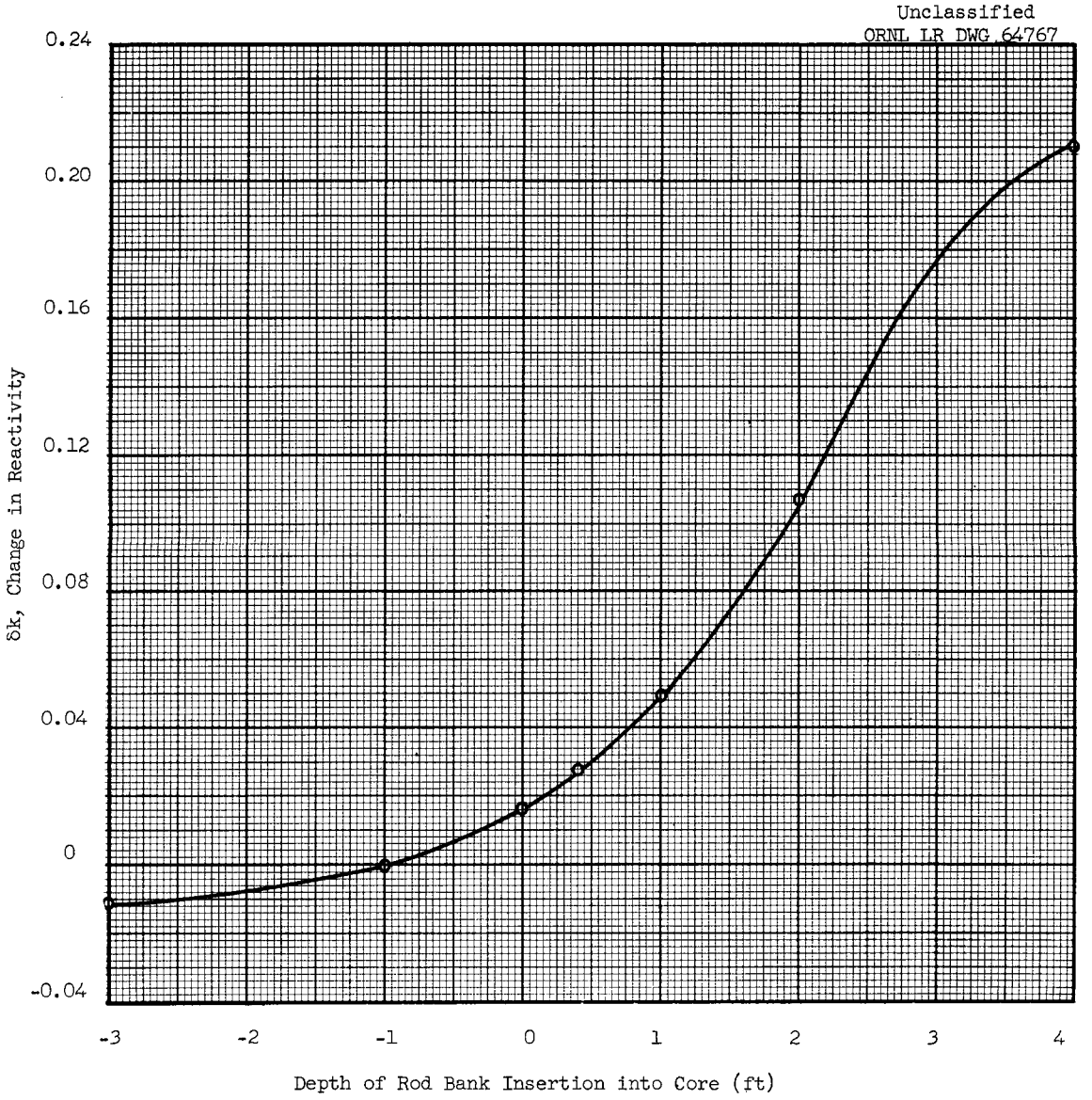

Fig. 6.7. Differential Control Rod Worth (Normalized to Zero at Point of Maximum Allowable Control Rod Withdrawal).

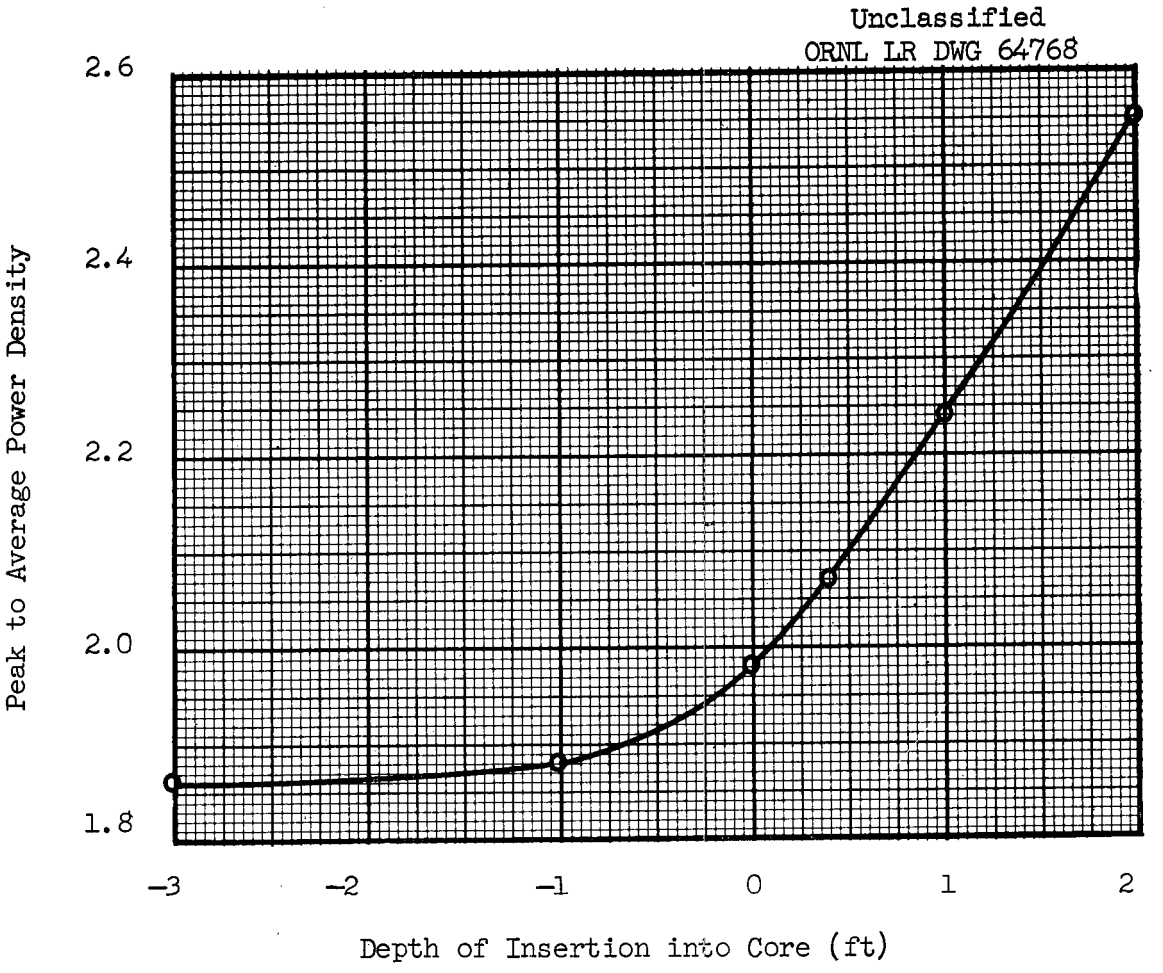

Fig. 6.8. Ratio of Peak to Average Power Density versus Depth of Insertion of Control Rod Bank.

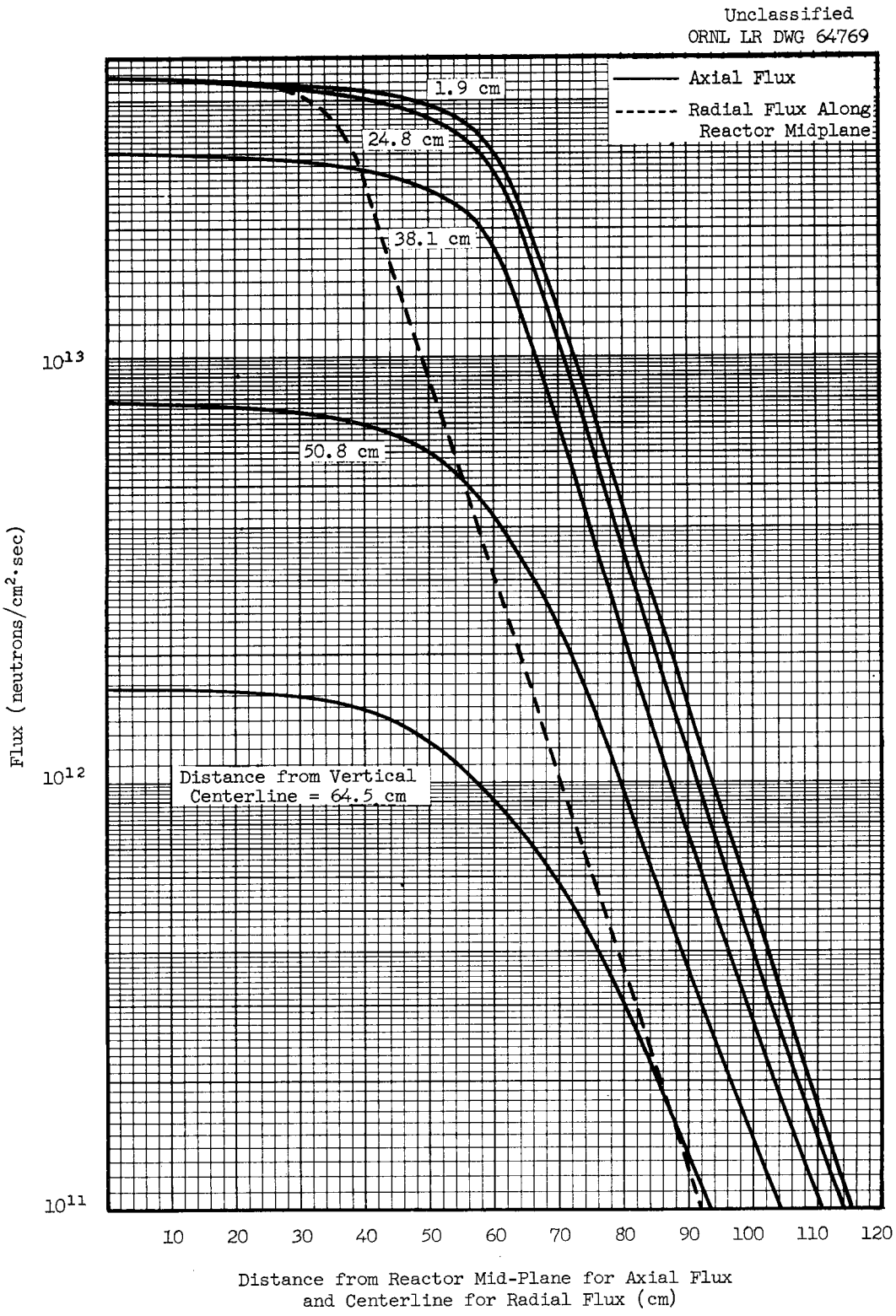

Fig. 6.9. Radial and Axial Flux Traverses for Fast Flux (E > 0.18 Mev) with Control Rods Withdrawn.

The heating from the capture gamma rays in the steel was calculated in three energy groups for the gamma-ray sources. The thermal-neutron flux was taken from the multigroup calculations, in which it was assumed that the reflector contained no boron, in order to obtain a maximum possible heating rate. The heat generation is shown in Fig. 6.10. The thermal stress at the inner surface of the pressure vessel was then conservatively estimated to be only 360 psi, indicating that this factor would not be a problem, even without boron in the reflector.

The dose rate at the outer surface of the main biological shield was estimated for 8- and 9-ft concrete thicknesses, and for 0, 0.5 and 1% boron in the outer 4 in. of the reflector. The results of the calculations are summarized in Table 6.3. The strong effect of small quantities of boron in the reflector on shielding requirements, principally on the reduction in pressure vessel capture gamma rays, is clearly indicated.

Table 6.3. Effect on Dose Rate at Biological Shield Surface of Boron Content of Reflector and Shield Thickness

Source	Dose Rate (mr/hr)		
	No Boron	0.5% Boron	1% Boron
	8-ft Concrete Shield		
Core	0.285	0.285	0.285
Reflector	0.006	0.004	0.004
Pressure vessel	52.920	0.520	0.099
Shield	3.228	0.269	0.215
Neutron penetration	0.304	0.282	0.265
Total	65.74	1.36	0.87
	9-ft Concrete Shield		
Core	0.045	0.045	0.045
Reflector	0.001		
Pressure vessel	9.268	0.091	0.017
Shield	0.483	0.040	0.032
Neutron penetration	0.026	0.025	0.023
Total	9.82	0.20	0.12

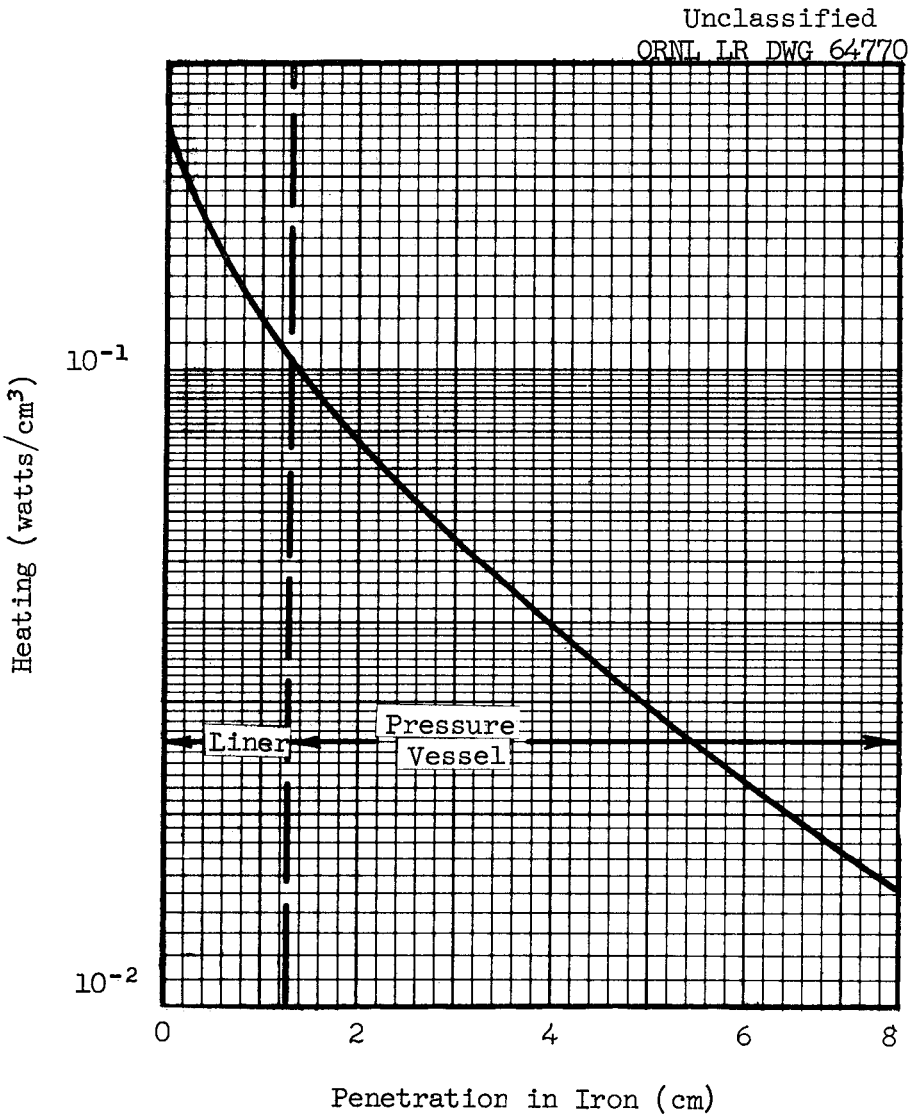

Fig. 6.10. Heating of Pressure Vessel by Iron Capture Gamma Rays.

The calculations for Table 6.3 were based on thermal neutron fluxes from the one-dimensional multigroup calculations. The dose rate from the core was obtained by using an equivalent line source, while the dose rates from the reflector and pressure vessel were obtained by breaking these regions into multiple equivalent plane sources and summing the contributions to the dose rate at the shield surface. The source strength in the shield was estimated by assuming thermal-neutron absorption at one mean free path into the shield and fast-neutron penetration attenuation as predicted by removal-theory cross sections.

The heat load on the inner surface of the biological shield from neutron slowing down in the shield and gamma rays was estimated for each of the boronated cases studied. The results are given in Table 6.4. In any event, the heat load from neutrons and gamma rays is much lower than that from thermal radiation of the uninsulated pressure vessel. The tentatively chosen boron concentration (0.5%) may not give a sufficiently high flux for the compensated ion chambers; a full-power flux of 10^{10} neutrons/cm^2·sec is desired.

Table 6.4. Effect of Boron in Reflector on Heat Load on Biological Shield Inner Surface

Source	Heat Load on Shield (Btu/hr·ft^2)		
	No Boron	0.5% Boron	1% Boron
Core	2.13	2.13	2.13
Reflector	0.37	0.23	0.22
Pressure vessel	161.10	1.99	0.38
Shield capture gammas	27.65	2.32	1.16
Neutron slowing down	0.03	0.03	0.03
Total	191.3	6.7	3.9

Calculations show that little increase in the flux can be expected from a graphite thermal column, so the only way to increase the flux is by decreasing the boron concentration in the reflector. A correlation of maximum flux in the shield vs dose rate at the surface of the 8-ft shield (which also depends primarily on flux in the adjacent pressure

vessel) shows that a flux of 10^{10} neutrons/cm^2·sec can probably be achieved with a surface dose rate of 10 mr/hr. Since areas around the shield are all limited access areas, this dose rate should be satisfactory.

Economic Basis for Reference Design

Previous work at ORNL on a pebble-bed reactor experiment[2] used as a reference design the 350-Mw(thermal) system described by Sanderson & Porter.[3] The Sanderson & Porter design used fuel balls with 10 wt % UO_2 plus ThO_2 (8.8% Th plus U). Therefore, for this study, an analysis of the effect of fuel composition on fuel cycle costs was undertaken in order to define more closely a realistic reference design. While it is realized that some of the cost data are not very well known, it was hoped that a cost analysis could delineate the range of compositions of interest and also point out which costs are most important.

The fuel lifetime for each of a wide range of initial fuel compositions was taken from a recent parametric study of homogeneous, graphite-moderated reactors.[4] It was implicitly assumed that the reactor was operated on an equilibrium fuel cycle, with graded exposure, that the core leakage probability was 0.05, that 0.01 k was available for shim control, and that sufficient reactivity was provided to override peak samarium poisoning.

The fuel cycle cost items included were the following:

1. fabrication of coated particles at $0.175 per gram of uranium plus thorium,
2. fabrication of fuel spheres at $1.10 per sphere,
3. head-end reprocessing at $30.39 per kilogram of uranium plus thorium plus graphite,

---

[2]A. P. Fraas et al., Preliminary Design of a 10-Mw(t) Pebble-Bed Reactor Experiment, ORNL CF-60-10-63 rev. (May 8, 1961).

[3]Sanderson & Porter, Pebble-Bed Reactor, Part 2: System Analysis, S&P 1963 (May 1, 1958).

[4]R. S. Carlsmith and A. M. Perry, Effect of Fission Products on Fuel Reactivity Lifetime, ORNL-TM-41 (Oct. 30, 1961).

4. "Thorex" recovery processing at $34,000 per day for 600 kg of thorium per day or 44 kg of uranium per day, whichever was smaller; this includes one day of turn-around time per day of operation and assumes that the throughput rate is so small that shipments of less than 8 days plant capacity are made,[5]
5. U^{235} makeup at $13.70 per gram,[5]
6. thorium makeup at $0.017 per gram ($7.72 per pound),[5]
7. use charge on the U^{235} at 4.75% per year; the amount of fissionable material included[5] was (a) the equilibrium amount of U^{233} plus U^{235} in the core, (b) 275 days supply of U^{235} in fresh fuel being fabricated, and (c) 275 days supply of U^{233}, U^{235}, and Pa^{233} in spent fuel being reprocessed,
8. the working capital charge on thorium at 12.5% of its value,[5]
9. the working capital charge on fuel fabrication cost (items 1 and 2) at 60% of 12.5% of its cost,[5]
10. credit for all U^{233}, U^{235}, and Pa^{233} recovered, and
11. credit for all thorium recovered.

A thermal efficiency of 40% and a plant factor of 80% were assumed. In any case in which the total cost of items 3, 4, and 7c exceeded the credit from items 10 and 11, the case was designated a "throw-away cycle" and all costs and credits for these items were omitted. Most of the cases of interest were throw-away cycle cases, because of the high cost of the head-end reprocessing and the low concentration of recoverable material. The inclusion of items 8 and 9 should be noted. These are fixed-cost items which are often not associated with the fuel cycle. However, it is appropriate to consider their effect on optimum fuel composition whether they are included in the fuel cycle cost or elsewhere.

The costs for 1 1/2-in.-diam fuel spheres are given in Figs. 6.11, 6.12, and 6.13. In conjunction with the fuel costs it is necessary to consider an additional parameter, the ratio of peak-to-average power density caused by depletion of the macroscopic fission cross section during burnup (independent of spatial variations of the flux), as indicated in Figs. 6.14, 6.15, and 6.16. A high value for this power ratio implies a low average core power density and, consequently, excessive capital costs.

The range of fuel compositions of interest is chosen by specifying, somewhat arbitrarily, that the fuel cycle cost be less than 1.8 mills/kwhr

[5]Nuclear Power Plant and Cost Evaluation, Vol. 4, USAEC, Division of Reactor Development.

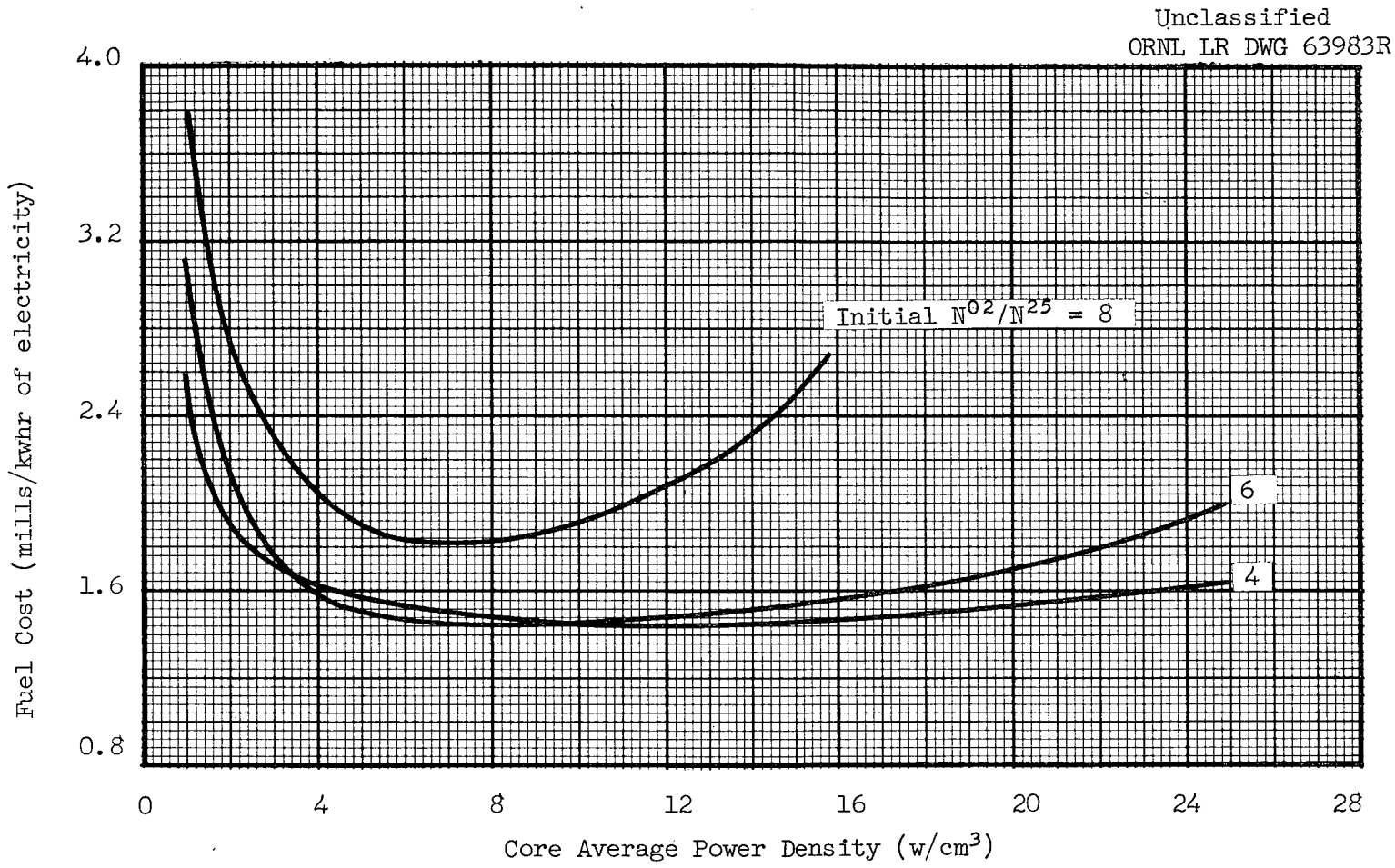

Fig. 6.11. Fuel Costs for 1.5-in.-diam Spheres with an Initial Carbon-to-U^{235} Atom Ratio of 2000.

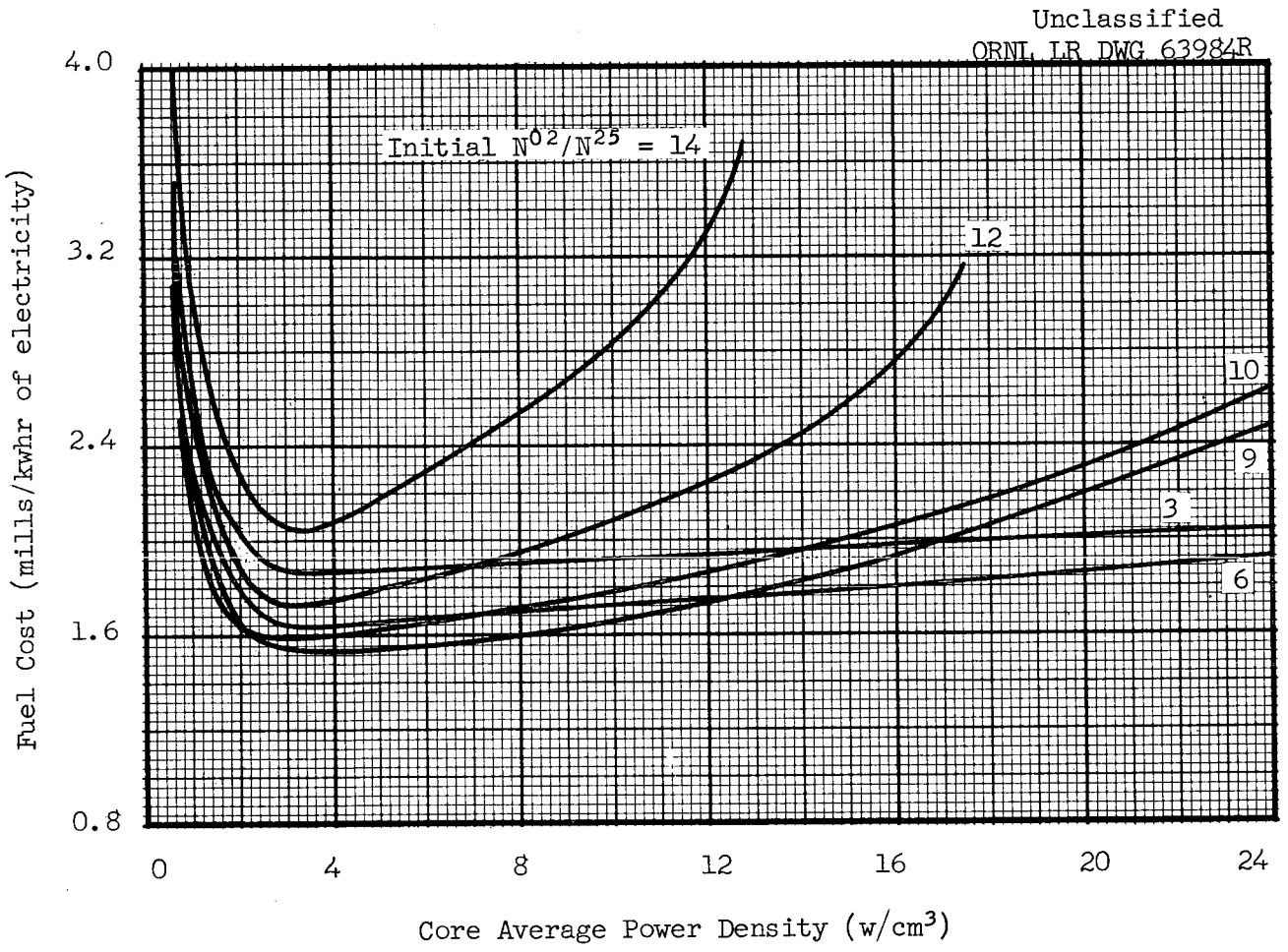

Fig. 6.12. Fuel Costs for 1.5-in.-diam Spheres with an Initial Carbon-to-U^{235} Atom Ratio of 4000.

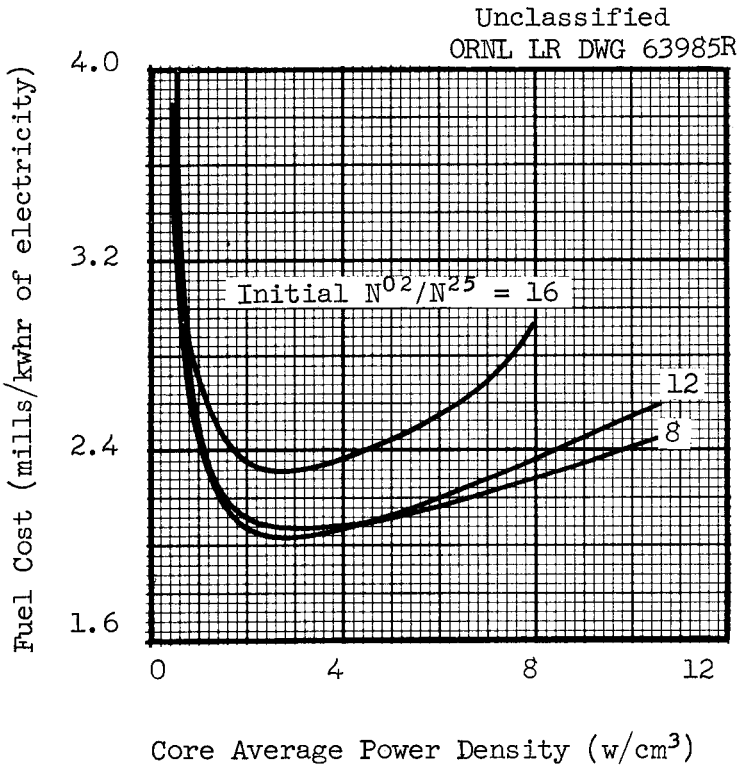

Fig. 6.13. Fuel Costs for 1.5-in.-diam Spheres with an Initial Carbon-to-U^{235} Atom Ratio of 8000.

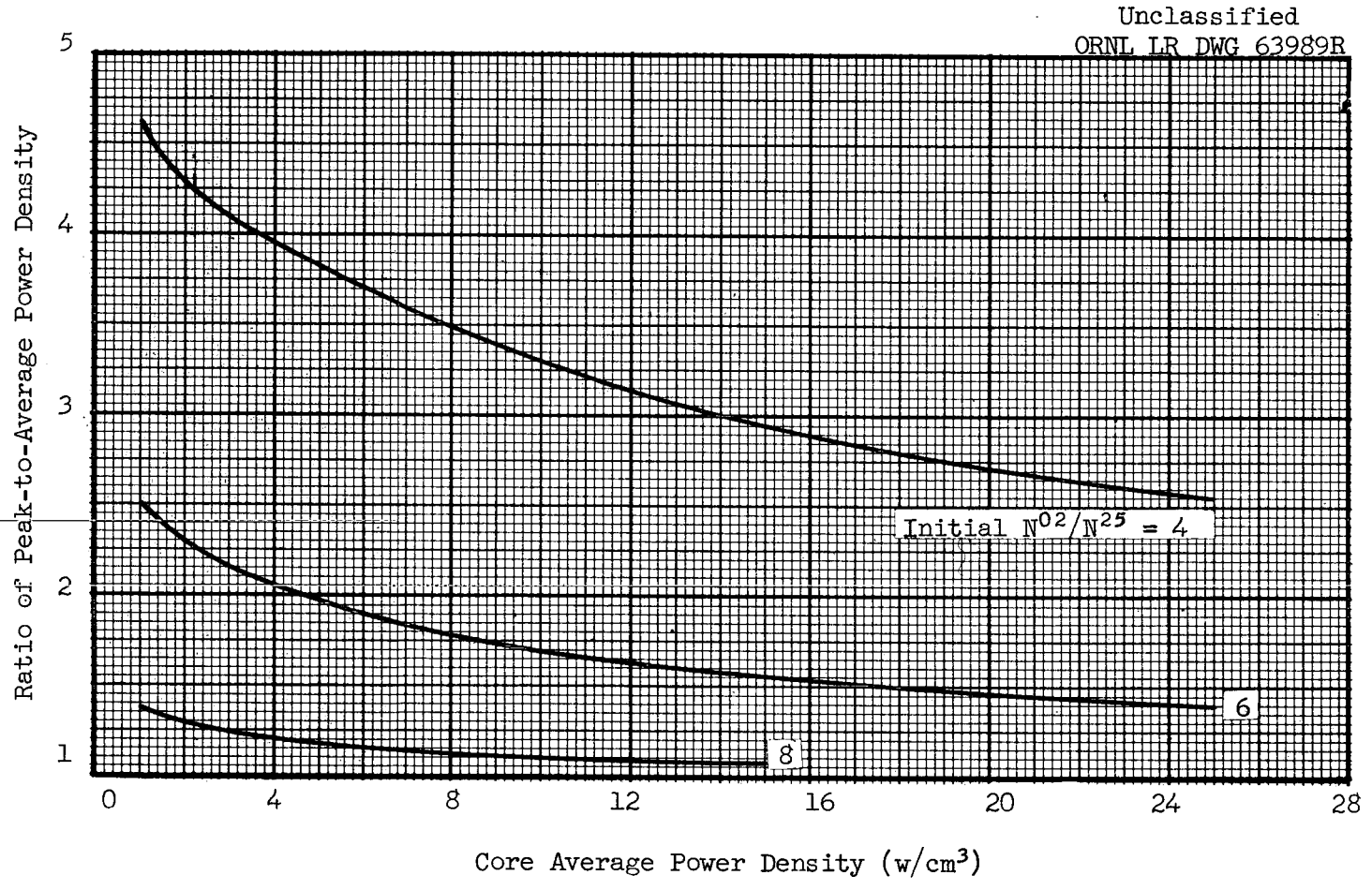

Fig. 6.14. Effect of Burnup on Peak-to-Average Power Density Ratio as a Function of Initial Thorium-to-Uranium Ratio and Average Power Density; Graded Exposure, Initial Carbon-to-U^{235} Ratio of 2000.

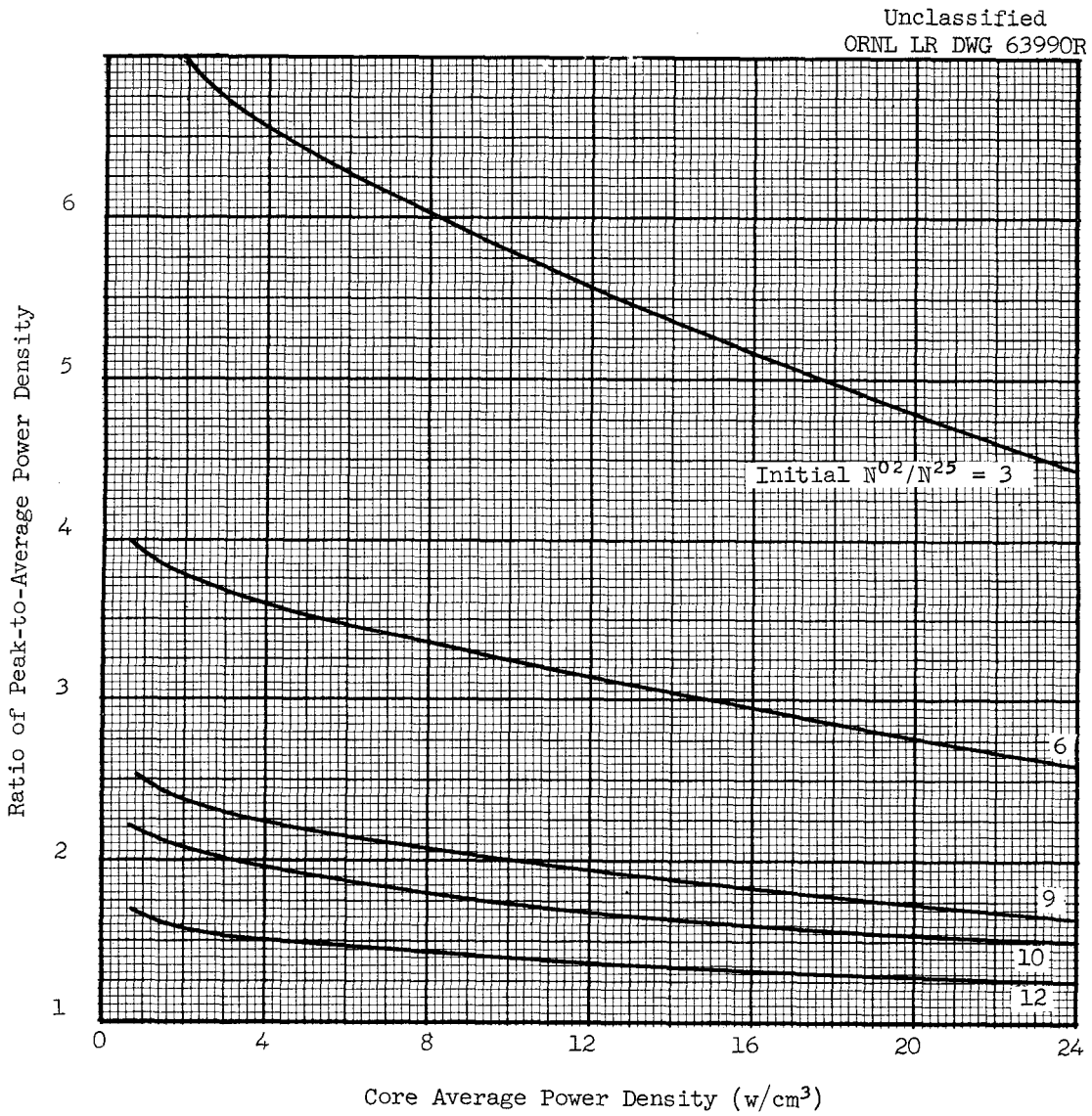

Fig. 6.15. Effect of Burnup on Peak-to-Average Power Density Ratio as a Function of Initial Thorium-to-Uranium Ratio and Average Power Density; Graded Exposure, Initial Carbon-to-U^{235} Ratio of 4000.

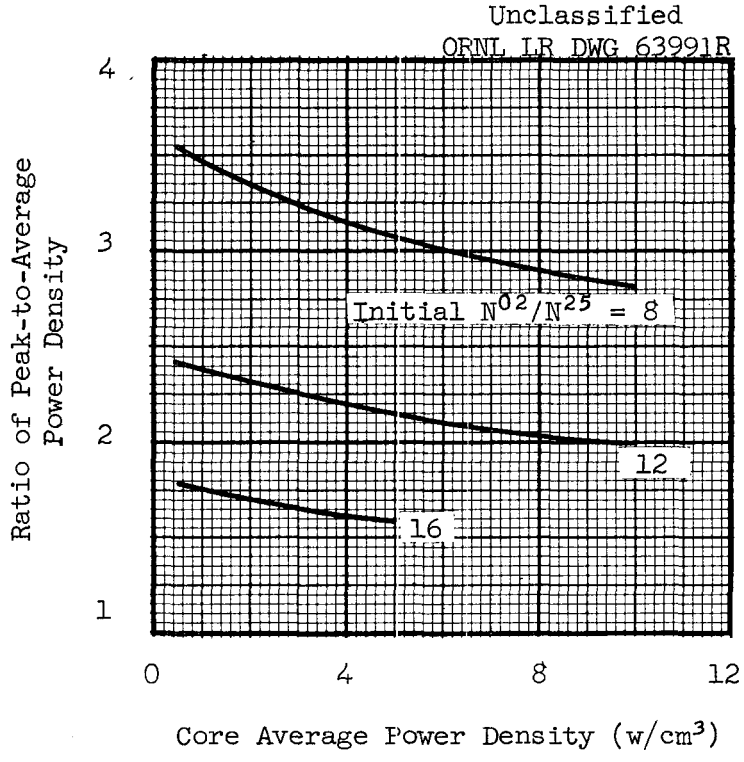

Fig. 6.16. Effect of Burnup on Peak-to-Average Power Density Ratio as a Function of Initial Thorium-to-Uranium Ratio and Average Power Density; Graded Exposure, Initial Carbon-to-U^{235} Ratio of 8000.

of electricity and the peak-to-average power ratio from burnup be less than 2.0. The fuel compositions which meet these conditions are:

N^C/N^{25}	N^{02}/N^{25}	Uranium + Thorium (wt %)
4000	8–12	4.2–5.9
2000	5.5–7	5.9–7.2

Fuel cycle costs were also computed for 2 1/2-in.-diam fuel spheres on the same basis as that used for analysis of the 1 1/2-in.-diam spheres. An additional, slightly dubious, assumption was made that the fuel sphere fabrication cost would remain $1.10 per sphere, regardless of the sphere size. The results are given in Figs. 6.17, 6.18, and 6.19. The principal difference in cost between the reactors with 1 1/2-in.-diam spheres and those with 2 1/2-in.-diam spheres is an advantage in the order of 0.4 mills/kwhr of electricity for the latter. The optimum fuel composition is shifted slightly toward the more lightly loaded systems (higher carbon-to-uranium ratio), but the range of interesting fuel compositions is essentially the same.

Although the fuel costs for both sphere sizes have been plotted over a wide range of power densities, it should be kept in mind that not all these power densities are attainable. In an upflow core the power density is limited by bed floatation. In this case the smaller spheres would impose a lower limit than the larger spheres. There are also likely to be limitations on maximum sphere temperature and on maximum sphere power density as a result of thermal stresses. These limitations, which have not yet been precisely determined, would be more severe with larger spheres.

For typical reference design points near the optimum, the cases given in Table 6.5 may be considered. The costs in this table are the fuel cycle costs only, that is, the working capital charges on thorium and fuel fabrication cost which were included in the previous discussion are excluded here.

The two cost items which seem most uncertain are the head-end reprocessing (dissolving the uranium and thorium from spent fuel elements) and fuel fabrication, including coated-particle fabrication. With both items the uncertainty arises from the fact that no large-scale experience

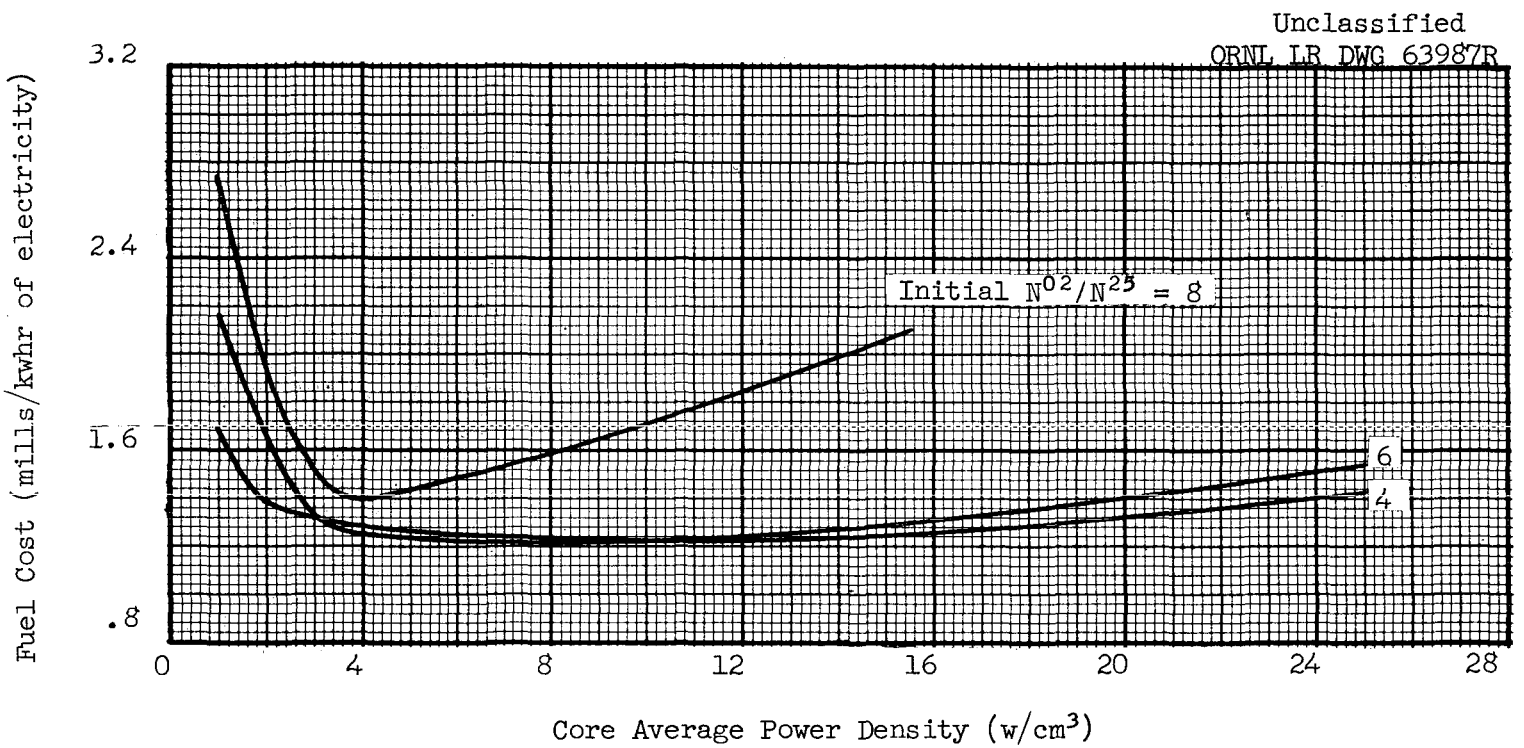

Fig. 6.17. Fuel Costs for 2.5-in.-diam Spheres with an Initial Carbon-to-U^{235} Atom Ratio of 2000.

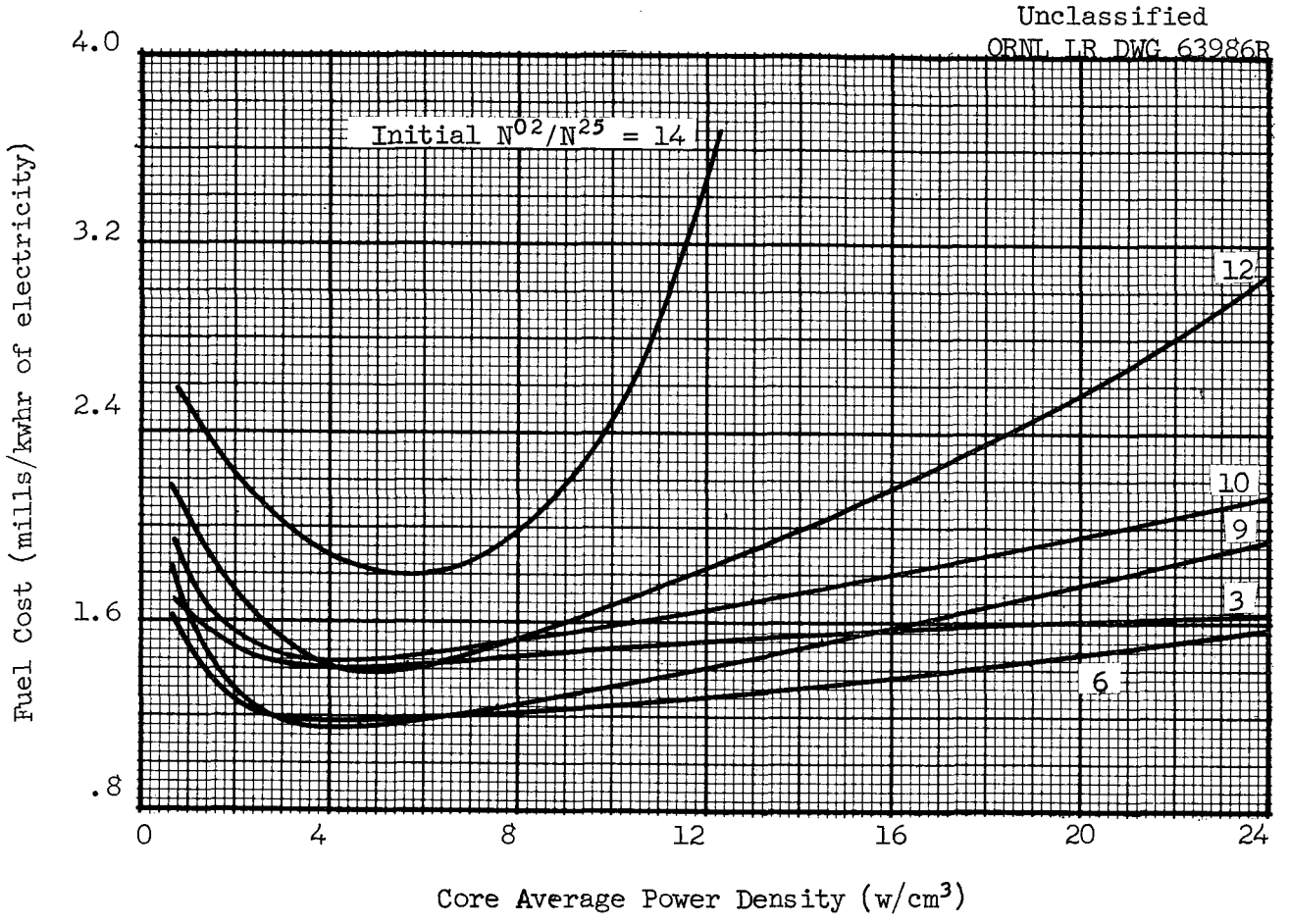

Fig. 6.18. Fuel Costs for 2.5-in.-diam Spheres with an Initial Carbon-to-U^{235} Atom Ratio of 4000.

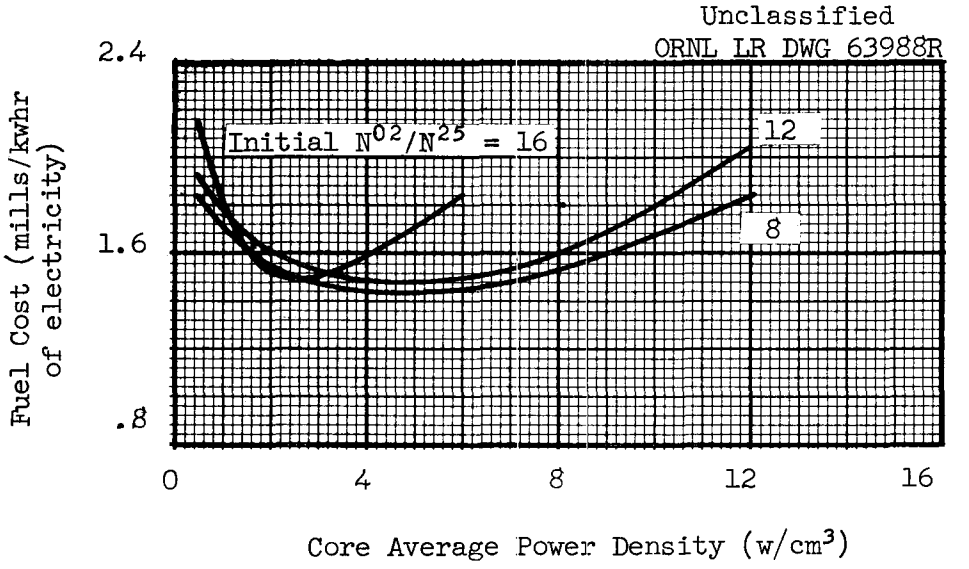

Fig. 6.19. Fuel Costs for 2.5-in.-diam Spheres with an Initial Carbon-to-U^{235} Ratio of 8000.

Table 6.5. Pebble-Bed Reference Designs

Fuel sphere diameter, in.	1.5	2.5	1.5	2.5
N^C/N^{25} in fresh fuel	4000	4000	2000	2000
N^{02}/N^{25} in fresh fuel	10	10	6	6
Uranium plus thorium in fresh fuel, wt %	5.0	5.0	6.3	6.3
Core average specific power, Mw/kg of fissile material	3.1	3.1	2.8	2.8
Core average power density, w/cm^3	9.0	9.0	16	16
Core average conversion ratio	0.64	0.64	0.61	0.61
Fuel cycle cost, mills/kwhr of electricity	1.6	1.5	1.4	1.3
Peak-to-average power ratio from burnup	1.7	1.7	1.5	1.5
Fuel lifetime, fissions/initial fissile atom	1.5	1.5	1.2	1.2
Fuel lifetime, fission/cm^3 of fuel sphere	3.1×10^{19}	3.1×10^{19}	5.0×10^{19}	5.0×10^{19}

is available upon which to base costs — and indeed, the exact processes have not been defined. Of the two, the fuel fabrication costs appear to have the most decisive effect on the system. A different ratio of coated particle cost to fuel sphere cost would lead to distinctly different values for optimum fuel composition. A very much higher fuel fabrication cost could make this type of reactor impractical.

7. COOLANT SYSTEM ACTIVITIES AND IMPURITIES

The helium coolant of the PBRE will be contaminated by both radioactive and chemically active impurities. The concentration of radioactivity in the coolant has significance in two respects: (1) the circulating activity itself presents shielding and hazards problems, and (2) activity deposited from the coolant onto surfaces adds to the shielding requirements and increases the difficulty of maintenance. The major radioactive contamination will consist of fission products and their daughters, although there will also be relatively insignificant quantities of tritium, activated corrosion products, and activated coolant impurities. In determining the requirements for a fission-product cleanup system, specific attention was given to xenon, krypton, and iodine, which are expected to contribute strongly to the coolant stream activity. Other species may also be quite important, for example, strontium, with regard to hazards, or barium and cesium, with regard to shielding and maintenance; not enough is known about their mobilities, however, to permit consideration of their behavior in the design of the purification system.

The chemically active contaminants may consist of (1) oxidizing impurities, such as water, carbon dioxide, and oxygen; (2) reducing impurities, such as hydrogen and carbon monoxide; and (3) relatively inert impurities, such as nitrogen. These impurities are introduced by graphite outgassing, by system inleakage during normal operation, by makeup helium, and by the necessity for opening the primary system during maintenance and inspection. The major restriction on the concentrations of chemical contaminants in the PBRE is associated with limiting damage to the fuel and the reflector. At the low contaminant levels imposed by graphite, there should be no problems of compatibility between the coolant and metals.

Purification System

The helium purification system provided for the PBRE and described in Section 3 is composed of a fission-product delay trap and a chemical cleanup system that operate in parallel. A portion of the total reactor

coolant system flow is diverted through each path and them combined and returned to the coolant system by an auxiliary compressor. The fission-product delay trap is composed of charcoal beds that operate at room temperature. The chemical cleanup system contains a heated CuO bed for the oxidation of CO and H_2, followed by a room-temperature molecular-sieve adsorber for the removal of CO_2 and H_2O.

Gaseous Fission-Product Activity

In a previous study of the PBRE,[1] the thermal power of the reactor was 10 Mw, the coolant pressure was 1000 psia, the main coolant flow rate was 11 lb/sec, and the helium was heated from 550 to 1250°F in passage through the core region. Based on 1% bypass flow through the fission-product cleanup system, the delay trap was sized to give a 30-min holdup time for krypton, a 6-hr holdup time for xenon by dynamic adsorption in the charcoal bed, and irreversible removal of a minimum of 99.9% of the iodine contained in the bypass stream. Deposition of iodine on other surfaces was not considered, although some adsorption may occur on the colder surfaces in the system.

At the operating conditions currently proposed for the PBRE, that is, a thermal power level of 5 Mw, a coolant pressure of 500 psia, a helium flow rate of 5.4 lb/sec, a temperature rise across the reactor core from 550 to 1250°F, and 1% bypass flow to the delay trap, an adsorber bed of the size previously considered would have essentially the same holdup times and minimum iodine-removal efficiency. The decontamination factors which would be obtained for xenon, krypton, and iodine, and the system activity levels based on the fission-product-release rates given in Section 10 are listed in Table 7.1. Since the turnover time of the reactor helium inventory through the fission-product trapping system is approximately 20 to 25 min, the delay trap will have little effect on the activity due to short-lived (<5-min half-life) radioactive species in the coolant. In addition, the activity from the very long-lived species,

[1]A. P. Fraas et al., Preliminary Design of a 10 Mw(t) Pebble Bed Reactor Experiment, ORNL CF-60-10-63, rev. (May 1961).

Table 7.1. Decontamination Factors and System Activity Levels

Isotope	Half-Life	Activity in Coolant (curies)		Decontamination Factors
		Without Purification	With Purification	
Kr^{83m}	114 m	1.7	0.82	2.0
Kr^{85m}	4.36 h	7.9	3.8	2.1
Kr^{85}	10.6 y	28.6	20.0	1.4[a]
Kr^{87}	78 m	7.7	3.9	2.0
Kr^{88}	2.77 h	15.5	7.5	2.1
Xe^{131m}	12 d	1.7	0.14	11.7
Xe^{133m}	2.3 d	3.0	0.21	14.0
Xe^{133}	5.27 d	198	13.9	14.3
Xe^{135}	9.13 h	62	5.3	11.8
I^{131}	8.05 d	102	0.16	630
I^{132}	2.4 h	102	14.7	6.9
I^{133}	20.8 h	75	1.1	69
I^{134}	52.5 m	17.8	4.7	3.8
I^{135}	6.68 h	38	1.7	23
	Total	661	78	

[a]Effect of 0.1% per day leakage.

typified by 10.6-y Kr^{85} will not be significantly reduced by the delay trap because practical holdup times will be short compared with the half-lives. The delay trap will be of significant value in its effect on the noble gases having half-lives of the same order of magnitude as the economically obtainable delay times and on those species which are strongly adsorbed on charcoal (for example, the iodine isotopes). Other radioactive species that have condensed or reacted with other materials present in the helium circuit will also be efficiently filtered by the charcoal bed if they are carried to this point by the helium stream. It is felt, however, that most of these fission products will be deposited at various points in the coolant circuit as carbides, metals, or oxides, and that only a small portion of these materials maintained in suspension in the gas stream will ever enter the fission-product trap.

It is possible to reduce the activity in the coolant by increasing the fraction of coolant bypassed to the cleanup system or by increasing

the delay time of the charcoal beds. A significant improvement could not be made by increasing the side-stream flow, however, without going to an undesirably large bypass fraction. It does not appear advantageous to make an appreciable increase in delay time. Increasing the delay by a factor of 10, which would require a tenfold increase in the size of the charcoal trap, would only reduce the total activity of the nuclides listed in Table 7.1 from 78 to 51 curies. Provision of a system, such as a refrigerated or a liquid-nitrogen-cooled charcoal trap, that would give essentially infinite holdup times would reduce the total-activity value of Table 7.1 only to 29 curies. Since there will be activity deposited in the coolant system that is not affected by side-stream purification at all, it does not appear worthwhile to provide a more elaborate purification system than the one selected.

Deposited Fission-Product Activity

Detailed knowledge of the types and amounts of activity that will deposit throughout the coolant system would be of great value in the design of the PBRE. Information on specific nuclides is needed so that gamma energy levels and half-lives can be considered in evaluating shielding requirements and planning maintenance procedures; knowledge of chemical forms would be helpful in preparing decontamination procedures. Unfortunately, there is little information available on the behavior of nongaseous fission products, and much of what is available appears to be contradictory. Thus the present inexact knowledge of escape of activity from the fuel is compounded by greater uncertainties regarding the mobility and deposition of activity in the system.

The deposition problem is discussed in Section 16 and a research program for obtaining the needed data is outlined. Operation of the PBRE will, of course, provide valuable information on activity distribution in a reactor, and this represents an important objective of the experiment. To facilitate the study of activity deposition in the PBRE, ion chambers will be mounted at typical locations throughout the reactor system to record gross activity buildup on the primary piping, reactor

components, charcoal beds, etc.; a multichannel analyzer and scintillation detector will be arranged so that sections of the heat exchanger and flow system can be probed after shutdown to identify longer lived fission-product species (the analyzer will also be used to identify activities in the decontamination solutions); removable dummy tubes will be installed in the heat exchanger to give more exact knowledge of plateout; and a charged-wire analyzer will continuously monitor the coolant gas and identify the fission products present.

In spite of the many uncertainties involved, it is useful to estimate the level of deposited activity in order to establish the magnitude of the unshielded radiation to be encountered in maintenance of the PBRE. This has been done making the following assumptions:

1. The nuclides Br, I, Kr, Xe, Rb, Cs, Se, Te, Sr, Ba, and Ce escape from the fuel at the rate given by Eq. (1), Section 10, with the half-life used in the equation being the sum of the half lives of the nuclide and its mobile precursors.[1]

2. Except for the noble gases, all the elements which escape and their daughters deposit on surfaces in the primary system.

3. The purification system has no effect on activity deposition.

4. The reactor had operated at full power for two years.

Table 7.2 lists the activities of those gamma enitters (of all energies) having chain yields exceeding 0.1% and half-lives less than 10^5 y which the analysis indicates would be deposited in the primary system. The values in Table 7.2 are conservative in that equal mobility is ascribed to Ce, Ba, Sr, and the other listed nuclides and to the noble gases; no allowance is made for the effect of the purification system (in contrast, for example, with the assumption made regarding iodine in estimating circulating activity).

If the activity indicated in Table 7.2 were deposited uniformly on all metal surfaces in the PBRE (~1500 ft^2), the dose rate outside one of the lines between the blower and heat exchanger, for example, would be about 35 r/hr during operation. Because much of the dose rate is contributed by long-lived hard-gamma activity, the level would only fall to 26 r/hr one day after shutdown and to 22 r/hr after one week. Results

Table 7.2. Fission Products Deposited in System

Nuclide	Ratio of Release Rate to Birth Rate, R/B	Deposited Activity (curies)		
		During Operation	After One Day	After One Week
	$\times 10^{-3}$			
Se-85	0.04	0.35		
Br-83	0.1	2.0		
-84	0.04	2.1		
-87	0.007	0.54		
Rb-88	0.1	17		
Sr-91	0.1	46	14	
Y-90	30.0	320	320	320
-91m	0.06	5.9	3.5	
-91	0.06	15	15	15
-92	0.9	25	2.2	
-93	0.02	5.9	1.8	
-94	0.01	3.0		
Zr-95	0.0001	0.27	0.27	0.22
-97	0.0001	0.27	0.13	
Nb-93m	0.02	1.9	1.9	1.9
-95	0.02	0.27	0.27	0.27
-97m	0.0001	0.27	0.13	
-97	0.0001	0.27	0.13	
Sb-126	0.1	0.81		
-127	0.6	6.2	6.2	2.1
Te-129m	1.7	24	24	21
-129	0.1	0.59		
-131m	0.3	5.9		
-131	0.05	6.5		
-132	0.1	3.2	2.5	
-133m	0.06	12		
-133	0.06	16		
I-131	1.0	120	110	85
-132	0.1	32	29	16
-133	0.2	73	44	
-134	0.07	25		
-135	0.1	40	6.5	
Cs-138	0.5	3.2		
Ba-137m	30.0	380	380	380
-139	0.07	17		
-140	1.0	270	250	190
La-140	1.0	270	260	230
-141	0.03	8.4		
-142	0.02	5.1		
Ce-141	5.2	1300	1300	1300
-143	0.3	95	66	
-144	5.0	1300	1300	1300
-146	0.02	4.1		
Pr-144	5.0	1300	1300	1300
-146	0.02	4.1		
	Total	5700	5400	5100

from the few plateout experiments[2-5] performed to date suggest that most of the activity actually will not be distributed uniformly, as assumed, but will be deposited principally in cooler regions in the core and reflector and on low-temperature surfaces, such as the heat exchanger. This is not fully reassuring, however, with regard to a component such as the blower, since in some cases accumulation of activity in high-turbulence flow-separation regions has been observed.[4]

Considering all the uncertainties in this analysis, little can be concluded with confidence. The results do indicate, nevertheless, that radiation levels will be low enough for semiremote maintenance of most PBRE components to be practical without decontamination. Whether direct approach to components exposed to the primary helium will be possible cannot be determined until more knowledge is obtained of fission-product transport and deposition phenomena, as well as fission-product escape from the fuel and the feasibility of in situ decontamination.

Oxidizing Impurities

Coated Fuel

The allowable level of oxidizing impurities in the PBRE coolant stream is primarily a function of the amount of graphite oxidation which can be sustained in the core region without compromising the operation of the reactor system. If the fuel spheres are protected by an oxidation-resistant coating, the moderator graphite is the primary target of attack. Since the moderator graphite is massive compared with the fuel spheres, has a generally lower operating temperature, and a lower surface-to-volume ratio, coolant purity is less critical in this case. If, on the other

---

[2]P. K. Conn et al., Isotope Deposition Hazards in Gas-Cooled Reactors, Annual Meeting ANS, Gatlinburg, Tenn. (June, 1959).

[3]J. M. Tobin et al., An Experience in the Plateout of Fission Products from Helium Gas Stream, TID-7610 (October, 1960).

[4]M. F. Osborne, Fission-Product Deposition and Decontamination of BNL Gas-Cooled Loop, ORNL CF 61-7-49 (July, 1961).

[5]M. N. Myers, Laboratory Plate-Out Study I: Special Loop Installed in CTF During IET 21 and 25, APEX-617 (April, 1961).

hand, uncoated fuel is used, the fuel balls themselves must be assumed to absorb most of the damage, and coolant purity becomes extremely critical.

In a detailed design study of the purification system[6] for a PBRE using coated fuel spheres, the following assumptions were made:

1. Water inleakage was limited to 0.1 lb/day.

2. The allowable graphite burnup was 1% of the core, exclusive of fuel spheres, during a two-year period.

3. Steady-state graphite outgassing was 0.003 ft^3 (STP)/ft^3 of graphite, and the gas was composed of 50% CO_2, 10% CO, 15% H_2O, and 25% hydrocarbons.

4. Oxidation by H_2O was irreversible according to the equation

$$H_2O + C \rightarrow H_2 + CO \quad .$$

5. Oxidation by CO_2 was controlled by the rate of mass transfer across a gas film.

6. The CO was completely converted to CO_2 in the cooler regions of the helium system.

Based on these assumptions, an allowable CO_2 level of 21 ppm (by volume) was determined for the coated-fuel-sphere system. Maintaining this CO_2 concentration and limiting water inleakage to 0.1 lb/day seems to be practical for the reactor system under consideration; however, the difficulty of providing a completely reliable coating for the fuel spheres dictates examination of the coolant purity requirements when using uncoated fuel.

Uncoated Fuel Spheres

In the study of the PBRE using uncoated fuel spheres, reaction rates of H_2O and CO_2 obtained by British workers in the field of high-temperature reactor technology were used to determine the allowable H_2O and CO_2 levels, based on the following assumptions:

---

[6]B. C. Finney, C. D. Scott, J. C. Suddath, The Helium Purification System for the Proposed Pebble Bed Reactor Experiment, ORNL CF-60-10-31 rev. 1 (October, 1960).

1. The allowable graphite loss from the fuel spheres is 1% during a normal life span of three years.

2. Reaction rates are a direct function of impurity partial pressure.

3. One per cent of the main coolant flow is diverted to a chemical purification system having a removal efficiency of 50% for H_2O and CO_2.

4. The $CO \rightarrow CO_2$ back reaction in the cooler region of the helium circuit is considered complete in one case and negligible in another.

5. Water inleakage is considered to be the only source of CO_2, H_2O, and CO during normal operation.

Based on these assumptions, the equilibrium CO_2 and H_2O levels in the helium coolant are those given in Table 7.3. It may be seen that allowable oxidizing impurity levels are quite low when prevention of excessive damage to uncoated fuel spheres is the primary criterion. Special analytical techniques would be required to sense the helium purity at these low impurity levels; this requirement is discussed further in Section 16.

Table 7.3. Allowable Water Inleakage Rate and Oxidizing Impurity Levels for PBRE Using Uncoated Fuel Spheres

	$CO \rightarrow CO_2$ Reaction	
	Complete	Negligible
H_2O, ppm by volume	0.0052	0.0162
CO_2, ppm by volume	0.172	0.068
H_2O inleakage, g/day	1.84	5.8
Ratio of H_2O to CO_2 damage	1/3	2/1

The primary control exercised on fuel-sphere damage would be derived from designing the helium coolant system to essentially eliminate water inleakage during normal operation. The purification system will be useful in removing water and CO_2 during periods of graphite outgassing and after maintenance shutdowns, but during normal operation, the core graphite must be considered as the primary "getter" for these two impurities when

they are present. As a consequence of this "gettering" effect, the pebble-bed system tends to be self-cleaning, and the design of the purification system does not need to provide for effective operation at extremely low oxidizing impurity levels if water inleakage is held to the allowable value.

Nonoxidizing Impurities

The maximum levels of the nonoxidizing impurities H_2, N_2, and CO in the helium coolant are affected by several factors. In a discussion of helium purity for high-temperature gas-cooled reactors, British investigators bring out the following points:

1. Hydrogen and CO are capable of reducing oxide scale formed on the coolant piping during periods of high-level contamination resulting from graphite outgassing or the entrance of air into the system. Thus, these two reducing impurities can contribute to graphite damage by CO_2 and H_2O formation.

2. Hydrogen and CO are effective in surpressing the reaction of H_2O and CO_2 with graphite.

3. Based on thermodynamic calculations, the reactions

$$CO + H_2 \rightarrow C + H_2O$$

$$CO + 3H_2 \rightarrow CH_4 + H_2O$$

should not be of major importance in a high-temperature gas-cooled reactor if the impurity contents are kept below 100 ppm by volume.

4. Carbon transport from the cooler to the hotter portions of the helium circuit by the reaction

$$C + 2H_2 \rightleftharpoons CH_4$$

is extremely slow compared with the carbon transport to cooler regions resulting from the graphite oxidation process.

5. Carbon transport by the reaction

$$H_2 + 2C + N_2 \rightleftharpoons 2HCN$$

is important where temperatures exceed 1100°C and HCN formation becomes of significance.

6. Chromium-bearing steels may be oxidized and carburized by CO and by traces of CO_2 and H_2O. Embrittlement of steels by H_2 should not be a problem at low-impurity partial pressures.

Since the allowable levels of CO_2 and H_2O are very low when using uncoated fuel balls, the principal factor in determining allowable H_2 and CO levels might be the generation of oxidizing impurities by the reduction of iron oxide scale in the coolant system. It would be beneficial to reduce the formation of this scale by measures designed to minimize exposure of the piping system to evolved impurities and by preventing the entry of air during system maintenance.

On the basis of mass transfer rates measured by other investigators at 20 atm, CO and H_2O concentrations of 100 ppm each would result in graphite mass transfer equivalent to approximately 1/25 of the allowable loss from the fuel spheres (1% in three years). These values are in rough agreement with unpublished British mass transfer measurements for a similar system. The former results incorporate both the disproportionation reaction of CO and the combination reaction of CO and H_2 and indicate the latter to be more important to carbon deposition, particularly at higher H_2 concentrations.

In spite of the favorable condition indicated by those specific results, there is still much uncertainty about the possibility of appreciable mass transfer. Results forthcoming from experimental programs in progress or planned at several installations will aid in evaluation of the problem.

Coolant Purity Requirements

The tentative allowable coolant impurity specifications for the PBRE, based on the above considerations, are listed in Table 7.4. Further work

Table 7.4. Allowable Impurities in PBRE Coolant

Impurity	Allowable Concentration (ppm by volume)
H_2O	$\ll 1$
CO_2	<1
O_2	0
CO	<10
H_2	<10
N_2	<50

will be required to define exact limits for an unclad fuel sphere system and to establish whether such limitations are practical in an operating reactor. Investigations along these lines may establish that it is mandatory to provide some type of protective coating for the fuel, especially if localized attack at regions of maximum temperature is expected.

Impurity Sources

Major sources of short-term high-contamination levels in the coolant will be graphite outgassing and entry of air when the system is opened for maintenance. Since graphite outgassing decreases with time, it is of interest to estimate the period during which the graphite is a primary source of oxidizing impurities. Assuming a degassing rate and gas composition typical of EGCR moderator graphite (no pretreatment), it can be shown that the graphite outgassing will be of lesser significance than the maximum allowable inleakage of water as a source of graphite damage after 200 to 250 hr. If it is considered advantageous, graphite outgassing can be minimized by pretreatment of the graphite to drive off the major portion of the adsorbed gases and volatile materials. The pretreated graphite would be cooled in a controlled atmosphere and protected from exposure to air and moisture until ready for installation in the reactor. These precautions would minimize the release of contaminants to the coolant system when the reactor is started up.

Maintenance procedures which could result in introduction of air into the coolant system must be conducted in a manner which will minimize this effect. A blanket gas, such as argon or nitrogen, will reduce the amount of oxygen trapped in the system and adsorbed on the core graphite. Use of a vacuum purge before recharging the system with helium will lower the contaminant concentration, and operation of the purification system for a period prior to reactor reheat should help in re-establishing the required purity levels.

Main Stream Filtration

Use of a full-flow filter in the main coolant circuit to reduce the concentration of entrained solids in the helium is under consideration. The compressor impeller and bearings may require protection from erosive and abrasive materials, while valve bearings and sealing surfaces will benefit from the removal of particulate matter. Some limitation on the spread of condensible fission products may result from the use of such a filter.

System Analysis

The helium purification system currently proposed for the PBRE should give adequate control of radioactive and chemical contaminants in the reactor coolant. The fission-product removal system does not have stringent performance requirements, since the reactor is designed for safe operation with activity in the coolant circuit. The charcoal delay trap will serve primarily to reduce the system activity from intermediate half-life nuclides of the noble gases and to cut down the concentration of biologically hazardous iodine isotopes in the reactor leakage and offgas.

The chemical clean-up system will be effective in reducing the concentration of reactive impurities to satisfactory levels following startup or an inadvertant admission of air or water into the system. During sustained periods of reactor operation, however, the core graphite will tend to "getter" the oxidizing impurities before they are withdrawn in the side stream, and graphite damage will be a function of the success

achieved in limiting the inleakage of oxidizing impurities to the helium coolant system. Hydrogen and carbon monoxide concentrations will be controlled by the chemical cleanup system during normal operation.

8. REACTOR CONTROL AND SAFETY SYSTEMS

Reactor Control System

The function of the control system of a nuclear reactor is to assist the operator in carrying out the objectives of reactor operation. In the case of the PBRE, the prime objective is considered to be the establishment of conditions of temperature, flow, coolant composition, and fuel burnup that will provide satisfactory tests of the performance of the fuel and the reactor system. This is in contrast to the objective of operating a power reactor to provide heat at a certain temperature in varying amounts to satisfy a variable demand or a research reactor to provide a constant neutron flux.

Three regimes of operation that the PBRE control system will be asked to accommodate are described below as means for permitting the operator to approach design-point conditions through a series of gradual intermediate stages and for allowing him to separate the key operating variables in order to observe their individual effects:

1. "Zero" power isothermal operation at power levels up to about 1 kw with the heat dump not operating will permit the operator to select the coolant flow (0 to 100%) that will achieve the desired system temperature in equilibrium with heat losses by radiation and convection. This operating regime will be used for critical experiments, reactivity coefficient measurements, etc. under manual flux control.

2. The low-power regime is defined as the range 0 to 200 kw with manual flux control, coolant flow of 20 to 100%, a gas inlet temperature of $\leq$600°F, and a gas temperature rise of 0 to 140°F. The inlet temperature may be controlled but the outlet temperature will not, although it will, of course, be monitored by the safety system. This regime will be used to produce significant quantities of fission products under modest conditions of fuel temperature and fuel temperature difference.

3. Operation in the power range 200 kw to 5 Mw will be accomplished with automatic temperature control at outlet temperatures above 690°F, coolant flow of 20 to 100%, an inlet gas temperature of approximately

550°F, and a gas temperature rise in the range 28 to 700°F. The inlet and outlet gas temperatures and reactor power will be independently selected, provided, of course, that the combination is consistent with safe temperature limits. This regime will be used to approach rated conditions in controlled steps and to operate in steady state at any conditions up to and including the design point.

In the startup and intermediate ranges the reactor operator will be required to manipulate shim rods to attain criticality and to establish the desired level of flux. Instrument channel supervisory interlocks will be used to provide orderly operation and prevent flux excursions which might necessitate safety actions during these operations. Some minimum flow of coolant will be required so that during startup the reactor outlet gas temperature will not approach design-point values unless there is a failure of the control system.

Although the operation is manual at these low levels, the system will probably require that the operator choose an automatic control mode of operation which will take over when the lower demand limit is reached. In short, the automatic rod control system (servo system) will never be turned off, but in low-level operation, the regulating rod will be stationary at its withdrawn limit and the servo will not interfere with manual operation.

If the reactor is to be taken to power, the manual operation will proceed until the servo system takes over and controls the reactor at the minimum servo set point. At this time the operator may choose to establish a "run" mode of operation, in which it is possible for him to raise the servo demand set point. Before the operator can initiate the "run" mode, the control system must be required to check itself by the usual interlocks which indicate proper functioning of the servo system. These check reactor period and regulating rod position, and verify that the servo is controlling at the proper level.

The servo control mode is one in which the primary control parameter is reactor outlet gas temperature. Because of the time-response characteristics of the system, stabilization will be required. A scheme has

been suggested that will probably prove adequate.[1] The outlet gas temperature control range desired is from 690 to 1250°F, with flow adjustable by the operator from 20 to 100% of design point. In this scheme, the reactor power is variable from about 4 to 100% of design point, depending on the conditions chosen by the operator. In this mode of operation, the transition between "start" and "run" may occur at any point between 4 and 20% of design point flux. Such a system could provide independent control of temperature profile and approximate power by the operator.

Reactor system parameters and the proposed methods of controlling them in the various operating regimes are summarized below:

Parameter	Control Method
Coolant pressure	All regimes: not directly controlled; helium inventory selected so that the pressure is ≤500 psia when the average temperature is 900°F; inventory under operator control, not automatic
Coolant flow	All regimes: no automatic control; blower speed set manually to achieve desired operating conditions
Gas inlet temperature	Regime 1 (R-1): not automatically controlled; manually set by setting blower speed and helium inventory
	Regimes 2 and 3 (R-2 and R-3): controlled by regulation of feedwater temperature
Gas outlet temperature	R-1 and R-2: uncontrolled but subject to safety limits
	R-3: manual set point; closed loop controller manipulating regulating rod
Flux level	R-1 and R-2: manual control by control rod positions
	R-3: servo-controlled through outlet gas temperature regulation of control rods; operator manually sets blower speed to achieve desired combination of reactor power and temperature rise

[1]A. P. Fraas et al., Preliminary Design of a 10-Mw(t) Pebble-Bed Reactor Experiment, pp. 11.1 ff, ORNL CF-60-10-63 (May 8, 1961).

Control rod position	Shim rods: manually controlled in all regimes
	Regulating rods: servo-controlled as discussed in text
Steam pressure	All regimes: manual set point; controlled by throttle valve
Feedwater temperature	All regimes: manual set point; controlled by steam bypass valve
Feedwater flow rate	All regimes: level control in steam drum

It should be pointed out that a good control system, including a good automatic controller, can do much to ensure long uninterrupted runs by reducing the probability that the reactor parameters get into the region where safety action is required.

The nuclear instrumentation channels to be provided, along with their functions, are the following:

1. Startup Channel. Two logarithmic counting channels, capable of continuously monitoring neutron flux and reactor period over the entire operating range of the reactor are recommended. One of these will be considered an installed spare. The wide range will require that the detector be movable during operation, either automatically or under operator control from the operator's station. It is not necessarily required that such a channel be capable of indicating absolute reactor power, but may only be required to indicate relative reactor power for any one chamber position.

2. Wide Range Logarithmic Channel. There will be a "log N" channel, using a compensated ionization chamber, that will provide continuous flux-level and reactor-period monitoring over about the upper six decades of the operating range of the reactor without chamber movement. The compensating mechanism and chamber position will be adjustable from outside the containment vessel.

3. Wide Range Linear Channel. A linear current channel, utilizing a compensating ionization chamber with range change mechanisms in the amplifier circuits, will be used to provide monitoring of the flux level over approximately the upper six decades of the operating range of the reactor without chamber movement. The compensating mechanism and chamber position will be adjustable from outside the containment vessel. The range

change will be accomplished by the reactor operator from his operating position. This channel will not be connected into the control system except through the operator.

4. Automatic Control (Servo) Channel. This channel, using an ionization chamber, will provide neutron-flux information for servo control of the reactor in the "power" range. The chamber position will be adjustable from outside the containment vessel. The automatic control mode described above will use information from this linear flux channel and various nonnuclear channels, such as flow, gas temperatures, etc. The servo will use one of the shim rods as the regulating rod, with limited servo-controlled span. The span will be adjustable in position, but not in length, by the operator for shim control. The techniques for using a shim-regulating rod are well known and appear to be satisfactory for the PBRE.

System Control Characteristics

A preliminary analog analysis of a model of the PBRE reactor system has been made, but future revision of the model used will undoubtedly change some of the results. The important results of the analysis are discussed below:

1. The "fuel time constant," defined as the time required for 63% response of the core mid-point fuel surface temperature to a step change in power, was 50 sec at design flow. This varies approximately inversely as the coolant flow rate.

2. On scram from full power at full coolant flow, the gas outlet temperature and mean fuel temperature both had a maximum rate of change of about 350°F/min. The temperature rate of change for fuel in the upper portion of the core would be greater.

3. Blower coastdown on a 10-sec time constant and blower seizure caused about the same transient. Without any rod motion and with a minimum fuel temperature coefficient, the outlet gas temperature reached almost 1800°F, and the mean fuel temperature reached about 1550°F, in both cases. Convection flow rates of 4 to 5% of design-point resulted. With scram after 10 sec, the outlet gas temperature for blower seizure reached

only about 1425°F. The mean fuel temperature, with scram, rose from 1100 to 1200°F.

4. Very slow ramp reduction in coolant flow with constant rod position resulted in shutdown of the reactor, with some increase in gas temperature and a slight decrease in mean fuel temperature. The latter decrease is due to heating up of the reflector. Damped oscillations of the temperatures and reactor power on very long (>5 min) periods were observed.

5. Step and ramp increases in reactivity were run, with the outlet gas temperature peak always delayed behind the mean fuel temperature peak. As would be expected the delays were much longer for low flow conditions.

The analog model will be refined as the design progresses, and more specific control problems will be investigated.

Reactor Safety System

The function of the reactor safety system is that of sensing the departure of certain critical parameters from some previously defined region of safety and the actuation of mechanisms to return the reactor to a safe condition. In many instances the parameters that are measured, and to which safe limits are assigned, are not those that must be limited for safety reasons. For example, neutron flux is usually considered to be a reactor safety parameter. However, high flux, per se, does not necessarily imply an unsafe condition. The safety implication of high flux arises from the fact that when the power generation exceeds the cooling rate the fuel temperature must rise. In most cases, the choice as to what parameters are measured for safety is dictated by the availability of sensory information, the time response characteristics of the sensors and the reactor system, and the reliability of these devices in determining that the reactor is indeed in or near an unsafe condition.

The safety system for the PBRE will be required to protect the system against excessive temperatures and excessive rates of change of temperature. Preliminary analog analyses indicate that the thermal time constants in the system are very large and that sensing temperatures alone would not suffice for certain fast transients. It is clear that the fuel

temperature can increase only when the rate of cooling is exceeded by the rate of heating. If the difference between these rates is held below some maximum value, the rate of change of fuel temperature can be limited. If, on the basis of analysis, an upper limit is assigned to this rate of change of fuel temperature which ensures that no temperature in the system increases too rapidly, a "safe" excess of reactor power over cooling rate can be established. These two parameters are measurable by flux, flow, and gas temperature instrumentation and can provide the basis for a safety system to protect against excessive rates of change of temperature. For slower transients the temperature sensors alone can provide adequate signals for the safety system.

The rapid change in the relationship between heating and cooling rates can come about in the PBRE as a result of rapid changes in flux or coolant flow or both. The PBRE will operate at various flows from about 20 to 100% design point. It is clear that the "safe" flux level for 20% flow is much lower than that for 100% flow. For this reason, it is not sufficient to use a flux signal or a flow signal for safety action, but it is necessary to combine information from both these to determine that a safe condition exists.

Preliminary analog analyses have shown that very fast nuclear transients starting at low level, if terminated by scram at about 150% of design-point flux, do not produce serious temperature transients, even if the coolant flow is as low as 10% design point. This is apparently due to the very narrow width of the power peak and the large heat storage capacity of the fuel. Although the startup accident has not been simulated, it appears reasonable at this time to consider a flux safety trip at near the 150% design point that is not related to coolant flow.

In summary, the PBRE should have a reliable nuclear safety system capable of shutting the reactor down on any of the following:

1. high coolant outlet temperature,
2. some function of reactor neutron flux and coolant flow which ensures that temperature rates of change will not be excessive.
3. neutron flux in excess of some fixed upper limit above design point,
4. loss of reactor pressure, which constitutes a loss of coolant.

In addition to these primary safety requirements, there are at least two more conditions which deserve consideration, since they indicate that one or more of the four conditions listed above will exist unless corrective action is taken.

1. A very short reactor period indicates a failure of the reactor control system and should produce a scram to limit the severity of the transient. It should be noted that the mechanism for producing such a scram is not usually considered to require the reliability indicated by the four conditions listed above on the basis that its function is to prevent a flux level scram which is disorderly but tolerable.

2. The reactor should not be started (or should be shut down) unless the coolant flow is greater than some minimum value. This is not included as a primary safety condition because of the possibility that very low power runs of an experimental nature may be desirable. It is included in the interest of orderly operation and could be considered a reactor control requirement.

The reliability of the safety system is of utmost importance. Redundancy, with monitoring or testing to detect failures within the system, will be used. At the present time it is proposed to use auctioneering logic in the safety system. Three identical and independent safety channels will be installed. As in existing reactors at ORNL, two of these channels must be presumed to be operating, on the basis of tests and monitoring, for operation of the reactor to be permitted. The third channel will be considered an installed and operating spare, preventing the necessity of stopping a run on detected failure of a single channel. Of course, many types of failure will automatically shut down the reactor. It is hoped that sound design, installation, and maintenance will minimize failures of all types.

Four shim safety rods will be used to provide shutdown margin and reactivity control. These will be located in holes in the graphite reflector and symmetrically placed about the reactor vertical centerline on a 40-in.-diam circle. The reactivity balance is given in Section 6.

The safety rods are supported and driven from the bottom. The poison section consists of a hollow B_4C cylinder, 3 in. o.d. and 4 ft long.

Below this is a graphite follower and a drive tube coupling the rod to the drive mechanism through an electromagnet. Each rod mechanism is enclosed in the pressure vessel and a nozzle extension. The rods scram downward. The coupling to the magnet is designed so that the rod can fall away from its drive, upon interruption of the magnet current, but cannot be raised above the position established by the drive mechanism (as by a gas pressure differential); in addition a large downward force can be exerted by the drive mechanism in the event that the rod fails to drop on scram. The arrangement of the control rods and drives is illustrated in Section 3. The maximum speed of the rods will be determined in further analytical work.

Primary Coolant System Instrumentation

Some unusual problems will be encountered in instrumenting the PBRE, since the coolant system will contain fission products which may contaminate the primary measuring elements. Development of a special group of primary elements could be necessitated by high radiation levels, and provision for remote calibration, maintenance, and decontamination may be necessary (although it may be possible to install traps in the pressure taps to the instruments to protect them from activity).

Metallic-sheathed, MgO-insulated, Chromel-Alumel thermocouples will be used for all temperature measurements during operation of the reactor near design conditions; thermocouples for higher temperature operation are discussed in Section 16. Adequate spares will be provided, and a number of thermocouples in the primary system will be made replaceable by installing wells or guide-tubes inside of the reactor.

Moisture detectors will be used to detect a steam leak into the main coolant stream. These detectors will be connected into the reactor safety system to scram the reactor and isolate the heat exchanger from the steam system when a leak is detected.

Gross activity deposition at different levels in the heat exchangers, in the blower, and at various other points in the system will be monitored by permanently installed ion chambers. In addition, spectral information

permitting identification of the activities of specific nuclides will be measured during shutdown periods using scintillation detectors and a multichannel analyzer. A study is planned for determining the feasibility of using either a data logger or a combined data logging and computing system for processing the experimental data.

9. STRUCTURAL ANALYSIS OF SYSTEM

Investigations were made to determine the structural integrity of critical regions in the proposed system. Where applicable, design evaluations were made in accordance with the 1959 ASME "Unfired Pressure Vessel Code," Section VIII, and "Tentative Structural Design Basis for Reactor Pressure Vessels and Directly Associated Components," PB 151987, 1 December 1958 Revision, Department of Commerce, Office of Technical Services. These design bases will be referred to as the "ASME Code" and the "Navy Code" in subsequent discussions.

Three separate types of stresses were considered in the design evaluations: these are primary, secondary, and thermal. The primary stresses are direct or shear stresses developed by the imposed loading which are necessary to satisfy only the simple laws of equilibrium of external and internal forces and moments. Simple membrane pressure stresses in shells are an example of primary stresses. Secondary stresses are direct or shear stresses developed by the constraint of adjacent parts or by self-constraint of the structure. These differ from primary stresses in that they may be relaxed by yielding of the material. Bending stresses caused by structural discontinuities are an example of secondary stresses. Thermal stresses are internal stresses produced by constraint of thermal expansion. Thermal stresses are similar to secondary stresses in that they are relieved by yielding of the material.

The ASME Code is generally accepted as the basis for evaluating primary membrane stresses. However, the Navy Code extends beyond the ASME Code in that it considers secondary and thermal stress evaluations in addition to primary stresses. When the analysis of stresses in a member reveals a biaxial or triaxial stress condition it is necessary to make some assumption regarding the failure criterion which is to be used. The Navy Code uses the maximum shear theory of failure. The stresses upon which limitations are established are defined as the "equivalent intensity of combined stresses" and are numerically equal to twice the maximum shear stress. According to the Navy Code the primary-plus-secondary stress intensities must not exceed the smaller of 90% of the yield strength or 60%

of the ultimate strength. No stress limitations are considered with regard to thermal stresses except those which remain constant during any normal steady-state power operation; however, the combined effects of all stresses, including thermal, must be evaluated in terms of resistance to cyclic fatigue. This latter evaluation requires a detailed examination of all the different types of stresses occurring in a region together with an accurate knowledge of the number of cycles for each operation which the system will be subjected to. In the preliminary evaluations described herein, only the stresses in the top access nozzle, which is subjected to large thermal stresses, were evaluated in terms of cyclic fatigue. In the final design all regions must be examined on a fatigue basis.

Since graphite is a brittle material, stress analyses of graphite structures require an entirely different basis for evaluation than that used for ductile metal structures. Further discussion of the failure criterion for graphite is deferred to that portion of the structural analyses dealing with the reflector graphite structure.

In order to specify the design for the reflector graphite, the mechanical properties and radiation-induced shrinkage data for nuclear grades of graphite must be available. Complete information relating to the thermal conductivity and the coefficient of thermal expansion is also required, since the thermal stresses are functions of these properties. From the existing evidence there appear to be optimum combinations of mechanical properties and radiation shrinkage characteristics for obtaining maximum longevity before shrinkage cracking occurs. Shrinkage data are being obtained at Hanford on various grades of graphite, and it is proposed that these studies be augmented with a research and development program for determining:

1. the mechanical and physical properties of both irradiated and unirradiated graphite,
2. the combined effects of stress and shrinkage in graphite,
3. the influence of geometry and extrusion size upon the useful lifetime of a graphite structure.

The detailed program is outlined in Section 16, Research and Development.

In order to properly assess the effects of thermal stresses in the fuel balls, applicable physical and mechanical properties of fueled graphite must be available. Specifically, values of thermal conductivity, coefficients of thermal expansion, and strength are needed. A program designed to yield this required information is also outlined in Section 16. The physical and mechanical properties of graphite are dependent on such factors as temperature, the type of coke, the type of binder, the amount of graphitization, the method of fabrication, and the orientation of the grains. In nuclear applications the fast-neutron exposure, as well as the irradiation temperature, affects the properties. When fueled graphite is considered, the effects of the fuel must be taken into account. Thus, all the above factors must be considered in the fueled-graphite investigations in order to furnish data applicable to the fuel balls.

The structural investigations are discussed below in four parts: the reactor pressure vessel, the pressure-vessel support system, the steam-generator support system, and the graphite reflector structure. Each part contains a discussion of the problems involved, statements of the applicable design criteria, summaries of the stress analyses, and interpretations of the results obtained.

Pressure Vessel

The reactor pressure vessel material is type A212, grade B, carbon steel plate. The design pressure and temperature are 625 psi and 650°F, respectively. In order to allow for decontamination effects, a corrosion allowance of 1/16 in. was applied to all structural members of the vessel. This allowance is the minimum specified by the ASME Code when actual corrosion effects are indeterminate.

The reactor pressure vessel is shown in Fig. 3.10. The structural analyses of the basic shell (heads and cylindrical portion), the nozzle attachment regions, the liner, and the core support plate are discussed below.

Heads and Cylindrical Portion of Vessel

The necessary thicknesses of the cylindrical portion of the pressure vessel and of the torispherical heads were determined in accordance with the ASME Code. The code allowable stress for type A212, grade B, carbon steel at 650°F is 17 500 psi. The minimum thickness for the cylindrical portion of the vessel is given by

$$t = \frac{PR}{SE - 0.6P} + C \quad ,$$

where

P = design pressure, 625 psi,
R = inside radius of shell, 54.5 in.,
S = maximum allowable stress value, 17 500 psi,
E = joint efficiency, 0.9,
C = corrosion allowance, 0.0625 in.

Based on the above, the minimum required thickness of the cylindrical portion of the vessel is 2.28 in. The next larger standard plate size is 2.5 in., which was taken as the thickness of the cylindrical portion. The minimum thickness of the torispherical heads is given by

$$t = \frac{PLM}{2SE - 0.2P} + C \quad ,$$

where, in addition to the notations previously given,

L = inside spherical or crown radius of the torispherical head,
$M = (1/4)(3 + \sqrt{L/r})$,
r = inside knuckle radius.

The ASME Code further specifies that the inside crown radius to which an unstayed head is dished shall not be greater than the outside diameter of the skirt of the head, and that the inside knuckle radius of a torispherical head shall not be less than 6% of the outside diameter of the skirt or the head but in no case less than three times the head thickness. Based on these considerations, a crown radius, L, of 80 in. and a knuckle radius,

r, of 12 in. were chosen. The minimum required head thickness is 2.28 in. A standard plate thickness of 2.5 in. was therefore chosen for the top and bottom heads.

The discontinuity stresses in the vicinity of the head-to-cylinder junction (see Fig. 3.8) were analyzed[1] by assuming that the torispherical head was ellipsoidal in shape with a minimum-to-maximum radius ratio of 1/2. The stress and stress intensity indexes (factors by which the circumferential membrane stress in the cylinder is multiplied to obtain the stresses and stress intensities of interest) were obtained by interpolating between tabulated values given by Kraus et al.[1] The indexes, maximum stresses, and maximum stress intensities are given in Table 9.1. The circumferential membrane stress in the cylinder is 13 940 psi. The greatest stress intensity is 20 800 psi, and it occurs at the inner surface of the knuckle.

Table 9.1. Stress Indexes, Stress Intensities, and Stresses in the Head-to-Cylinder Junction Region Created by an Internal Pressure of 625 psi

	Crown	Knuckle	Cylinder
Maximum stress index	1.24	1.40	1.10
Maximum stress intensity index	1.24	1.49	1.10
Maximum stress	17 300 (xo)[a]	19 500 (xi)	15 300 (co)
Maximum stress intensity	17 300 (o)	20 800 (i)	15 300 (o)

[a]Letters in parentheses following the stress indicate the location of the stress; x indicates axial; c, circumferential; o, outer surface; i, inner surface.

The maximum allowable primary-plus-secondary stress intensity given by the Navy Code for type A212, grade B, carbon steel at a temperature of 650°F is 24 000 psi. Since the maximum stress intensity in the vessel (20 800 psi) is less than the allowable value, the vessel without nozzle attachments is adequately designed.

[1]H. Kraus, G. G. Bilodeau, and B. F. Langer, Stresses in Thin-Walled Pressure Vessels with Ellipsoidal Heads, Journal of Engineering for Industry, pp. 29–42 (February 1961).

Nozzle Attachment Regions

The nozzle attachment regions in the heads are reinforced by locally increased nozzle stub and shell thicknesses. The local increases in shell thickness are not shown in Fig. 3.10. The transition from the heavy wall of a stub to the thinner nozzle region is made using a tapered section in accordance with ASME Code procedures. In the case of the top access nozzle, the thickness is uniform throughout the entire length. The pertinent nozzle dimensions are given in Table 9.2. The thicknesses of the control rod and top access nozzles differ, as follows, from those shown in Fig. 3.10.

	From Fig. 3.10	From Table 9.2
Control rod nozzle thickness, in.	1.25	1.50
Top access nozzle thickness, in.	3.0	3.25

The model used for analyzing the local bending and membrane stresses in the nozzle regions of the heads was a single nozzle radially attached to a spherical shell. Although the control rod nozzles are not radially attached, the analysis made is acceptable for design purposes. The gas inlet nozzle is attached to the cylindrical wall of the vessel and an exact analysis is not available. Hence, this nozzle was designed on the basis of the Navy Code procedure of area replacement. With the exception of the top access nozzle, which is 12 in. long, the nozzles were assumed to be semi-infinite in length, and all the nozzles were taken as thin-walled cylinders. The pressure stresses at the nozzle-to-shell junctions for the control rod, fuel removal, and top access nozzles are given in Table 9.3.

From Table 9.3 the maximum primary-plus-secondary stress intensity for a control nozzle is 24 900 psi. Although this value is slightly above the 24 000-psi limit, the thin-walled cylinder representation for the nozzle is conservative and the design is acceptable. The values for the remaining nozzles are below the limit given.

The gas inlet nozzle was designed using the procedures outlined in the Navy Code. The required thickness of the vessel wall is 2.04 in., and the required nozzle thickness is 0.25 in. The corresponding area

Table 9.2. Nozzle Dimensions Pertinent to the Analysis[a]

Nozzle	Inside Diameter (in.)	Nominal Thickness (in.)	Reinforced Thickness (in.)	Length of Reinforcement (in.)	Length of Taper (in.)	Total Length (in.)
Control rod	4.026	0.237	1.5	3.75	5.0	Long
Gas inlet	13.126	0.437	2.5	6.25	9.0	Long
Fuel removal	15.0	0.50	2.5	6.25	8.0	Long
Top access	30.0		3.25	12.0	None	12.0

[a]The thickness of the vessel was assumed to be 3 in. for the analysis of the control-rod, gas-inlet, and fuel-removal regions; for the top access nozzle region it was taken as 3.25 in.

Table 9.3. Pressure Stresses at Junctions of Nozzles and Vessel and at Top Access-Nozzle Flange

Nozzle	Nozzle Stresses (psi)				Vessel Stresses (psi)			
	Axial		Circumferential		Meridional		Circumferential	
	Outer Surface	Inner Surface	Outer Surface	Inner Surface	Outer Surface	Inner Surface	Outer Surface	Inner Surface
Control rod	17 800	-16 600	18 600	8 300	6 600	-800	12 400	15 900
Fuel removal	13 700	-11 500	18 000	10 500	11 700	-5100	15 300	14 500
Top access (at junction)	15 000	-11 800	18 700	10 700	16 400	-9700	17 500	12 900
Top access (at flange)	-9 100	12 300	-2 700	3 700				

replacement needed is 27.03 in.^{2}. The replacement area available in the nozzle, taking into account the 1/16-in. corrosion allowance, is 27.34 in.^{2}, and the available replacement area in the vessel wall is 11.80 in.^{2}. The total area for replacement is, therefore, 39.14 in.^{2}, and the nozzle is adequately designed.

The thermal stresses in the nozzles will be low as a result of maintaining the pressure envelope at a uniform temperature. However, it may be desirable to limit the temperature of the flange on the top access nozzle to about 300°F for sealing purposes. In order to evaluate the stresses associated with the temperature distribution, an exponential function that has the value of 550°F at the nozzle-to-shell junction and 300°F at the top flange was used to describe the distribution. The temperature function is given by

$$T = 550\ e^{-0.0505x} ,$$

where x is the axial distance along the nozzle. This expression gives a greater decay of temperature with distance along the nozzle than does the so-called "fin" equation. The stresses at the two ends of the nozzle are given in Table 9.4.

The maximum stress intensities corresponding to the combined thermal and pressure stresses are 24 100 psi at the shell end and 49 000 psi in

Table 9.4. Thermal Stresses at Junction of Top Access Nozzle and Vessel and at Flange

Location	Axial or Meridional Stresses (psi)		Circumferential Stresses (psi)	
	Outer Surface	Inner Surface	Outer Surface	Inner Surface
At junction, nozzle	9 100	-9 100	-2 800	-8 300
At junction, vessel	9 500	-8 300	-8 400	-2 500
At flange, nozzle	-36 700	36 700	-11 200	10 800

the flange region of the nozzle. The maximum stress intensity in the shell is 28 400 psi. The maximum value exceeds the 42 000-psi limit given by the Navy Code, and a modification in length or thickness or both will be required if the 300°F limit is imposed.

A fatigue analysis was also made. The stress concentration factor applied to the bending component of the thermal stresses in the nozzle is 1.75 for a fillet radius of 1.0 in. The stress summary is given in Table 9.5. The three stress intensities on the outer surface at the ends of the nozzle and the corresponding mean values are given in Table 9.6. An allowable alternating stress of 66 000 psi was adopted based on 500 cold start-up cycles and a usage factor of 0.4. The applicable fatigue diagram is shown in Fig. 9.1, where it may be seen that the stress values lie within the safe region.

Stresses may be induced in the gas inlet nozzle and the adjacent shell region as a result of relative vertical displacement of the two ends of the gas inlet line. This relative displacement is due to thermal expansion effects in the system and to probable misalignment of the pressure vessel relative to the steam generator during erection. Displacements from four separate sources combine to produce the total relative displacement from thermal-expansion effects. These four sources (see Fig. 3.10) are described below:

1. Vertical displacement of pressure vessel as a result of rotation of the support plates as the reactor is heated from room temperature to operating temperature. This displacement is discussed in the section of this chapter on the pressure vessel support system, and it is shown that the vertical displacement is 0.024 in.

2. Vertical movement of the steam generator support platform because of curvature in the support columns. This displacement is discussed in the section of this chapter dealing with the steam-generator support system and is equal to 0.019 in., assuming that the steam generator moves to one side of the normal position as the system is heated from room temperature to the operating temperature.

3. Vertical displacement of steam generator as a result of rotation of the members which support the steam generator from the support platform.

Table 9.5. Summary of Outer Surface Stresses of Top Access Nozzle

Location	Time	Condition and Source	Axial Stress (psi)			Circumferential Stress (psi)		
			Basic	K[a]	Actual	Basic	K	Actual
At vessel and flange	Initial	Isothermal, zero pressure	0		0	0		0
At vessel	At full power	Internal pressure, 625 psi	15 000	1.0	15 000	18 700	1.0	18 700
		Discontinuity thermal						
		Bending	9 100	1.75	15 900	2 700	1.75	4 700
		Membrane	0		0	-5 600	1.0	-5 600
		Total			30 900			17 800
At flange	At full power	Internal pressure, 625 psi	-9 100	1.0	-9 100	-2 700	1.0	-2 700
		Discontinuity thermal						
		Bending	-36 700	1.75	-64 200	-11 000	1.75	-19 300
		Membrane	0		0	-200	1.0	-200
		Total			-73 300			-22 200

[a]K = stress concentration factor.

Table 9.6. Stress Intensities and Associated Alternating and Mean Stress Intensities for Top Access Nozzle

Location	Stress Intensity (psi)			Alternating Stress Intensity[a] (psi)			Mean Stress Intensity[a] (psi)		
	S_{12}	S_{23}	S_{31}	S_{12}	S_{23}	S_{31}	S_{12}	S_{23}	S_{31}
At vessel	13 100	17 800	30 900	6 600	8 900	15 500	6 600	8 900	15 500
At flange	51 100	22 200	73 000	25 600	11 100	36 700	16 400	11 100	5 300

[a]The numerical subscripts 1, 2, and 3 on S(stress intensity) refer to the axial, circumferential, and radial directions, respectively.

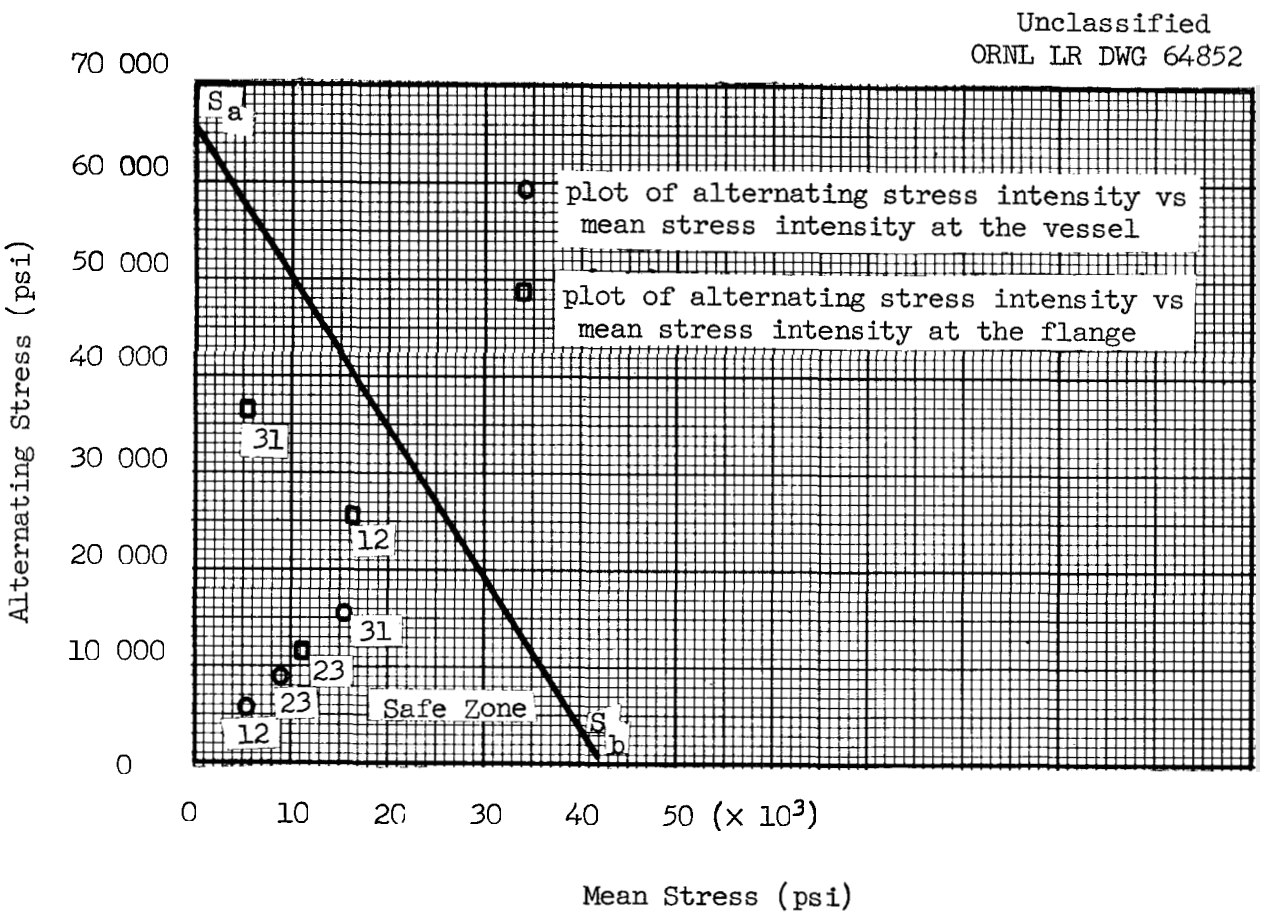

Fig. 9.1. Goodman Diagram for Fatigue Analysis of Top Access Nozzle.

4. Axial thermal expansion of that portion of the steam generator between its support plane and the plane of the concentric gas ducting.

By proper design the movements described in items 3 and 4, together with those described in items 1 and 2, can be made self-compensating so that the net relative vertical displacement of the ends of the gas inlet line will be negligible. There remains the possibility that a slight vertical misalignment might occur during erection. This effect is less serious than the thermal effects, which would be cyclic in nature, because the associated stresses may be relieved through deformation without deleterious effects.

The effects of a relative displacement, δ, were examined by considering the gas inlet line to be a beam fixed against rotation at both ends and subjected to a displacement, δ, at one end. Each half of the line thus behaves as a cantilever beam subjected to an end displacement of $\delta/2$. The force, in lb, at the end of the cantilever beam as a function of the misalignment is given by

$$F = \frac{1.5\ EI\delta}{l^3} ,$$

where

E = modulus of elasticity, psi

I = moment of inertia, in.^{4}

l = length, in.

For a 14-in. sched.-40 pipe, 6 ft long,

$$F = 41\ 380\ \delta ,$$

and the moment, in in.-lb, at the junction of the nozzle and shell is

$$M = 248\ 300\ \delta .$$

The stress values in the nozzle and shell corresponding to this moment loading were evaluated.[2] The axial stress (psi) in the nozzle is

[2]P. P. Bijlaard, Welding Research Council Bulletin Series, No. 50 (May 1959).

the greatest, and its value is 94 730 δ. Thus, a relative displacement of 0.10 in. gives a stress of 9473 psi, which clearly indicates that only a small amount of misalignment can be tolerated.

Liner

The pressure vessel liner is made of type 304 stainless steel. The configuration is a cylindrical shell with a head in the form of a conical section and a spherical upper portion (see Fig. 3.3). The design conditions for the liner are an external pressure of 3 psi at 1250°F. The working pressure will actually be approximately 2 psi and the temperature will be nearer 550°F (because of the insulation on the upper portions of the liner).

The minimum liner thickness was determined in accordance with the ASME Code requirements for shells subjected to external pressure. However, the code rules are limited to spherical and cylindrical shells. The code states that vessels intended for service under external working pressures of 15 psi or less, which are to be designed in compliance with the rules for external pressure, shall be designed for a maximum allowable external pressure of 15 psi or 25% more than the maximum possible external pressure, whichever is smaller. Thus, since the actual external pressure on the liner will be approximately 2 psi, the 3 psi design value meets code requirements. The liner thickness was arbitrarily chosen as 1/2 in. which, after allowing for corrosion, gives an effective thickness of 3/8 in. The Code charts indicate that the allowable external pressure for the cylindrical portion is 8.8 psi, and the value for the spherical portion is 20.2 psi. Since it is reasonable to assume that the conical portion of the liner will have a greater resistance to buckling than the cylindrical portion, the liner is adequate from the standpoint of resistance to external pressure.

During normal operation, differential thermal expansion between the liner and the pressure vessel causes the liner end of the gas outlet line to move vertically 0.19 in. relative to the gas inlet nozzle. If the portion of the liner in the upper plenum reached a temperature of 1250°F, this relative displacement would become approximately 0.86 in. In either

event, large stresses may occur in the regions of the gas outlet nozzle attachment to the liner. These stresses could be appreciably reduced by using an expansion joint, which would allow rotation at the steam generator end of the line. The stress analysis of such a nozzle-to-conical shell attachment does not lend itself to accurate theoretical analysis, and an experimental stress analysis will be required for the final design. The required experimental analysis is discussed further in Section 16.

The pressure vessel liner is welded to the support plate, and thus thermal stresses corresponding to the difference in the coefficients of expansion for type 304 stainless steel and type A212, grade B, carbon steel will be induced upon heating. Since the plate is more rigid than the liner, the radial expansion will be dictated by the plate. The lower portion of the liner will, therefore, behave as a cylinder with the end fixed against rotation and subjected to a radial deflection.

Using this model the stresses in the liner were calculated[3] for a temperature of 550°F. The mean coefficients of expansion were taken as 9.45×10^{-6} in./in.·°F and 7.15×10^{-6} in./in.·°F for the stainless steel and carbon steel, respectively, giving a difference in radial expansion of 0.058 in. The corresponding axial and circumferential stresses are 52 500 and 44 700 psi, respectively. Hence a design modification is needed to bring these values within acceptable limits. The required reduction can be achieved by constructing the lower section of the liner from a material with a coefficient of expansion lying between the values for type 304 stainless steel and type A212, grade B, carbon steel or by using a stainless steel support plate.

Core Support Plate

The carbon steel plate that supports the core and reflector rests on lugs attached to the cylindrical portion of the pressure vessel. The stress magnitudes given below are based on the assumption that the fuel-removal mechanism extends up into the fuel cavity through a 12-in.-diam

[3]F. J. Witt, Thermal Stress Analysis of Cylindrical Shells, ORNL CF-59-1-33 rev. (January 1959).

hole at the center of the plate, and there are 296 holes 3/4 in. in diameter on a 1 1/2-in. triangular pitch between the edge of the 12-in.-diam hole and a circle with a radius of 30 in. to allow for the passage of coolant gas from the lower plenum into the fuel bed (see Fig. 3.10). For a graphite density of 1.7, the distributed load on the plate is 7.4 psi.

Based on these data, the maximum stress in the unperforated portion of the plate was found to be ~4300 psi. This stress is in the tangential direction and is located at the outer edge. The stress concentration factor[4] at the edge of one of the small holes is ~2.0, while the value midway between holes[5] is ~1.7. Thus the maximum stresses at these locations in the perforated region are ~10 000 and ~7700 psi, respectively. From these data it is apparent that a margin of safety exists in the design of the plate to allow for irradiation effects and accident conditions.

Pressure Vessel Support System

The pressure vessel support system is designed to permit differential radial growth between the pressure vessel and supporting structure. The system is depicted in Fig. 3.7, which shows both the pressure vessel and the steam generator support system, and in Fig. 3.9, which is a pictorial drawing of one of the supports. The 11 support plates bear against plates attached to the pressure vessel and to the support frames which, in turn, are supported from the biological shield. Flat bearing surfaces were chosen for the pressure vessel lugs and plates attached to the biological shield because difficult machining and alignment problems are associated with other forms. The gear rack and pinion tooth arrangement at the top and bottom of each support plate are designed to absorb the horizontal components of force in the system. The side thrust plates prevent rotational

---

[4]R. E. Peterson, Stress Concentration Design Factors, John Wiley and Sons, New York, 1953.

[5]C. C. Wilson and R. L. Maxwell, An Experimental Investigation of the Stresses and Deflections of a Perforated Plate in Bending, Part 1, University of Tennessee Engineering Experiment Station, Department of Mechanical Engineering, Report No. ME-61-1 (June 1961).

and translational motion of the pressure vessel with respect to the biological shield.

As the reactor is heated from room temperature, radial thermal expansion of the pressure vessel causes the support plates to rotate, with their cylindrical ends rolling on the bearing plates. At the same time, the gear teeth roll in the gear racks according to the fundamental characteristics of spur gearing. The entire support system must be designed to withstand seismic loadings without permitting translations or rotations of the pressure vessel relative to the support framework.

The design and stress analyses of the support system for each of the above requirements are presented below in two parts. The first part is concerned with the design and analysis of the system for normal operating conditions; the second part considers the effects of seismic loadings.

Design and Stress Analysis for Normal Operating Conditions

Under normal conditions it is assumed that the weight of the pressure vessel and contents (145 000 lb) is equally supported by 11 support members, which are each 36 in. long. The vertical load normally carried by each support member is thus 824 lb per inch of support plate length. Actually, since the support members are not equally spaced around the entire circumference of the vessel (see Fig. 3.8), the two supports nearest the gas inlet nozzle will carry approximately 985 lb/in. and the support opposite the gas inlet line will carry only 672 lb/in. The rolling surfaces on the ends of the support members were sized so that the contact stresses would be within acceptable limits. For a rolled steel roller on a flat plate of the same material, the maximum acceptable load per inch is given by[6]

$$P' = 700\ d \quad ,$$

where P' is the load per inch and d is the roller diameter. For a 2-in.-diam roller the maximum acceptable load is 1400 lb/in. Thus, the contact stresses developed in the rollers and in the flat bearing plates are,

[6]S. Timoshenko, Strength of Materials, Part II, p. 343, D. Van Nostrand, New York, 1956.

during normal conditions, within acceptable limits. It is assumed that the formula for the allowable load is unchanged for temperatures up to 550°F.

The upward thrust on a support lug attached to the pressure vessel induces bending in the shell. The load is applied at a distance of about 3.25 in. with a resulting moment of approximately 42 000 in.-lb. No accurate model for evaluating the stresses is available; however, an estimate of the maximum stress may be made by using methods developed for analyzing single nozzle-to-shell attachments[7] when interaction between adjacent attachments does not exist. The value in this case was found to be ~1200 psi, which is almost insignificant. However, additional investigation is required in the vicinity of the gas outlet nozzle where the interactions and combined stresses may be important.

The total axial load (per inch) transmitted by the support plates is 830 lb/in. The critical buckling load for the plates is 18 500 lb/in. Thus the support plates are more than adequate from the standpoint of stability during normal operation.

The thickness of the gear teeth was established on the basis of bending stresses in the teeth. A thickness of 1/2 in. was found to be satisfactory, assuming the gear material to be forged carbon steel (SAE 1030).

As the pressure vessel expands radially, the rotation of the support plates causes a vertical displacement of the entire pressure vessel assembly. The radial expansion of the pressure vessel in going from room temperature to the design operating temperature is 0.216 in. The corresponding vertical movement of the pressure vessel at the support level is 0.024 in. upward. This displacement can be balanced by a corresponding displacement of the steam generator end of the gas inlet line.

Effects of Seismic Loads

In the design of the PBRE, the maximum horizontal and vertical accelerations resulting from earthquake loadings are taken, respectively, as 10% and 5% of that due to gravity. These values are twice those used

---

[7]Op. cit., Bijlaard.

in the design of the EGCR. The reactor pressure vessel support members are designed to resist downward loads only, and it is essential that, at no time during an anticipated seismic disturbance is the vessel tipped off of any support member.

The 11 support members are spaced at 30-deg intervals around the pressure vessel (see Fig. 3.8). A twelfth member was omitted because of the presence of the gas inlet nozzle; hence, there is a 60-deg interval between the members in this vicinity. The center of gravity for the pressure vessel and the internal components lies on the reactor center line approximately 62.4 in. below the support circle. The entire supported weight, w, was assumed to be 145 000 lb.

The case in which downward load (called positive in the remaining discussion) on one member is a minimum will occur when the horizontal force through the center of gravity acts in the direction opposite to that of the gas inlet line. For identification purposes, it is assumed that the support members are numbered in a clockwise direction, when viewed from above, with number one being located at an interval of 30 deg from the centerline of the gas inlet nozzle. From symmetry, the force on member number one, F_1, equals that on member number 11, F_{11}, etc. Therefore, six relationships are needed to determine the reaction forces. Two of these are determined from static relationships. Assuming that the maximum horizontal and vertical accelerations occur simultaneously

$$2F_1 + 2F_2 + 2F_3 + 2F_4 + 2F_5 + F_6 = 0.95\ w \qquad (1)$$

is the expression obtained from $\Sigma F_v = 0$. The summation of moments about a diameter perpendicular to the one through the gas inlet nozzle equals zero, or

$$\Sigma M = 0 \quad .$$

Thus,

$$F_1\sqrt{3} + F_2 - F_4 - \sqrt{3}\,F_5 - F_6 - \frac{d}{r}\,(0.2\ w) = 0 \quad , \qquad (2)$$

where d is the distance to the center of gravity and r is the radius to the support plate. The other four relationships can be obtained by

considering the strain in each of the supports. The support ring will deflect downward and tip through a small angle, ϕ. Since planes remain plane after deformation, expressions may be written for the individual deflections, δ_i, and the force relations follow from the deflections in each support. Thus

$$F_1 = [1 + (\sqrt{3}/2)]F_3 - (\sqrt{3}/2)F_6 \tag{3}$$

$$F_2 = (3/2)F_3 - (1/2)F_6 \tag{4}$$

$$F_4 = (1/2)F_3 + (1/2)F_6 \tag{5}$$

$$F_5 = [1 - (\sqrt{3}/2)]F_3 + (\sqrt{3}/2)F_6 \quad . \tag{6}$$

The solution of these six equations gives the force on the support member opposite the gas inlet nozzle:

$$F_6 = +4400 \text{ lb} \quad .$$

This force is positive, so the vessel will remain seated on its support structure during the seismic disturbance postulated. The largest force on a member is

$$F_1 = +21\ 070 \text{ lb} \quad .$$

The vertical deflections caused by these loads are

$$\delta_6 = 0.30 \times 10^{-3} \text{ in.}$$

$$\delta_1 = 1.28 \times 10^{-3} \text{ in.}$$

The maximum force on a support plate corresponds to a load of 1320 lb/in. which is well below the 18 500 lb/in. value required for buckling. The deformations are also small and the effects upon the stresses in the gas inlet piping should be negligible.

In order to fully study the characteristics of the system under earthquake conditions, a vibrations study should be made to determine the

fundamental frequencies. Thus, an investigation for this purpose is outlined in Section 16.

Steam Generator Support System

A flexible support system is proposed for the steam generator. The system will allow the steam generator to move freely in a single horizontal direction and thus accommodate the thermal expansion of the pressure vessel, the steam generator shell, and the primary coolant piping between the steam generator and the pressure vessel. A 1/8-scale model of the proposed support system is shown in Fig. 9.2. The support system consists of beam columns (beams subjected to axial compression while simultaneously supporting lateral loads) with small moments of inertia corresponding to the desired direction of motion. The ends are fixed against rotation. In order to allow for radial expansion of the steam generator shell, the steam generator is supported from the support platform by bars hinged at both ends. To facilitate removal of the steam generator from above, the bars will probably be mounted above the platform, as shown in Fig. 3.7, rather than below the platform as in Fig. 9.2. In order to depict the horizontal motion which the support system is capable of absorbing, a triple exposure photograph of the model in the normal position and in a position to either side of the normal is shown in Fig. 9.2. The range of motion shown corresponds to approximately 7 in. in the actual support system. A displacement of approximately 1 1/2 in. will occur during a normal reactor power cycle.

The lateral force required to displace the steam generator horizontally depends on the ratio of the compressive load carried by each beam column to the critical buckling load for each column. If this ratio becomes equal to one, zero lateral force is required to move the steam generator through a small horizontal displacement.[8] One of the columns is shown diagramatically in Fig. 9.3a. Figure 9.3b depicts the column in its

[8]By definition, the critical load is the axial compressive force which is just sufficient to maintain the column in a slightly bent form when the lateral force is removed.

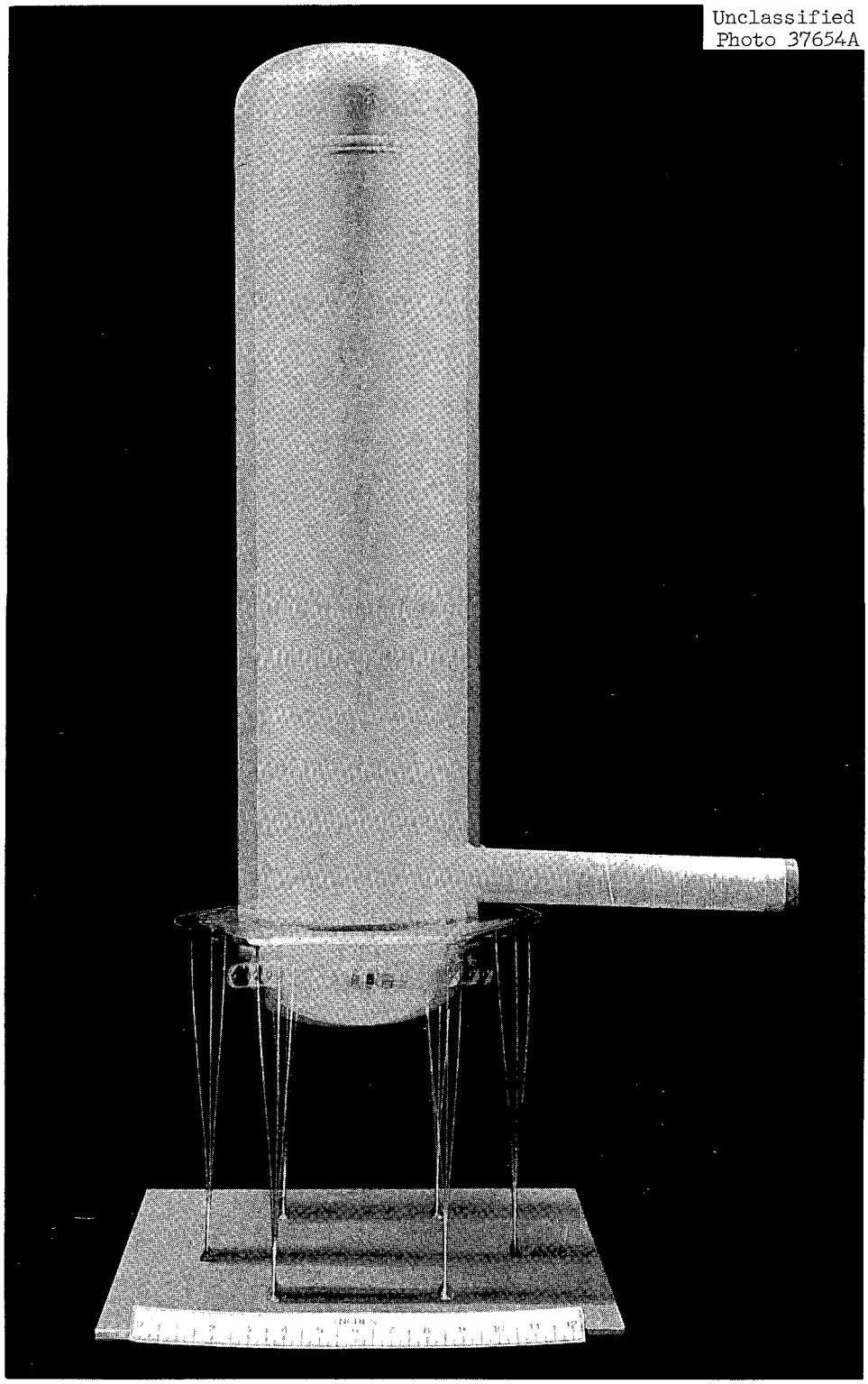

Fig. 9.2. Scale Model of the PBRE Steam Generator Flexible Support System Depicting Horizontal Movement of the Steam Generator. Original reduced 18%.

deformed shape. The critical load in this case is given by

$$P_{cr} = \frac{\pi^2 EI}{l^2} ,$$

where E is the modulus of elasticity, I is the moment of inertia, and l is the column length. If the relative displacement of the two ends of the column is limited to a small value (or to zero, as shown in Fig. 9.4), the critical buckling load, P_{cr}, is

$$P_{cr} = \frac{4\pi^2 EI}{l^2}$$

or greater. Thus if the relative lateral displacements of the ends of the beam-column supports are limited by stops and by the coolant pipe, each beam-column support could carry an axial load equal to its critical load and yet be supporting only one-fourth, or less, of the load necessary to actually produce failure.

In order to properly design a support system of the type proposed, relations between the lateral load, Q, on each beam column, and the lateral and axial relative displacements of the ends of a beam column are needed. The following equations, derived from strain energy considerations, express these relations:

$$\delta = \frac{8Ql^3}{EI\pi^4} \sum_{n=1}^{\infty} \frac{1}{n^2(n^2 - \alpha)} \sin^2 \frac{n\pi}{2}$$

and

$$\lambda = \frac{4Q^2 l^5}{(EI)^2\pi^6} \sum_{n=1}^{\infty} \frac{1}{n^2(n^2 - \alpha)^2} \sin^2 \frac{n\pi}{2} .$$

Here δ and λ are the relative lateral and axial displacements of the ends of a beam column, respectively, and α is the ratio of the axial load, P, to the critical load and is given by

$$\alpha = \frac{Pl^2}{EI\pi^2} .$$

Unclassified
ORNL LR DWG 64853

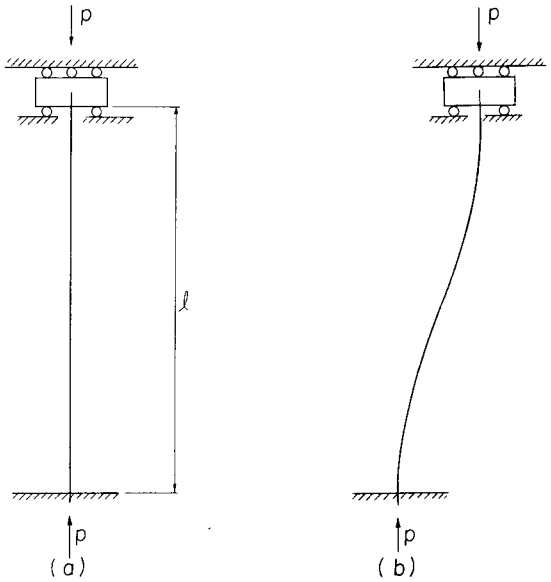

Fig. 9.3. Buckling Form of Steam Generator Support Columns When Lateral Deflection is Permitted.

Unclassified
ORNL LR DWG 64854

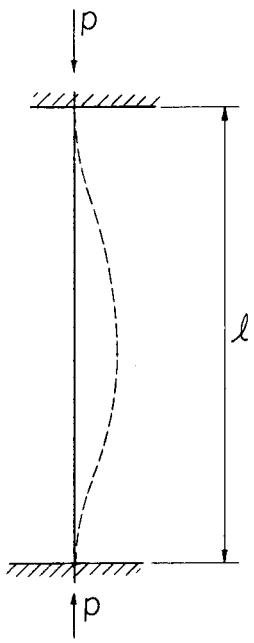

Fig. 9.4. Buckling Form of Steam Generator Support Columns When Lateral Deflection is Prevented.

The preliminary design of the support system was based on the use of six identical beam columns. In the absence of final steam generator design, the columns were examined by using an arbitrary steam generator weight of 26 000 lb. The columns were assumed to be steel, 6 ft long, and 8 in. wide. Three ratios of the compressive load on each column to the critical load were considered:

$$\alpha = P/P_{cr} = 1.0,\ 0.75,\ \text{and}\ 0.5 \quad .$$

The horizontal load, Q, required to displace the steam generator 1 1/2 in. from the vertical position, the vertical displacement of the tops of the beam columns, λ, and the required column thickness, t, are given in Table 9.7 for each value of α. It should be remembered that Table 9.7 is based on an estimated steam generator weight and will be corrected when a final steam generator design is selected. The final selection of a column thickness (or P/P_{cr} ratio) will depend on the allowable axial load which the gas inlet line can transmit without producing excessive stresses in the line or in the pressure vessel or steam generator attachment regions.

Table 9.7. Design Parameters for the Steam Generator Beam-Column Supports for Three Ratios of the Axial Load to the Critical Load

$\alpha = P/Pr_{cr}$	t (in.)	λ (in.)	Q (lb)
0.5	0.61	0.019	663
0.75	0.533	0.019	221
1.0	0.485	0.019	0

Graphite Reflector Structure

The rapid decay of the radial fast-neutron flux in the inner portion of the graphite reflector will produce significant differential radiation shrinkage in the reflector. On the basis of available shrinkage and rupture-elongation data and the present knowledge concerning graphite behavior, it must be assumed that strains induced by fast-neutron irradiation

will cause failure after some exposure interval. This interval depends on the graphite configuration and on the ability of the graphite to withstand deformation without rupture.

The cylindrical portion of the graphite reflector is 96 in. in outside diameter and 30 in. in inside diameter. In order to gain an insight into the severity of the problem, an anisotropic elastic analysis was used to predict the axial, circumferential, and radial stress distributions in the first 12 in. of the reflector, assuming that this portion of the reflector is made up of a single thick-walled cylinder. Generalized plane strain conditions were assumed. The flux data were approximated by an exponential function, and the resulting exposure equation is

$$\phi = 1.12 \times 10^4 \, e^{-0.26d} \quad ,$$

where d is in inches from the core-reflector interface and ϕ is in Mwd/AT per year. The exposure is expressed in megawatt days per adjacent tonne of fuel in the Hanford reactors because shrinkage data are ordinarily given in terms of this unit. The exposure distribution represents that at the mid-plane of the reactor. It was assumed that the longitudinal axis of the cylinder coincides with the direction of extrusion and that the mechanical properties and shrinkage rates are the same in the radial and tangential directions.

The mean temperature of the reflector at the mid-plane of the reactor was assumed to be 1000°F. Based on this temperature and assuming the graphite to be needle-coke AGOT, the shrinkage rates were taken as 3.4×10^{-7} and 1.5×10^{-7} (in./in.)/(Mwd/AT) in the axial and perpendicular directions, respectively. The modulus of elasticity was taken as 1.5×10^6 psi in the axial direction and 1.1×10^6 psi in the perpendicular direction.

The results of the calculation for the thick-walled cylinder, 12 in. thick, are presented in Fig. 9.5, where the axial, radial, and tangential stresses are plotted as a function of the radial distance from the core-reflector interface. The stresses shown represent those occurring after one year of full power operation of the reactor. The maximum tensile

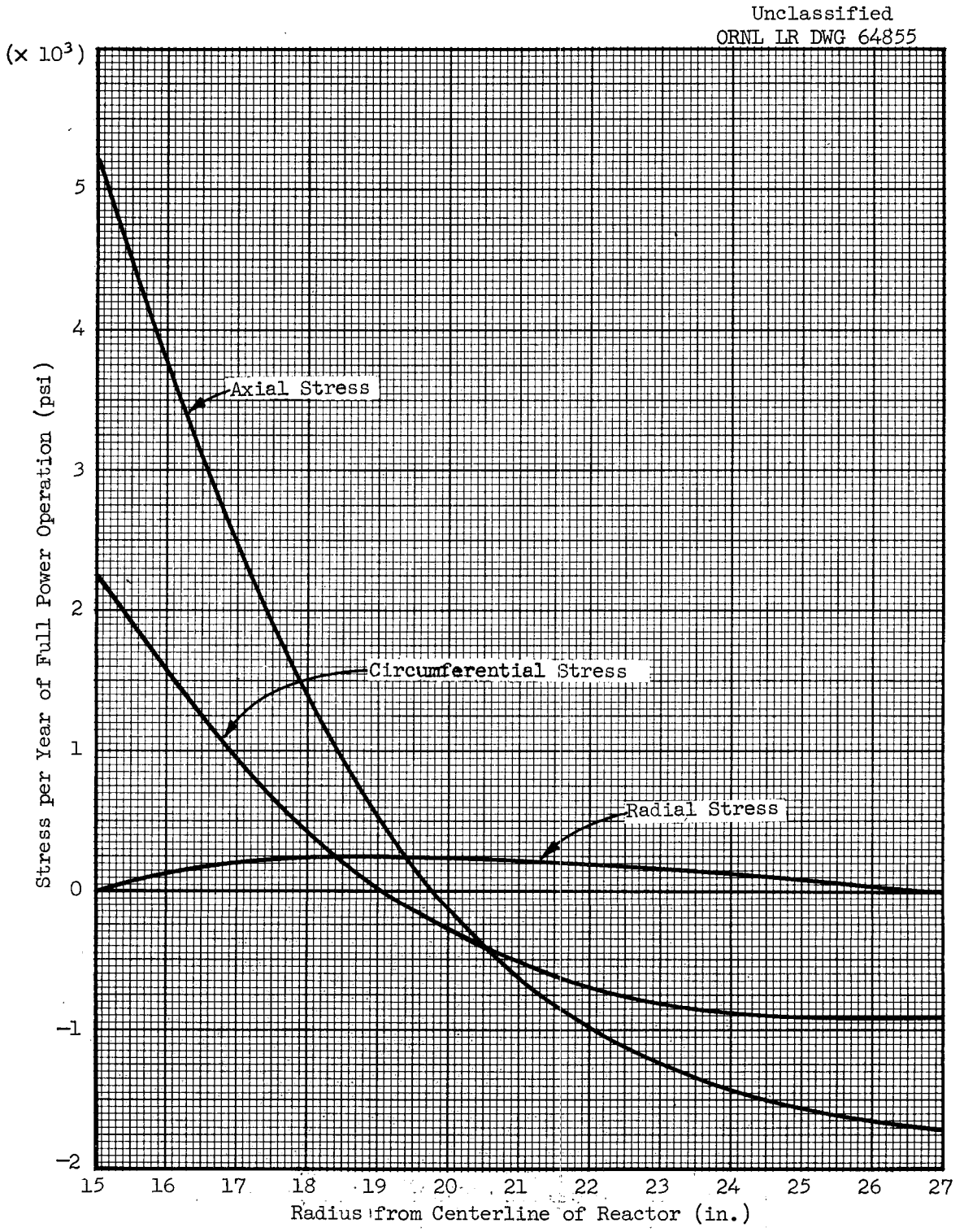

Fig. 9.5. Stresses in First 12 in. of Graphite Reflector After One Year of Full Power Operation, Assuming a Single Cyclinder 12 in. Thick.

strains (only those portions of the strains which are associated with stresses are considered) occur at the inner surface and are given by ϵ_θ = 1230 μin./in. per year of full power operation and ϵ_z = 2820 μin./in. per year of full power operation, where θ and z correspond to the circumferential and axial directions, respectively.

The rupture properties of graphite vary widely from specimen to specimen and even within the same specimen. Thus, fracture predictions can be made on a statistical basis only. A typical set of rupture data from uniaxial tensile tests on needle-type AGOT graphite performed at ORNL[9] are given in Table 9.8. Not enough data were obtained to provide

Table 9.8. Uniaxial Tensile Data for Needle-Type AGOT Graphite

	Rupture Stress (psi)	Fracture Strain (%)
Axial direction		
Minimum	2270	0.16
Average	2310	0.19
Maximum	2360	0.21
Perpendicular direction		
Minimum	1650	0.30
Average	1790	0.35
Maximum	1890	0.41

a statistical basis for predicting fracture. Minimum, average, and maximum values of rupture stress and fracture strain in the directions parallel and perpendicular to the extrusion axis are presented. Other sets of tests at ORNL have yielded much lower minimum values. For instance, fracture strains, in the axial direction, as low as 0.086% have been reported.[10] The National Carbon Company obtained fracture stresses for a large number of samples from the EGCR moderator blocks. Enough data were obtained to

[9]GCR Quar. Prog. Rep. June 30, 1960, ORNL-2964, p. 99.

[10]Letter to L. H. Jackson, AEC, from R. A. Charpie, ORNL, dated April 15, 1961, Subject: Engineering Test Status Report for EGCR-Sect. 1.

form a statistical basis for predicting fracture stresses. The fracture data included very low fracture stresses. For example, the probability that a specimen (taken perpendicular to the extrusion axis) will fail before a stress of 700 psi is reached is 0.25.

Based on the above discussion of fracture data for needle-type AGOT graphite, it is possible to make some inference about the exposure times for the 12-in.-thick cylinder before cracking occurs. Using the minimum fracture values given in Table 9.8, the predicted time to cracking was determined based on both the principal stress theory of failure and the principal strain theory of failure. These times are given below:

Life based on principal strain theory	30 weeks
Life based on principal stress theory	22 weeks

For the fracture strain of 0.086%, the exposure time before cracking occurred would be only 16 weeks. For the fracture stress of 700 psi, it would be only 13 weeks. Actually, it is meaningless to compare elastically calculated stresses with fracture stresses. This is due to the nonlinearity of the stress-strain diagrams for graphite. Since strains are the applied conditions, it is only correct to compare calculated strains with uniaxial fracture strains. Therefore, the principal strain criterion for rupture is believed to be the more realistic.

The graphite reflector structure, shown in Fig. 3.4, illustrates the general type of arrangement which might be used in the final design to facilitate removal. However, the final design of the core will be based on obtaining a maximum graphite lifetime before replacement becomes necessary because of excessive deformation or cracking. Several graphite configurations have been proposed to reduce stresses resulting from radiation shrinkage. A discussion of one such method was given in a previous report.[11] Concentric cylinders were proposed for the first several inches of the reflector. These thinner cylinders were subjected to radiation shrinkage stresses which were appreciably smaller than those for thicker cylinders in the same region. Such a solution has not been used in the present case because of the large diameters required for the cylinders.

---

[11]A. P. Fraas et al., Preliminary Design of a 10-Mw(t) Pebble-Bed Reactor Experiment, ORNL-CF-60-10-63 rev., sec. 9 (May 8, 1961).

However, thin segmented concentric cylinders might be used. Cuts in the segments would further reduce the stresses. With present methods,[12] assuming plane strain conditions, it is possible to investigate general configurations, and such investigations are in progress. It is entirely plausible to assume that a graphite configuration could be found which will extend the life of the inner portion of the reflector to several years of full power operation.

---

[12]Robert F. Redmond, Lewis E. Hulbert, and Richard W. Clark, Numerical Solution of Reactor Stress Problems, BMI-1503 (February 1961).

10. FUEL ELEMENTS AND GRAPHITE COMPONENTS

Fuel Elements

Considerable information concerning the behavior of fuel elements of the type required for the PBRE has been generated since the initial design study on this subject.[1] The purpose of this section is to review the fuel element problem in the light of this information and to discuss the reference configuration which has been selected for the PBRE.

The approach used in arriving at a reference fuel element has been a conservative one. This approach is felt to have been appropriate in view of the uncertainties which surround the actual requirements of the PBRE fuel elements and because pertinent data on the behavior of fueled graphite simply are not available for the limiting conditions of reactor operation which are anticipated. Research and development programs designed to clarify this situation are described in Section 16 of this report.

Requirements and Operating Conditions

The required fuel element characteristics and pertinent operating conditions for the PBRE are tabulated below:

Configuration	Sphere
Size (diameter), in.	1 1/2
Number of spheres in core	11 700
Fuel loading, wt % of U + Th in fuel sphere	5
Thorium-to-uranium atom ratio	0.61
Enrichment of uranium in U^{235}, %	93
Carbon density, g per cm^3 of net graphite volume	1.70
Average power density, w/cm^3	
Reactor core	9
Fuel spheres	14.8

[1] A. P. Fraas et al., Preliminary Design of a 10-Mw(t) Pebble Bed Reactor Experiment, ORNL CF-60-10-63 rev. (May 8, 1961).

Mean surface heat flux, Btu/hr·ft^2	29 700
Sphere operating temperatures, °F	
Average volumetric	1090
Average center-to-surface temperature difference	120
Estimated hot-spot conditions	
Surface	~1900
Center	~2100
Irradiation exposure (burnup)	
Fissions per cm^3 of fuel sphere	3.1×10^{19}
Mwd per ton of U + Th	130 000
Atom per cent of initial U + Th	13.6

Fission-Product Retention

The major requirement for the fuel elements is associated with fission-product release from the standpoints of both hazards and system maintenance. Although it is difficult to define precisely what is meant by adequate fission-product retention in the present application, the criterion most frequently cited is with regard to the inert gas species, such as Kr^{87} (78 m), Kr^{88} (2.8 h), Xe^{135} (9.20 h), Kr^{85m} (4.4 h), and Xe^{133} (126 h) which are readily measured in irradiation experiments. Release factors, defined as the steady-state ratio of release rate to birth rate (R/B), in the range of 10^{-6} to 10^{-4} for these species appear to represent reasonable design goals in the development of a satisfactory fuel element for a pebble bed reactor.[2] The major uncertainties in this area are due to inadequate experimental data on the transport and deposition characteristics of troublesome fission products and the effect these characteristics will have on the maintenance problem.

In order to fulfill the major requirement cited above, the graphite-base sphere in the PBRE must include one or more features which serve to retain or hold up fission products under the mechanical, thermal, chemical, and irradiation environments which will exist in service. Since

[2]A. P. Fraas et al., Design Study of a Pebble-Bed Reactor Power Plant, ORNL CF-60-12-5 rev. (May 11, 1961).

normal molded graphite matrices are not sufficiently impermeable, the retentive character required for both volatile and nonvolatile species must derive from suitable coatings on the fuel particles, impregnation of the matrix, or coatings on the fuel spheres themselves. The extent to which recourse must be taken to these three methods of approach is not completely clear at the present time. If, however, the fuel is to be in the form of thorium-uranium carbide particles, as presently conceived, it will be necessary to provide particle coatings for handling purposes during fabrication, and a potential fission-product barrier would thereby be built into the fuel element. Accordingly, the development of impermeable pyrolytic-carbon coatings which are stable with respect to the environmental conditions cited above has been a matter of major emphasis during the past year.

If existing experimental programs indicate that oxidizing impurities in the helium coolant require a protective coating, such as siliconized-silicon carbide (Si-SiC) on the sphere to prevent mass transport of carbon to the cooler portions of the system, another method for retaining fission products would be incorporated into the design. Graphite impregnation techniques are available and have been used in other programs. This method of approach may receive attention if the method of particle coating appears to be inadequate.

Results on graphite fuel elements containing bare fuel particles have indicated that the rates of release of the various radioactive species are dependent on the half life. A plot of the logarithm of the R/B ratio for the various species versus the logarithm of the half life has shown a slope of one-half. This correlation suggests that for bare particles the controlling release mechanism is the diffusion of recoils through the graphite matrix or fission-product diffusion in the fuel particles.

For reference purposes, the results obtained in the Sanderson & Porter program[3] on the FA-23 specimen in the SP-5 sweep capsule are useful. The FA-23 specimen was a 1 1/2-in.-diam molded-graphite sphere containing uncoated uranium carbide particles, with a 1/8-in. unfueled shell and a 0.008-in. coating of Si-SiC. The specimen operated at surface and central

---

[3]Fuel Element Development Program for the Pebble Bed Reactor – Final Report, NYO-9064, April 30, 1961.

temperatures of 1300 and 1500°F, respectively, and the sphere coating failed after about 21 days during startup of the third reactor cycle. After the coating failed, the R/B factors increased by a factor of 10^5 and remained essentially constant for a period of 11 days. Samples taken some four months later, after a burnup of approximately 5 at. % U^{235}, showed that further increase in the release rate had occurred. The data obtained during the final 15 days of the 170-day experiment are plotted as a function of half life in Fig. 10.1. Since operating conditions in the SP-5 capsule were similar to the average conditions proposed for the PBRE, uncoated PBRE fuel elements containing bare fuel particles would be expected to give about the same release rates as those observed for the FA-23 specimen.

It seems reasonable to assume that with whatever features are built into the PBRE fuel element to retard the release of fission products, the release rates could be reduced by a factor of 50 relative to the rates from fuel elements containing bare particles. Thus, a reasonable estimate for the maximum R/B ratio for a given species in the PBRE is provided by the relationship

$$R/B = 10^{-6} \sqrt{T_{1/2}} \quad , \qquad (1)$$

where $T_{1/2}$ is the half-life, in seconds, for the given species. This relationship is plotted in Fig. 12.5. As shown in Section 12, the release factors computed from this equation are more than adequate from the standpoint of normal leakage of activity from the PBRE. Uncertainties in the behavior of non-volatile fission products in the coolant system preclude a similarly clear-cut statement with regard to maintenance problems.

Mechanical Effects

During fabrication, coated particles are subjected to mechanical damage during blending and molding. In addition, coated particles at the surface of a molded graphite sphere are subjected to more or less severe mechanical damage by abrasive action, impact, and compressive forces during handling in fabrication, during loading and unloading in the reactor, and during reactor operation. Because of the potential

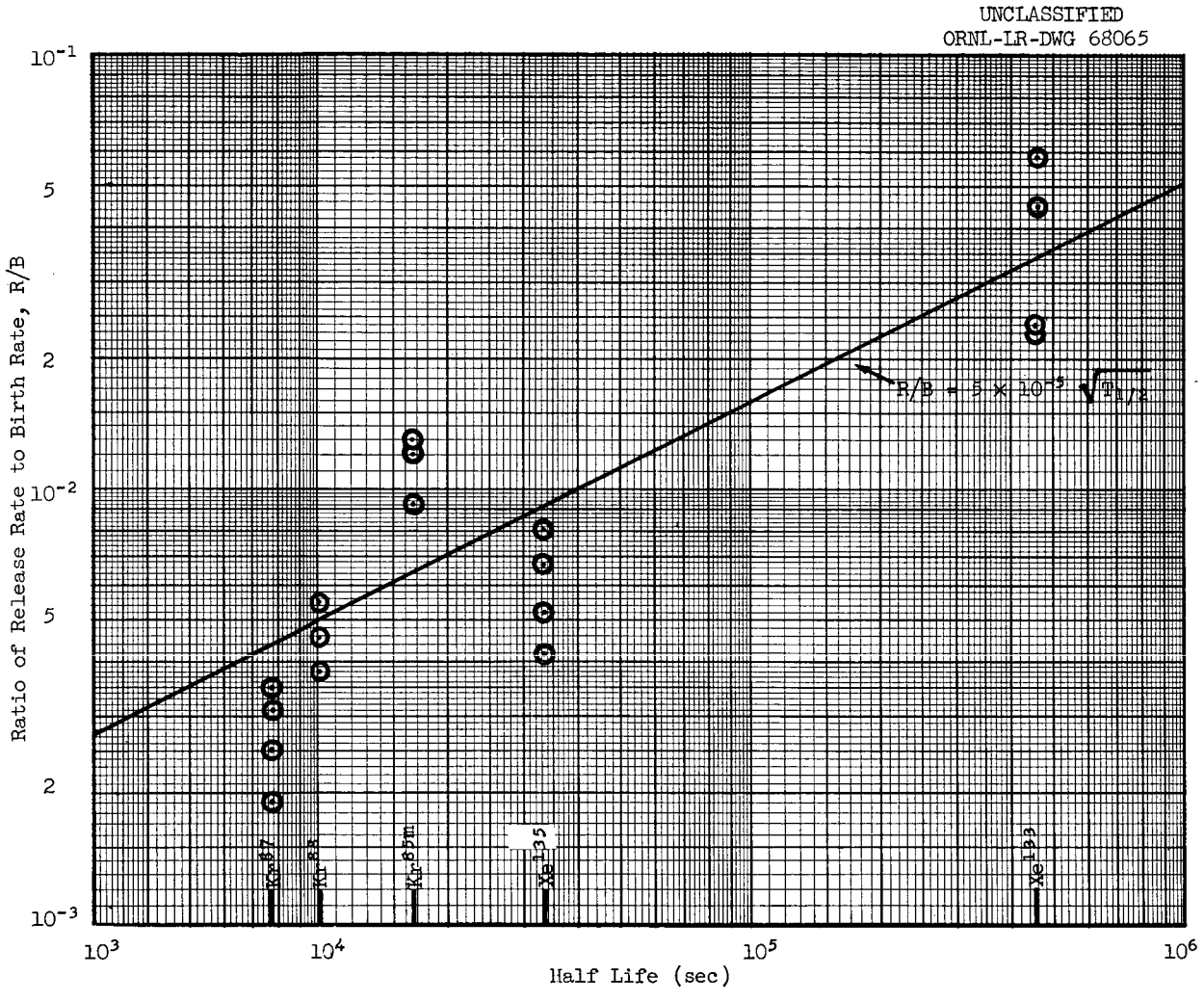

Fig. 10.1. Relationship Between R/B and Half Life for Fueled Graphite Containing Uncoated Uranium Carbide Particles at 1300°F. (Data for FA-23 specimen in SP-5 capsule of Sanderson & Porter program as described in text.)

damage to surface particles by these mechanical effects, it is evident that protection in the form of an unfueled graphite shell must be included in the reference design. Whether adequate protection against this mechanical damage would be provided by an oxidation-resistance coating, particularly for coated particles which partially protrude from the surface, is doubtful, but this possibility deserves investigation. First attempts at fabricating unfueled-shell configurations in the Sanderson & Porter program[3] were regarded as unsuccessful because cracks developed in the shells during capsule irradiation tests. Improved fabrication techniques may be required to overcome this limitation.

Notwithstanding the effects on surface particles, the PBRE fuel spheres must retain their integrity under the stresses imposed during loading and unloading and during reactor operation. As discussed in Section 5, a set of unfueled graphite spheres will be used for testing the fuel-handling system and will be available for use during the loading of fueled spheres in the reactor. Thus, impact loads are expected to be minimal and no problem is anticipated during this phase of the operation. The abrasive action of balls in contact during movement of the bed as fuel is extracted periodically may create a dust problem. Lateral compressive loads during operation may arise from thermal expansion, although preliminary tests performed in the Sanderson & Porter program[4] indicate that the pebble bed would expand on heating with no change in the fractional void volume and, therefore, no significant generation of lateral compressive stresses. The maximum vertical compressive load on a ball on the bottom of a 4-ft-high bed would be less than 4 lb.

Thermochemical Effects

Requirements for chemical stability of the fuel element include not only oxidation resistance but also phase stability within the fuel particle and compatibility of the fuel-particle coating with the fuel particle and the matrix graphite. Possible catastrophic reactions in case of a steam leak must also be considered. From the standpoint of thermochemical

---

[4]Progress Report on Pebble-Bed Reactor for Period June 1, 1959–October 31, 1960, Sanderson & Porter, NYO-9071.

stability, a fuel element containing pyrolytic-carbon-coated uranium-thorium dicarbide particles appears to be the most attractive of several which have been considered. Disproportionation of uranium dicarbide to yield the sesquicarbide, U_2C_3, and graphite under PBRE hot-spot conditions has been reported,[5-7] although evidence for this reaction has not been seen in experiments involving coated uranium carbide particles. While the equilibrium phase situation in the ThC_2-UC_2 system is not precisely known, it is possible that the addition of thorium would tend to have a stabilizing effect on the disproportionation reaction under consideration. In any case, it is conceivable that if phase instability of this type presents a problem, an appropriate heat treatment could be used prior to the time the fuel elements are inserted in the reactor. The added effects of irradiation must be studied, however, before final decisions can be made. The use of ThO_2-UO_2 solid solution material for the fuel particles is not entirely out of the question. Pyrolytic carbon coatings on oxide fuel particles can be compatible if the coatings do not crack and allow release of the gaseous products of the reaction between these phases. In addition, the oxide fuel particle concept will be preferred if experiments now in progress show that severe attack of carbide particles with damaged coatings would occur in case of a steam leak. Oxide coatings, such as Al_2O_3 and BeO, on oxide fuel particles have not been removed from consideration entirely, although based on existing information this concept does not appear as attractive as that involving carbon-coated carbide fuel particles.

Irradiation Effects

The irradiation effects of concern are those which would render the fuel element mechanically and chemically unstable and thereby promote the release of fission products. Cracking of particle coatings during

---

[5]M. W. Mallett, A. F. Gerds, and H. R. Nelson, The Uranium-Carbon System, J. Electrochem. Soc., 99: 197–204 (May, 1952).

[6]W. Chubb and F. A. Rough, An Evaluation of Data on Nuclear Carbides, BMI-1441 (May, 1960).

[7]M. W. Mallett, A. F. Gerds, and D. A. Vaughan, Uranium Sesquicarbide, AECD-3060 (December, 1951).

irradiation, as discussed in subsequent sections, can be attributed to the singular or combined effects of particle swelling, neutron-induced shrinkage of the particle coating, and pressure buildup from fission gases within the coated particle. There is a need for better understanding of why particle coatings fail so that modifications to the fabrication procedures can be made intelligently. For example, the merit of providing a substantial void volume within the coated particle and of incorporating a porous intermediate coating between the particle and the outer, impervious coating may deserve careful evaluation.

The Reference Fuel Element

Based on existing knowledge and the considerations discussed in the previous section, a reference fuel element has been selected. This element is a molded, 1 1/2-in.-diam graphite sphere containing a uniform dispersion of pyrolytic-carbon-coated uranium-thorium carbide particles, a 1/16-in.-thick unfueled graphite shell, and a 0.006- to 0.008-in.-thick coating of Si-SiC. The nominal diameter of the fuel particles is 180 ± 20 μ and the coating thickness is 80 ± 20 μ. Other properties such as the thorium-to-uranium ratio and fuel loading are tabulated in the previous section.

The choice of the unfueled shell thickness was based on optimization with respect to protection against mechanical damage to coated particles and thermal stress states which could promote separation at the interface between the fueled and unfueled portion. The particle diameter is felt to be optimum with respect to particle separation for a given fuel loading and fission-product retention within the particle. The coating thickness was chosen because of the significant drop in alpha count (due to uranium contamination) which has been reported at a coating thickness of 50 to 60 μ.

Status of Coated Particle Fuel Element Development

Development work on fuel elements based on the coated particle concept is being conducted at Oak Ridge National Laboratory (ORNL), Battelle

Memorial Institute (BMI), General Atomic (GA), and in varying degrees by several private industrial concerns. The major emphasis by far has been on the preparation of pyrolytic-carbon-coated carbide fuel particles and evaluation of these particles both in the unsupported condition and as incorporated into graphite bodies.

Investigation of oxide-coated UO_2 particles has been restricted for the most part to preparation and evaluation studies at BMI; similar studies on pyrolytic-carbon coated thorium-uranium carbide particles has been the item of principal interest at GA. The emphasis at ORNL has been on the evaluation of commercially produced, pyrolytic-carbon-coated uranium carbide particle materials in an extensive irradiation test program. Recently, some limited fabrication studies have been initiated at ORNL. Considerable information concerning the techniques used in all phases of PBRE-type-fuel element fabrication has been accumulated by commercial suppliers.

The summarizing comments listed below are intended to convey the more important features of the development work which are pertinent to the PBRE fuel element problem. The material has been categorized in terms of the several types of coated particles under consideration. Data of a preliminary nature are not included in the discussion.

Pyrolytic-Carbon-Coated Uranium Carbide Particles

The uranium carbide particles which have been studied represent multiphase systems containing UC_2 as the major phase, UC as Widmanstätten-type platelets, and varying amounts of graphite flakes. Under certain restricted conditions it is apparently possible to prepare particles which are essentially all UC_2. All particles of this type which have been examined are high-density spheroids, 150 to 300 μ in diameter, covered with 5 to 15 μ of a porous graphite layer which persists as an intermediate layer during the pyrolytic coating process.[8]

Uranium carbide particles have been coated with carbon by the pyrolysis of hydrocarbons at temperatures ranging from 950 to 2000°C. Depending

---

[8]C. K. H. DuBose and R. J. Gray, The Metallography of Pyrolytic Carbon Coated Uranium Carbide Spheres, ORNL-TM-91, in publication.

upon the deposition temperature and rate, the microstructure of the coating assumes a smooth, laminar appearance or a columnar, more granular appearance. High temperatures and low rates favor the columnar form. The coating density passes through a minimum in the temperature interval from 950 to 1800°C.[9-12]

Alpha-counting and acid-leaching techniques have shown that contamination of the coatings prepared by a variety of techniques can be kept to acceptable levels. Thermal cycling of coated particles between room temperature and 1400 to 1600°C results in a slight increase in the amount of exposed fuel due, presumably, to fuel migration through the coatings. When these particles are heated to temperatures higher than 2100°C for prolonged periods, extensive reactions are detected at the carbide-coating interface and the amount of exposed fuel increases by a factor of 10.[13]

Fission-gas release studies using neutron-activation techniques have shown that the fractional release of Xe^{133} from unsupported coated particles is approximately 1×10^{-6} after 3 hr at 1400°C. In studies at ORNL laminar-type coatings were observed to spontaneously rupture at 2050°C; columnar-type coatings did not rupture at 2180°C, but diffusion of Xe^{133} through the coatings was observed after 20 hr. In no case did thermal cycling between room temperature and 1800°C cause rupture or release of significant quantities of Xe^{133}. Release of Ba^{140} has been detected at temperatures greater than 1400°C in neutron activation tests.[13]

Static-capsule irradiation tests to approximately 8 at. % burnup (approximately 3000 hr) have been performed on both laminar- and columnar-type coated uranium carbide particles in the temperature range 2000 to 2500°F. In both cases, 0.1 to 0.2% of the Kr^{85} generated was detected

---

[9]R. W. Dayton and C. R. Tipton, Jr., Progress Relating to Civilian Applications During July, 1961, BMI-1534.

[10]R. W. Dayton and C. R. Tipton, Jr., Progress Relating to Civilian Applications During August, 1961, BMI-1541. (Classified)

[11]R. W. Dayton and C. R. Tipton, Jr., Progress Relating to Civilian Applications During September, 1961, BMI-1546.

[12]R. W. Dayton and C. R. Tipton, Jr., Progress Relating to Civilian Applications During October, 1961, BMI-1549. (Classified)

[13]GCR Quar. Prog. Rep. for Period Ending Dec. 31, 1961, ORNL-3254.

in the gas after the tests and from 2 to 4% of the particle coatings were cracked.[13]

At ORNL, fueled-graphite specimens containing coated uranium carbide particles have been obtained from two commercial sources. It has been shown by acid-leaching and neutron-activation tests that, with one exception, damage to the particles occurred during fabrication of the specimens. Fractional release of Xe^{133} after 20 hr at approximately 1000°C in neutron-activation tests has ranged from 2×10^{-5} to 8×10^{-4}, with the lower value being associated with lower molding pressure. For the one exception this value was 2×10^{-7}.[13] In many cases the uniformity of distribution of particles has been observed by radiographic techniques to be poor. Sweep tests on fueled graphite bodies containing coated particles are in varying states of progress and, except for the ORNL-MTR-48-5 experiment,[14] only preliminary results have been obtained.

In the MTR-48-5 experiment, a cylindrical specimen 1 in. in diameter by 1 1/2 in. long containing laminar-type coated particles was tested. A molding pressure of 30 000 psi was used in fabricating the specimen, and the fractional release of Xe^{133} from a similar specimen in neutron-activation tests was 5×10^{-4} in 22 hr at 1000°C. Estimated central fuel temperatures and approximate times at temperature during the test were as follows: 1750°F for 99 hr; 2600°F for 880 hr; 2350°F for 24 hr; 2050°F for 247 hr; 1600°F for 875 hr; and 1750°F for 275 hr. The initial release factors for Kr^{88} were in the order of 10^{-3} but increased exponentially during the 2600°F exposure. At 1600°F, the release factors decreased but were higher than the initial values by factors of 2 to 6. They remained essentially constant during the 1600°F exposure. The burnup in this experiment was estimated to be 15 at. % of U^{235}. The results have been interpreted to indicate that in the as-fabricated condition from 1 to 5% of the particle coatings were damaged and that additional damage to the particles occurred during the test. Postirradiation examinations have not been performed.[13]

---

[14]GCR Quar. Prog. Rep. for Period Ending Sept. 30, 1961, ORNL-3210.

Pyrolytic-Carbon-Coated Uranium-Thorium Carbide Particles

Development in this area has been carried out at GA in connection with the HTGR. It is important to note that because of the internal purge system and low-permeability graphite sleeve in the HTGR fuel element, fission-product retention by particle coatings was not a primary objective in the GA program. In addition, the HTGR fuel-element temperatures are substantially higher than those proposed for the PBRE.

Techniques have been developed at GA for producing pyrolytic-carbon-coated spheroidal $(Th,U)C_2$ particles and for incorporating these particles into cylindrical graphite bodies by hot-molding methods.[15] The protection afforded by the coatings is measured by exposure to moist air at 50°C. For example, after 20 hr, a variety of coated particles showed a weight gain of 0.1 to 0.3% as compared with 11 to 20% for uncoated particles. The pyrolytic coatings are laminar in structure and are deposited at 1400°C. The fractional release of Xe^{133} is of the order of 10^{-5} in 24 hr at 1000°C in neutron-activation tests.

High-burnup (approximately 20 at. % U^{235}) low-temperature tests (less than 100°C) have been performed using compacts containing low-density coated particles of 105 to 250 μ particle diameter and a nominal coating thickness of 30 μ.[15,16] The thorium-to-uranium ratio was 2.25:1. Post-irradiation heating experiments indicated that approximately 17% of the coated particles had failed during irradiation. Sweep-capsule tests[15] at temperatures of 960 to 1550°C on bodies of this type showed that R/B ratios for Kr^{88} ranged between 1×10^{-3} and 12×10^{-3} after approximately 20 at. % burnup of the U^{235}.

Pyrolytic-Carbon-Coated Uranium Dioxide Particles

Carbon coatings have been applied in the temperature range of 1200 to 1700°C to uranium dioxide particles by the same methods used on uranium

---

[15]W. V. Goeddel, The Development and Evaluation of Graphite Matrix Fuel Compacts for the HTGR, GA-2289, Aug. 8, 1961.

[16]40 Mw(E) Prototype High-Temperature Gas-Cooled Reactor Research and Development Program, Quar. Prog. Rep. for Period Ending March 31, 1961, GA-2204.

carbide particles and with similar results for coating density.[10,11] Acceptable surface contamination, as determined by alpha assay, has been obtained. Coatings applied at 1700°C have shown higher surface alpha activities, and, in one run, an unexplained high porosity, as evidenced by the 1.2 wt % UO_2 removed by acid leaching.

Al_2O_3-Coated Uranium Dioxide Particles

Aluminum oxide has been applied to uranium dioxide particles by direct hydrolysis of gaseous Al_2Cl_6 with water vapor and by indirect hydrolysis with a mixture of hydrogen and carbon dioxide gases.[17] Coatings applied at 500 to 900°C tend to be porous and amorphous, but at 1000°C they are nearly of theoretical density and are transparent. At temperatures between 900 and 1100°C, the α-Al_2O_3 structure becomes pronounced. Uranium oxide particles coated with aluminum oxide at 1000°C are essentially unaffected by heating in air at 650°C. Heating of fine-grained aluminum oxide coatings to temperatures above their application temperature promotes grain growth and may lead to stresses that will cause failure of the coating. There is some evidence that a course-grained structure is conducive to failure by oxidation.

The difference in thermal expansion of aluminum oxide and uranium dioxide can also cause coating failure. Coatings applied at 1000°C undergo cracking when heated to approximately 1400°C. A solution has been sought in higher application temperatures. Coatings applied at 1400°C were similar in appearance to those obtained at 1000°C but gave inferior response to acid leaching whether in the as-produced, heat treated, or oxidized condition. In addition, the crushing strength for 1400°C aluminum oxide is about 50% of that for 1000°C coating.

A preferred crystal orientation of one type was obtained for application temperatures of 1000 to 1250°C. A preferred orientation was also found for 1400°C coatings, but the orientation was rotated at 90 deg to that obtained at the lower temperatures.

---

[17] M. F. Browning et al., Alumina Coating of UO_2 Shot by Hydrolysis of Aluminum Chloride Vapor, BMI-1471, Oct. 25, 1960.

Results of inpile tests in the SP-5 sweep capsule on aluminum-oxide-coated uranium dioxide supported in a graphite matrix (Spec. No. FA-22)[1] have become available.[9] Fractional release data have been plotted as a function of fission-gas decay constant, λ. An analysis of the form of the data plot suggests that the mechanism of fission-product escape to the sweep gas was not diffusion through the particle coating. Some re-release by particle-surface contamination was observed, but the principal release mechanism involved particle-coating cracking. Some coating cracking occurred at less than 1% burnup and much more at 3 to 5% burnup. Postirradiation examination disclosed that about 3.6% of the particles in the sphere possessed cracked coatings. About 86% of the particles with cracked coatings were located within 10 particle diameters of the surface of the sphere.

An additional sweep capsule experiment has been performed using a sample machined from a prototype of the FA-22 sphere.[12] The sample temperature was 1070°C, and acceptable fission-product retention (R/B for Kr^{85m} of 10^{-6}) was observed during the first cycle of operation, which was for a period of 201 hr. A capsule leak at that time required termination of the sweep test.

BeO-Coated Uranium Dioxide Particles

Beryllium oxide coatings have been applied at BMI at temperatures between 1000 and 1400°C to uranium dioxide particles by hydrolysis of gaseous $BeCl_2$. Dense, transparent, and nonporous coatings were obtained for BeO having up to 1% SiO_2 or Al_2O_3 impurities. Lowering these impurities to 100 ppm gave a porous and opaque coating in the range 700 to 1100°C. Efforts to improve the quality of high-purity BeO coatings have thus far been unsuccessful.[12]

Sphere Surface Coatings and Low-Permeability Graphite

Sphere Surface Coatings

Isotropic grades of graphite coated with Si-SiC that are completely oxidation resistant in air at 1000°C are available from commercial sources.

Coatings of this type have been applied to molded, fueled graphite spheres as discussed in the previous PBRE design report.[1] Coating failures during irradiation have been sufficiently frequent, however, that it is clear that without further development work, Si-SiC coatings alone cannot be depended upon to provide the fission-product retention required in the PBRE.

Low-Permeability Graphite

Tests designed to evaluate the effectiveness of low-permeability graphite sleeves have been performed in the ORNL-MTR-48 facility.[14] The permeabilities of the specimens ranged between 10^{-8} and 10^{-9} for helium at room temperature and a pressure difference of 1 atm. While these experiments have been plagued with failures in the silicon-base brazes used to seal the bottles, it is reasonable to conclude that release factors of the order of 10^{-3} can be achieved. The measured temperatures within the sleeves ranged between 1050 and 1500°F in these tests.

Graphite Components

The PBRE reflector and a boronated thermal-neutron shield will be fabricated of graphite. Detailed design of these components is discussed in Section 3. Essentially, the graphite structure consists of an 8 1/2-ft-diam, 10-ft-high right-circular cylinder containing a centrally located 2 1/2-ft-diam, 4 ft-high cylindrical cavity for the pebble bed. Additional graphite will be located in the upper hemispherical head of the pressure vessel. The outer layer of graphite will contain 1/2 wt % boron to serve as a thermal neutron shield. In order to facilitate handling and to reduce the coolant gas leakage from the core, it is desirable to minimize the number of graphite pieces used; that is, large components are desired.

Under normal operation, the graphite will be subjected to temperatures of 550 to 1250°F, flowing helium at 500 psi containing impurities, fast-neutron bombardment, and mechanical loads. The major problems anticipated derive largely from the nonuniformity of the environment. Temperature gradients will induce thermal stresses and, in combination with

flowing impure gas, can lead to carbon and possibly boron mass transfer. The fast-neutron flux gradient through the graphite sections will cause differential shrinkage, which, in turn, will lead to stresses which eventually can exceed the fracture stress unless relieved by creep. Under these conditions, the graphite must not fracture or undergo major dimensional changes. The coolant flow passages, control rod channels, and the fuel element feed and discharge channels are all part of the graphite structure.

Although the operating requirements of the reflector graphite and boronated thermal-neutron shield graphite are similar in many respects, certain problems are unique to one or the other. Therefore, this discussion will consider the two types of graphite separately.

Reflector Graphite

Consideration of the design and operating requirements of the PBRE reflector graphite indicate that the major problems are concerned with cracking from radiation-induced shrinkage and oxidation. Similar problems are faced in the EGCR. Furthermore, the AGOT needle-coke graphite used in the EGCR moderator columns and the isotropic, coatable 901 RYL grade used in the fuel-element support sleeves of the EGCR are logical candidates for the PBRE reflector. Typical physical and mechanical properties of these grades of EGCR graphites are therefore presented for reference in Table 10.1.

Radiation Shrinkage Cracking. Fast-neutron bombardment of graphite induces dimensional changes which depend on exposure, temperature, type of graphite, and direction with respect to the extrusion axis of the graphite. At the temperatures of the PBRE reflector, the dimensional changes will be negative, that is shrinkage will occur. Because of the fast-neutron flux gradient through the graphite sections, differential shrinkage will be induced. The stresses generated thereby can eventually exceed the rupture stress unless relieved by creep. The consideration of radiation shrinkage cracking is important because it may limit the operating life of the graphite components.

Table 10.1. Properties of EGCR Graphites

Property	AGOT Moderator Graphite[a]			Fuel Element Support Sleeve Graphite, 901 RYL[b]		
	Average	Maximum	Minimum	Average	Maximum	Minimum
Bulk density, g/cm^3	1.71	1.73	1.68	1.71	1.75	1.67
Tensile strength, psi						
Longitudinal[c]	1080	1270	840	1670	1980	1200
Transverse[c]	750	930	650	1190	1530	850
Longitudinal[c] flexure strength, psi	2150	2480	1830	2850	3540	2320
Young's modulus, psi						
Longitudinal[c]	1.60×10^6	1.75×10^6	1.39×10^6	1.53×10^6	(e)	(e)
Transverse[c]	0.85×10^6	0.96×10^6	0.71×10^6	(e)	(e)	(e)
Coefficient of thermal expansion, $10^{-6}/°C$[d]						
Longitudinal[c]	0.71	0.89	0.58	4.55	(e)	(e)
Transverse[c]	2.36	2.66	2.14	5.50	(e)	(e)
Ratio	3.32	2.99	3.69	1.22	(e)	(e)
Thermal conductivity, cal/cm·sec						
Longitudinal[c]	0.532	0.599	0.401	0.39	(e)	(e)
Transverse[c]	0.359	0.430	0.293	(e)	(e)	(e)
Thermal-neutron absorption cross section,[f] mb	3.94	4.10	3.87	3.90	4.03	3.76
Boron content, ppm	0.27	0.5	0.1	0.55	0.94	0.24
Ash content, ppm	160	240	80	26	110	<10
Oxidation rate[g] at 600°C, g/g·hr	0.015	(e)	(e)	0.015	(e)	(e)

[a]Extrusion size 18 in. × 18 in.

[b]Extrusion size approximately 5 1/2 in. in diameter.

[c]Directions are with respect to the extrusion axis.

[d]Temperature range of measurement: AGOT, room temperature to 100°C; 901 RYL, 100 to 600°C.

[e]Not determined or not reported.

[f]For neutrons with an average velocity of 2200 m/sec.

[g]Determined in air at a pressure of 1 atmosphere.

The radiation-damage characteristics of the EGCR graphites are being studied at Hanford.[18] It has been shown that at 475°C, the AGOT moderator graphite contracts 0.36% in the parallel direction and 0.18% in the perpendicular direction after an exposure of 17 000 Mwd/AT. These rates are lower than those based on earlier results which form the basis for the calculations in Section 9. The contraction rate was observed to increase with exposure; however, there were not enough data to establish an accurate, quantitative relationship in this regard.

After an exposure of 3000 Mwd/AT at 500°C, a contraction of 0.034% was observed for samples of 901 RYL graphite in a direction parallel to the axis of extrusion. Other samples were irradiated at 1200 to 1400°C to an exposure of 5000 Mwd/AT.[19] The contraction observed in the 901 RYL graphite was approximately equal to that for the AGOT moderator graphite in the parallel direction. The contraction in the perpendicular direction, however, was six times as large as that of the moderator graphite.

No data have been reported for the effect of irradiation on the strength properties of graphite irradiated at temperatures of interest to the FBRE. The out-of-pile creep properties of the EGCR moderator graphite have been studied at ORNL at temperatures up to 1100°F and a tensile stress level of 1800 psi.[20] After small initial strains of less than 0.015% during the first 10 to 30 hr of the experiments, no further creep was detected for periods as long as 2000 hr. Based on the limits of detection, it was estimated, therefore, that after the initial strains the creep rates were less than 5×10^{-9}/hr.

Experiments[21] have shown creep of various grades of nuclear-grade graphite when stressed under irradiation at temperatures up to 300°C.

---

[18]Preliminary Results of Second Irradiation of EGCR Graphite, Letter Report from J. M. Davidson, GE-HAPO, to W. J. Larkin, OROO, July 18, 1961.

[19]Private communication from D. R. de Halas, Hanford, to Fred L. Carlsen, Jr., ORNL, December, 1961.

[20]GCR Quar. Prog. Rep. March 31, 1961, ORNL-3102, p. 116.

[21]N. C. Fielder et al., Irradiation Induced Plasticity in Graphite, Paper presented at the Fifth Biennial Conference on Carbon, University Park, Pa., June 19–23, 1961.

In some cursory experiments, creep constants of approximately 2×10^{-6}/psi per 1000 Mwd/T were observed. This value appears to be applicable for specimens irradiated between room temperature and 300°C at stresses up to 500 psi. The exposures for these experiments were less than 1000 Mwd/T.

The thermal conductivity of graphite has been observed to decrease under irradiation.[22] After an exposure of 4500 Mwd/AT at 500°C, the room-temperature thermal conductivity of samples of grade CSF was reduced by about a factor of 3.

The effect of neutron irradiation on Young's Modulus has been studied by a number of workers.[23-27] For room-temperature irradiations, this property increases and appears to reach a constant value, on extended exposure, that is two to three times the unirradiated value. For higher irradiation temperatures, the effect of irradiation is less pronounced. For example, at 350°C, the modulus was found to be 1.4 times the unirradiated value after an exposure of approximately 700 Mwd/AT.[24]

---

[22]R. E. Nightingale et al., Damage to Graphite Irradiated up to 1000°C, Proceedings of the Second United Nations International Conference on the Peaceful Uses of Atomic Energy, Geneva, 1958, Vol. 7, pp. 295–360, United Nations, New York, 1958.

[23]J. H. W. Simmons, The Effects of Irradiation on the Mechanical Properties of Graphite, in Proceedings of the Third Conference on Carbon Held at the University of Buffalo, pp. 559–568, Pergamon Press, New York, 1959.

[24]J. H. W. Simmons, The Effects of Neutron Irradiation on the Physical Properties of Graphite, in Industrial Carbon and Graphite, Papers Read at the Conference Held in London, Sept. 24–26, 1957, pp. 511–518, Society of Chemical Industry, London, 1958.

[25]G. H. Kinchin, The Effects of Irradiation on Graphite, in Proceedings of the International Conference on Peaceful Uses of Atomic Energy, Geneva, 1955, Vol. 7, pp. 472–478, United Nations, New York, 1956.

[26]W. K. Woods et al., Irradiation Damage to Artificial Graphite, in Proceedings of the International Conference on Peaceful Uses of Atomic Energy, Geneva, 1955, Vol. 7, pp. 455–471, United Nations, New York, 1956.

[27]H. W. Davidson and H. H. W. Losty, The Effect of Neutron Irradiation on the Mechanical Properties of Graphite, in Proceedings of the Second United Nations International Conference on the Peaceful Uses of Atomic Energy, Geneva, 1958, Vol. 7, pp. 307–314, United Nations, New York, 1958.

It is clear that many additional data are required to accurately assess the graphite-cracking problem. A research program designed to provide these data is outlined in Section 16.

Oxidation. The reactions between graphite and the impurities in the helium coolant stream are discussed in detail in Section 7. The behavior of various grades of graphite when heated in air, including the effects of protective coatings, has been investigated and the results are of interest for comparative purposes in connection with potential PBRE graphite components.

Experiments conducted in flowing air indicate that the oxidation rates of the two types of EGCR graphite are essentially the same at 600°C. The temperature dependence of the oxidation rates for both grades are also similar, and in the approximate temperature range of 500 to 700°C the "activation energy" was determined to be approximately 50 kcal/mole.

As discussed in Sections 7 and 12, protective coatings on the reflector graphite do not appear necessary in the PBRE. In addition it is not clear that acceptable coatings of Si-SiC could be applied to the large graphite components. The degree to which Si-SiC coatings are protective depends upon the isotropy of the graphite upon which they are applied. For example, coatings of this type on EGCR moderator graphite components develop cracks on cooling from the application temperature and these cracks provide direct contact with the oxidizing environment. More specifically, this cracking is related to the low coefficient of thermal expansion for the graphite in the perpendicular direction, as compared with that for the Si-SiC coating.

Only preliminary information is available on the effects of irradiation on the protectiveness of coatings on graphite specimens.[28-30] In one experiment six grades of graphite coated with Si-SiC by three manufacturers were tested for oxidation resistance after an exposure of approximately 8×10^{20} neutrons/cm^2 ($E > 1$ Mev) in an atmosphere of helium

---

[28]Private communication from R. E. Dahl, Hanford, to J. O. Kolb, ORNL, June 29, 1961.

[29]GCR Quar. Prog. Rep. March 31, 1961, ORNL-3102, p. 110.

[30]J. L. Jackson, The Effect of Irradiation on Siliconized-Silicon Carbide Coatings for Graphite, HW-68494, February, 1961.

and carbon dioxide at 500°C. There was no evidence of radiation damage to the coatings and only one of the nine specimens of a coated isotropic grade failed when heated in air at 1000°C.

Boronated Graphite for Thermal-Neutron Shield

Questions relating to the availability, manufacture, properties, irradiation effects, possible boron loss, and cost of boronated graphite are discussed in this section. Boronated graphite components are available from at least three manufacturers. The material is not a stock item with any of these manufacturers, but is made to order for special applications. Boronated graphite can be made by normal processing techniques, and the comments concerning available sizes of the reflector components in the previous section apply to the boronated product as well.

In general, the properties of graphite with low boron content are about the same as boron-free graphite manufactured in the same manner. Some properties[31] of graphites with boron contents of 0.2 to 5 wt % are given in Table 10.2. The high strengths of specimens of grade 8710 are the result of the low firing temperature.

Specimens of the grades described in Table 10.2 were irradiated for two cycles in the GETR at 1200°F. Negative dimensional changes of approximately 0.2% were observed based on measurements which were accurate to ±0.1%. Because of the low exposures anticipated for the thermal-neutron shield, radiation-induced shrinkage should not present a problem.

The loss of boron from boronated graphite is being studied by General Atomic.[32] An extrapolation of the boron vapor pressure over boronated graphite yields a vapor pressure of 10^{-24} atm at 1300°F, indicating that the loss of boron under PBRE conditions would be small. However, there may be a significant loss of boron as a result of reactions with impurities in the helium coolant. It can be shown that even with partial

---

[31] 40 Mw(E) Prototype High-Temperature Gas-Cooled Reactor Research and Development Program, Summary Report for the Period Jan. 1, 1959 to Dec. 31, 1959, and Quar. Prog. Rep., Oct. 1, 1959–Dec. 31, 1959, GA-1235, p. 25.

[32] 40 Mw(E) Prototype High-Temperature Gas-Cooled Reactor Research and Development Program, Quar. Prog. Rep. for the Period Ending Sept. 30, 1960, GA-1774, p. 15.

Table 10.2. Properties of Some Boronated Graphite

Sample designation	8 710	8 734	8 736
Boron content, wt %	~0.3	~0.2	~5
Firing temperature,[a] °C	850	>2 700	>2 700
Density, g/cm^3			
As received	1.64	1.69	1.63
After heating to 2000°C in vacuum	1.62	1.68	1.56
Weight loss on heating to 2000°C in vacuum, %	1.95	0.11	3.81
Crushing strength,[b] psi			
Longitudinal	12 000	8 100	3 400
Transverse	8 100	7 000	4 700
Coefficient of thermal expansion,[b] 10^{-6}/°F			
Longitudinal	1.5	1.0	0.9
Transverse	2.6	2.0	1.1

[a]As reported by manufacturer.

[b]Directions are with reference to grain orientation.

pressures of hydrogen and CO of the order of 10^{-3} atm, the very volatile boric oxides and boric acid will be formed. In the General Atomic experimental program boron losses at 2000°C were observed to be 100 times higher than the losses predicted from the boron vapor-pressure measurements. This effect was attributed to the more volatile boron compounds formed by reactions with impurities. The extent to which impurities in the coolant would present a problem with regard to boron loss at the low temperatures in the PBRE shield is uncertain.

The cost of boronated graphite components depends primarily on the boron content and the machining requirements. The cost of B_4C powder ranges between \$3 and \$11 per lb, depending upon purity and particle size. Unmachined material containing 1/2 wt % boron would cost approximately \$1 per lb.

11. MAINTENANCE OF CONTAMINATED SYSTEMS AND COMPONENTS

The extent and distribution of fission products throughout the PBRE coolant-circulating system cannot be precisely predicted but, as discussed in Section 7, will be one of the things to be determined in the course of the experiment. Although removal of deposited activity has been performed on a laboratory scale, the ability to effectively decontaminate components in situ at PBRE conditions has yet to be demonstrated. The maintenance design is therefore predicated on the assumption that all components that are contacted by the coolant gas or that handle exposed fuel elements will be too contaminated for direct approach; maintenance can be performed, however, in the fashion successfully demonstrated on circulating-fuel reactors.

In order to provide conditions most favorable for repair or replacement, the proposed plant layout provides for access from above to the majority of the operating components by the removal of modular shielding blocks. A work shield similar to the one illustrated in Fig. 11.1 can be placed over the opening left by the removal of a shielding block, and maintenance can be accomplished through openings by semiremote techniques (see Fig. 11.2). The normal maintenance procedure will probably be the replacement of components rather than their repair in place.

A decontamination facility is provided in the secondary enclosure. After examination to determine the nature and extent of contamination, components and test sections removed from the reactor system can be decontaminated by the methods described at the end of this section and then repaired by conventional methods. Provision will also be made in the design of the PBRE for the decontamination of some components in place. The information gained will aid in designing future reactors for in-place decontamination which will permit direct maintenance of most components.

The major components and auxiliary systems are compartmentally shielded from each other. In the event of a major system revision or the replacement of a major component, the contaminated equipment can be disconnected and removed from its compartment by remote methods. With the source thus removed from a compartment, the new equipment can be installed by direct-

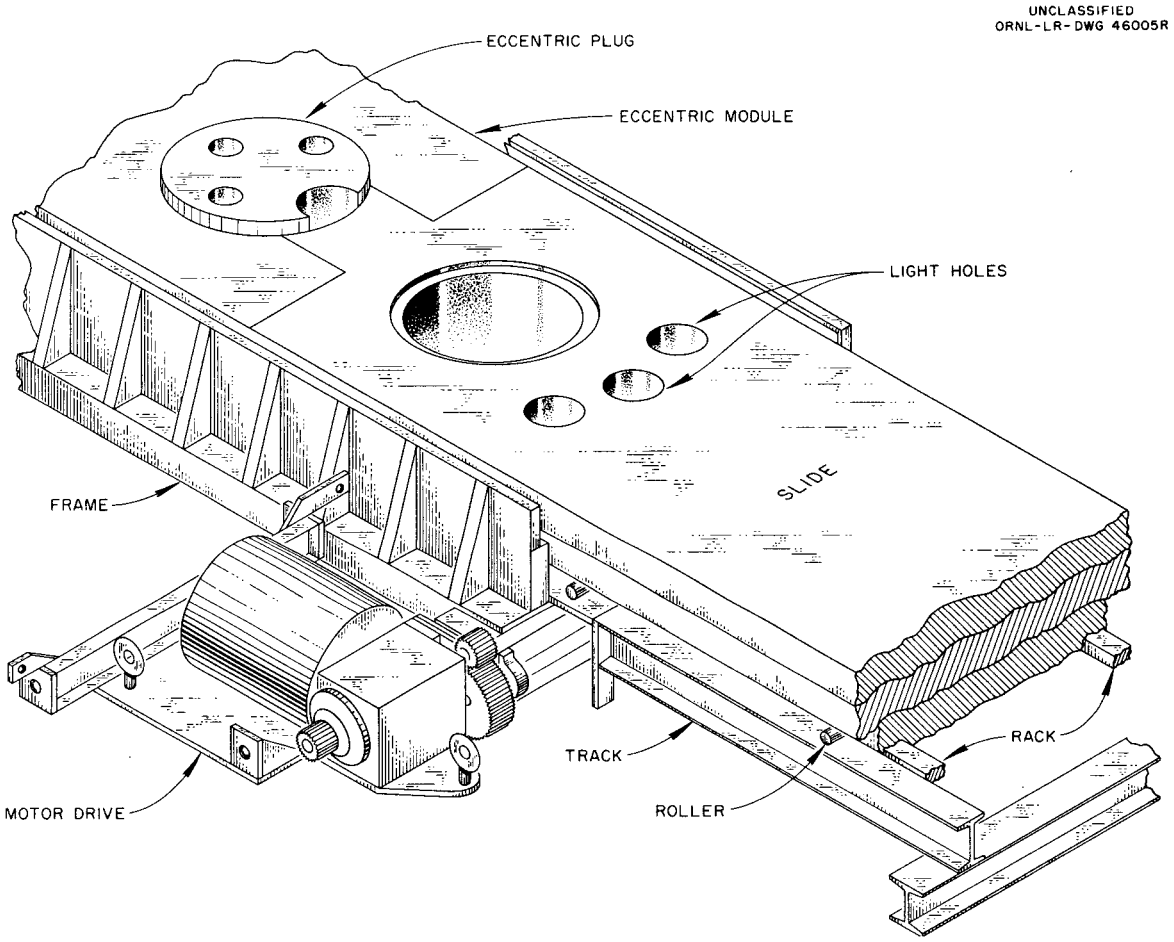

Fig. 11.1. Work Shield for Maintenance on Contaminated System.

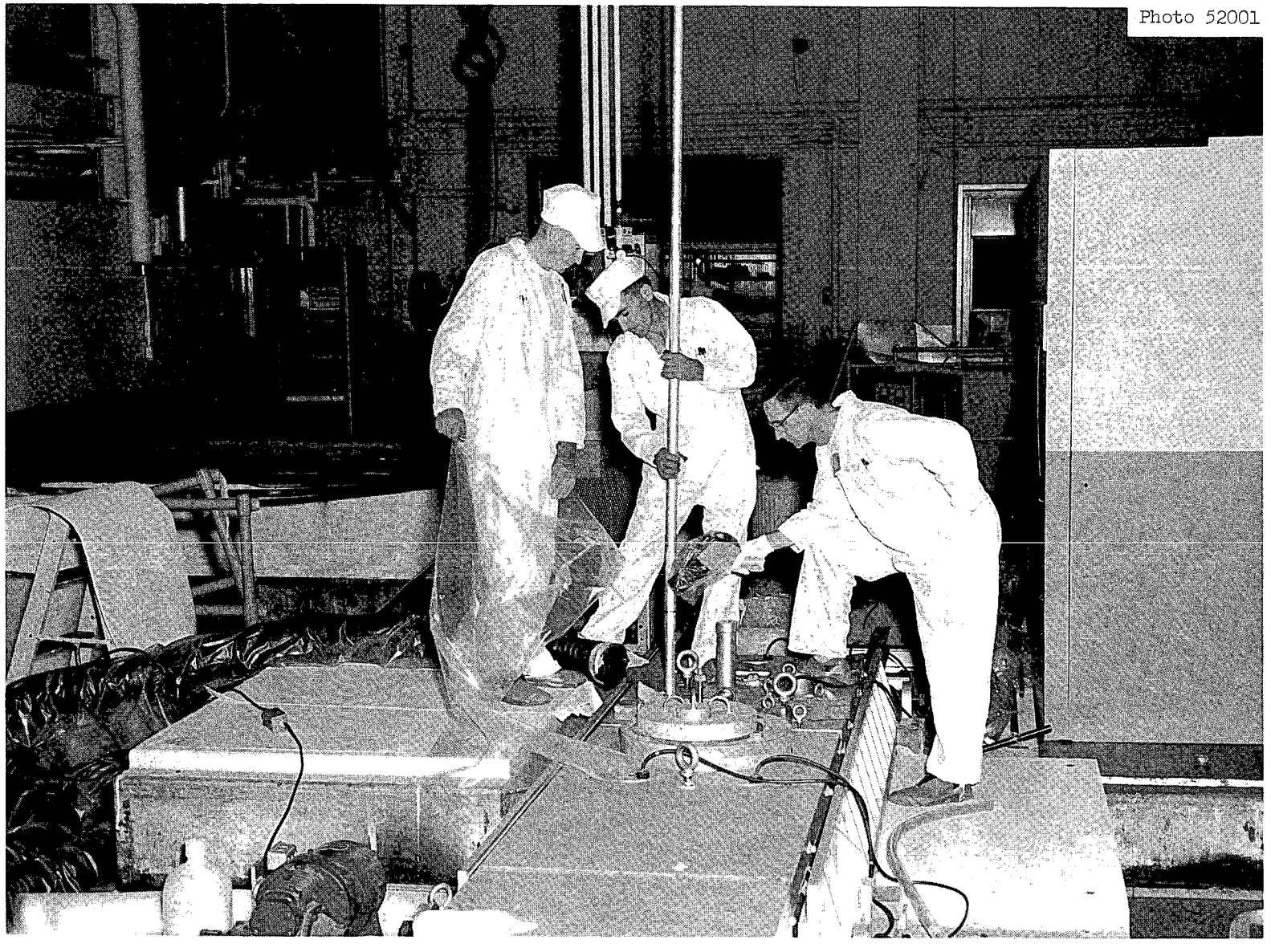

Fig. 11.2. Maintenance Work By Semiremote Techniques Through Opening in Work Shield.

approach methods. Concrete-block shielding will be stacked between major pieces of equipment in the coolant decontamination, offgas, ventilation, and other contaminated systems to reduce the radiation levels encountered during maintenance of components.

The control rods and fuel-discharge machinery extend below the reactor vessel into a shielded room. Gross particulate contamination of these components is possible, and particulate matter would be expected to fall out when the closures are opened. Hence access to this room for equipment maintenance seem unlikely. The drives for the control rods and for the fuel-discharge equipment are therefore brought out through shielding so that the drive mechanisms can be repaired or replaced by direct approach. Other equipment in the room below the reactor vessel will be designed for unit replacement by the manipulation of as few disconnects as possible, and a service machine capable of removing and replacing this equipment will be provided. A shielding window and manual manipulator will permit an operator to view and assist the operation of the service machine. The manipulator will be mounted on a rail that will allow it to be used for changing tools on the service machine or to be moved into the hot cell for use there.

The specific maintenance problems anticipated and the contemplated methods of handling them are discussed in the following sections.

Main Circulating Blower

The main blower is described and illustrated in Section 3. As shown, it is located in a shielded compartment to isolate it from direct radiation originating in the reactor core or the heat exchanger. Access for maintenance is provided through the top shielding. The motor and rotary element are contained in a housing having a flanged closure at the end. Electrical and instrument connections are made through remotely operable disconnects, and any auxiliary services, such as cooling water, lube oil, or buffer gas, are connected through mechanical joints. If blower replacement becomes necessary, the reactor will be shutdown and depressurized, the work shield placed over the blower, and the concrete shielding block removed. The mechanical joints will be unbolted with long-handled wrenches

and the electrical and instrument leads disconnected. After withdrawal from the casing on a track, the blower can then be raised through the work shield into a preplaced container with the building crane. With proper preparation made in advance and personnel excluded from the areas involved, the blower can be transferred to either the decontamination tank or to the remote-maintenance facility on the first level without use of a shield cask; a shielded container will be required if the unit is to be removed from the building without decontamination.

After removal of the blower is complete, a replacement unit will be installed and connected, the shield block replaced, and the work shield removed. The reactor system will then be ready to operate.

Heat Exchanger

The heat exchanger is installed in a shielded compartment with access through the top shielding. The helium coolant piping is completely welded, but the water and steam lines are connected by mechanical joints. As illustrated in Section 3, the heat exchanger drums and tube bundle are supported from the flanged head. A spare head and bundle are provided.

In the event that tube-bundle replacement becomes necessary, the reactor will be shut down and depressurized, the work shield set over the heat exchanger, a shield modular unit removed, and the mechanical joints unbolted with long-handled wrenches. The building crane, operated remotely by personnel in a shielded location, will be used to raise the bundle and place it in the previously prepared decontamination tank. The replacement bundle will be installed, connected, and the shielding replaced. The damaged bundle will be decontaminated and transferred to the shop for direct maintenance.

Replacement of the entire heat exchanger can be done if substitution of a unit of a different design is desired. After removal of the tube bundle, the pipe connecting to the blowers and the reactor core will be cut with torches using long-handled tools. Openings in the shell will then be plugged and the shell flooded with decontamination fluids which

can be added, agitated, and removed through openings in the work shield. The shell can then be removed with the building crane. Temporary shielding, as needed, will then be put in the openings between the heat-exchanger compartment and the blower and core compartments. The activity level in the heat exchanger compartment should be sufficiently low at this point to permit installation of a new unit by direct machining and welding of the helium lines. Provision of space for the steam lines of the new exchanger will have to be made at the time the shield is built.

Core Servicing

It is anticipated that, as a result of radiation damage, some of the graphite reflector may have to be replaced. The graphite reflector blocks have therefore been sized to pass through the access in the top of the vessel; they will be designed to be gripped by the replacement tool, and will be keyed for location and locking in the assembly. A packaging facility and conveyor can be provided to be placed above the reactor vessel within the biological shield. In order to avoid frequent removal of the service tool, the conveyer will operate through an opening made by removal of shield plugs in the side of the shield (see Section 3). A work shield is provided for use in core servicing operations. If reflector replacement becomes necessary, the reactor will be shut down, depressurized, and emptied of fuel. The work shield will be placed over the reactor vessel, the conveyor and packaging facility installed, and the flange and fuel charging mechanism removed (see Fig. 11.3).

The graphite-handling tool, containing conventional lighting and a periscope, will then be lowered into the vessel. The operator will successively grip the blocks to be removed, raise each block and place it in a container positioned on the conveyor, and move it into a carrier located outside the shield for transport to storage. The ventilation is arranged to prevent particulate matter from floating above the biological shield into the work area. When removal and examination are complete, the replacement graphite will be conveyed through the shield opening, picked up by the servicing tool, and stacked in the vessel.

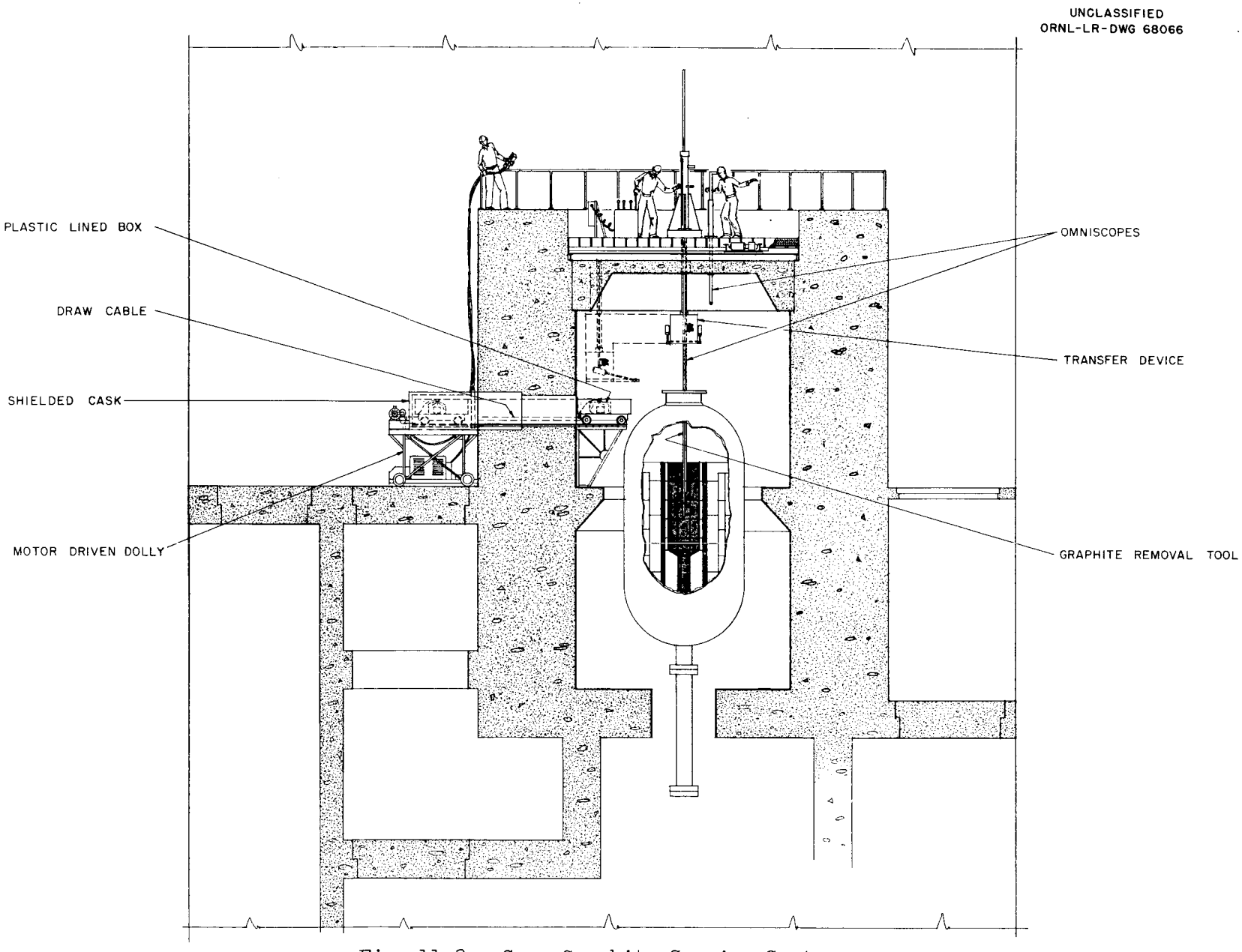

Fig. 11.3. Core Graphite Service System.

Control-Rod and Fuel-Discharge-Machine Drives

The control rods and the rotating elements in the fuel-discharge machine are actuated by pinions on the ends of shafts which extend through the shield wall into a service area. This arrangement permits direct servicing of the drive units. Although, as shown in Section 3, the rods and drives are enclosed within the primary-system pressure envelope, there will be seals on all the pinion shafts. These seals will keep activity out of the drive units; in addition, by permitting maintenance on the drives with low-pressure helium in the reactor, they will eliminate the necessity of completely removing the helium when servicing is required.

Control Rods

The control-rod tubes, as mentioned earlier, terminate in a shielded room below the reactor vessel that contains a service machine and manipulator and can be viewed from the service room through a shielding window. Access to this room is expected to be extremely limited, and any maintenance needed will be performed by an operator using the service machine and manipulator. In the design described in Section 3, control rods would be separated into shorter sections and withdrawn and replaced remotely from the bottom of the reactor with this equipment. However, if the top reactor vessel access is enlarged as suggested in Section 3, full length control rods can be withdrawn upward and replaced from above. This step would drastically reduce the maintenance operations and equipment required below the reactor vessel.

Fuel-Discharge Machine

The fuel-discharge machine, illustrated in Section 5, extends into the room below the reactor vessel and terminates in a mechanical closure. The motor unit and drive shaft can be removed through the mechanical joint outside the biological shield. With the drive shaft unit removed, the lower flange can be remotely removed and the columnator unit lowered out of the reactor by use of the service machine described in Section 3.

The assembly containing the ball discharge gas locks can be removed, when necessary, with the service machine after the two flanges have been opened using the manipulator. Any of the units from the subreactor room can be carried to the crane shaft or placed in the hot cell by the service machine.

Auxiliary Equipment

The components of auxiliary systems that are exposed to activity are located in functionally designed shielded compartments. Access to each of these compartments is through its top shielding and the work shield. Faulty components will be replaced with units connected into the system with mechanical joints. Items to be repaired will be decontaminated and repaired by direct maintenance.

Decontamination Procedures

Replacement of contaminated components would be considerably easier, and repair in place perhaps feasible, if activity levels could be reduced by in situ decontamination. As discussed in Section 16, however, means for hydraulically isolating components and for contacting surfaces with reagents remain to be developed. Techniques for decontaminating components after removal from the reactor are better established, and a system to be used in preparing equipment for repair, transfer to another area, or disposal is described in Section 3.

Contaminated components which are removed from the reactor will be placed in a decontamination tank located within the containment vessel. Unshielded (but bagged) equipment can be transferred to the tank with the building crane after evacuation of personnel.

The procedure outlined below will then be followed:

1. The component will be sprayed or filled with a solution of hot non-foaming detergent to remove water-soluble contamination and wash away any graphite dust. The rise and fall of the waste-line gamma activity will be monitored.

2. If this decontamination is adequate, the component will then be rinsed with water; if not, the procedure in item 3 will be followed.

3. The equipment will be sprayed or filled with oxalate-peroxide solution.[1]

4. If decontamination is adequate, the component will be rinsed with water; if not, the oxalate treatment will be repeated as in item 3.

5. If further decontamination is required, the solution used will depend on the fission products remaining, as revealed by a gamma scan with the spectrometer. Neutron-activation peaks such as those from Co^{60} and Fe^{59} in the structure of the metal cannot be reduced. Ruthenium and cerium may be decontaminated further by alkaline permanganate,[1] followed by a water rinse and an oxalate-peroxide treatment. A broad spectrum of fission products may indicate residual dust containing irradiated fuel either in inaccessible places or tightly adhering to metal surfaces.

6. The decontamination cycle is concluded with water rinsing until the drain-line sample is free of chemical residues. The equipment is then dried to minimize rust.

These procedures should provide decontamination by a factor of 50 to 10 000, depending on the initial activity level and on the effectiveness of contacting all contaminated surfaces. In most cases this should reduce the activity from the magnitudes estimated in Section 7 to levels which permit direct approach of components.

---

[1]A. B. Meservey, Decontamination of EGCR and PBRE, Revised Procedures, CF 61-8-89 (Aug. 31, 1961).

12. HAZARDS

The PBRE is being designed, as far as possible, to minimize all reliance on the functioning of equipment to guarantee that no accident to the plant will endanger the safety of the public, operating personnel, or buildings and equipment. Thus, the approach in the hazard analysis is not only to show that various serious accidents are unlikely (every effort will, of course, be made to prevent them) but, also, to show that even if they should occur, the consequences would be acceptable. Examples of this approach are cited below.

1. Complete combustion of the core is assumed, as well as a high leakage rate from the containment shell, in evaluating off-site doses. The arrangement of the shield ventilation system should, however, prevent combustion by limiting the amount of air which can reach the core.

2. Complete loss of power is assumed in assessing after-shutdown cooling requirements, and the design will provide for natural-circulation heat transfer circuits. An emergency power supply will, however, be provided.

3. Conversion to steam of all water in the steam system is assumed in evaluating the possible pressure buildup in the containment shell. Shutoff valves will, however, be included in the steam and feedwater lines to limit the amount of water that could leak into the reactor.

A preliminary analysis indicates that even with such conservative assumptions, operation of the PBRE at an ORNL site would not present any unacceptable hazards.

Integrity of the Containment Shell

The PBRE containment shell will be 66 ft in diameter, and fabrication considerations indicate that its thickness will be 5/8 in. It will thus be capable of withstanding an internal pressure of 15 psig.[1] Possible causes of a pressure rise in the shell are discussed below.

---

[1]Based on a 16 000-lb working stress, 80% weld efficiency, and 25% reduction in allowable pressure to account for external loads.

Helium Escape from System. The helium inventory in the primary system is approximately 11 000 scf or 1000 ft^3 at 500 psia and 900°F. Escape of this helium into the containment shell volume (4×10^5 ft^3) without heat transfer would increase the pressure in the containment shell by only 1.25 psi.

Graphite Combustion. Although the shield ventilation system is designed to retard the access of air to the primary system in the event of a rupture, the consequences of graphite combustion were examined. The containment shell volume of 4×10^5 ft^3 has an oxygen content of 1×10^5 gram-moles. Combination with graphite to form CO_2 (94 kcal/mole) would add 0.94×10^{10} cal (3.7×10^7 Btu) to the system. If all this energy were absorbed only in the containment shell atmosphere, the temperature and pressure rises would be intolerable. It is not reasonable to assume, however, that no other heat capacity would be available, since consumption of all the oxygen would take several hours. This can be shown by noting that even if the main helium blower is operating, it can circulate air at atmospheric pressure only at the rate of 11 000 lb/hr; since there is 2.8×10^4 lb of air in the building, circulation of all the air through the core would require 2.5 hr. Establishment of the open loop necessary for the blower to circulate air through the core is in fact unlikely because of the concentric character of the helium system; a break would have to occur in a line joining the blower to the steam generator or in the annular, cold duct between the steam generator and the reactor vessel without damage to the inner (hot) duct. Finally, the oxygen consumption rate would be limited by the chemical reaction rate to a value below the circulation rate at graphite temperatures below 1800°F. Indeed, calculations indicate that for a uniform bed temperature of 1800°F, the full flow of air at any temperature below 800°F would cool the graphite and extinguish the fire. (The average bed temperature under normal operating conditions is 1100°F.)

It is established, then, that even if combustion of the graphite could proceed to the point of complete oxygen consumption, it could not do so at a very rapid rate. Much of the heat of combustion would therefore be stored in various solids, including the containment shell itself. The heat capacities of some of these materials are listed in Table 12.1, along

Table 12.1. Air Temperature and Pressure Rises in Containment Shell Atmosphere

Component	Heat Capacity (Btu/°F)	Cumulative Heat Capacity (Btu/°F)	δT_{air} (°F)	δp (psi)
Air (4×10^5 ft^3)	5.5×10^3	5.5×10^3	6700	200
Containment shell × 1/2	0.38×10^5	0.44×10^5	840	24
Containment shell × 1/2	0.38×10^5	0.82×10^5	450	13
Graphite (5.5×10^4 lb)	0.22×10^5	1.04×10^5	355	10
Primary system (10^5 lb)	0.12×10^5	1.16×10^5	318	9
Concrete				
4000 ft^3 (a)	1.2×10^5	2.4×10^5	154	4.4
8000 ft^3 (b)	2.4×10^5	3.6×10^5	100	2.8
50 000 ft^3 (c)	15×10^5	16×10^5	23	

[a]All exposed surfaces to a depth of 1 in.; available in about 1 hr.

[b]All exposed surfaces to a depth of 2 in.; available in about 4 hr.

[c]All concrete in building (~2000 yd, of which approximately half is in biological shield); available only after several days.

with the temperature and pressure rises that would result if the energy released by complete oxygen consumption were stored in the components in proportion to their capacities. The heat capacity of each component is listed separately and, in addition, the combined capacity is noted for all those in the list down to and including the one opposite which a given entry appears in column 3; it is for this combined capacity that the pressure and temperature rises were computed. (The 630 000-lb containment shell is listed as two components of equal capacity.) This analysis is recognized as being rather arbitrary, since the temperatures of the solid components are initially quite different, the heat transfer rates are by no means uniform, and the components are not equally accessible for heat transfer. Nonetheless, the general conclusion may be reached that sufficient heat capacity is available in any of several combinations to limit the pressure rise to safe values.

The calculations summarized in Table 12.1 do not allow for several additional factors, some of which would operate to increase and some to

decrease the pressures given. These factors, discussed in subsequent paragraphs are:

1. sensible heat of reactor components (increase),
2. water leak, conversion to steam (increase),
3. loss of heat from containment shell (decrease), and
4. removal of heat by shield cooler (decrease).

Conversion of Water to Steam. The heat dump for the PBRE is a saturated-steam boiler operating typically at a temperature of 486°F and a pressure of 600 psia. The water content of the steam drum is about 1000 lb. Valves are provided in the steam and feedwater lines to isolate this portion of the steam system in the event of an internal boiler leak to the helium circuit. Although many details of the steam system remain to be worked out, it does not appear that the entire water inventory will exceed 10 000 lb.

Pressure increases for release of these quantities of steam into the containment vessel atmosphere have been computed. At the final temperatures indicated, these are

δp = 1.3 psi for 1000 lb of steam at 400°F,
δp = 13 psi for 10 000 lb of steam at 400°F,
δp = 17 psi for 10 000 lb of steam at 700°F.

The amount of heat required to produce 1000 lb of steam is roughly 10^6 Btu, and 10^7 Btu is required for 10 000 lb. That there is plenty of energy available may be seen from the summary of available energy sources in Table 12.2.

Table 12.2. Available Energy

Source	Energy (Btu)
Graphite, sensible heat above ambient	1.8×10^7
Primary system, sensible heat above ambient	0.6×10^7
10^4 lb of H_2O at 486°F	0.5×10^7
Graphite combustion, 10^5 moles at 94 kcal	3.7×10^7

Heat Loss from Containment Shell. The surface area of the containment shell exposed to the outer atmosphere is ~16 000 ft^2. Calculations of convective heat transfer show that about 2×10^6 Btu/hr could be transferred from the surface at 200°F, if uninsulated, or about 2×10^5 Btu/hr, if insulated. These rates are not sufficient to prevent some initial pressure rise in the accidents discussed above but, at least in the uninsulated case, would drop the pressure in a few hours following the accident. The higher transfer rates that would prevail at higher temperatures (for example, 6×10^6 Btu/hr at 400°F, 8×10^6 Btu/hr at 500°F, 1×10^7 Btu/hr at 600°F) would prevent occurrence of the temperature and pressure rises given in the first two or three lines of Table 12.1.

Although the effect of vaporizing 10^4 lb of water is to increase by 50% the number of moles of gas and vapor in the containment shell, the energy required would reduce the energy effectively available from graphite combustion in practically the same ratio. Further analysis will be helpful in clarifying the various possible combinations of events, but it does not appear that any reasonable combination of steam and air pressure could exceed the design pressure of the containment shell.

Heat Loss to Shield Cooler. Heat transfer from the uninsulated portion of the pressure vessel, by radiation and convection, will be on the order of 2×10^5 Btu/hr. While important for some purposes discussed under "Emergency Cooling," this cooling rate is too small to be relevant to the present discussion.

Hydrogen Formation. Hydrogen in air is flammable if present in concentrations between about 4 and 74 vol %. If the concentration is between 18 and 59 vol %, detonation is possible. In the rapid-burning case, an upper limit to the pressure rise may be obtained by assuming that all the heat of combustion is retained in the atmosphere. In the case of detonation, peak pressures an order of magnitude higher may be reached. Temperature and pressure rises as a function of hydrogen concentration are shown in Table 12.3.

If the hydrogen formed by dissociation of 1000 lb of steam (2.5×10^4 moles), the maximum available with the shut-off valves in steam and feedwater lines closed, were distributed uniformly in the building, its

Table 12.3. Hydrogen Combustion and Detonation (approximate values)

H_2 Concentration (mole %)	Q^a (kcal)	ΔT (°C)	Δp^b (psi)	Δp^c
5	2.9	580	28	
10	5.8	1160	57	
15	8.7	1740	86	
20	11.6	2320	115	up to 1400 psi

[a]Per mole of atmosphere.

[b]Combustion.

[c]Detonation, up to 12 times combustion pressure.

concentration would be about 5%; this is well below the detonation limit and close to the lower limit for flammability (probably below that for downward flame propagation). There is no assurance, however, that such hydrogen as is formed will be uniformly distributed, and, since H_2 is lighter than other gases, it may be assumed that concentrations of hydrogen above the average would in fact occur. Eventually, for example, much of it might collect at the top of the containment shell, or in other pockets, with high local concentrations. The possibility exists, therefore, that even much less than 2.5×10^4 moles of H_2, by detonating in a small confined space, could create a missile which could breach the containment shell.

The hope that difficulties of this sort can be circumvented rests primarily in the fact that the reactions by which H_2 is formed will proceed extremely slowly in the PBRE. To illustrate this point, rates for the reaction $C + H_2O \rightarrow CO + H_2$ under various conditions are given in Table 12.4. The basic reaction rate data employed are those of Mayers.[2] They were obtained between 850 and 1160°C, with specimens ~0.82 in. in diameter and 0.55 in. in length. These specimens evidently have a much larger surface-to-volume ratio than the fuel balls of the PBRE and very

[2]M. A. Mayers, J. Am. Chem. Soc., 56: 1879 (1934).

Table 12.4. Approximate Rates of Dissociation of H_2O in the PBRE[a]

Quantity of Graphite		Temperature (°F)	Steam Dissociated (lb/hr)	Heat Required (Btu/hr)	Cooling Rate[b] (°F/hr)
Pounds	% of Total				
17 000[c]	30	1300	1.1		
55 000[d]	100	1300	3.6	0.1×10^5	
		1400	13	0.4×10^5	
		1500	55	1.8×10^5	8
		1600	150	4.8×10^5	22
		1700	370	1.2×10^6	55
		1800	1500	4.8×10^6	220
1 200[e]	2.2	1600	3.3	1×10^4	22
		1700	8	2.6×10^4	55
		1800	33	1×10^5	220

[a]Reaction rates are those of Mayers (ref 1) and are for a steam pressure of about 1 atm.

[b]Cooling rate of stated quantity of graphite.

[c]Top 3 ft of graphite, assumed (somewhat arbitrarily) to be 50°F above gas outlet temperature; reaction of cooler graphite assumed negligible.

[d]All graphite assumed isothermal at given temperature; the highest temperature (1800°F) is possible with afterheat only after 20 days, if no heat is transferred away from the graphite.

[e]Fuel graphite.

much larger ratio than the reflector blocks. What allowance, if any, should be made for these differences is not clear, and it is not clear whether the reactions should be expected to proceed more rapidly in the presence of radiation.

It will be apparent from this discussion that this aspect of the hazards evaluation requires much additional work, both analytical and experimental. Since this appears to be the primary threat to the integrity of the containment shell, it will be intensively studied in preparing the hazards report for the PBRE.

Fission-Product Leakage from Containment Shell

Escape of fission products from the containment shell is predicated on complete combustion of the fuel balls, on a leakage rate of 1% per day of the containment shell atmosphere, and (as is customary) on the least favorable weather conditions; in addition, release at ground level is assumed. The leakage rate used in the calculations is higher than the minimum rate that can probably be achieved. A design level of 0.4%/day has been tentatively adopted, and this implies that testing equipment will have to be provided that is capable of verifying such a leak rate. Given the calculations for the 1% per day rate, results for a lower rate can be readily inferred.

Release of fission products from the fuel during combustion of the graphite matrix was assumed to be 100% for the noble gases, 50% for the halogens, and 5% for all others. In addition, 50% of the halogens that do escape are assumed to be adsorbed on surfaces within the containment shell, so that 25% is available for escape from the shell. The fission-product inventory in the fuel is based on two years of operation at 5 Mw. The residence time of individual fuel balls may exceed two years, but the average age in the reactor at any time will be two years or less. The only important nuclide whose concentration is significantly affected by the assumed exposure time is Sr^{90}. The inventory of the several nuclides that are of importance in this connection is given in Table 12.5. Integrated doses from inhalation of the contaminated atmosphere are shown in Fig. 12.1 for the following conditions:

1. release of activity (1% per day) at ground level,
2. continuous exposure for 8 hr,
3. no allowance for decay during 8 hr (would be a small downward correction),
4. large inversion condition: wind velocity 3.3 mph, atmospheric diffusion constant c = 0.1, and
5. large lapse condition: wind velocity = 5.1 mph, atmospheric diffusion constant c = 0.3.

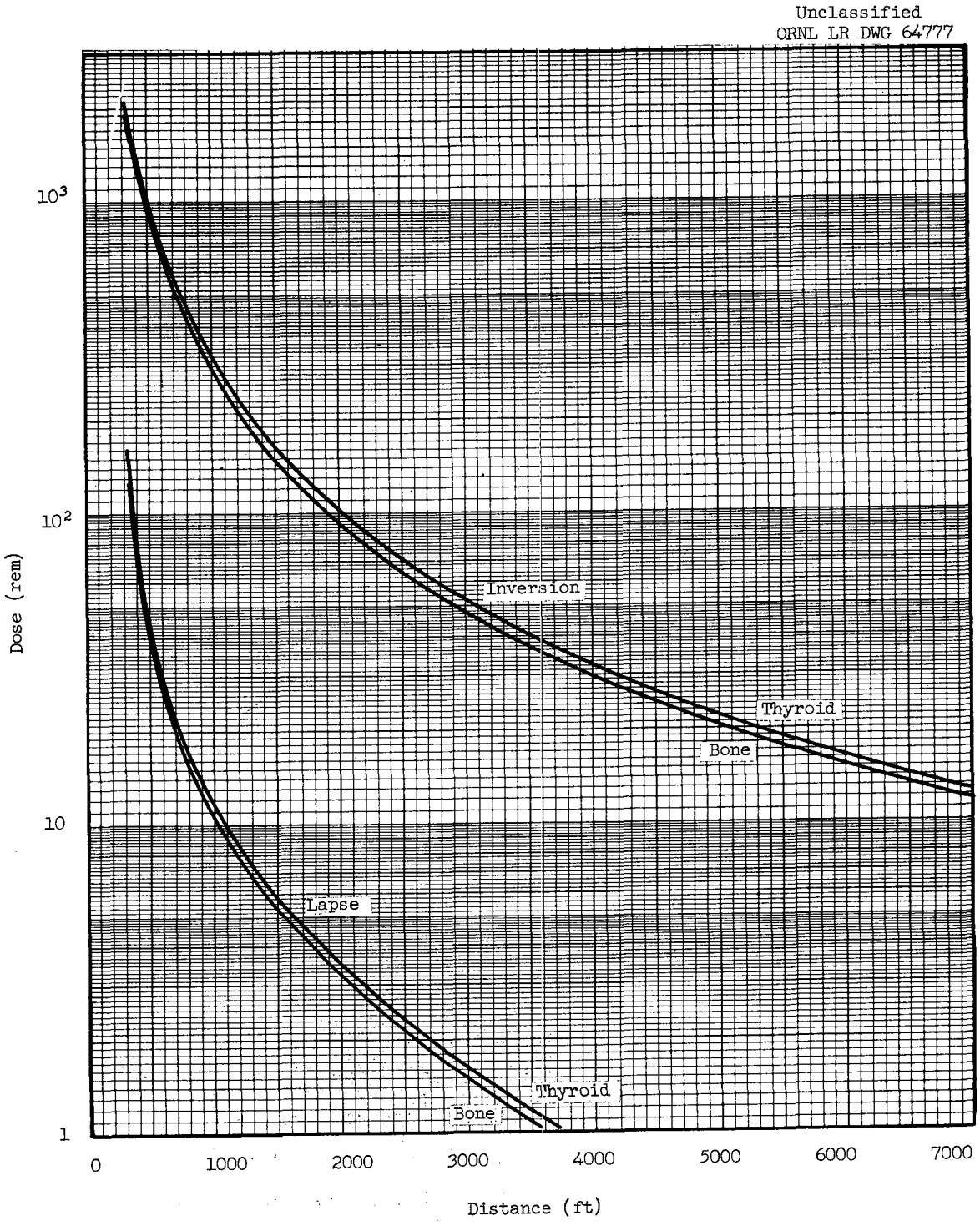

Fig. 12.1. Integrated Dose to Bone and Thyroid Versus Distance From Release Point for an 8-hr Exposure.

Table 12.5. Inventory of Fission Products After Two Years of Operation at 5 Mw

Nuclide	Activity[a] (curies)	Activity Available for Leakage[b] (curies)
	$\times 10^5$	$\times 10^4$
I^{131}	1.22	3.05
I^{132}	1.85	4.63
I^{133}	2.73	6.83
I^{134}	3.18	7.98
I^{135}	2.47	6.18
Sr^{89}	2.01	1.00
Sr^{90}	0.13	0.065
Y^{91}	2.47	1.23
Zr^{95}	2.68	1.34
Ba^{140}	2.64	1.32
Ce^{141}	2.52	1.26
Ce^{144}	2.00	1.00

[a]Total primary system activity, almost entirely in fuel.

[b]25% of iodines; 5% of bone seekers.

These meterological conditions were employed for the hazards analyses of the ARE and the EGCR.[3-4]

The reason for computing the dose for an 8-hr exposure is that this is presumed to be an adequate time for evacuating uncontrolled areas downwind from the reactor. Within the controlled area, speedier evacuations should be possible. Thus, the doses at the smaller distances in Fig. 12.1 would be reduced to allow for faster evacuation, for example, a 1-hr exposure would give one-eight of the indicated dose. As discussed in Section 14, either of the Oak Ridge sites considered is two miles from the nearest boundary of the Oak Ridge reservation. At this distance, maximum 8-hr doses of less than 10 rem to bone and to thyroid are to be expected.

The doses shown in Fig. 12.1 were computed on the basis of instantaneous release of fission products from the fuel. As discussed earlier, however, the fuel cannot be expected to burn very rapidly, and it is therefore of

[3]The Aircraft Reactor Experiment, ORNL-1407.

[4]Experimental Gas-Cooled Reactor Preliminary Hazards Summary Report, ORO-196 (May 1959).

interest to determine the effect of continuous release of the fission products from the fuel linearly over various periods of time.

For instantaneous release, the dose accumulated in time t is

$$D(t) = D_0 t \quad ,$$

where D_0 is the dose per hour of exposure. It is easily shown that if the fission products are released from the fuel steadily over an interval of time T, the doses are then

$$D(t) = \frac{D_0 t^2}{2T} \qquad \text{for } t \leq T$$

$$= D_0 \left(t - \frac{1}{2} T\right) \qquad \text{for } t > T \quad .$$

The results have been plotted, in Fig. 12.2, in the form of the time in which evacuation must be accomplished to limit the dose to 25 rem as a function of the distance from the ground-level leakage point and as a function of fuel-release time, T. The results indicate, as one would expect, that a finite release time may make a great difference to persons close to the reactor at the time of the postulated accident, but it is of much less significance to persons already several thousand feet away.

In order to see what doses would result if the ventilation valves on the containment shell should fail to close, calculations were made based on the assumption that the exposure time equals or exceeds the release time from the fuel; thus the entire inventory of released fission products escapes from the building and is assumed to pass by the point of exposure; the person being exposed does not leave the zone of maximum concentration during that time. Additional assumptions were that the air intake valve at the top of the containment shell (elevation 100 ft) and the outlet valve to the stack (height 100 ft) were open and that the stack filter efficiency for iodine was 95% and for other fission products (except gases) was 99.9%. For release above ground level, a maximum ground-level dose occurs at a distance from the release point that increases with increasing elevation of the release point. These distances, along with the values of the maximum doses, are listed in Table 12.6.

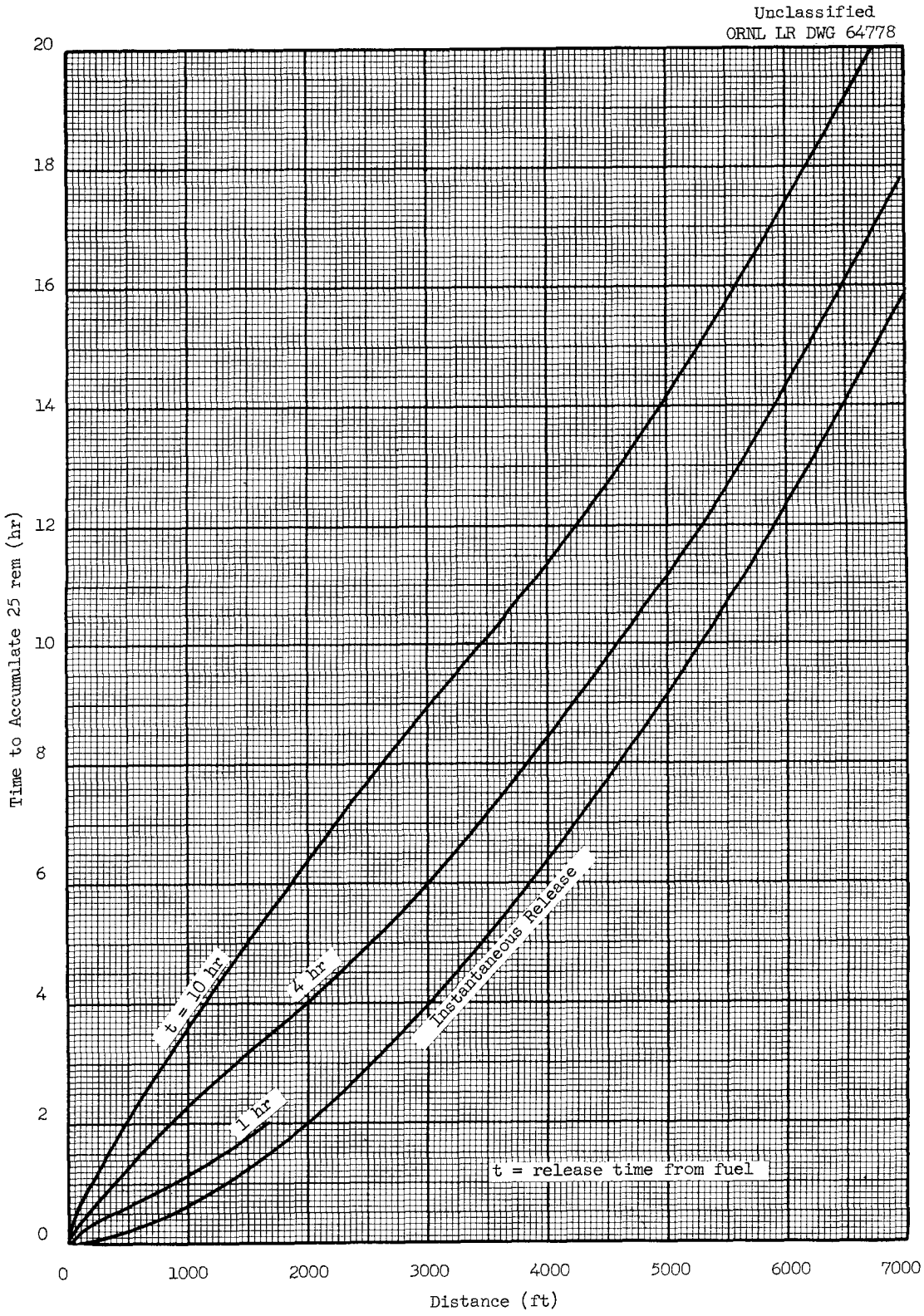

Fig. 12.2. Evacuation Time Versus Distance.

Table 12.6. Doses Following Uncontrolled Fission-Product Release

Release Point	Height (ft)	Filter Factor	Meteorological Condition	Distance (ft)	Maximum Dose (rem)	
					Thyroid	Bone
Stack	150	0.05[a], 0.001[b]	Inversion	5500	104	1.9
			Lapse	964	67	1.3
Stack	150	1.0[c]	Inversion	5500	2070	1930
			Lapse	964	1345	1254
Containment shell top	100	1.0[c]	Inversion	3380	4655	4340
			Lapse	607	3044	2838

[a]Factor for dose to thyroid.

[b]Factor for dose to bone marrow.

[c]Unfiltered.

The figures given in Table 12.6 show that discharge to the stack of all fission products released from the fuel during complete combustion of the core would not lead to excessive doses to bone or thyroid, provided the effluent air is filtered, as assumed. Unfiltered release from either the stack or the top of the containment shell would produce intolerable doses even at distances of 2 miles or more from the reactor, if there were no evacuation. If, on the other hand, evacuation were effected in one-tenth the time for release of the fission products from the fuel, even this extreme accident would probably produce no casualties.

Direct Radiation Dose Rate

Even if all fission products that might be released from the fuel as the result of an accident are confined within the containment shell, a significant radiation level will exist in the vicinity of the reactor because of the strong gamma-ray source in the shell. The gamma dose rate at a distance of 1000 ft from the reactor is shown in Fig. 12.3 as a function of time after the postulated accident (primary system rupture, core burns). Other conditions in the calculation are

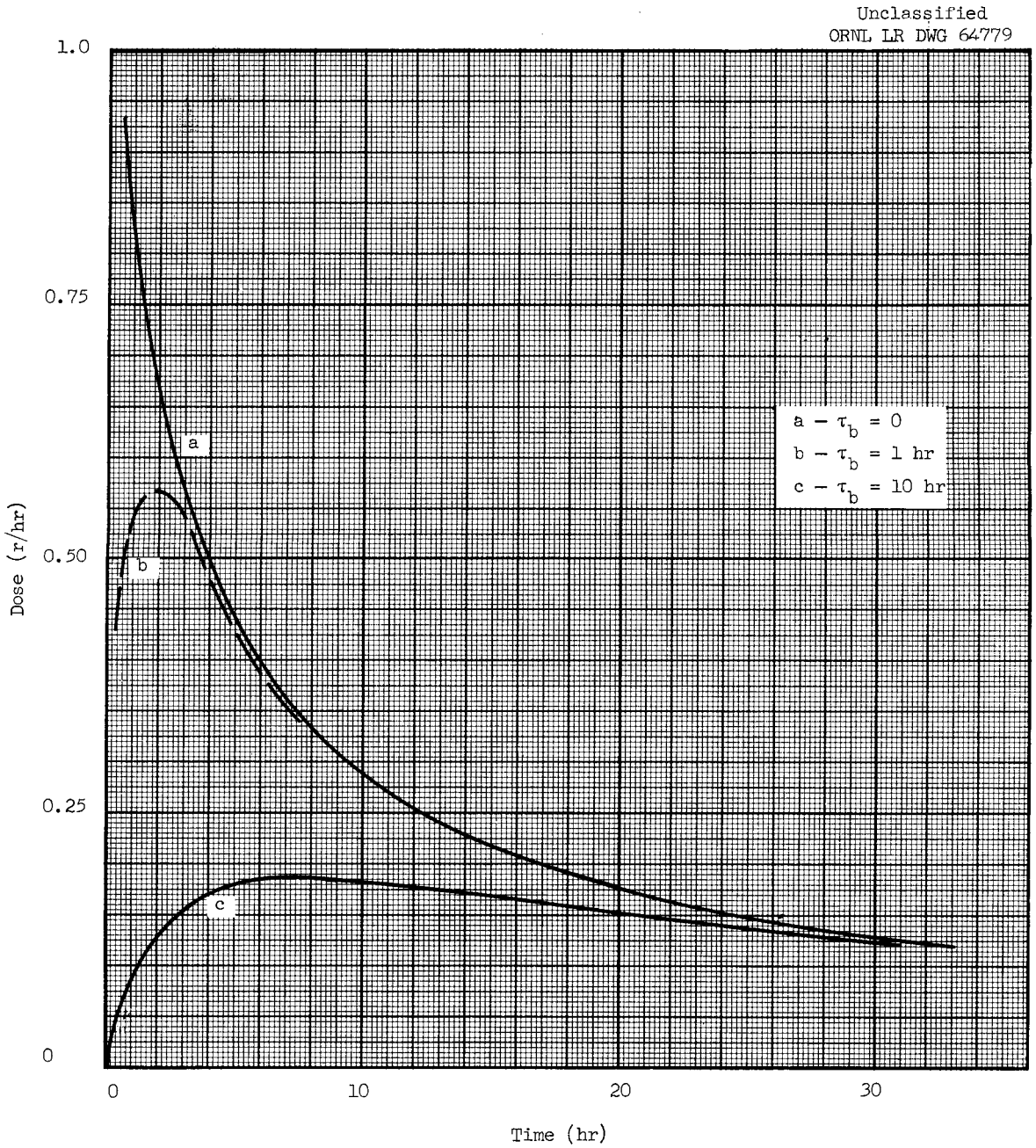

Fig. 12.3. Dose from Direct Radiation at 1000 ft for Exponential Burning Rate.

1. fission product release:

   100% of Xe, Kr

   50% of I, Cs, Br, Rb

   5% of all other fission products

2. gamma attenuation:

   internal structures, factor of 2 reduction

   containment shell, 5/8 in.

   air, 1000 ft

3. graphite burns at exponentially decreasing rate with a mean life (for burning) of 0, 1 hr, or 10 hr

As indicated by Fig. 12.3, direct dose rates, especially if slow burning is assumed, will be limited to a few hundred mr/hr at 1000 ft. In this circumstance, the dose rate 1500 ft away at the MSRE, for example, might be sufficient to require temporary evacuation of that facility. The main Laboratory area would be shielded by Haw Ridge.

Shield Ventilation System

Details of the shield ventilation system are given in Section 3. Attention is drawn here merely to those aspects of the design that are important from the viewpoint of safety.

1. Graphite Combustion. Immersion of the reactor primary system in an inert atmosphere is required only in the event of a rupture of the high-pressure circuit, which could be followed by air flow to the core. The guiding principle in the design was to use the escaping helium to displace or dilute the air surrounding the pressure circuit, and to prevent or retard any flow of air from the atmosphere outside the shield. Pressure-relief valves, which are required in any case to limit pressure rise in the shield space, will be located in each major compartment housing components of the high-pressure circuit. These will be loaded to close when the pressure differential between the atmospheres inside and outside the shield falls below a preset value, for example, several inches of water. The considerable number of penetrations in this envelope will be sealed with flexible boots suitably supported to prevent blowout; these

are intended to act as diffusion barriers, rather than as tight seals. As the design progresses, the desirability of actually making the shield a pressure-tight enclosure will be considered, and the difficulty of doing so will be assessed.

The volume of air initially present in the connected compartments composing this reactor enclosure is estimated to be about 8000 ft^3. The volume of helium in the reactor, if computed at standard temperature and pressure, is slightly larger, so significant dilution of the air may be expected. In any case, the air available represents less than 2% of the air in the containment shell. With this amount of air, about a thousandth of the graphite or a twentieth of the core could be oxidized, with the release of less than 10^6 Btu of energy. This energy, distributed over all the graphite, would raise its temperature 50°F.

Energency Cooling

It was pointed out above that the PBRE is being designed to avoid the requirement for a guaranteed power supply as a safety factor (although an emergency power supply will, in fact, be provided). The after-shutdown power levels are sufficiently low, and the heat capacities available sufficiently high, that the reactor could absorb all its afterheat for a very long time without excessive temperatures being reached. Temperature rises as a function of time after shutdown are shown in Fig. 12.4. Some of the salient factors are discussed below.

1. If all the afterheat were retained entirely in the fuel, the temperature rise would be ~600°F in the first hour and 1000°F in the first 2 hr. The average fuel temperature would rise from 1100 to 1700 or 2100°F, respectively.

2. If all the afterheat were retained in the graphite (core plus reflectors), the temperature rise would be about 500°F in the first week and 1100°F in a month. The average graphite temperature would rise from 90 to 1400 to 2000°F, respectively.

As a matter of fact, the afterheat cannot be retained in the graphite for extended periods of time, since heat transfer by radiation,

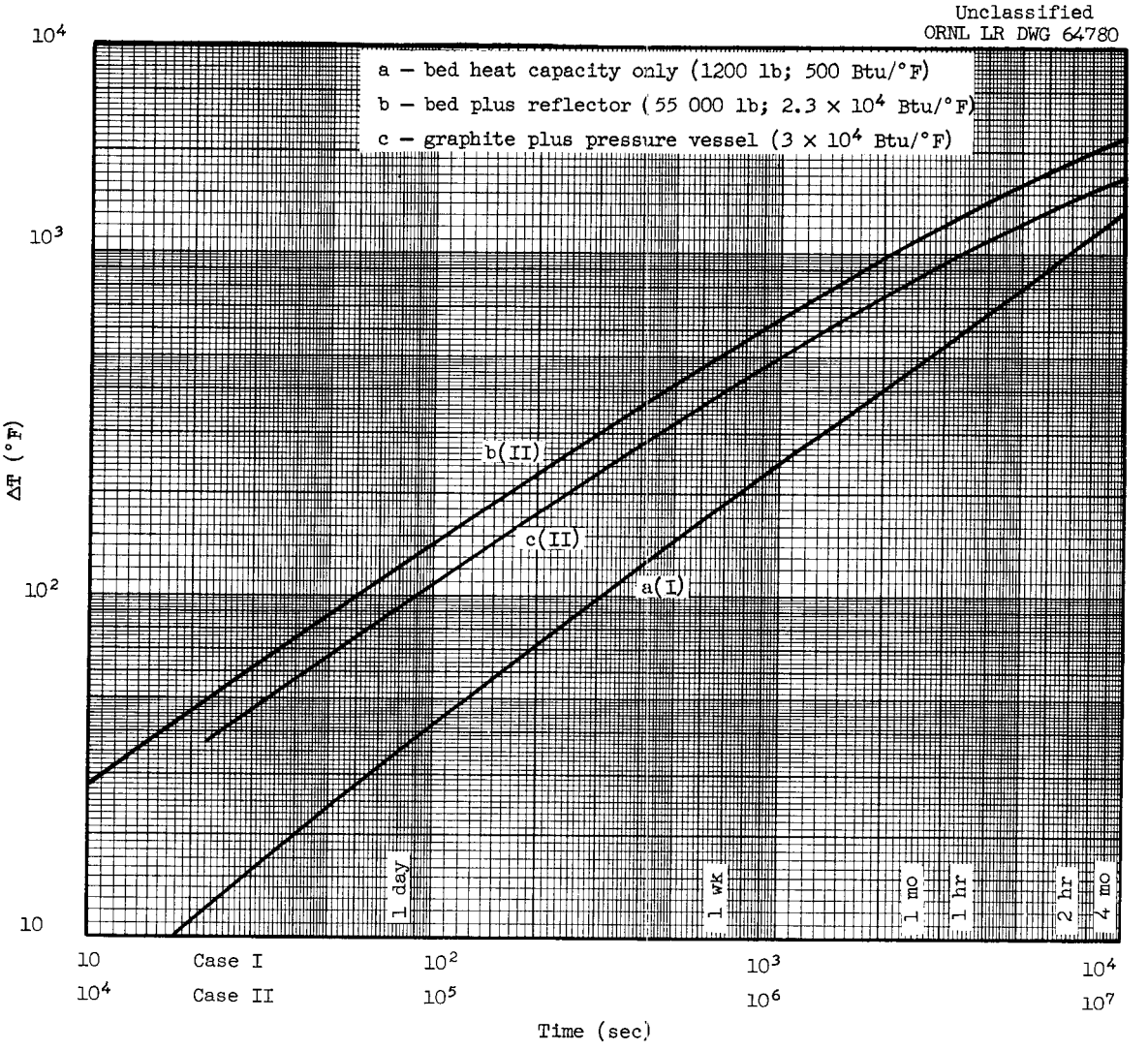

Fig. 12.4. Uncooled Temperature Rise of PBRE.

conduction, and convection will inevitably occur. The emergency cooler has ample capacity to remove afterheat if the main heat exchanger fails. On boiler failure without loss of helium pressure, convection cooling of the core will continue by natural circulation. This is discussed in detail in Section 4. For the case of system pressure loss, the heat can be transferred by radiation from the pressure vessel surface, a portion of which is left uninsulated for this purpose. (This is also discussed at greater length in Section 4.) The heat transfer rate by radiation from one-half the pressure vessel surface will be 3×10^5 Btu/hr, with the pressure vessel at 600°F and the opposing surface (shield cooler) at 212°F; this equals the afterheat rate 25 min after shutdown. (Afterheat for the first hour could be absorbed in the pressure vessel with a temperature rise of only 45°F.)

It is not yet clear what detailed temperature distribution would result under the postulated conditions (complete loss of power and helium pressure). Sensible heat will be redistributed, and temperature gradients will obviously be required to transfer even the modest amounts of heat involved. More elaborate calculations than those performed to date will be required to provide detailed results. Nonetheless, it is clear that both ample heat capacity and ample heat transfer mechanisms are available to accommodate all afterheat without excessive temperatures being reached.

It must be shown, of course, that certain critical components do not exceed allowable working temperatures during these transient conditions. The important cases are the core support plate and the control rods. Preliminary calculations of the core support plate temperature indicate that it will remain within safe limits. The control rods can withstand the maximum reflector temperatures quoted above, although they would not be expected to reach these temperatures in normal service.

Dissipation of the heat from the emergency boiler or from the shield cooler requires additional heat sinks. In the case of the emergency boiler, it is tentatively planned to condense its steam in a supplemental, low-pressure boiler which may be vented to the outside atmosphere. In this way, a relatively small quantity of water can take care of afterheat for many months, if necessary. For example, the total afterheat up to

100 days after shutdown will be about 4.8×10^7 Btu. Boiling of about 6000 gal of water would dissipate this heat. A 10 000 gal supply is presently planned. A similar solution may be employed for the shield cooler, but detailed design has not yet been undertaken.

Release of Fission Products from Fuel

Release of fission products from fuel during normal operation and subsequent leakage from the high-pressure helium system are not primarily a matter of safety, since far greater releases have already been examined in the core-combustion accident. In normal operation, however, the fission products that do leak from the pressure vessel will be discharged up the stack (after some delay and filtering), and it is therefore worthwhile to determine the levels of radioactivity that may prevail in the surrounding atmosphere. These levels were reported as part of the previous study of a 10-Mw Pebble-Bed Reactor Experiment.[5] The results depend, of course, upon the assumed characteristics of the fuel, as well as the effectiveness of the internal helium cleanup system and the assumed leakage rate from the primary high pressure circuit.

At the present time, it is not possible to characterize the fuel with much assurance; many additional fuel-irradiation experiments will be required, and the fuel specifications will undoubtedly undergo significant changes during this program. Nonetheless, some limiting leakage rates should be adopted as a design basis, with the expectation that actual operating experience will prove to be much more favorable. For this purpose, the results of the previous study are probably as good a basis as any. They were derived, however, from experimental results obtained with alumina-coated UO_2 particles rather than with the presently planned pyrolytic-carbon-coated UC_2 particles. Preliminary information from experiments with carbide particles suggests that greater leakage may be expected for short-lived nuclides and less leakage for long-lived nuclides than was indicated by the correlation employed in the previous study.

---

[5]A. P. Fraas et al., Preliminary Design of a 10-Mw(t) Pebble-Bed Reactor Experiment, ORNL CF-60-10-63 rev., p. 19.12.

A correlation between release rate and half-life based on existing data is presented in Section 10. Correlations of release rate to nuclide half-life for both UO_2 and uranium carbide are shown in Fig. 12.5. The still-tentative correlation for carbide fuel has been used to recompute fission-product releases from the fuel, the primary system, and the stack. In these calculations, several assumptions employed in the previous study were adopted:

1. Only Br, Kr, Rb, Te, I, Xe, and Cs are actually released from the fuel. Daughters of these may appear outside the fuel as a result of decay.

2. Where both a parent and a daughter escape, the effective half-life of the daughter is taken as the sum of the half-lives of both nuclides.

3. The fission-product cleanup system, with a flow rate equal to 1% of the main helium flow, operates on various chemical species as follows: Kr held up 1/2 hr; Xe held up 6 hr; Te and I removed essentially completely; Sr not removed.

In computing the concentrations of active nuclides in the shield ventilating system and the maximum ground level concentrations outside the building, the following additional assumptions were made:

1. The leakage rate from the helium pressure circuit is 0.1% per day.

2. The exhaust rate up the stack is 250 cfm while the volume of the enclosures designated as contaminated atmosphere zones is 60 000 ft^3. This includes reactor, boiler, and blower vaults, service machine vault, contaminated helium storage room, helium cleanup equipment room, etc.

3. Filters in the recirculating ventilation system were assumed to be 95% efficient for I, nil for the gases, and 99.9% efficient for Sr and Te.

Table 12.7 lists the following quantities for selected nuclides that make the dominant contributions to the biological doses:

1. core activity, based on two years of operation at 5 Mw,
2. R/B – release rate of fission products from fuel divided by production rate from fission,
3. primary loop activity without cleanup,

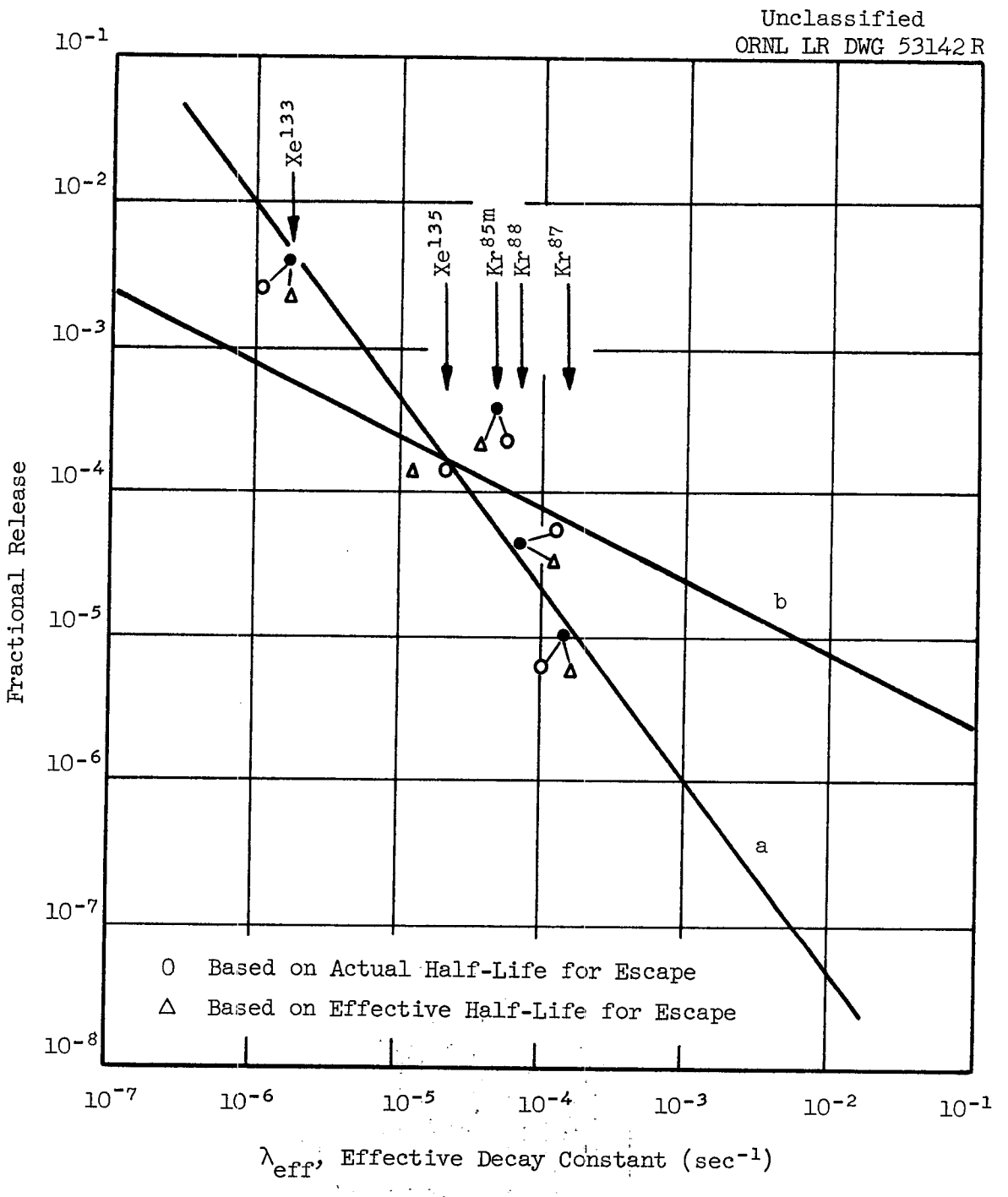

Fig. 12.5. Fractional Fission-Product Release from Fuel Balls. (a) Alumina-Coated UO_2 (see ref. 5). (b) Pyrolytic-Carbon-Coated UC_2 with 2% of the Coatings Assumed to be Cracked.

Table 12.7. Activities in Core, Helium, Building, and Outside Atmosphere

Isotope	Core Activity (curies)	Fractional Release Rate from Fuel (R/B)	Primary Loop Activity (curies)		Activity in Contaminated Zones (fraction of occupational MPC)		Activity Sent up the Stack (curies/day)	Maximum Ground-Level Concentration for Inversion Conditions (fraction of nonoccupational MPC)[a]		
			Without Cleanup	With Cleanup	Unfiltered	Filtered		A	B	C
Kr^{85}	1.59×10^{3}	1.80×10^{-2}	28.6	20	0.66	0.66	2.0×10^{-2}	1.8×10^{-5}	1.8×10^{-5}	1.8×10^{-5}
Xe^{131m}	1.26×10^{3}	1.31×10^{-3}	1.65	0.14	0.003	0.003	1.4×10^{-4}	9.2×10^{-8}	9.2×10^{-8}	9.2×10^{-8}
Xe^{133}	2.72×10^{5}	7.28×10^{-4}	198	13.9	0.45	0.45	1.4×10^{-2}	1.2×10^{-5}	1.2×10^{-5}	1.2×10^{-5}
Xe^{135}	2.60×10^{5}	2.39×10^{-4}	62.2	5.25	0.39	0.39	4.0×10^{-3}	1.1×10^{-5}	1.1×10^{-5}	1.1×10^{-5}
I^{131}	1.22×10^{5}	8.35×10^{-4}	102	0.16	5.2	0.50	1.5×10^{-5}	1.4×10^{-4}	1.4×10^{-5}	7.0×10^{-7}
I^{132}	1.84×10^{5}	5.35×10^{-4}	102	14.7	6.6	1.22	1.0×10^{-3}	1.8×10^{-4}	3.3×10^{-5}	1.7×10^{-6}
I^{133}	2.72×10^{5}	2.74×10^{-4}	75	1.1	9.5	1.01	1.0×10^{-4}	2.6×10^{-4}	2.7×10^{-5}	1.4×10^{-6}
I^{135}	2.47×10^{5}	1.55×10^{-4}	38	1.7	3.0	0.38	1.6×10^{-4}	8.0×10^{-5}	1.0×10^{-5}	5.0×10^{-7}
Sr^{89}	2.01×10^{5}	3.08×10^{-5}	6.2	5.7	56	5.35	5.5×10^{-4}	1.5×10^{-3}	1.5×10^{-4}	1.5×10^{-7}
Sr^{90}	1.19×10^{4}	1.28×10^{-5}	0.15	0.11	109	10.2	1.0×10^{-5}	2.9×10^{-3}	2.8×10^{-4}	2.8×10^{-7}
Te^{127m}	2.34×10^{3}	2.79×10^{-3}	6.52	9.2×10^{-4}	0.002		8.8×10^{-8}	4.6×10^{-8}		
Te^{129}	1.42×10^{4}	1.69×10^{-3}	24	9.3×10^{-3}	0.09	0.009	8.9×10^{-7}	2.5×10^{-6}	2.6×10^{-7}	
Te^{132}	1.84×10^{5}	5.26×10^{-4}	97	0.38	0.92	0.09	3.7×10^{-5}	2.5×10^{-5}	2.4×10^{-6}	
A^{41}					573	573	2.33	1.6×10^{-2}	1.6×10^{-2}	1.6×10^{-2}

[a]No internal filtering in building; no stack filtering; stack flow rate of 250 cmf.

[b]Internal filtering, 2500-cfm flow through filters; no stack filtering; stack flow rate of 250 cmf.

[c]Same as B, but with stack filters; efficiencies as listed in text.

4. primary loop activity with cleanup,
5. activity in contaminated zones without credit for filtering, expressed as fraction of maximum permissible concentrations for workers,
6. activity in contaminated zones with filtering, expressed as fraction of occupational MPC,
7. activity sent up the stack without filtration, curies/day,
8. maximum unfiltered ground-level concentration outside the building, expressed as fraction of nonoccupational tolerances (taken as 10% of occupational tolerances).

It may be noted that the 1.8-h Ar^{41} activity is the most significant. This activity is a function of flow rate to the stack, since at low flow rates argon has an opportunity to decay inside the building; however, the differences are slight for flows above a few hundred cubic feet per minute.

Results of Analyses

The analyses carried out to date indicate that the PBRE could be operated at the proposed Oak Ridge site without undue risk to the public or to neighboring facilities. Rather extreme accident conditions, with simultaneous failure of the protective equipment provided to minimize their consequences, would not appear to produce exposures in excess of tolerable limits.

If the design features provided to prevent graphite combustion should fail and air should reach the core at the maximum possible rate, there appears to be ample heat capacity and heat transfer capability available to keep the internal pressure rise within design limits. If shutoff valves in steam and water lines should fail to close and should admit all available water to the core, the resulting pressure rise in the containment shell would not exceed its design capability. If the core should burn and the valves in the off-gas line to the stack should fail to close, stack filters and stack height would limit the maximum exposures to safe values. If standby emergency power supplies should fail to start on demand, adequate heat transfer mechanisms and heat sinks will be available

to carry away all afterheat. If fission-product leakage from the fuel and the helium system should prove to be ten times greater than assumed, no off-site hazard would exist even without filtering the stack effluent.

The principal hazard that appears to remain potentially troublesome is that of hydrogen formation by the steam-graphite reaction. The nature of the risk involved is not fully understood at this time, and more work in this area will be required.

13. HIGH-TEMPERATURE OPERATION

A tentative objective established for the PBRE is the study of the behavior of core materials at conditions in which the outlet helium temperature is in the range 2000 to 2500°F. This objective is to be pursued, however, only if provisions for its accomplishment do not compromise the basic purposes of the reactor that are stated in Section 2.

The design that has evolved for the PBRE is well suited to the generation of ultra-high temperatures if two conditions are accepted. These are (1) that the hot gas will be attemperated with colder gas before emerging from the reflector structure and (2) that the power level of the reactor will be reduced below the design level for normal operation. The first restriction permits study of core conditions without requiring that the hot gas ducts and heat exchanger be designed for very high temperature operation. The second restriction is precautionary and may not be necessary; it is stated to avoid prescribing commitments for the reactor designers until more detailed studies are performed. Operation at lower power may ease problems associated with protecting the structural parts of the core from high temperatures, removing heat from the control rods and the reflector, restricting the fission-product activity evolved from the fuel, providing for the removal of afterheat, and avoiding hazardous conditions.

Alterations Required for High-Temperature Operation

Operation of the PBRE at very high temperatures would be attempted only after it had been operated for sufficient time with exit gas temperatures near 1250°F to satisfy the basic objectives of the experiment. At this point the PBRE would be altered by (1) installing equipment needed to provide for gas attemperation, (2) possibly installing a thermal-insulating liner around the cylindrical portion of the ball bed and the upper reflector, (3) replacing the initial control rods with rods made from higher temperature materials or having reflective insulation cladding, and possibly providing for increased coolant flow through the rod

channels and nearby graphite reflector, and (4) installing high-temperature thermocouples at appropriate points in the system.

Attemperation would be achieved by diverting part of the gas returning from the heat exchanger into the graphite chamber at the top of the core. The closure in the upper plenum liner, shown in Fig. 3.3, would be replaced with one having a tube which would extend downward into this chamber; an orifice in the line would restrict the fraction of return coolant which bypasses the core and would at the same time act as a flow-measuring device. It may be feasible to install an adjustable flow-regulating device, as well, so that changes in the bypass flow can be made without opening the reactor vessel. A total helium flow capable of giving a mixed mean temperature of 1250°F would, with this arrangement, result in temperatures in the steam generator, gas ducting, blower, shield, and auxiliary system identical to those existing at normal design conditions.

During high-temperature operation, parts of the graphite reflector will be at temperatures as high as the exit gas temperature, that is, in the range 2000 to 2500°F. While this will not create problems with regard to the graphite, because of its satisfactory mechanical properties at high temperatures, it will be necessary to assure that the high thermal conductivity of the reflector does not result in excessively high temperatures in the control rods, core support plate, core liner, and pressure vessel.

The control rods proposed for initial installation in the PBRE are designed for normal operation at temperatures in the range of 1400°F, with a maximum temperature of 1700°F permissible for short periods. Unless further studies indicate that rod temperatures can be restricted to this range, installation of rods suitable for high-temperature operation will be necessary. It may be possible to satisfy this requirement by providing a high-temperature nickel-base alloy sleeve or sleeves about the absorber section to act as reflective insulation, with perhaps an increase in coolant flow as well. An alternative and probably more desirable procedure would be to use a control rod capable of operating at temperatures in the range of 2000°F. Use of B_4C protected by or dispersed in graphite, with a molybdenum central rod for tensile strength, might be

adequate for this service; problems associated with the development of a high-temperature control rod are discussed in Section 16.

Consideration has been given to the use of a thermal-insulating liner around the fuel bed and the section of the reflector which is above the core to restrict the region of high temperature and allow the control rods and the remainder of the reflector to operate at near normal temperature levels. Pyrolytic graphite and porous carbon are materials which might serve as insulation. Manufacturers indicate that pyrolytic graphite of the type used for rocket nose-cones can be made in sections large enough for this application, with existing facilities being capable of producing a hollow cylinder as large as the PBRE core. The thickness is limited, however, and more than one layer may be required.

Porous carbon has been used successfully as the bed liner in the Induction Simulated Reactor at the Morgantown Research Center of the Bureau of Mines. In one case, a carbon liner in contact with heated spheres was not noticeably damaged during a 1000-hr run[1] in which the exit helium temperature was 2500°F.

Estimates of heat transfer rates are given in Table 13.1 for examples of pyrolytic graphite and porous carbon core liners. Although as shown, the heat loss would be reduced considerably by use of either material, in further consideration of a core liner attention will have to be given to the mechanical properties of the materials and their behavior under irradiation.

Temperatures in the reflector can be limited by providing an increased coolant flow through the control rod channels and the graphite structure, so that there should be no significant difficulty in controlling the temperatures at the stainless steel core liner or at the support plate. An appreciable rate of heat removal would occur, however, if sufficient flow were provided to keep the rod channel cool. This is illustrated by the first set of values in Table 13.1. As shown, the heat loss could be reduced by providing a gap filled with stagnant helium in

---

[1]N. H. Coates, J. P. McGee, and G. E. Fasching, Simulated Nuclear Reactor System for High-Temperature Process Heat: 1000-hr Demonstration Run at 2500°F, Bu Mines Report RI-5886, 1961.

Table 13.1. Effect of Insulation on Heat Transfer Through Core Wall When Maximum Control Rod Channel Temperature[a] is 1250°F

Conditions	Thermal Conductivity (Btu/hr·ft·°F)	Heat Transfer (kw) for Two Helium Exit Temperatures from Core	
		2000°F	2500°F
No core insulating liner[b]		250	420
No core insulating liner; one gap filled with stagnant helium in reflector		180	300
1 in. of pyrolytic graphite insulation	0.7	70	120
2 in. of porous carbon insulation	1.0	50	85
2 in. of pyrolytic graphite insulation		35	60

[a]Temperature assumed to be controlled by adjustment of coolant flow through control rod channel.

[b]The thermal conductivity of graphite is 20 Btu/hr·ft·°F.

the reflector. Since radiation is the predominant mode of heat transfer, the gap width is not critical.

It is expected that measurement of gas and reflector temperatures in the range above 2000°F will require replacement of the original thermocouples with ones capable of operating at higher temperatures. This should present no unusual difficulty if adequate high-temperature thermocouples are available, since the core thermocouples will be designed to be replaceable. Development of thermocouples and sheaths for use in the PBRE core environment at temperatures above 2000°F is discussed in Section 16.

Replacement of all or part of the graphite reflector structure may be required before operation of the reactor at high temperature. Changes could be occasioned by the need to provide insulating sections and/or additional cooling passages, as discussed above, to alter the upper dome structure for installation of the attemperation system, or to remove the

boronated outer layer of graphite blocks. The necessity for these changes will be indicated by further design studies and possibly by the results of research and development activities.

Fuel Problems of High-Temperature Operation

The volumetric average fuel temperature during operation at 1 Mw (thermal) with an outlet gas temperature of 2500°F will be about 1750°F; for the same conditions, if the sphere packing were uniform, the fuel temperature in the hottest region of the reactor would be about 2600°F. The existence of closely packed clusters in a randomly packed bed, however, may cause temperatures at points to exceed considerably the values calculated for average conditions.

An estimate of the maximum fuel temperature was therefore made using the analytical procedure described in Section 4. The computed hot spot was about 3200°F for the conditions stated. The computed temperature is this high because the lowered helium flow rate results in the heat transfer coefficient being reduced considerably below the normal design value. At this temperature level, however, the effects of internal bed conduction and radiation would be more important than at design conditions and could decrease this temperature considerably.

Since fuel element temperatures during the high-temperature gas experiment will exceed 2500°F, consideration has been given to the behavior of the fuel under these conditions. At temperatures this high, Si-SiC sphere coatings could not be used, since they would deteriorate quickly. Thus, if protection against oxidation of the graphite is found to be necessary, a different type of coating, for example NbC, would have to be developed. Damage to uncoated elements may be little worse than at design conditions since, as discussed in Section 7, the rate of attack will be determined by the water inleakage rate.

With regard to the reference fuel element discussed in Section 10, fuel migration rates may increase by several orders of magnitude, and severe reactions resulting in apparent mass movement of carbide particles through the pyrolytic carbon coatings could occur. The instabilities thus introduced would have the effect of promoting the release of fission

products to levels considerably higher than those which have been considered achievable with the reference fuel element. Diffusion of such nonvolatile fission products as Ba^{140} would also occur under these conditions. If oxide-coated UO_2 particles were used instead of those discussed in Section 10, reactions between graphite and Al_2O_3 or BeO coatings would introduce instabilities at the higher temperatures. A heavily impregnated graphite matrix may provide a partial solution to the fission product-retention problem, but developmental work will be required.

It is reasonable to state that dimensional and mechanical stability could be achieved in the fuel element under the conditions of the high-temperature experiment. Based on present knowledge, however, the activity level in the coolant system will probably be much higher than at normal design conditions.

Reactor Physics and Control

The specific physics and control problems associated with an increase in core temperature will depend on the power level at which the reactor is operated, the fuel lifetime desired, the decrease in core diameter if an insulating sleeve is inserted, and the nuclear properties of any insulation used. No difficulties are anticipated, although a change in fuel enrichment might be required if the core diameter were reduced. This itself would not be particularly undesirable, since reloading at that time would probably occur anyway, but care would have to be observed that a reduction in the thorium loading did not have a seriously adverse effect on the fuel temperature coefficient.

Hazards Considerations

Reactor hazards considerations would have to be carefully re-examined before operating the PBRE at high temperatures. The major questions that would arise would be related to (1) control rod infallibility, (2) after-heat removal, (3) temperatures which could exist during accident conditions, (4) more rapid rate of graphite oxidation on air admission, and (5) production of hydrogen from a steam leak. The first three questions have been mentioned previously. With regard to the fourth, it is worth

noting that the analysis in Section 12 of the consequences of air admission is based on the assumption that reaction with hot graphite occurs at the rate the gas enters the core; therefore no more severe condition could be assumed for higher temperature conditions.

The steam-graphite reaction can be expected to proceed much more rapidly for a steam leak occurring during high-temperature operation than for the corresponding accident under reference design conditions. Since the influence of the reaction rate on the severity of the resulting hazard is not fully apparent, it is difficult to say whether a more serious danger would exist in the high-temperature case. This matter would certainly require further study.

Additional Costs of High-Temperature Operation

The initial increase in reactor cost to provide for the possibility of high-temperature operation appears small. Means by which the coolant flow through the reflector can be increased may have to be provided in the original structure, but all the other changes mentioned can be made when needed. The cost of modification at the time the change in conditions is to be made will be in the range of $200,000 to $500,000, the difference largely depending on whether replacement of the entire reflector is required.

There will also be the expense of developing high-temperature thermocouples and control rods for this application (discussed in Section 16). In addition, the research and development programs for other areas include some costs associated with extending the range of experiments to the condition of interest for high-temperature operation.

Conclusions

There appears to be no significant impediment to operation of the PBRE with gas outlet temperatures in the range 2000 to 2500°F if fuel elements adequate for operation at those conditions are developed. More detailed studies will be required before a firm conclusion can be made,

but, tentatively, it appears possible to increase the temperature level to this high range with only limited alteration of the reactor structure.

14. SITE SELECTION

Introduction and Conclusions

Representative sites at the Oak Ridge National Laboratory and at the National Reactor Testing Station were investigated to provide information for making a site recommendation based on engineering and economic considerations. These investigations indicated (1) that there would be an appreciable advantage in locating the PBRE near enough to ORNL for members of the scientific and engineering divisions to participate expeditiously in the planning and analysis of reactor operations, and (2) that the construction cost of the reactor would be less at Oak Ridge than at NRTS.

Savings of approximately $900,000 achieved by using existing HRE-2 facilities in Oak Ridge would more than offset a cost advantage of several hundred thousand dollars achieved by housing the reactor in a conventional building at NRTS rather than in a containment vessel at Oak Ridge. In addition, since construction costs are 22.5% higher at NRTS than in Oak Ridge, it is estimated that excess facility construction costs in the order of $1,000,000 would be encountered in Idaho. It does not appear likely that appreciable cost savings could be obtained by using the GE-ANP maintenance facility at NRTS without seriously compromising the objectives of the reactor experiment.

The accessibility advantages of an Oak Ridge location and the additional costs associated with development of an NRTS site are partially offset by other considerations. Location of the PBRE at an NRTS site would reduce the possibility of damage to ORNL or to properties adjoining the Oak Ridge controlled area and would give some increase in latitude in design and utilization of the PBRE. It does not necessarily follow, however, that more hazardous experiments would be performed with the PBRE at Idaho; continued availability of the reactor as a development tool would dictate a prudent approach to operations and would inhibit the performance of experiments that could damage the facility.

Two sites at ORNL and two sites at NRTS were considered. The sites at ORNL have been designated as Site 1, at the HRE-2 facility, and Site 2, an area on Melton Valley Drive east of the HRE-2 facility (Fig. 14.1).

Unclassified
ORNL LR DWG 64851

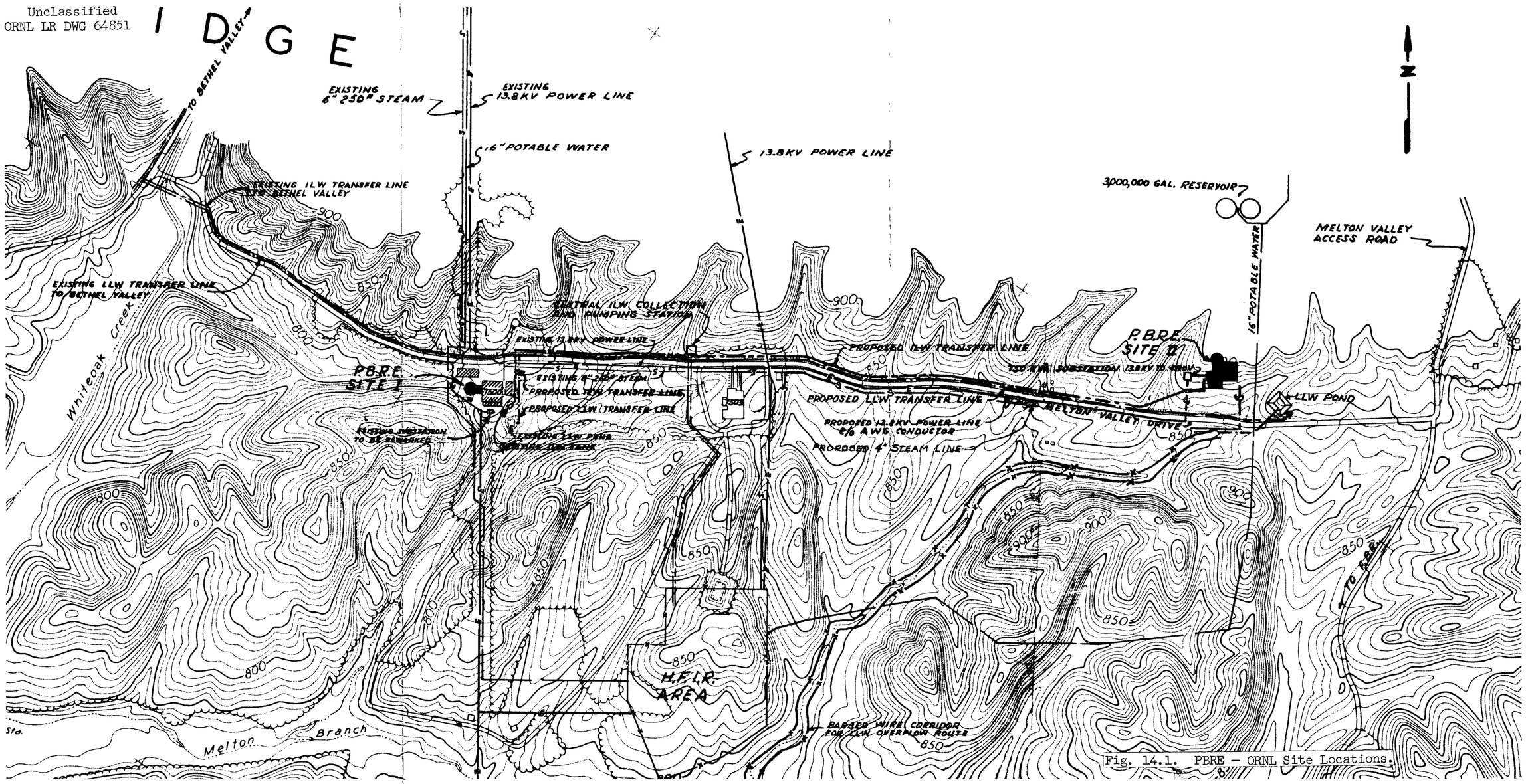

Fig. 14.1. PBRE – ORNL Site Locations.

Sites considered at NRTS are Site 1, between the SPERT and GCRE areas, and Site 2, at the ANP area (see Fig. 14.2).

Hazards Considerations

Selection of a site for the PBRE involves questions of hazards to the public, to neighboring installations such as the Oak Ridge National Laboratory, if at Oak Ridge, or to other reactor sites, if at NRTS, and to the personnel operating the experiment. In evaluating hazards questions, the most serious accident has been assumed to be a rupture of the high-pressure helium system followed by complete combustion of the reactor core and release of fission products from the reactor vessel (see Section 12). The analysis has been based on 100% release of the noble gases, 50% of the halogens and alkali metals, and 5% of all other fission products from the core.

The containment vessel that would be provided at Oak Ridge would largely retain the fission products evolved from the reactor. In estimating activity escape from the containment shell, a persistent leakage of 1% of the containment vessel atmosphere per day, following the accident, was assumed; the additional assumption was made that one half the iodine that escaped from the core would be retained on surfaces within the containment vessel. Under those conditions, it is found that either of the Oak Ridge sites considered would be acceptable as far as public safety is concerned. Both sites are two miles within the nearest boundary of the Oak Ridge reservation, although the Bearden Creek embayment of Melton Lake will be approximately one mile from Site 2. Under the most unfavorable atmospheric conditions (wind velocity 3 mph, large inversion), the dose from fission products escaping from the containment vessel would be 0.8 rem to the thyroid and a like amount to the bone for each hour of exposure at a distance of 2 miles, and 3 rem for each hour of exposure at a distance of one mile. Under typical daytime atmospheric conditions, the doses would be less than one-tenth these amounts. At a distance of 2000 ft, the dose to bone and to thyroid could be 12 rem for a 1-hr exposure, which indicates that prompt action would be required to evacuate the area near the reactor.

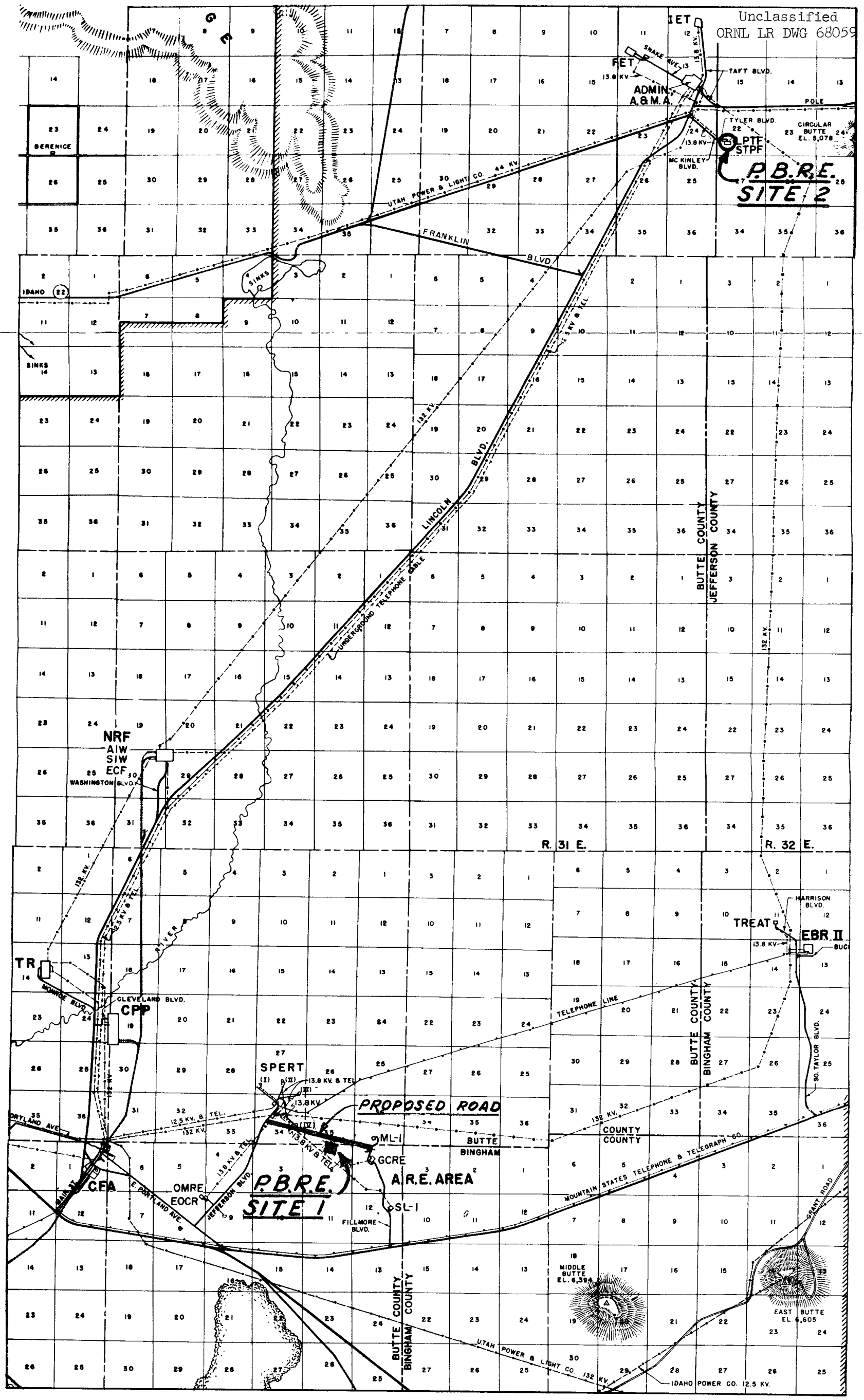

Fig. 14.2. PBRE – NRTS Site Locations.

The main ORNL area is one-half mile or more from either site and is on the other side of Haw Ridge. While there might be concern about fission products being carried through the gap in the ridge at the western end of the Laboratory, measurements show that a wind blowing toward the Laboratory through the gap is accompanied by a wind blowing in a northeasterly direction (SW wind) up the valley in which Sites 1 and 2 lie, that is, away from the gap.

Another danger to neighboring facilities would be from direct radiation of gamma emitters within the containment vessel. At the MSRE site, which is approximately 1500 ft from the HRE-2 site, the direct dose rate would be a few hundred mr/hr at most. While this would pose no particular danger to personnel there, it could prevent use of that facility for a time.

No hazards problems are visualized for location of the reactor at either of the NRTS sites. Containment vessels are not required at NRTS, reliance being placed on isolation and on the partial containment that may be provided by the reactor building. A serious accident with the PBRE could endanger other facilities in the area, in the absence of containment, but this would be a small risk which presumably would be acceptable as part of the operating philosophy at NRTS.

Utilization of the Facility

Since the PBRE is to be an experimental facility, there is a significant advantage to be gained by locating it at an Oak Ridge site. The staff of the reactor will be relatively small and their time will be fully occupied with the details of operating the system. If the facility is conventiently nearby, however, many ORNL staff members would participate in the planning and analysis of reactor operations. Hence, the reactor staff would be backed up by a much larger body of engineers and scientists, several hundred of whom will have participated in the research, development, and design activities which led to the construction of the facility. As an example, at times during operation of the HRE-2, many members of the Reactor Experimental Engineering Division, Reactor Chemistry Division,

Chemical Technology Division, Metallurgy Division, and others, who were not members of the reactor operating staff, participated day-by-day in observing and analyzing the behavior of the reactor, conducting experiments, performing remote maintenance operations, etc.

This participation would also occur if the reactor were located at NRTS, but to a much lesser degree. The travel time from Oak Ridge to Idaho would greatly limit the frequency and extent of visits to the site. Coordination within the ORNL organization by the transmission of reports would be obviously less effective than direct participation when day-to-day operation of the reactor was involved.

In contrast to the advantages of an Oak Ridge site, there would be some gain in flexibility in design and operation of the system if it were located at NRTS. Elimination of the containment vessel would make the reactor more accessible for connection of services and passage of equipment, and scheduling of construction might be simplified. The design of a heat dump, for example, might be easier if there were no requirement of secondary containment. There would be greater freedom in the discharge of gaseous wastes than at Oak Ridge.

The simplification achieved by use of an NRTS location, however, is limited. Shielding would still be required to protect the operating personnel when the reactor was at power and to make components accessible for inspection and maintenance when it was shut down. Continued availability of the reactor as a development tool would necessitate operation in a manner that would preclude experiments that could damage or contaminate the facility. The possibility of releasing a significant fraction of the fission product in the reactor to the surroundings would restrict the type of experiments which could be performed, even at an NRTS location.

Sites at ORNL

Site 1, at HRE-2 Facility

Since the HRE-2 has been shutdown, there are certain advantages in locating another reactor of similar size at the same site (see Fig. 14.1)

to utilize the existing facilities and services. The existing building can be used for the control room and administrative and service areas. The existing air-cooled condenser can be used to dissipate the heat generated by the reactor, and the existing electrical and water services can be extended to the reactor containment vessel at minimum cost.

Site 2, East of the HRE-2 Facility

Site 2 is located by Melton Valley Drive on Haw Ridge, approximately 4000 ft east of the HRE-2 facilities and 2500 ft east of the MSRE facility (see Fig. 14.1). This site is considered because of its proximity to ORNL electrical and water distribution systems. It is typical of several potential reactor sites in the Haw Ridge–Melton Valley area.

Sites at NRTS

Site 1, Between SPERT and GCRE Areas

Site 1, between the SPERT and GCRE areas (see Fig. 14.2), was considered because, of the undeveloped sites available, it has the advantages of being close to an access road which is to be built between the SPERT and GCRE areas, it is adjacent to the power distribution line, and it is a reasonable distance from existing reactors. In addition, the site is in an area which receives central-facility services, consisting of craft help, heavy equipment, laundry, technical library, transportation, hospital, food service, central warehousing, central shops, fire and security protection, utilities, maintenance, and waste disposal.

Site 2, at ANP Area

The only available developed sites at NRTS are at the ANP area. Consideration was given to sites in this area to determine whether a reactor using the existing facilities would be compatible with the objectives of the experiment. Three design variations were considered to permit using NRTS Site 2 at the ANP area.

1. A stripped-down reactor installation with little or no shielding mounted on one or more flat cars with provisions for coupling instrumentation,

electrical, and other supply lines into receptacles at a remote site could be used. The flat car could be hauled into the GE-ANP A & M building hot cell whenever maintenance work might be required.

2. A fixed reactor installation inside the A & M building was considered. The remote-handling facilities could be employed directly for maintenance and the complications of flat-car mounting, breaking connections, etc., could be avoided.

3. A fixed installation could be made at the LPTF to take advantage of existing utilities.

Flat-car mounting of a reactor is most suitable for short-term tests of compact systems. In contrast, long-term operation of the PBRE will be necessary to achieve significant burnup of the fuel and to investigate fission-product deposition problems. Further, an appreciable height is required if fuel-handling systems applicable to a power reactor are to be studied. Without shielding of the system, maintenance procedures would be fully remote rather than semidirect and direct as proposed for power reactor systems. The flat-car proposal was rejected for these reasons as seriously compromising several objectives of the PBRE.

There are similar objections to construction of the reactor in the GE-ANP A & M building. The hot cell height of only 61 ft would considerably limit the system. Further, the concrete shielding in the ceiling and upper portion of the side walls of the hot cell is only 2 ft thick. Hence, additional shielding around the reactor might be required to reduce the neutron and gamma dose level during reactor operation. Some shielding for isolating and separating highly radioactive components would also be required if direct and semiremote maintenance on the less radioactive portion of the system were to be possible. Full reliance on the available remote manipulators for maintenance would require the erection of a considerably more complex assembly without eliminating the need for many special-purpose tools. It is thus questionable whether appreciable savings could be achieved by use of the A & M building hot cell. Constructing the experiment in the hot cell would also sacrifice a costly facility which might be used more advantageously sometime in the future.

The use of the LPTF facility adjacent to the STPF in the ANP area was also considered. These facilities have their own utilities. Since it has been proposed that the STPF be utilized for the EBOR Project, the adjoining LPTF has the disadvantage of proximity and possible hazards.

A further disadvantage in selection of a site in the ANP area is that central-facility services are not provided. Thus services must be duplicated at considerable additional cost.

Site Cost Comparisons

The estimated cost of items which differ at the various sites are given in Table 14.1. Costs for the NRTS site were estimated on the basis of costs at ORNL and adjusted by a construction cost index ratio[1] of 1.225. Comparison of the costs at the undeveloped sites in both areas shows that several hundred thousand dollars saved by elimination of the containment vessel at NRTS is offset by the additional cost of construction there. Table 14.1 shows further that approximately $900,000 is saved by using existing HRE-2 facilities rather than by developing a new site in either area.

In addition to the amounts in Table 14.1, roughly $4,000,000 of the total cost of the plant may be allocated to on-site construction work. The NRTS construction cost differential, when applied to this on-site work, results in an "excess" facility construction cost of $1,000,000. Thus there is a saving of approximately $1,900,000 to be achieved by building the PBRE at the HRE-2 site in Oak Ridge rather than at a site at NRTS.

---

[1]AEC Construction Cost Differential as of January 23, 1961:

$$\frac{\text{NRTS}}{\text{ORNL}} = \frac{1.31}{1.07} = 1.225$$

Table 14.1. Building and Site Development Costs Summary

	ORNL		NRTS Site 1 Between Spert and GCRE
	Site 1 At HRE-2	Site 2 East of HRE-2	
Site preparation	$ 20,700	$ 90,300	$ 90,300
Roads	1,400	12,000	8,200
Storm sewer		2,700	2,700
Fencing		12,300	12,300
Building alterations	55,000		
Containment shell			
Excavation	152,600	206,500	
Shell	610,000	610,000	
Concrete	74,000	74,000	
Reactor building			
Excavation			206,500
Building			150,000
Concrete			160,000
Administration and service building		451,000	451,000
Sanitary waste facilities		5,100	5,100
Power	10,800	28,800	28,800
Water	5,000	25,700	160,000
Steam		85,400	99,100
Liquid radioactive waste facilities	11,400	94,700	42,000
Subtotal	940,900	1,698,500	1,416,000
NRTS cost differential (22 1/2%)			318,600
Contingency (20%)	188,100	339,500	346,400
TOTAL	$1,129,000	$2,038,000	$2,081,000

15. CONSTRUCTION COST ESTIMATE

The design and construction costs of the reactor described in this report have been estimated in as much detail as is feasible at this stage of the project. The estimate was performed in such a way as to assign a price to every major component of each process system, as well as to major plant features. To provide a basis for assigning costs, components were characterized by performance criteria, by flow diagrams and descriptive sketches, and by discussions with project personnel. Estimates were solicited from industrial firms on equipment which could be sufficiently described, and the cost experience of EGCR, HFIR, MSRE, and other projects was heavily drawn upon. All top charges such as escalation, contingency, and overhead were applied. A summary of the project costs is presented in Table 15.1 in conventional format.

Considerable effort has been spent in attempts to reduce the cost of the plant, and the original concepts of several major features have been altered. Design changes were made to achieve economics only where they were consistent with the accomplishment of project objectives. The PBRE must have a fuel-handling system similar to one which would be used on a large power reactor; the fuel must be subjected to a nuclear, chemical, and physical environment similar to that in a large pebble-bed reactor; the product of power density and use factor must be sufficient to produce full fuel burnup in a reasonable time; it must be possible to operate and maintain the reactor with a relatively high release of fission products from experimental fuel elements; means must be provided for studying fission product escape, migration, and deposition in the system; the useful life of the plant must be adequate for performance of the desired experiments; and the reactor must unquestionably be safe to operate.

The cost estimates of Table 15.1 are felt to be as realistic as it is presently possible to make them. Economy will, however, continue to be a prime consideration in the development. The current estimate for a 5-Mw PBRE exceeds the estimate of $9,096,000 made 1 1/2 years ago[1] for a

[1]A. P. Fraas et al., Preliminary Design of a 10-Mw(t) Pebble Bed Reactor Experiment, CF 60-10-63 rev. (May 8, 1961).

Table 15.1. Preliminary PBRE Cost Estimate

	CPFF	Fixed Price	ORNL	Total
Direct Construction Costs		2,706,000	4,016,000	6,722,000
1. Building Cost to 5-ft Line				
(a) Modification to Building 7500 for reactor control, service, and administration		75,700	2,000	77,700
(b) Reactor building (new), including containment shell, shielding, and services		1,967,500	4,000	1,971,500
2. Installed or Fixed Equipment (nuclear plant and auxiliaries)		636,000	4,004,000	4,640,100
Sub Total		(2,679,200)	(4,010,000)	(6,689,200)
3. Movable Equipment				
4. Improvements to Land		1,400		1,400
5. Outside Utilities		25,400	6,000	31,400
Engineering Design and Inspection		204,000	1,032,000	1,236,000
Design		204,000	914,000	1,118,000
Inspection			118,000	118,000
Indirect Costs			1,213,000	1,213,000
Escalation to FY 1965		349,000	712,000	1,061,000
Allowance for Contingencies		641,000	1,387,000	2,028,000
Gross Total Project Cost		3,900,000	8,360,000	12,260,000
Salvage Credits for Reused Equipment				
Net Total Project Cost		3,900,000	8,360,000	12,260,000

10-Mw PBRE. There was at that time only seven weeks available for the preparation of both the conceptual design and the estimate. Many plant features, particularly instrumentation, maintenance, and auxiliary systems, have appeared on further study to be more costly than previously expected. Recent experience with other reactor projects at ORNL has shown that the standard 10% allowance for contingencies is inadequate and that an allowance should also be made for escalation. Accordingly, the current estimate provides 19% for contingencies and 12% for escalation. Further, construction is now assumed to be based on operating rather than capital funds, with a consequent increase in overhead of from 25 to 100% on direct labor.

If consideration is given only to cost per Mw, the $12,260,000 PBRE estimate makes pebble-bed reactors appear expensive relative to other types. This seemingly unfavorable comparison occurs because several of the major PBRE cost items (reactor building, instrumentation, fuel-handling equipment, maintenance equipment, and engineering) are nearly as expensive for this 5-Mw reactor as they would be for one many times that power. If the PBRE power were doubled, for instance, the incremental cost would be less than $1,500,000. A significant comparison may be made of the costs previously estimated for the 10-Mw(t) PBRE[1] and an 800-Mw(t) PBR[2] ($62,761,000, which is $190/kwe). For an 80-fold increase in thermal power, the cost increased only by a factor of 7. Hence the high cost of the reactor experiment does not imply that a full-scale power plant based on the pebble-bed concept will be uneconomical.

In preparing the cost estimate of Table 15.1, all design, engineering, fabrication, construction, and installation costs were included in operating funds to which overhead was charged at 100% of direct labor. All contracted labor and material were included as material charges, with profit and overhead added. All plant costs were estimated on the basis of the layout of Fig. 3.25. If it is decided that a superheated-steam system should be used, the estimate will have to be increased to cover the cost of the more complex system and, possibly, apparatus for indirect maintenance.

---

[2]A. P. Fraas et al., Design Study of a Pebble-Bed Reactor Power Plant, CF 60-12-5 rev. (May 11, 1961).

Spare equipment and parts are not included in the estimate, and it is considered that a minimum of $233,000 of reactor operating funds should be allocated for those items that should be available at startup. The spare equipment should include a main blower, a steam generator tube bundle, control rods and rod drives, auxiliary system components, and instruments. In addition, a minimum of $50,000 of reactor operating funds should be available at startup for shielded casks for fuel handling and maintenance.

The cost of the fuel is similarly not included in the estimate of capital costs. The fuel for the first core loading will be charged to operating funds.

16. RESEARCH AND DEVELOPMENT

Research and development problems for the PBRE fall into three broad categories: (1) those necessary for completing the design for fabrication and construction; (2) those necessary for developing the information needed for providing the first fuel loading, evaluating hazards, preparing for decontamination and maintenance, preparing for evaluation and interpretation of results, and operating the reactor; and (3) those necessary for providing future advanced fuels, for fuel processing, and for revising the core to achieve gas temperatures above 2000°F.

Some of the principal problem areas to be considered are:

1. The fuel: its composition, physical properties before and after irradiation, dusting characteristics, outgassing properties, chemical stability, fission-product retention characteristics, and behavior in the presence of air or steam under accident conditions.

2. The fuel bed: its void fraction, pattern of sphere movement through the bed, temperature distribution, levitation characteristics, and coolant velocity profiles and fluid dynamics in the bed.

3. Fuel charging and removal: the fuel-addition system; gas locks; devices to control velocity of entry and minimize free fall and breakage problems; fuel movement in the bed; the discharge device; fuel-sphere counting, classification, storage, and examination devices; and equipment to return unspent and new fuel to the addition system.

4. Moderator graphite: its structural properties, behavior under irradiation, evaluation of boronated graphite, detection of cracks in the reflector, and gas evolution.

5. Helium coolant: purity requirements and purification processes, analysis techniques, flow and mixing problems, and mass-transfer and fission-product-deposition phenomena.

6. Components and auxiliary systems: control rods and drives, blowers, joints, valves, insulation, the steam generator, special instrumentation, and the purification system.

7. Maintenance: decontamination techniques, servicing and equipment-handling techniques, and the need for special tools and techniques for assuring the integrity of equipment which is reassembled remotely.

The research and development program described below comprises the tasks and experiments which need to be completed in part or in whole to assure satisfactory performance of the pebble-bed reactor experiment. However, many of the studies discussed in this section are already being conducted as continuing programs for the general development of gas-cooled reactor technology. Results of these general studies will contribute directly to the specific needs of the PBRE.

Schedules and cost estimates for the program outlined are given at the end of this section. A comparison of the proposed research and development schedule with the PBRE design and construction schedules indicates the two to be mutually consistent.

Fuel Element Development

As described in Section 10, considerable information has been accumulated in experimental fuel element development programs since publication of the last PBRE study,[1] and some limitations associated with the coated-particle concept, particularly the pyrolytic-carbon-coated uranium carbide element, have become reasonably clear. What remains to be done is to investigate modifications of existing techniques, as well as new techniques, in an effort to improve the performance of coated-particle fuel materials. The present practice of maintaining close liaison with potential suppliers and particularly with related projects at Battelle Memorial Institute, General Atomic, General Electric NMPO, OEEC Dragon, and Brown-Boveri-Krupp, will, of course, be continued.

The major areas of interest in the fuel element development program include studies of (1) mechanical and physical properties; (2) fabrication; (3) chemical stability; (4) fission-product behavior in the fuel; (5) the effects of irradiation on items 1 through 4; and (6) chemical processing. Extensive irradiation testing is required to demonstrate the feasibility of an all-ceramic fuel with the good fission-product-retention properties desired for the PBRE. Because of the time required for design, preparation,

---

[1]A. P. Fraas et al., Preliminary Design of a 10-Mw(t) Pebble-Bed Reactor Experiment, ORNL CF 60-10-63 rev. (May 8, 1961).

operation, and complete evaluation of irradiation experiments, the fuel element research and development schedule is established to a large extent by this phase of the program. In view of this consideration, it is estimated that at least a two-year period will be necessary before firm recommendations can be made for purchase of the most promising PBRE fuel elements. The specific research and development programs discussed below have been formulated on this basis.

Mechanical and Physical Properties

A comprehensive test program is required to evaluate the physical and mechanical properties of the fuel elements in the light of proposed PBRE conditions. In general, these tests apply both before and after irradiation. The mechanical properties of interest are crushing strength, impact resistance, and abrasion resistance. The physical properties of chief concern are related to thermal effects and include thermal conductivity and the coefficient of thermal expansion. Other characteristics of interest include density and particle distribution as determined by radiographic techniques; microstructures of particles, matrix, and sphere coatings as determined by metallographic techniques; sphere-coating integrity as determined by oxidation and "hot oil" tests; and exposed fuel present as surface contamination and damaged particles as detected by alpha-counting and acid-leaching techniques.

Nondestructive Inspection of Fuel Elements

The development of inspection techniques for fuel materials and fuel elements will be necessary to complete the specifications and acceptance criteria for fuel spheres. Recent preliminary studies with low-voltage radiography indicate excellent potential for coated-particle dimensional gaging and the possibility of evaluating the integrity of particle coatings. Another test that may be useful for evaluating the integrity and impermeability of particle coatings on large quantities of fuel particles is the galvanic cell method. Feasibility studies on these techniques should determine the adaptability and need for further development.

The determination of fuel distribution within fuel elements will require the development of techniques and acceptance standards for radiographic inspection. The detection of cracks in fuel spheres may also be possible by this technique. The thickness and continuity of bonding of the unfueled shell, on the other hand, may require investigation of other techniques, such as eddy current or ultrasonic inspection.

The thickness and integrity of the siliconized-SiC coating on the fuel spheres must be carefully specified and controlled. Preliminary work on similar coatings for the EGCR fuel assembly sleeves demonstrated the feasibility of eddy currents for the measurement of coating thickness.[2] A galvanic-cell method for the detection of flaws in the coating was also shown to be promising.[3]

Fabrication Studies

One of the limitations of the coated-particle fuel element is associated with the effects of fabrication variables. It is noted in Section 10, for example, that studies on commercially produced materials have shown that many coated particles have been damaged in some manner during fabrication of the fueled-graphite specimens. It is important, therefore, that the methods used for preparing and coating the particles, for incorporating the particles in suitable graphite matrices, for applying protective sphere coatings, and for impregnating molded graphite matrices be understood by the materials personnel responsible for the PBRE fuel. The need for first-hand knowledge of fabrication variables becomes particularly apparent when an attempt is made to establish a reasonable set of fuel element specifications and to negotiate intelligently with the potential suppliers of fuel spheres for the PBRE. It has become evident that the understanding required must stem from actual fabrication experience.

Chemical Stability

Experimental studies are required to evaluate the chemical stability of the various component phases within the fuel sphere and the stability

---

[2]GCR Quar. Prog. Rep. June 30, 1961, ORNL-3166, pp. 97–98.

[3]GCR Quar. Prog. Rep. March 31, 1961, ORNL-3102, p. 116.

of the fuel sphere with respect of its environment. Interactions involving the fuel particle, its coating, and the matrix material; interactions between sphere coating and the matrix; phase stability in the uranium-thorium-carbon system or the uranium-thorium-oxygen system represented by the fuel particle; and effects of time, pressure, and temperature on the self-welding tendency of sphere coatings must be studied. Environmental effects studies will include investigations of the effects of steam and oxidizing contaminants in the helium coolant.

Fission-Product Behavior

Certain out-of-pile experiments are required in order to study the behavior of both volatile and nonvolatile fission products in the fuel sphere. In this connection, experimental data are required on the rates and mechanisms of diffusion of fuel and fission products through particle coatings and matrix materials.

Effects of Irradiation

By far the largest effort and cost in the fuel element development program is associated with irradiation experiments on unsupported particles, fueled-graphite specimens of sizes and shapes which are compatible with existing capsule designs, and full-scale PBRE fueled-graphite spheres. The types of experiments include (1) fission-product release and deposition during postirradiation heating after light irradiation (the so-called "neutron-activation" method); (2) static capsule in-pile tests; (3) sweep capsule in-pile tests; and (4) in-pile loop tests.

The capsule irradiation facilities to be used are the LITR; the B-9, C-1, and poolside facilities of the ORR; and the ORNL-MTR-48 facility.

The GCR-ORR loop No. 2 irradiation facility will be utilized for tests of full-size fuel spheres under conditions closely simulating those of the PBRE bed. Variables which can only be fully evaluated by forced-convection cooling, including non-uniform heat transfer, contact between spheres, particle erosion, and the effects of coolant impurities at low concentration levels, will be studied and data will be obtained on fuel behavior and fission-gas retention. Actual assemblies will utilize several

full-size fuel spheres axially aligned and surrounded with unfueled dummies in various packing configurations which will readily fit into the loop facility. Testing of a bed containing two or three parallel rows of fueled spheres can be accommodated by reduction of sphere size or by revision of the loop to afford a larger test region. The loop is capable of operation with helium cooling at 300 psia and with gas inlet and outlet temperatures at the fuel element of 1200 and 1500°F, respectively. Tests of each fuel sphere assembly will be continued for several months. Three to four experiments will be scheduled to fully utilize the loop during the first two years of its operation.

Chemical Processing

Although the development of fuel reprocessing procedures is not a prerequisite to the design and construction of a reactor experiment, an economical chemical recovery process for the spent fuel must be developed if the pebble-bed reactor concept is to have a place in the long-range nuclear power reactor program.

Graphite Components

The research and development program on graphite components for the PBRE has two major objectives: (1) to select the best grade of graphite and (2) to provide the required reactor design data. Stresses resulting from neutron-induced dimensional changes are expected to impose limiting conditions on design and operating life of the graphite structures. Existing evidence indicates the possibility of selecting a grade of graphite for maximum longevity on the basis of an optimum combination of its mechanical properties and behavior under irradiation. Growth data are being obtained on various types of graphite at Hanford; it is proposed that these studies be augmented with a program for determining (1) the mechanical and physical properties of various types of graphite and the effect of irradiation on these properties, (2) the influence of extrusion size and shape on the properties of graphite, and (3) the combined effects of applied stress and radiation-induced shrinkage on graphite.

With respect to the boronated-graphite thermal-neutron shield material, the major question requiring study is the possible migration of boron under exposure to the temperatures and the radiation and chemical environments which will exist in the PBRE. The detailed graphite component research and development program is outlined in the following sections.

Physical and Mechanical Property Tests

The properties of interest are thermal conductivity, coefficient of thermal expansion, and stress-strain relationships under both tensile and compressive loads. Because of the nonuniform variation of materials properties in a given graphite, enough data will be obtained to provide a statistically sound basis for comparison of the various types of graphite. The materials to be tested will include the grades of moderator graphite for which data on effects of irradiation are being obtained at Hanford.

The extrusion size and shape are known to influence the mechanical properties of graphite. In order to design the optimum section sizes in the reflector, the extent of this effect must be determined. One or two of the best grades of graphite discovered in the test program on physical and mechanical properties will be extruded in various sizes and shapes. Complete tensile and compressive stress-strain diagrams will be obtained on a sufficient number of samples cut from mutually perpendicular directions to provide statistically significant data.

Irradiation Tests

The best graphite selected on the basis of the out-of-pile tests will be irradiated at different temperatures for extended fast-neutron exposures. The objectives will be to determine irradiation-induced changes in physical and mechanical properties and to establish the relationship between radiation-induced shrinkage and stress and strain for constrained specimens. The thermal conductivity and creep characteristics, including strain versus time correlations, rupture strain, and rupture stress, will be determined as functions of fast-neutron exposure and irradiation temperature.

Boronated Graphite Studies

The vapor pressure of boron over boronated graphite at the PBRE operating temperatures is expected to be low enough to make loss by direct vaporization negligibly small. However, very volatile boric oxides and boric acid may be formed by reaction with impurities in the helium. It is proposed that tests be performed to determine the magnitude of the boron migration problem under PBRE conditions. The loops designed for graphite oxidation studies in connection with the helium purification problem can be used for these tests. The work at General Atomic on boronated graphite will continue to be followed, although the GA studies are being made at very high temperatures and boron concentrations much higher than the 0.5 wt % considered for the PBRE. Some studies, made in conjunction with the commercial suppliers, may be in order to establish uniformity and reproducibility of boron content and physical and mechanical properties of the boronated graphite components.

Coolant Purification

Stringent purity requirements are imposed on the helium coolant of the PBRE to minimize hazards, reduce the damaging effects on materials and components exposed to the helium, and to ease decontamination and maintenance problems. The removal and control of impurities involves studies of the sources and kinds of contaminants, filtration, and bypass cleanup techniques.

While these problems are amenable to analysis to a degree, experimental verification of their magnitude and severity with respect to the PBRE is required. Consequently, the over-all program on coolant purity will be designed for laboratory-scale experiment and for system testing to the extent necessary to define the nature of the sources of contamination, the effects of contaminants on materials, and the effectiveness of the purification equipment in keeping the situation under control.

Gas Evolution from Reflector and Fuel Graphite

It will be necessary to determine the outgassing characteristics, including the constituents of the outgassed material, as functions of

both temperature and time for PBRE fuel spheres. Similar work has already been carried out on many representative reactor-grade graphites, but degassing information on the specific graphite chosen for the PBRE reflector-moderator may be required, especially at extreme temperature levels (up to 2500°F). The readsorption characteristics of graphite when cooled and stored in selected atmospheres and subsequent degassing characteristics will also be studied to determine whether such special storage prior to installation in the PBRE will be economically advantageous in controlling system contamination levels.

The data obtained from the experiments suggested will assist in determining loads to be handled by the purification equipment and in defining special operating procedures during periods of high outgassing rates.

Graphite Oxidation and Mass Transfer

The specification of the helium purity for the PBRE will rest, in part, on the extent of chemical reaction between the contaminants and graphite.

The rate of graphite oxidation by helium sweep gas containing controlled quantities of O_2, H_2O, and CO_2 will be determined analytically and experimentally. The work will cover the effects of impurity partial pressure, specimen and helium temperatures, helium pressure and flow rates, as well as the effects of CO and H_2 on reaction rates. Specimens tested should include moderator graphites and fuel spheres. The program will be initiated with bench-scale, once-through flow tests where variables can be closely controlled and reaction rates accurately determined. It will be expanded to close-circuit loops containing graphite sphere beds through which helium can be circulated at conditions matching reactor operation to check tendencies toward localized attack at hot spots. The latter loops will provide, in addition to graphite oxidation data, further information on effects of outgassing and a definition of the problems of graphite mass transfer as functions of system operating parameters and materials of construction. Specimens of various metals with differing surface treatments which may be encountered in the PBRE system will be

inserted in the cooler regions of the loops to examine the roles of these features in the deposition of carbon. It will also be of interest in these loops to determine the extent to which carbon dust is produced and transported in the helium stream.

Purification System and Components

Filter Development. Because of the nature of the PBRE core, graphite particles, carbon dust, and, possibly, graphite coating material may be carried around the coolant circuit in such a way as to damage the coolant circulator and valve seats or to cause plugging of instruments and bleed lines. Full-flow filters may be required in the main coolant circuit of the PBRE to remove this particulate matter. Some benefits may also be derived in limiting the spread of condensed fission products by concentration on the filter medium. Filter designs will be tested to demonstrate that they possess the required effectiveness and efficiency under simulated reactor operating conditions. The structural integrity of the filter and filter medium must be demonstrated in long-term tests, and the pressure-drop characteristics of various promising designs will be determined. Test rigs and prototype test components obtained for this work can be used subsequently for proof tests of reactor hardware.

Fission-Product Cleanup System. The dynamic-adsorption coefficients for krypton, xenon, and iodine on charcoal at the temperatures and pressures of interest to the PBRE are reasonably well established at the present time. A limited amount of additional testing and evaluation may be necessary to answer specific questions as the PBRE detail design develops.

Poisoning of the charcoal bed by adsorbed iodine does not appear to be a problem in the PBRE application. Some additional work will be required to investigate the possibility of iodine transport through the charcoal trap on minute particulates present in the helium stream.

Chemical Cleannup System. Considerable work has been done on the kinetics of the oxidation process[4] and on the coadsorption of CO_2 and

[4]C. D. Scott, Removal of Hydrogen, Carbon Monoxide, and Methane from Gas-Cooled Reactor Helium Coolants, ORNL-TM-20 (Nov. 15, 1961).

H_2O on molecular sieves. However, further work will be required to verify the performance of the oxidizer at H_2 and CO levels of specific interest to the PBRE and to establish the dynamic adsorption capacity of molecular sieves for CO_2 and H_2O at extremely low partial pressures. These studies require laboratory experiments with prototype or reduced-scale components.

Gas-Analysis Equipment. Analytical techniques must be developed for monitoring helium purity at the low contamination levels required for the PBRE. Gas chromatography has been useful in the past for on-stream monitoring of helium purity, but the thermal-conductivity detector normally used with these instruments does not possess the required sensitivity for the PBRE application.

A development program is required to provide equipment with which the required degree of sensitivity can be achieved and the low-level contamination measured. The application of ionization detectors to gas chromatography shows promise of increasing sensitivity a thousand-fold or more over the thermal-conductivity detector. Another possible approach to increased sensitivity involves concentration of the impurities (by diffusion of H_2 and helium through a palladium or silica barrier) to a sufficient degree that conventional analytical techniques may be employed. Although sample concentration would interpose a greater time delay between sampling and readout, the development of such a technique should be pursued as a backup effort.

Purification System Mockup

The foregoing programs are devoted to developing understanding of individual processes and system components. To resolve uncertainties on the relative magnitudes of the problems that will be encountered when all processes are occurring simultaneously, a working prototype of the purification system should be operated to simulate, with the possible exception of fission products, as much of the over-all PBRE contamination-handling problem as possible. The system could be attached to one of the closed-cycle mass-transfer rigs. These experiments should reveal oversights not detectable in the individual investigations; and, in addition, they should permit development of appropriate parts of the PBRE

operating manuals in advance of PBRE operation. The mockups will also provide sites for proof-testing PBRE purification system components.

Fission-Product Transport and Deposition

An important problem in the evaluation of gas-cooled reactors is the behavior of fission products in the coolant streams and their effects on hazards and leaktightness specifications, life of equipment, shielding requirements, maintenance techniques, and purification system performance. Although fission product behavior is particularly important in ceramic-fueled reactors, where some release of activity is to be expected, similar problems are encountered when defects occur in metal-clad fuel elements of other types of gas-cooled reactors.

Fission products that remain in the gaseous state at reactor conditions will be continuously removed from general circulation by the purification system. Many elements, however, will be condensed or adsorbed on surfaces in the core, primary coolant circuit, and auxiliary systems; some will deposit directly on component surfaces while others may react first with particulate matter in the gas stream. The particular activities deposited in the system and their distributions will determine shielding requirements, the decay and decontamination criteria to be observed before maintenance is begun, and, of major importance, the extent to which maintenance must be performed by indirect techniques.

As discussed in Section 7, little is known about the transport and deposition of activity in gas-cooled reactors. The information that exists is fragmentary and often appears contradictory; generally, it is a byproduct rather than a primary result of an experiment, and in most cases is from UO_2 rather than the uranium-carbide graphite fuels, which may result in quite different fission-product spectra and deposition patterns.

Transport and deposition of fission products in helium systems, with particular emphasis on PBRE conditions, will be studied using four approaches: (1) theoretical and experimental studies of the chemical behavior of fission products, (2) out-of-pile annealing experiments using lightly irradiated fuel, (3) experiments with in-pile fission-product

sources using both existing loops and new facilities, and (4) studies performed with the PBRE itself. Some studies of the first two types are presently being performed at ORNL. Experiments using the PBRE are discussed in Section 11.

Chemical Studies

To improve the understanding of fission-product behavior in the reactor, it will be desirable to perform theoretical and experimental studies of the fission-product species released from PBRE fuel in order to establish (1) the chemical forms of the important species, (2) the nature of interaction between the species and materials in the system, and (3) the nature of interactions with possible particulate matter in the gas stream. Studies of the interactions of fission products will in some cases involve rates of interaction and in others (such as where saturation occurs) will involve equilibria. These studies will be conducted in conjunction with fuel development work and with experiments conducted for developing the purification system, and they may require experiments using artificially heated activated specimens.

Activation Studies

The fission-product retention abilities of PBRE-type fuel samples are being studied with neutron-activation techniques. Specimens heated after irradiation are used to identify species which escape and to determine rates of release. Experiments of this type are also being performed to obtain preliminary information on fission-product deposition as a function of surface temperature; fission products evolved from the fuel are conducted past heated surfaces and the locus of deposition of particular species obtained. Further annealing experiments in which materials, surface conditions, chemical composition of the gas, Reynolds number, and channel geometry are varied will provide information on other aspects of the problem. This technique is limited, however, in that only the longer lived species evolved directly from the fuel can be studied.

In-Pile Experiments

In-pile loops and facilities involving in-pile radiation sources will be used for studying fission-product behavior at conditions similar to those which will exist in PBRE. With an in-pile experiment, the important category of nonvolatile daughters which escape from the fuel as volatile or gaseous precursors can be studied.

When it is completed, GCR-ORR loop No. 2 will provide deposition data, in addition to serving as a fuel test bed. Although some controlled studies of fission-product deposition will be possible, the most important deposition information obtained from the loop will probably relate to activity accumulation on components and the operating problems created by its presence.

Ultimately, a flexible deposition facility using an in-pile fission-product source will be built for a systematic evaluation of the problem. The facility will be designed for variation of temperatures, gas velocity, flow geometry, surface material and finish, coolant impurity level, and particulate content of the gas in a fashion which will permit development and testing of models of fission-product behavior. The system presently visualized will have easily replaceable test sections permitting orderly series of tests.

Core Cooling Problems

The inquiry into the heat transfer and fluid flow characteristics of the PBRE core region may be considered in two classes, each of which affects in a different manner the operating performance of the reactor. First, there are the mean value problems which determine the average reactor operating conditions. Included in this category are such items as the mean axial and radial distribution of voids, the mean sphere-bed heat-transfer coefficients, and the radial and axial turbulent diffusivities of heat and momentum. Superimposed upon these are a second group, the extreme-value problems, which perturb the mean reactor characteristics and limit performance to ensure against high rates of fission product release and physical damage to the fuel elements. Within this area, a

prime problem affecting PBRE operation is that of undercooled local regions resulting from close-packed sphere clusters or the possibility of flow-passage blockage by fractured spheres.

Many of these factors have received exhaustive attention in the general technical literature. Thus, sufficient data exist to effect a core design which, while preliminary, will still allow reasonable feasibility judgments. For any specific design, however, sufficient disagreement exists in the literature to warrant the development of improved analytical models and the resolution of uncertainties by appropriate supporting experiments.

Mean Bed Void Fraction

The mean bed void fraction in the PBRE core may be influenced by the methods of addition and removal of spheres, by the geometry of the core bottom, and possibly by the flow of gas through the bed. These factors may also influence the radial and axial variation of void fraction, and, in particular, the shape of the container bottom will affect the void fraction in the lower part of the core. Bed voidage affects the coolant flow and temperature distributions in the core and is a factor in the physics of the reactor.

With present knowledge, there is uncertainty in both the mean void and void distribution in the PBRE. Hence, information on the void fraction will be developed using both full-scale (as mentioned later) and part-scale models of the PBRE core.

Flow Distribution and Pressure Drop

The flow distribution within a packed bed is one of the major nonnuclear factors affecting the temperature distribution within the reactor core. Although there is little information on gas velocity distributions within sphere beds, measurements of velocity profiles are available for the region immediately downstream of the bed surface. By carefully locating the sensors, such measurements permit a reasonably accurate estimate of the velocity profile within the bed. The available measurements both within the bed and immediately downstream from the bed are in

qualitative agreement, indicating a maximum in the velocity profile adjacent to the core wall in the same region as the maximum power generation from flux peaking. The quantitative agreement of the data from the different investigations is not, however, so satisfactory. Therefore, velocity profiles will be measured in the downstream face of the full-scale mockup in an attempt to resolve the disagreement. These tests will be made at various bed depths in order to verify the common belief that the entrance region in packed beds amounts to only a few sphere diameters. In addition, some time will be devoted to the development of instrumentation and techniques suitable for measuring velocity profiles within the bed.

Available data on the average friction factor in packed beds appear well grounded even at low superficial flows and should be valid for purposes of core design. Since measurements on pressure drop as a function of flow rate can, however, be easily obtained using the full-scale model, the pressure-loss characteristic for the PBRE core will be verified.

Additional Flow Problems

The hot-spot problem depends closely upon both the bed voidage and the flow patterns within the bed. A wealth of data on the radial and axial eddy diffusivities within a packed sphere bed allow estimation of either the radial or axial spreading of a labeled tracer as a function of distance from the source. These data, combined with simple analytical models of the distribution of voids within a packed bed, will permit a rough estimate of the effect of local clustering on the development of hot spots in the vicinity of the cluster. Another uncertainty is the frequency and extent of clusters of close-packed spheres within a randomly packed bed.

Experiments aimed at a more detailed understanding of the clustering problem are in progress. The first phase of this program consists of a study of the local rates of mass transfer from a single soluble sphere packed in a regular array of inert spheres. This technique will then be extended to the investigation of rates of transfer in the wake of closely packed sphere clusters. The influence of the wall on the solution

distributions will also be considered. From these data, average and local heat transfer coefficients may be estimated. In addition, the packed-bed eddy diffusivity close to the wall (0 to 5 sphere diameters) will be investigated using a point-source tracer dispersion technique.

An estimate of the frequency of occurrence of clusters will be obtained from planned tests with a bed formed entirely of soluble (or sublimating) spheres. If necessary, a more detailed measurement of the frequency of clustering can be obtained by detailed dissection of randomly packed beds.

The influence of the inlet velocity pattern (as dictated by the number and distribution of slots or holes at the inlet face of the bed and by the shape of the lower, noncylindrical portion of the core) on the downstream profiles and on the approach to established flow are of concern in the specific design of a PBRE core. This problem will be investigated using the full-scale model or lesser-scale models where deemed advisable.

As the velocity through a packed bed having an unrestrained upper face is increased, a point is reached at which the drag forces on the spheres which are tending to move them in the direction of flow are equal to the gravitational forces which are acting to keep the bed fixed. This condition is termed incipient levitation, and it is observed that at this point the spheres on the upper surface of the bed begin to spin. Since the abrading action associated with such movement is undesirable, it is planned to verify the incipient levitation limit for the reference PBRE core.

Full-Scale Flow Model

Since most of the problems outlined above are concerned with the specific PBRE reference design, a full-scale model of the system will be a useful and necessary adjunct to the program. Initially, this system will consist only of a plastic model of the core region; provision will be made for expanding the mockup to include other features (fuel sphere introduction and removal devices, moderator region, etc.) as the development evolves. An air blower adequate for the needs of this program is presently available.

Thermal Studies

The program discussed to this point has been concerned with obtaining sufficient information under isothermal conditions to permit the development of analytical models for estimating both mean and extreme bed temperature distributions. Based on the outcome of these studies, it may be found desirable to perform some experiments by alternately passing hot and cold gas through the bed and observing the response characteristics of a number of properly instrumented spheres located at predetermined positions within the bed. If the hot gas is held to temperatures below 180°F, it should be possible to utilize the full-scale plastic model for such investigations.

Fuel Handling

The fuel-handling problems of the PBRE fall into two general areas: (1) selection of the shapes of the core bottom and fuel-discharge device that will give a desirable pattern of fuel movement through the ball bed and (2) the development of reliable equipment for the addition, removal, examination, sorting, and storage of fuel elements.

Movement of Spheres in the Core

The preferred pattern of fuel-sphere movement through the core would match the fuel residence time to the flux pattern in such a way as to give a uniform burnup of all elements. While a close correspondence between the fuel flow pattern and the flux may not be obtainable, the deviations from the average burnup can be limited by proper design of the lower end of the core. Preliminary model studies which have been made of this problem are summarized in Section 5.

Determination of sphere flow patterns through the core as a function of the bed configuration and the design of the sphere discharge device will be continued using small-scale plastic models and marbles. Eventually full-scale tests of the most promising designs will be performed using graphite spheres and flow of air through the bed (to reproduce the effect helium drag forces will have on the sphere movement);

the full-scale test will be performed using the facility discussed with regard to cooling studies.

Component Development

As described in Section 5, the fuel-handling equipment consists of gas locks with appropriate valves for transition from the atmosphere in the fuel-handling area to the reactor environment, sphere counters, a fuel-addition system, a discharge device for controlling the release of spheres from the core, sphere classifiers and sorters, an instrument for determining the fissile material content of a fuel element, storage facilities, and a conveyor to return unspent fuel to the charging chute. Means must be provided for removal of fuel elements from the core or from entry and discharge lines in the event of equipment malfunction.

A number of components for performing these functions will have to be tested or developed. Full-scale tests of equipment will be required to ensure that satisfactory performance can be achieved; particularly questionable items must be studied individually, and eventually a mockup in which key aspects of the system can be tested will be needed. The actual fuel-handling system will be extensively tested on the reactor with dummy fuel elements during the time provided in the schedule (Section 17) before actual fuel loading is begun.

PBRE Instrumentation and Control

The research and development effort required for the PBRE instrumentation and control systems includes analog studies, reactor control and safety system development, development of nonnuclear equipment for reactor control and safety, development of devices for use in the containment system, development of components for use in the fuel-handling system, and the development of instruments for high-temperature operation. As the design of the plant proceeds, additional development work, unanticipated at this time, is expected.

Analog Analysis

The ORNL analog computer is being and will continue to be used to study the transient behavior of various parts of the reactor system. Studies will be made of the effect of various perturbations of the steady state on temperatures, flux levels, etc. These will include studies of the requirements of the control system as well as those of the safety system. As the design nears completion, the analog model will be refined on the basis of the latest design information, and the transient behavior of the entire system will be studied.

Reactor Control and Safety System

The reactor control and safety systems were discussed in detail in Section 8 of this report. Many reactor control and safety devices are already available for use in these systems. However, development of some components and subsystems will be required. Among these are an automatic controller, a safety amplifier suitable for combining reactor coolant flow and flux level information, and a remotely controlled mechanism for positioning the safety chambers.

Nonnuclear Instruments and Equipment for Reactor Safety and Control

Primary coolant system instrumentation that will be exposed to gas-borne and deposited fission products present problems of calibration, maintenance, replacement, and possibly radiation damage. Pressure and flow transmitters and an instrument to detect a steam leak into the helium system are the key instruments in this category.

Methods must be devised for installing replaceable thermocouples in the reactor. The use of long thermowells or sealed guide tubes appears to be feasible, but a successful technique remains to be demonstrated.

Reliable power systems for safety instruments are needed. With the use of electrical instruments becoming more widespread, the development of a good, solid-state, dc-ac inverter that would operate from batteries would be an important contribution to this field.

Containment System Equipment

A modest development effort will be required to overcome shortcomings of existing valves and operators. For containment-vessel isolation it will be necessary to provide valves with low leakage rates and high reliability. Operators suitable for redundant systems (to improve system reliability) must be developed. The development of check valves that are leaktight for use in contaminated-area ventilation systems will be another aim of the program.

Pressure-relief and vacuum-relief valves are of great importance in any containment system. Existing equipment does not provide the reliability needed for such applications.

Fuel-Handling System

Most of the development problems for the fuel-handling system were described above. Specialized and reliable instrumentation is needed in connection with fuel-sphere counting and inventory control devices, sphere classifiers, and a fuel-burnup analyzer.

Development of Thermocouples for Measurements in the Range 2000 to 2500°F

The successful use of thermocouples for measurement of temperatures during very high-temperature operation of the PBRE will require the development and testing of new thermocouple assemblies. It will be necessary to measure helium and graphite temperatures in the range of 2000 to 2500°F. Although all core thermocouples will be replaceable, they should be reliable for a minimum of six months to one year at temperature. The sheath materials will be exposed to atmospheres containing low concentrations of carbonaceous gases, water, and hydrogen; in addition, the sheaths will be in physical contact with graphite over appreciable periods of time at elevated temperatures. The conditions under which these thermocouples will operate will be very similar to those expected for the HTGR, EGCR, and OEEC Dragon, except for the higher temperatures; therefore, close liaiscn should be maintained between these related projects.

The development of satisfactory thermocouple assemblies will require studies of (1) thermocouple wires, (2) metallic sheath materials,

(3) thermocouple insulation, and (4) compensating extension wires. In addition, it may be necessary to develop welding and replacement techniques for the types of thermocouples selected.

For periods of operation in the range 2000 to 2200°F, special Chromel-P vs Alumel and Geminol-P vs Geminol-N wires should give adequate life and reliability if properly sheathed. At temperatures above 2200°F the nickel-chromium alloys are unsatisfactory and the selection should be made from platinum, platinum-rhodium alloys, Platinel (Au-Pd-Pt vs Au-Pd), tungsten, rhenium, tungsten-rhenium alloys, molybdenum, niobium, and platium-molybdenum alloys.

Operation in the 2500°F region will require development of thermocouple sheaths which will not allow diffusion of carbon into the insulation. It is possible that double-sheathed assemblies may be necessary. The testing of a double sheath consisting of a layer of niobium over molybdenum seems indicated from results reported by the OEEC Dragon Project. Other sheath materials which should be considered include platinum, platinum-rhodium alloys, platinum-molybdenum alloys, and tantalum.

Preliminary screening tests should indicate whether any difficulties are to be expected from aluminum oxide or magnesium oxide insulation; magnesium oxide insulation should be satisfactory for these thermocouples. The necessity for compensating extension wires will be determined by the choice of thermocouple lead wires and the design of measuring instrumentation. Thermocouple assemblies made from promising combinations of materials should be tested under reactor atmospheric conditions.

Component Development

A primary objective of PBRE component development is to reduce the probability of primary and auxiliary system failure during operation by resolution of nonnuclear experimental features in advance of reactor construction. Some aspects of these problems, notably with regard to the purification system, fuel-handling equipment, and instruments and controls have been discussed above. Development work required in connection with control rods and drives, blowers and seals, mechanical joints, valves, the steam generator, and insulation are discussed below.

Control Rods and Drives

The four PBRE control rods are located under the reactor and move vertically. The mechanism for supporting and moving each rod is conceived to be electromechanical, and it will be canned to preclude escape of gaseous fission products.

Since the rod drives will be exposed in some degree to radioactive contaminants from the core, it will be necessary to establish the reliability of the electromechanical equipment and lubricants under these conditions. Limitations on activity will, in turn, determine sealing requirements. The choice of a lubricant may also affect sealing requirements.

The characteristics of electrical circuitry operating in helium are uncertain with respect to the dielectric strength of insulation and arc-over at switches and between terminals. Each electrical system must be tested in its operating environment at design conditions to assure proper operation, and some statistical proof-testing of individual components may be required. Functional testing of each production assembly will be required before installation in the reactor.

It is expected that the rod drive motors, motor brakes, power supply, and instrument readout system components will be commercially standard hardware; other hardware items, however, must be specially designed and individually tested for this application. These items include the mechanical power train, the latch-and-release mechanism, and the shock absorber. Finally, the over-all rod drive system must be tested for response, consistency, and reliability of performance consistent with reactor safety requirements.

Blowers

The PBRE requires primary coolant blowers to circulate large quantities of hot helium with relatively low pressure losses and auxiliary compressors to circulate small quantities of cool helium with larger pressure losses. While the design of the PBRE blowers will draw heavily on recently achieved technology for helium service, it will be necessary to

develop designs adapted to the specific PBRE conditions and to verify actual performances by tests.

The use of blowers using shaft seals can be ruled out because of the elaborate and costly auxiliary sealing systems that would be required. The use of totally enclosed blowers with oil-lubricated bearings would involve many of the same complexities as for blowers using shaft seals. A third alternative is, however, present: the use of totally enclosed blowers equipped with gas-lubricated bearings. The use of gas bearings will eliminate some complexities from the helium purification system and will obviate the need for a lubricant supply system.

Main Blower. A number of design study layouts will be made first. The operating limitations of the bearings will be explored by calculation and through discussion with consultants and manufacturers. Recent ORNL experimental and analytical work will be applied to the study of methods for cooling the motor and the bearings.

A full-scale experimental assembly will then be built to verify that the system selected will operate as predicted. Each assembly will include a full-scale set of bearings and electric motor and a flywheel to simulate the mass of the impeller. Tests will be carried out at the temperature and pressure which the blower will experience in the reactor. If the development of the PBRE design indicates that the system will be improved by using two main blowers in series or in parallel, the test assemblies will be modified to include impellers; and the joint performance of the blowers will be evaluated, including regimes of instability.

The third phase of the work will include the design, fabrication, and test of the prototype blower for the reactor, including the design and construction of a test loop to permit tests at maximum PBRE pressure and blower temperature conditions.

Auxiliary Blower. As described elsewhere in this report, the blower for the helium purification system will be equipped with gas-lubricated bearings, and will be of the hermetically sealed type. The development of the auxiliary blower will pass through the same three phases as that of the main blower, and most aspects of the studies and tests for the latter unit can be applied to the auxiliary blower.

The auxiliary blower may be equipped either with a centrifugal or a regenerative type of impeller, depending on the value of the pressure rise which must be provided for the final design of the helium purification system. If the regenerative system is selected, it will be necessary to modify the volute configuration to reduce the relatively high radial loads imposed on the bearings. This will be accomplished by reduced-scale experimental verification of studies that have been initiated.

Joints and Closures

The design of the PBRE requires that access to the core and steam generator internal components be possible and that components in the main coolant and auxiliary helium system be replaceable. Because of the level of radioactive contamination in these systems, opening and closing of joints and the handling of components to which the joints are attached must be accomplished behind shielding using techniques of the type described in Section 11. The joints must therefore be sufficiently accessible and advantageously positioned so that work performed on them can be accomplished quickly and effectively. Reassembly to original tightness specifications must be achievable, and it must be possible to validate this achievement by remote inspection. The joints and closures used must provide a high degree of seal integrity under all reactor operating conditions; and, where this performance cannot be guaranteed, double sealing and pressure or vacuum buffering of the interspace must be specified.

The PBRE will require joints in a variety of sizes to meet a wide range of conditions. Mechanical joints with double seals and gas buffering will be provided for large closures and connections. The majority of joints, however, will be in 1-in.-IPS or smaller auxiliary and service lines, and for these, single-seal mechanical joints may be satisfactory. In selecting mechanical joints and closures for these applications, use will be made of experience available from the design and development of experimental loops for the EGCR and also of favorable experience available from other gas-cooled reactor projects in the United States and the United Kingdom. The development in other programs of brazed and welded joints

which can be broken and remade remotely will be followed and evaluated for applicability to small lines in the PBRE. Joint types which show promise in various size and temperature ranges are listed and discussed in Section 3.

Because experience has indicated that the stringent tightness specifications for mechanical joints used in gas-cooled reactors can be met only by proof testing and design adjustment, a program is required to investigate the potential of promising designs of all sizes of interest to the PBRE and to determine the means associated with each for detecting leaks during operation. Tests will be conducted to determine the seal integrity and mechanical handling problems associated with promising joints and closures through representative temperature, pressure, and mechanical load cycling. Statistical evaluations will also be made of single-sealed types for small lines to determine confidence levels on reliability. The extent of reusability of the flanges and gasket material will also be demonstrated.

Slip Joints

In addition to mechanical joints and closures, the PBRE may require the use of a slip joint to accommodate differential thermal expansion in the concentric piping connecting the reactor pressure vessel to the steam generator. The primary criteria for such a joint are that it operate for the life of the reactor exposed to high-temperature helium containing small amounts of particulate matter without excessive wear, galling, or binding, and that the bypass flow of helium through the slip joint not become excessive during this period. A slip joint has been built and tested for GCR-ORR loop No. 2, but the size is much smaller and the requirements less stringent than those for the PBRE.

Development of the slip joint for PBRE will require design, fabrication, and evaluation of several concepts to allow selection of the more promising approaches. Evaluation tests should be carried out on prototype joints at simulated reactor operating conditions of temperature, pressure, and loading with the joints being cycled through typical motion cycles in a purified helium atmosphere for extended periods of time. Following

evaluation tests, a joint configuration for use in the PBRE can be selected and a full-scale unit should be built and endurance tested at reactor operating conditions.

Valves

The PBRE helium coolant and auxiliary gas-handling systems do not, in the present design, have any requirements for highly specialized valves; however, because of the nature of the system, the more-or-less standard valves to be applied must meet stringent performance specification with respect to reliability and allowable seat leakage. The fuel-handling system of the reactor will require a specialized valve capable of positive shutoff at the seat and designed to pass the fuel spheres when opened. Provisions must be made to prevent damage to the sealing surfaces and valve mechanism by particulate matter or broken fuel spheres.

A program is needed to screen the various types of valves available on the market which are applicable to the PBRE helium system. The experience of other projects with similar high-integrity valves must be investigated in the process of settling on the most promising designs. Long-term endurance and performance tests on activators, on seats and plugs, and on stem seals must be conducted at simulated operating conditions. The test facility for this investigation will be designed to accommodate a number of valves simultaneously, and these will be automatically cycled through a representative temperature and pressure range while being opened and closed at regular intervals.

Suitable fuel-handling valves must be tested under simulated operating conditions. Satisfactory leaktightness at the seat must be demonstrated throughout typical valve lifetimes, and the suitability for fuel handling must be demonstrated by installing the valves in a typical fuel feed system where their mechanical integrity can be demonstrated under adverse conditions.

Steam Generator Development

Although the PBRE steam generator probably will be procured from a vendor on the basis of performance specifications, some aspects of the

development and testing of the unit will remain the responsibility of the project. These include design and development of removable specimens for studying fission product and carbon deposition, and possibly tools for plugging tubes. The operation of the shutdown cooler is closely related to the hazards analysis of the reactor, and the adequacy of the design must be proved prior to freezing the steam generator design. In the event analytical studies do not suffice, models of the cooler will have to be constructed and tested to demonstrate satisfactory operation.

Experimental Stress Analyses

Large stresses may occur in the region of the gas outlet nozzle attachment to the reactor vessel liner as a result of differential vertical movement of the two ends of the gas ducting. The configuration, that of a nozzle-to-conical shell attachment, does not lend itself to accurate theoretical analysis, and an experimental stress analysis is required. This analysis may be made through the use of an appropriate model instrumented with strain gages. The end of the nozzle should be loaded or displaced in accordance with the conditions predicted for the reactor system. The results may then be used to specify an acceptable design.

The support scheme for the pressure vessel should also be investigated experimentally to evaluate the stresses in the vessel and to determine the vibrational characteristics of the system. Information concerning the latter is important in designing against earthquake loadings. An additional vibration study is required to evaluate the design of the steam-generator support system.

Materials Problems

The development activities described below, although providing information needed in the PBRE program, are in large part a continuation of the materials program planned for gas-cooled reactors in general.

Compatibility of Coolant and Decontamination Reagents with Metals

Since the coolant cleanup system is being designed to keep the levels of H_2O and CO_2 each below 1 ppm, no compatibility problems between the

structural materials and the coolant are expected at temperatures which will exist in the PBRE. Therefore, no experimental investigations of reactions between metals and gases appear to be needed.

It is not anticipated that the buffered oxalate-peroxide solution used in decontamination of components will damage the metal structures. This solution has been shown to attack carbon steel only mildly and would not be expected to affect stainless steels unless significant amounts of chloride were present. It will, of course, be required that the chloride content of the solution and rinse be severely restricted to avoid stress-corrosion cracking of any stainless steels exposed during the process. Equipment and materials tested for determining effectiveness of decontamination procedures will also be examined for unusual or unanticipated metallurgical deterioration, if any.

Compatibility of Graphite and Metal

In cases where contact between the graphite reflector and metal structures is inevitable, such as with thermocouples, it will be necessary to provide protection of the metal to prevent carburization and embrittlement. In recent tests, extensive carburization was observed at 1300°F in vacuum at the points of contact between type 304 stainless steel and graphite.[5] Preoxidation or copper plating of the stainless steel protected it at this temperature and would be expected to offer protection at somewhat higher temperatures. Thus, in situations where the interface temperature is above 1000°F, such protective measures should be provided and would be expected to minimize contact carburization during normal operation.

Welds of Upper Shroud, Concentric Tubing, etc.

The joining of type 304 stainless steel to carbon steel at the core support plates is not likely to be a problem. Procedures developed previously[6] for joining type 304 stainless to type A212, grade B, carbon

[5]GCR Quar. Prog. Rep. June 30, 1961, ORNL-3166, pp. 168–69.

[6]GCR Quar. Prog. Rep. Sept. 1960, ORNL-3015, pp. 95–96.

steel in the EGCR are probably adequate. Extensive testing of such joints showed that welds made with BP-85 filler metal could withstand many thermal cycles without failure.[7] If the temperature conditions are significantly different from the EGCR structural requirements, a few tests may be advisable to confirm the adequacy of the dissimilar-metal welded joints.

Special Compatibility Problems in High-Temperature Operation

Graphite-Metal Reactions. At temperatures much above 1500°F the protection of metal structures from contact carburization may be extremely difficult. Contact between graphite and thermocouple protection tubes or sheaths, or between graphite and stainless steel in the top plenum mixing chamber, may be inevitable in a reasonable design. Oxide films or copper-plated surfaces would protect stainless steel at 1500°F but could not be expected to remain protective at much higher temperatures. Thus, a solution to a difficult design problem plus a series of tests utilizing ceramic oxides or other materials compatible with graphite and metals may be necessary to assure reliability in the system.

Control Rods

The present control rod design utilizes the basic EGCR rod, having B_4C bushings supported in an annulus between stainless steel tubes. This rod is designed for normal operation at approximately 1400°F in the EGCR, with a maximum temperature of 1700°F for short periods. For normal operation of the PBRE, such a rod is deemed adequate and reliable. The surfaces of the rod are preoxidized to enhance emissivity and inhibit carburization, and the inner surfaces are copper plated to protect the stainless steel structures from reaction with the B_4C. However, at prolonged high temperatures (>1600°F) these protective features would no longer be reliable. For operation at high temperatures it would thus be necessary to use a set of special control rods that would be developed to withstand the severe service conditions.

A possible design would utilize B_4C protected by or dispersed in graphite and supported in a tube of molybdenum or other high-strength

[7]GCR Quar. Prog. Rep. Sept. 1961, ORNL-3210, pp. 46–47.

metal. While no irradiation test data have been generated on B_4C at such temperatures, it is considered adequate for the service, since at a range of lower temperatures the volume change occurring during irradiation is relatively independent of temperature. Certain nickel-base alloys might be adequate in place of the molybdenum if they were carefully protected from the B_4C and graphite. The structure of the control rod would be supported by a molybdenum rod through the center, which would allow some flexibility at the high temperature and would provide sufficient strength so that the control rod could be pulled into position. The compatibility of these higher temperature materials with PBRE gases and contaminants will require testing. No development of fabrication techniques for molybdenum are anticipated.

Protection of the metal structure (molybdenum or high-temperature alloy) from the B_4C and graphite would have to be reliable. Spray-coating techniques for applying protective oxides should be tested, as well as the use of other refractory metals.

Maintenance Problems

As discussed in preceding sections, the PBRE is to be constructed within shielded cells so that either remote or direct maintenance can be performed as activity levels permit. To simplify the approach, components and joints will be arranged for vertical access wherever possible. In any event, tools must be designed to reach and perform tasks wherever the joints may be located, to remove and replace equipment, and to restore the circuit to its original containment integrity. A particular problem in this connection is the development of methods of inspection of reassembled equipment, most of which may be in a field of radioactivity too high to allow entry of personnel. Other studies are required to indicate whether isolation and decontamination techniques in situ are feasible and to develop procedures for decontamination of equipment which is to be repaired or moved to storage.

Maintenance in the PBRE Cells

The development of remote maintenance techniques for use at the PBRE will require the use of scale models of the system to determine the accessibility of parts, routes to be followed in transporting defective and new equipment, and the motions required of tools to separate joints, extract components, disconnect leads, remove insulation, and replace all of the equipment for continued operation. The scale model may also be used to test models of proposed handling equipment to determine possible oversights or deficiencies in their design before they are fabricated for use in the PBRE.

The full-scale mockup discussed in the preceding section on fuel handling can be arranged in a geometry matching its proposed location in the reactor cells and enclosed by walls simulating cell walls and openings therein. Tests of the adequacy of disassembly and reassembly tools, inspection procedures, and leak-testing techniques using full-scale equipment would be conducted on some components and assemblies. As radioactive equipment is taken out of service, the component or part will require special handling, bagging, and storage to avoid spreading activity. The full-scale mockup will serve as a facility to check out the techniques developed for these purposes.

It may be necessary to close openings temporarily to prevent the spread of activity, and it is proposed to develop inflatable closures for these purposes.

Decontamination Studies

Three types of contamination problems for the PBRE can be identified:

1. In-cell activity resulting from inadvertent events or activity fall out while maintenance operations are being performed. Conventional cleanup techniques, possibly accomplished remotely, will probably be adequate to handle these situations.

2. Activity in or on equipment removed from the PBRE for servicing, examination, or destruction. Procedures for decontamination are being developed as a part of the gas-cooled reactor program; these studies will

be continued and related more directly to the PBRE as knowledge of fission-product deposition becomes available.

3. Removal of activity from reactor circuits in situ. While it may be possible to remove and replace every component of the PBRE, in many cases this will be undesirable and for full-scale power reactors replacement of large components may be completely impractical. In these cases it will be particularly desirable to rid the system of as much activity as possible before working on it.

Some kind of blowdown or wash down is visualized for in situ decontamination, but techniques for accomplishing this are untested at present. These problems will be studied, and in situ decontamination techniques developed. It may be desirable to test procedures for in situ decontamination in connection with full-scale components, where available, and to test the effectiveness of procedures for reducing activity in connection with fission-product deposition experiments.

Physics

There are four principal characteristics of the PBRE whose investigation might require a critical experiment. These are (1) criticality, that is, the fuel composition required to give a specified cold, clean multiplication factor for the clean core, (2) the reactivity effect of the control rods, (3) the temperature coefficients of reactivity, and (4) the power distribution.

While experimental verification of the analytical methods employed to study these characteristics is certainly required, it is likely that this verification can be found in existing critical experiment results. Analyses of criticality for Zenith and the HTGR and of the hot ART critical experiment should serve to determine whether neutron diffusion and thorium-resonance absorption are being taken into account properly. The analysis of control rod worth in Zenith, which like the PBRE has its rods in the reflector, should verify rod-worth calculations. The analysis of temperature coefficients for Zenith and for HTGR should indicate, at least, whether the range of uncertainty remaining in the temperature coefficient calculations for the PBRE is acceptable from the viewpoint of

control and safety. How much uncertainty can be regarded as satisfactory will depend on the computed values of the coefficients, as discussed in Section 5. These have not yet been computed with sufficient care to permit a final position to be taken on this point. The power distribution in the PBRE is quite favorable, and it is not expected that deviations of several per cent from the expected distribution would jeopardize the fuel element tests to be performed in the reactor.

Conservative estimates have been made of the uncertainties that are likely to remain after this analysis has been carried out and appropriate revisions, if any, made to the PBRE calculations. It is presently believed that adequate operating margins are being designed into the reactor to accommodate these remaining uncertainties. It is therefore proposed to carry out the analyses with the expectation that further critical experiments will not be found to be necessary.

Hazards Studies

In the event of air flow through the PBRE core following a primary system rupture, combustion of the graphite may proceed at a rate sufficient to raise the core temperature, thereby increasing the reaction rate and accelerating the rate and ultimate amount of fission-product release, as well as energy release. In the event of a steam leak into the reactor, hydrogen may be produced by reaction with graphite. Analysis of such accidents to obtain estimates of the hazards involved requires information on chemical reaction rates that at present is either lacking or inadequate.

Combustion of Fuel and Graphite. In the case of combustion of the fuel-graphite matrix, it is important to know whether any credit can be taken for protective coatings on the fuel spheres and on the fuel particles themselves. Although experiments on EGCR fuel sleeves have indicated only minor reductions in burning rate because of the presence of Si-SiC coatings, comparable experiments may be carried out for coated fuel spheres, in the hope that a significant amount of protection can be achieved by reason of improved coatings and the simpler element geometry. While UC_2-ThC_2 particles are known to react rapidly with oxygen at PBRE fuel

temperatures, pyrolytic-carbon coatings on the particles may provide a substantial measure of protection against fuel oxidation.

Burning experiments should therefore be carried out with coated particles, with graphite spheres not containing fuel particles, with graphite spheres containing uncoated fuel particles, and with graphite spheres containing coated particles, as well as with coated spheres. It is believed that low-pressure test facilities provided for the graphite oxidation and mass transfer studies discussed earlier can be modified to permit evaluation of reaction rates with gross air contamination as a function of specimen temperature, gas temperature, and gas flow rate.

Steam-Graphite Reactions. The seriousness of the graphite-steam reaction in terms of core damage and the amount of hydrogen produced will depend very much on the reaction rate. The effect of radiation on the reaction rate is unknown. Although information on the reaction rates in the absence of radiation is available at temperatures above 1500°F, extrapolations to much lower temperatures are not thought to be very reliable. Since, with the exception of periods of very high-temperature operation, most of the graphite in the PBRE will be below 1250°F (average fuel bed temperature in the PBRE will be 1100°F, average graphite temperature about 900°F), hydrogen formation rates cannot be estimated reliably from information currently available. The graphite-oxidation and mass-transfer experiments discussed previously will supply information on the extent of the reaction between moist helium and graphite at very low moisture content. For hazards studies, additional experiments should be planned to measure reaction rates over a range of steam pressures of at least 1 to 10 atmospheres and over the range of temperatures downward from 1800°F to the point where the reaction rate becomes too low to measure. This work will require test facilities (similar to those for the high-pressure graphite oxidation and mass transfer tests) wherein reaction rates of representative fueled-graphite specimens with gross steam contamination can be measured as a function of specimen temperature, vapor temperature and flow rate, and system pressure.

In-Pile Experiments. At the present time it is not possible to postulate the requirements for in-pile evaluation of the hazards associated

with graphite or fuel-matrix combustion with air or steam. This problem can be examined analytically based on the results of the out-of-pile testing, and the progress of other high-temperature gas-cooled reactor programs in this country and abroad will be followed closely. At some later date, the requirements for a minimum irradiation program will be more clearly defined.

Fission-Product Releases. The fractions of various fission products that would be released as a result of burning the fuel balls have not been determined experimentally. Hazards analyses to date have been based on information obtained from experiments involving the oxidation of UO_2 to U_3O_8. The analysis can be placed on a firmer basis when experimental results for coated carbide fuel particles become available. Such experiments can presumably be arranged within the scope of the present Nuclear Safety Program, and it is not believed that additional funding need be provided.

Nuclear Safety Pilot Plant. A proposal has been made for the construction at ORNL of a nuclear safety pilot plant for the investigation of reactor hazards problems. This facility is primarily designed for experiments on the meltdown of slightly irradiated fuels and the transport of fission products within a model containment vessel. The plant will, however, have the capability of performing tests on a full-size PBRE core with a minimum of modification. For such tests, the sphere bed would be heated electrically in an inert atmosphere to a temperature distribution which corresponds to thermal conditions at the time of an accident. The accident would then be simulated by circulation through the core of gas having a composition which represents that resulting from a depressurization of the reactor primary system, inleakage of steam from the heat exchanger, or other abnormal conditions.

Tests could be performed, for example, to determine the influence on the behavior of the system of intact Si-SiC sphere coatings, damaged sphere coatings, and the presence of UC_2 and ThC_2 in the fuel. Methods of inhibiting oxidation reactions could be tested as well. The rate of release of fission products from the core and their disposition in a containment vessel could be studied by using slightly irradiated fuel or radioactive tracers.

Funds for modification and operation of the nuclear safety pilot plant are not included in the PBRE research and development budget, since the existence of the facility is contingent on other activities. A program of experimentation with the facility, however, would add considerably to an understanding of the hazards associated with the chemical reactivity of graphite fuels.

Over-All Research and Development Program

The schedules and costs of the foregoing programs are summarized in Tables 16.1 and 16.2. The costs do not include certain future hazards experiments involving chemical reactions of air and steam with graphite because of incomplete definitions of the requirements at this time.

The amounts allocated for each type of effort that has either been budgeted already or may be considered a part of continuing general development for gas-cooled reactors are shown in Table 16.2 by subject and fiscal year. The total of the continuing general development effort represents about $6,822,000 over a four-year period. The additional increment due specifically to the PBRE is estimated as $5,043,000 over a five-year period, including Fiscal Year 1962.

From the descriptions of tasks, it is apparent that PBRE research and development cannot be provided on the basis of the PBRE increment alone. However, it is interesting to note that of the continuing GCR development programs, about $4,062,000 of the required $6,822,000 is already scheduled in Fiscal Year 1962 and 1963 budgets.

In the tasks listed, most of the work is required to achieve ordinary temperatures of operation in the system. Specific mention is made, however, of thermocouple and control-rod materials development for operation at outlet gas temperature of 2500°F. There are also scattered provisions for work at higher temperatures in regard to fuel element development, core cooling, fission-product deposition, coolant purification, and hazards. The cost of thermocouple and control rod development is $315,000, but the incremental costs of the other programs have not been determined specifically.

Table 16.1. PBRE Research and Development Schedule

Title	FY-1962 Quarters				FY-1963 Quarters				FY-1964 Quarters				FY-1965 Quarters				FY-1966 Quarters			
	-1-	-2-	-3-	-4-	-1-	-2-	-3-	-4-	-1-	-2-	-3-	-4-	-1-	-2-	-3-	-4-	-1-	-2-	-3-	-4-
Fuel Element Devel.																				
Graphite Components																				
Coolant Purification																				
Fission Prod. Trans. & Dep.																				
Core Cooling Problems																				
Fuel Handling																				
Reactor Control & Inst.																				
Component Devel.																				
Materials Problems																				
Maintenance Problems																				
Hazards																				

Table 16.2 Division of Research and Development Showing PBRE Increments

	FY-1962	FY-1963	FY-1964	FY-1965	FY-1966	Total
Fuel Element Development	600	1660	1425	350		4035
Continuing GCR Development Programs	580	1065	655			2300
PBRE Increment	20	595	770	350		1735
Graphite Components	80	390	520	190		1180
Continuing GCR Development Programs	80	250	250	190		770
PBRE Increment		140	270			410
Coolant Purification	90	240	315	25		670
Continuing GCR Development Programs	90	155	155			400
PBRE Increment		85	160	25		270
Fission Product Transport & Deposition	210	540	725	525	200	2200
Continuing GCR Development Programs	210	540	515	225		1490
PBRE Increment			210	300	200	710
Core Cooling Problems	72	135	125	63		395
Continuing GCR Development Programs	72	100	100	50		322
PBRE Increment		35	25	13		73
Fuel Handling	50	325	75			450
Budgeted Phases	50	230				280
PBRE Increment		95	75			170
PBRE Instrumentation & Control	35	260	230	30		555
Continuing GCR Development Programs	25	160	120	25		330
PBRE Increment	10	100	110	5		225

Table 16.2 (continued)

	FY-1962	FY-1963	FY-1964	FY-1965	FY-1966	Total
Component Development	75	535	535	135		1 280
Continuing GCR Development Programs	30	210	180	30		450
PBRE Increment	45	325	355	105		830
Materials Problems		175	260			435
Continuing GCR Development Programs		50	150			200
PBRE Increment		125	110			235
Maintenance Problems	15	150	160	160	75	560
Budgeted Phases & Continuing GCR Development	15	110	45	45	15	230
PBRE Increment		40	115	115	60	330
Hazards		80	25			105
Continuing GCR Development Programs		40	10			50
PBRE Increment		40	15			55
Totals	1227	4490	4395	1478	275	11 865
Budgeted Phases & Continuing GCR Development	1152	2910	2180	565	15	6 822
PBRE Increment	75	1580	2215	913	260	5 043

17. SCHEDULE FOR DESIGN AND CONSTRUCTION

A project schedule for PBRE which includes research and development, design, and construction is presented in Fig. 17.1. The schedule calls for continuing the present conceptual design studies until July 1, 1962, at which time it will be necessary to start a Title I design effort. The time periods indicated for the design phases of the project have been made consistent with the requirements for acquisition of research and development data; the research and development schedule is presented in more detail in Section 16.

The experience of other reactor projects of comparable complexity (EGCR, MSRE, HFIR, BONUS) has been used as a guide to the time periods required to secure reviews and approvals, and to negotiate contracts. This experience has also been used to guide the allocation of time for procurement and installation of key components such as the pressure vessel, steam generator, blowers, instrumentation and control system, and other components indicated on the bar charts. A generous period has been indicated for engineering shakedown before power operation is attempted.

It is felt that the schedule presented is a realistic one, contingent upon the required approvals being secured when indicated and funds and manpower being assigned as required. Key dates are the following:

A-E subcontract	1/1/63
Complete Title I design	1/5/63
Site approval	5/1/63
Construction contract	5/1/63
Start site work	7/1/63
Complete Title II design	9/1/64
Procurement and installing period for major components	3/1/63 – 8/1/65
ACRS hearing	11/1/64
Operating approval	5/1/65
Beneficial occupancy	8/1/65
Construction complete	11/1/65
Startup and part power operation	4/1/66

FIG. 17.1. P. B. R. E SCHEDULE
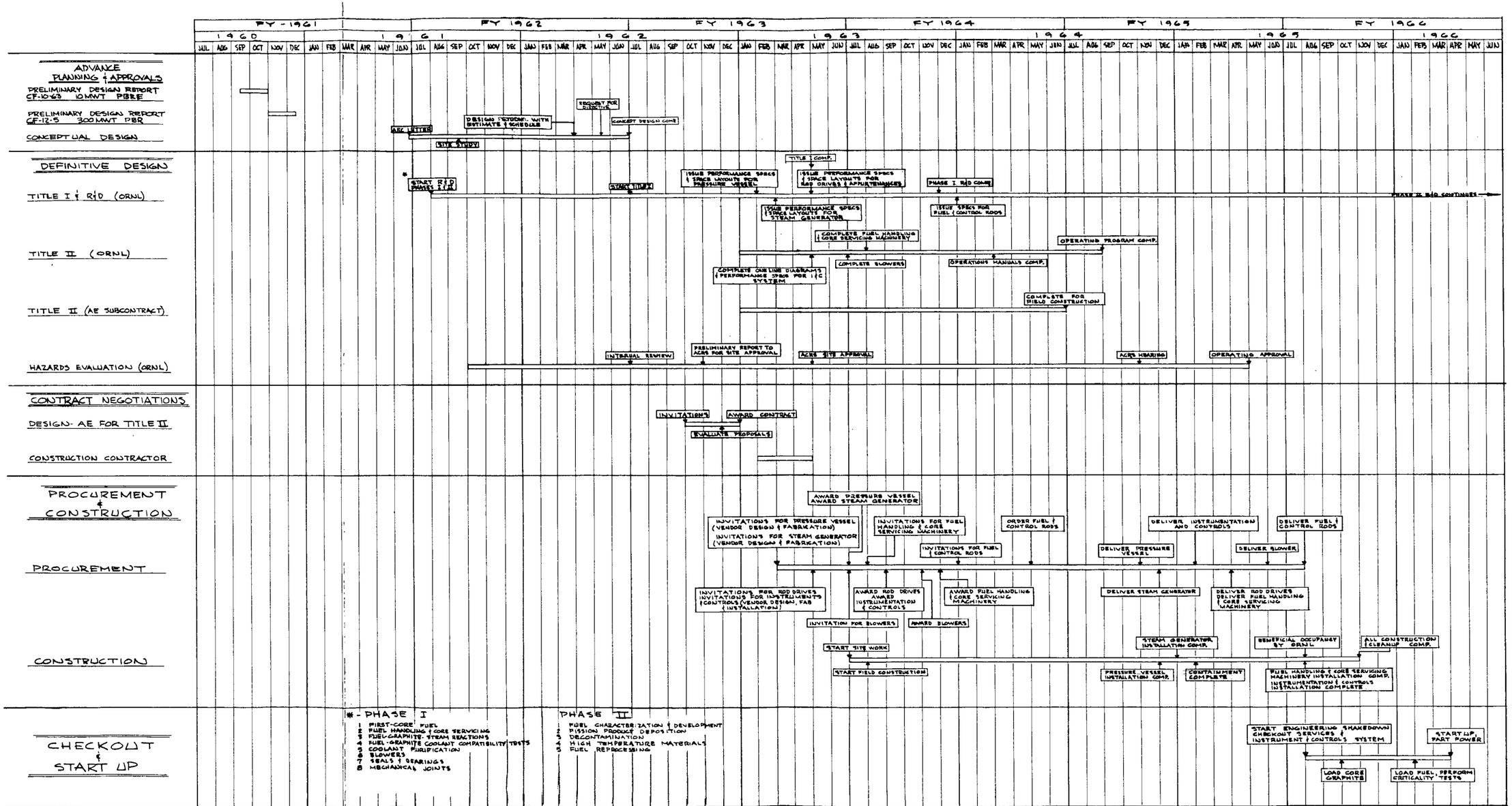
UNCLASSIFIED
ORNL-LR-DWG 68270